

**DEVELOPMENT OF GLASS-CERAMICS BY CONTROLLED NUCLEATION AND  
CRYSTALLIZATION OF GLASS SAMPLES PRODUCED FROM LOCAL RAW  
MATERIALS.**

**BY**

**ZAINAB SHEHU ALIYU**

**DEPARTMENT OF GLASS AND SILICATE TECHNOLOGY  
FACULTY OF ENVIRONMENTAL DESIGN  
AHMADU BELLO UNIVERSITY, ZARIA  
NIGERIA**

**JUNE, 2018**

## CHAPTER ONE

### 1.0 INTRODUCTION

Modern science and technology require new materials with special properties for diverse applications in our day to day activities. Among these new materials, one group plays a very special role and that is glass-ceramics material (Manfredini and Rinco, 1997). It occurred to Reamur in 1739 that dense ceramics could be made through crystallization of a base glass, but the invention of glass-ceramics through phase separation took place in the 1950s by the inventor S.D. Stookey (Holand and Beall, 2002). When the general theories on nucleation and crystal growth in glasses were well established, glass-ceramics have played vital role in a wide range of scientific and technological developments. In addition, there are great deal of text books, journal publications, conference proceedings describing the basis, characteristics, production, properties, advantages as well as wide variety of applications of these materials (Casasola and Rincon, 2012). Glass ceramics are polycrystalline materials produced from controlled nucleation and crystallization of carefully formulated base glasses (Shackleford and Doremus, 2008). They are inorganic materials and their microstructure is characterized by fine-grained randomly oriented crystals with some residual glass, without voids, micro crack or porosity and with two or more phases assemblage dispersed in the matrix of residual glassy phase (Daniela *et al.*, 2010 and Rezvani, 2011).

The chemical composition and microstructure of glass-ceramics are derived from primary base glasses, which are subjected to controlled heat treatment to nucleate crystals in the matrix of residual glassy phase (Mahdavi *et al.*, 2011). Nucleation is vital in glass-

ceramics production as it promotes the development of high density growth and crystallization (Alekseev *et al.*, 2010 and Jing *et al.*, 2013).

Glass-ceramics material is not a fully crystal because the microstructural configuration is 50 vol% to 95 vol% crystalline with the remainder being residual glassy phase (Salama *et al.*, 2002; Ali, 2008; Rezvani, 2011 and Bahman & Behzad, 2012b). Two or more phases assemblage may precipitate during controlled thermal treatment and their composition is completely different from the corresponding base glass, it follows that the composition of the residual glassy phase differs from the corresponding base glass (Carl and Hoche, 2002; Ali, 2008; Hussain *et al.*, 2010; Daniela *et al.*, 2010 and Khater *et al.*, 2013).

In the transformation of base glass to glass ceramics, nucleation is attainable heterogeneously or homogeneously. Bulk crystallization otherwise termed as heterogeneous nucleation involves utilization of various nucleating agents to promote the development of micro-heterogeneities and crystallization which result in the transformation of metastable base glass to stable microcrystalline glass-ceramics (Francis *et al.*, 2004; Ren-Ping *et al.*, 2007 and Bahman & Behzad 2012b). A wide variety of nucleating agents promote the crystallization process of base glass and enhance the formation of fine-grained microstructure. The most popular nucleating agents of base glasses are titania (TiO<sub>2</sub>), zirconia (ZrO<sub>2</sub>), chromium oxide (Cr<sub>2</sub>O<sub>3</sub>), iron oxide (Fe<sub>2</sub>O<sub>3</sub>), phosphorus pentoxide (P<sub>2</sub>O<sub>5</sub>), fluorides such as calcium fluoride (CaF<sub>2</sub>), sodium fluoride (NaF) and noble metals like; gold, silver and copper among others (Holand and Beall, 2002). The role of these substances is to promote micro phase separation in various base glass systems permitting the development of glass-ceramics. Bulk crystallization with the aid of nucleating agent is the most desirable crystallization technique and it is used in the

manufacture of almost all commercial glass-ceramics as it assures a uniform microstructure with high crystalline content (Salama *et al.*, 2002; El-Meliegy and Richard, 2012). Homogeneous nucleation occurs due to randomness or disordering of atoms without the aid of nucleating agent (Tulyaganov *et al.*, 2002). Also, glass-ceramics are made through powder processing technique in which glass powders (frits) are shaped with the help of a binder, sintered and then crystallized by heat treatment without the incorporation of nucleating agent (Tomohiro *et al.*, 2004; Garkida, 2007 Ali, 2008 and Isah, 2016).

Glass-ceramics have numerous advantages over conventional ceramics and glass because of their highly uniform microstructure with crystal sizes less than 10  $\mu\text{m}$  (Strnad, 1986). In addition, they possess better properties over glass and conventional ceramics such as high strength, excellent toughness and hardness, near zero coefficient of thermal expansion, high machinability, high temperature resistance, low dielectric loss, good infrared radiation performance among other (Hans and Dieter, 2005 and Shackelford and Doremus, 2008).

Glass-ceramics have a wide variety of applications among which include dental restoration, heat exchangers, membrane and sensors, heating elements, electronic packaging, welding equipment, prototyping component for automobile, medical equipment, cookware, nose cones of rocket, telescope mirror, vision ware, cladding in building industry, floor and wall tiles, anti corrosive equipment, filters, dental restoration and bone implant among others (Noves de Oliveira *et al.*, 1994; Patridge, 1994; Hans and Dieter, 2005; Ali, 2008; Daniela *et al.*, 2010; El-Meliegy & Richard, 2012 and Isah, 2016).

Glass-ceramics developed from the quaternary base glass system  $\text{CaO-MgO-Al}_2\text{O}_3\text{-SiO}_2$  is inexpensive and environmentally friendly, the starting materials might be sourced from

naturally occurring raw materials and the expected dominant phase assemblage precipitated from the system is diopside ( $\text{CaO-MgO-2SiO}_2$ ). The microstructure of diopside is characterized by a significant increase in hardness and wear resistance, biomedical and high chemical durability which has made it a potential candidate for wear resistance applications (Kokubo *et al.*, 1986; Salama *et al.*, 2002; Garza-Garcia *et al.*, 2007; Daniela *et al.*, 2010 and Bahman & Behzad, 2012a). Similarly, other lesser phases assemblage can be crystallized from the system such as wollastonite ( $\text{CaO.SiO}_2$ ) and anorthite ( $\text{CaO-Al}_2\text{O}_3\text{-2SiO}_2$ ) and quartz ( $\text{SiO}_2$ ) with microstructures characterized by excellent flexural strength, hardness, toughness, resistance to thermal shock and chemical durability hence making them suitable for cladding in building industry and low-temperature cofired ceramics (LTCC) (Baldi *et al.*, 1995; Alizadeh and Marghussian, 2000a; Salama *et al.*, 2002; Torres and Alarcon, 2004; Beall, 2008 & Bahman and Behzad, 2012a). Pyroxenes are most desirable mineral phases precipitated in  $\text{CaO-MgO-Al}_2\text{O}_3\text{-SiO}_2$  base glass system due to their interesting properties (Salama *et al.*, 2002). The most effective nucleating agents for  $\text{CaO-MgO-Al}_2\text{O}_3\text{-SiO}_2$  system include; titania ( $\text{TiO}_2$ ), chromium oxide ( $\text{Cr}_2\text{O}_3$ ), calcium fluoride ( $\text{CaF}_2$ ) and phosphorus oxide ( $\text{P}_2\text{O}_5$ ) (Salama *et al.*, 2002; Daniela *et al.*, 2010; Bahman and Behzad, 2012a and Khater, *et al.*, 2013). Controlled nucleation and crystallization technique has been adopted for this research owing to the fact that it is more efficient, reliable and it has been in practice over the years. Also, the study had followed the approach utilized by Salama *et al* (2002) and Mahdavi *et al* (2011) who reported that adding 10 wt% titania to the base glass system  $\text{CaO-MgO-Al}_2\text{O}_3\text{-SiO}_2$  promotes achieving high density nucleation and subsequent crystal growth.

## **1.1 Statement of Problem**

The naturally occurring starting materials for making glass-ceramic are available in various locations across the country. Most of the available raw materials have not been characterized to determine their properties and suitability for making glass-ceramics using controlled nucleation and crystallization processes. However, efforts were made by some researchers such as Aykut (2005); Marques *et al* (2006) and Isah (2016) to developed glass-ceramics from silicate-based wastes as starting materials using sinter crystallization route and was able to produce new materials with desirable properties. Their findings indicated the possibility of use majorly for tiling. In addition, Ali (2008) successfully developed glass-ceramics using local raw materials by sinter crystallization process and the new materials produced have excellent properties. Therefore, an attempt will now be made in this research to find out the suitability of using local raw materials for making glass-ceramics by controlled nucleation and crystallization routes as this type of glass-ceramics material has a wide variety of applications. Notable examples are cookware, welding and medical equipment, sensors, dental restoration, bone implant and gyroscope among others (Holand and Beall, 2002; Salama *et al.*, 2002; Mahmud, 2007 and Daniela *et al.*, 2010).

## **1.2 Justification for the Study**

Reports from government agencies and research institutes such as Raw Material Research and Development Council (RMRDC, 1989) and National Metallurgical Development Center, Jos (NMDC, 1990) have shown that the starting materials for making base glasses and the resultant glass-ceramics are available in various locations across the country. The major raw materials for the production of glasses and the resultant glass-ceramics include; sand, feldspar, limestone, magnesite, dolomite and gypsum among others are available in

various locations across the country. These materials are easily obtainable, environmentally friendly, inexpensive and more importantly their processing temperatures are low between the range 600-1200°C (Eric, 2008 and Khater, 2012).

### **1.3 Significance of the Study**

The outcome of the study would save the country substantial amount of foreign exchange on the importation of glass-ceramics products for both industrial and household applications. In addition, glass industries and related institutes as well as students will benefit greatly from the outcome of this research as skills and technology for the production of glass-ceramics using locally available raw materials will be acquired leading to the establishment of new industries which will result in creating employment opportunities for the teeming population.

### **1.4 Aim of the Study**

The aim of this study is to produce glass samples from local raw materials (feldspar, limestone & magnesite) and transform them into glass-ceramics through controlled nucleation and crystallization processes.

### **1.5 Objectives of the Study**

To achieve the aforesaid aim, some objectives were set out as follows:

1. To characterize the starting materials (feldspar, limestone and magnesite) using standard methods (XRF, XRD and SEM-EDS) to determine the oxides compositions, mineralogical constituents, microstructure/elemental distribution respectively so as to ascertain their suitability in glass making and glass ceramics.

2.To formulate batches and determine the glass transition temperatures ( $T_g$ ) of the glass samples produced which further provides idea about the nucleation and crystal growth temperatures.

3.To subject the glass samples produced to heat treatment using controlled nucleation and crystallization processes.

4.To characterize the glass-ceramics samples produced using SEM and XRD.

5.To investigate some physicochemical properties of the glass ceramics samples (hardness, chemical solubility, apparent density, porosity and water absorption) using ASTM standard procedures and effect of varying heat treatment time and titania ( $TiO_2$ ) addition on the quality of glass-ceramics samples produced.

### **1.6 Delimitations of the Study**

The study was restricted to collection of samples locally (feldspar, limestone and magnesite) from their respective deposits (Matari, Kalambaina and Tsakesimptah) respectively. The samples were subjected to crushing, grinding and sieving to  $-105\mu m$  particle size distribution. Each sample was subjected to characterization using XRF, XRD, SEM-EDS analyses to determine oxides composition, mineralogical compositions, morphological study and elemental compositions respectively. This has been done with a view to ascertaining their suitability in making glass-ceramics. Chemical grade titania ( $TiO_2$ ) and sodium chloride ( $NaCl$ ) were used as nucleating agent and fining agent respectively. Batches were formulated and glass samples were produced, followed by

transformation of glass samples into glass-ceramics using controlled nucleation and crystallization processes. Furthermore, characterization of glass-ceramics samples using XRD and SEM were carried out, although, only samples heat treated for 2 and 4 hours were considered for X-ray diffraction (XRD) and scanning electron microscope (SEM) analyses. In addition, determination of some property tests were conducted on each sample. The property tests include: Hardness, apparent density, chemical solubility, porosity and water absorption using standard procedures.

### **1.7 Limitations of the Study**

The obstacles which the research encountered include lack of melting furnace and equipment that would measure the major and minor mineral phases present in each glass-ceramics sample under investigation as well as measurement of some properties such as bending strength, toughness and thermal expansion coefficient among others which are relevant to the research. Besides, the X-ray diffraction (XRD) and scanning electron microscope (SEM) analyses were limited to samples that were heat treated for duration of 2 and 4 hours only due to financial constraints.

## CHAPTER TWO

### 2.0 LITERATURE REVIEW

Glass-ceramics which are partly glassy and partly crystalline are developed by controlled nucleation and crystallization of glasses. Glass-ceramics constitute varying phases assemblage which are dispersed in the matrix of a residual glassy phase depending on the base glass composition (Holand and Beall, 2002). The crystallization of base glass into glass-ceramics depends on heat treatment schedule which transforms base glass into uniform microcrystalline glass-ceramics with superior properties (El-Meliegy and Richard, 2012). The development of a finely divided uniform microstructure results in improvement in the strength and promotes the development of a broad spectrum of desirable glass ceramics properties. Achieving controlled crystallization depends on the following factors namely: nucleation temperature, crystallization temperature, heating rate and the length of the heating time (El-Meliegy and Richard, 2012). The idea of controlled crystallization of glass sample shows the separation of phases assemblage from the glassy phase in the form of tiny crystals, their growth rate as well as their final size are controlled by suitable controlled heat treatment, and the crystalline phases are generated by crystal growth from a homogeneous amorphous glass (Pinckney and Beall, 2008 and Daniela *et al.*, 2010).

The properties of glass-ceramics are superior to their corresponding glass samples and conventional ceramics because they have combination of physical, mechanical, chemical, thermal and biological properties and these properties can be tailored by changes in composition and heat treatment (Shackleford and Doremus, 2008 and Mukherjee and Das, 2012). The properties of glass-ceramics depend on composition, phase assemblage and microstructure (Pinckney and Beall, 2008). During manufacture, complex shapes may be produced using standard glass forming techniques such as pressing, blowing, casting, pouring and drawing among others before crystallization and dimensional changes are not noticeable (Beall, 1985 and Mahmud, 2007).

The idea of transforming the base glass into crystalline material was initiated by Reamur, a French chemist in the 17<sup>th</sup> century. He discovered that if a glass bottle was put into a mixture of sand and gypsum and both were subjected to heating for several days, they would be transformed into opaque material. Reamur was unable to achieve the heat treatment processes which were pertinent for controlled crystallization. However, in the late 1950s, S.D. Stookey of Corning Glass Works made the break through and therefore expanded the theory of phase separation (Mahmud, 2007 and Holand & Beall, 2002). Phase separation involves heat treatment in two stages to give nucleation and crystal growth both achieved at low and high temperature holding processes. This results in the formation of two or more phases assemblage dispersed in the matrix of the residual glassy phase (Salama *et al.*, 2002; Mohammed *et al.*, 2003; Garza-Garcia, *et al.*, 2007; Russell and Edward, 2010 and Khater, 2012). The glassy phase acts as a bonding phase because each crystal is surrounded by small volume fraction of the residual glass (Holand and Beall, 2002 and Mahmud, 2007). Amorphous phase separation is generally the first stage in

glass-ceramics formation. Phase separation is the process in which amorphous homogeneous phase is divided into two immiscible phases of different compositions (Pinckney and Beall, 2008). In glass, the separation occurs spontaneously on cooling from the molten glass or on reheating the solid glass, and the resulting microstructural configuration constitutes finely dispersed droplets of glass or crystals in the matrix of glassy phase (Naruporn *et al.*, 2013). To effect internal nucleation, some nucleating agents are incorporated to the batch, this melt homogeneously into the glass but promote very fine-scale phase separation on heating (Pinckney and Beall, 2008). The dispersed phase could be metal, titanate, zirconate or fluoride which would be structurally incompatible with the base glass and highly unstable as a glass. Thus, precipitates as tiny nuclei on heating at temperatures near the annealing point of the base glass would be formed (Holand and Beall, 2002).

Glass is melted at temperature between 1450°C and 1600°C and formed during cooling using techniques based on high viscosity temperature characteristics of a Newtonian fluid. After cooling the formed glass object, it is given a heat treatment slightly above its transformation range to develop micro heterogeneities upon which crystallization can subsequently commences (El-Meliegy and Richard, 2012). Further heat treatment produces a predominant phase change from glass to crystals that commence at the low energy surfaces of the tiny nuclei and ends when the oxide raw materials of the major phases assemblage are depleted from the residual glassy phase (Holand and Beall, 2002). During this process, viscous flow is drastically impeded by the growth of crystals around the widely and uniformly scattered nuclei. As a result, glass articles of precise shape can be

formed by this process and precipitated without distortion into uniformly microcrystalline ceramics (Casasola and Rincon, 2012).

In addition, it is possible to develop glass-ceramics using a two-stage process based on controlled nucleation and crystal growth. Glass-ceramics which are partly glassy and partly crystalline state are usually developed from specially formulated compositions which contains nucleating agent, melted, formed using desirable glass shaping techniques, annealed and then cooled to room temperature (El-Meliegy and Richard, 2012). Thereafter, the base glasses would be subjected to heat treatment to initiate nuclei formation and subsequent crystal growth (Salama *et al.*, 2002). Such thermal treatment is carried out in two stages as follows; at temperature somewhat above transition region to develop nuclei in the bulk glass and then followed by further heat treatment at higher temperature to promote crystallization on the formed nuclei (El-Meliegy and Richard, 2012). The basis of controlled crystallization depends on efficient nucleation which results in the formation of fine-grained and uniform microstructure without micro cracks or voids which would be ideal for a wide variety of applications (Holand and Beall, 2002). Glass-ceramics developed using controlled nucleation and crystallization or double-stage process has several advantages over conventional powder-processed ceramics, such as very null porosity as well as uniform microstructural configuration which are reproducible. The phases assemblage precipitated in some glass matrices typically enhance and sometimes lead to entirely new combination of properties ( Thiana *et al.*, 2008).

Generally, glass-ceramics are inorganic materials, and they are either alkali or alkaline earth alumino silicates with reproducible fine-grained and uniform microstructural configuration without porosity or micro crack (Aykut, 2005; Mahmoud, 2007; Garza-

Garcia *et al.*, 2007 and Daniela *et al.*, 2010). Most glass-ceramics that are commercially based, they are from multi component base glass systems such as the quaternary base glass system like CaO-MgO-Al<sub>2</sub>O<sub>3</sub>-SiO<sub>2</sub>, ternary base glass system like Li<sub>2</sub>O- Al<sub>2</sub>O<sub>3</sub>-SiO<sub>2</sub> as well as binary base glass system such as Li<sub>2</sub>O-SiO<sub>2</sub> (Holand and Beall, 2002; Shelby, 2005 and Mahmud, 2007).

In principle, a metastable glass object is obtained as a result of cooling from a melt. During subsequent heat treatment, controlled crystallization occurs, with nuclei formation and subsequent crystal growth of phases assemblage. Thus, a glass-ceramics is a multi phase crystalline solid which consists of finely dispersed phases assemblage in the matrix of a residual glassy phase (El-Meliegy and Richard, 2012). The controlled crystallization of the base glass results in the formation of fine-grained crystals that are evenly distributed throughout the base glass which is the main target of glass-ceramic (Beall, 1993; Holand and Beall, 2002). The number of crystals, their growth rate and sizes are controlled by time and temperature of heat treatment (Al-Harbi and Khan, 2008; Kartelia, 2010).

## **2.1 Theoretical Review**

The study of the CaO-MgO-Al<sub>2</sub>O<sub>3</sub>-SiO<sub>2</sub> system was important for understanding the reactions taking place in rocks. Pyroxenes are the most desirable mineral phases crystallized in CaO-MgO-Al<sub>2</sub>O<sub>3</sub>-SiO<sub>2</sub> glasses due to their interesting properties and the major phase assemblage present is diopside (Barbieri *et al.*, 1992; Alizadeh and Marghussian, 2000a; Tulyaganov *et al.*, 2002; Mohammed *et al.*, 2003; Ren-Ping *et al.*, 2007; Daniela *et al.*, 2010; Khater, 2010; Bahman and Behzad, 2012a ) among others.

Khater (2001) studied the crystallizing phases from multicomponent silicate glasses in the system  $K_2O-CaO-MgO-Al_2O_3-SiO_2$  and the conclusion drawn was that diopside, anorthite and wollastonite were the primary crystalline phases present with a small amount of microcline.

Khater (2010) investigated glass-ceramics of  $CaO-MgO-Al_2O_3-SiO_2$  base glass system. Batches were melted, cast and then subjected to heat treatment to induce crystallization. XRD results revealed the presence of diopside ( $CaO-MgO-2SiO_2$ ) as the dominant crystalline phase, wollastonite ( $CaSiO_3$ ) and anorthite ( $CaO-Al_2O_3-2SiO_2$ ) were minor crystalline phases.

Alizadeh and Marghussian (2000a) investigated the crystallization process of ternary system  $CaO-MgO-Al_2O_3-SiO_2$  using a mixture of  $Cr_2O_3$  and  $Fe_2O_3$  as nucleating agents. Wollastonite ( $CaSiO_3$ ) and diopside ( $CaMgSi_2O_6$ ) were the two major phases assemblage identified after two-stage heat treatment process. Beyond the diopside and wollastonite phases, numerous phases assemblage can be crystallized from the  $CaO-MgO-Al_2O_3-SiO_2$  system (CMAS).

Similarly, Tulyaganov *et al* (2002) studied the sintering and characterization behaviour of glass powders for the calcium magnesium alumino silicate (CMAS) system and there were formations of anorthite ( $CaAl_2Si_2O_8$ ), Akermanite ( $Ca_2MgSi_2O_7$ ) and diopside ( $CaMgSi_2O_6$ ).

Khater and Hamzawy (2008) investigated the effect of different nucleation catalysts on the crystallization behavior within the  $CaO-MgO-Al_2O_3-SiO_2$  system. They found that glass-ceramics containing  $CaF_2$ ,  $Cr_2O_3$  and  $TiO_2$  is characterized by fine-grained textures,

whereas glass-ceramics containing LiF is characterized by coarse grain texture and the result of XRD revealed that diopside is the dominant phase assemblage.

Daniela *et al* (2010) investigated the significance of crystallization catalysts playing a vital role on the phase transformation and the development of glass-ceramics texture using  $\text{Cr}_2\text{O}_3$ ,  $\text{TiO}_2$  and  $\text{ZrO}_2$  as nucleation agents for nuclei formation and crystal growth. Gahnite ( $\text{ZnAl}_2\text{O}_4$ ), virgilite ( $\beta$ -quartz), enstatite ( $\text{Mg}_2\text{SiO}_6$ ), wollastonite ( $\text{CaSiO}_3$ ) and diopside ( $\text{CaMgSi}_2\text{O}_6$ ) crystal phases were precipitated in the matrix of the residual glassy phase and the presence of these crystals of course increased fracture toughness as well as resistance to abrasive wear of glass-ceramics sample.

Wang *et al* (2010) presented a new kind of large grain transparent glass-ceramics obtained by the method of crystal growth from a homogeneous glass, the simultaneous variation of the glass matrix and crystalline compositions during the crystallization results in the high transparency of large grain, high crystalline volume glass-ceramics. The refractive indexes of the crystals and the glassy phase are suitable for optical property. Optimum heat treatment schedule, microstructural study and crystal phases were carried out using DSC, SEM and XRD respectively.

Juan *et al* (2012) examined the crystallization of  $\text{SiO}_2$ - $\text{Al}_2\text{O}_3$ - $\text{CaO}$ - $\text{Na}_2\text{O}$  base glass system using Differential Thermal Analysis (DTA). The crystal growth process has been studied using isoconversional, invariant kinetic parameters, and master plots methods. The applied kinetic models have revealed activation energy values that are over 360 and 385 kJ/mol by employing the integral and differential kinetic methods respectively. The crystallization process schedule that was previously observed using scanning electron

microscopy has been corroborated in this study using the kinetic methods. The crystallization of wollastonite occurs through a complex two-stage mechanism, with early three dimensional growth of crystals on the surface of glass particles followed by one dimensional growth of needles toward the interior of grains.

De Vekey and Majumdar (1970) studied the nucleation and crystallization of some glasses in the CaO-MgO-Al<sub>2</sub>O<sub>3</sub>-SiO<sub>2</sub> System using numerous nucleating agents such as TiO<sub>2</sub>, ZrO<sub>2</sub>, V<sub>2</sub>O<sub>5</sub>, MoO<sub>3</sub>, CeO<sub>2</sub>, WO<sub>3</sub> and ThO<sub>2</sub> in the amount ranging from 5-12 wt%. All the oxides induced some degree of nucleation but high density nucleation was achieved using 10-12wt% TiO<sub>2</sub> incorporation. This was considered to be suitable for quaternary base glass system. During controlled heat treatment of the glasses, phase separation occurred. The nucleation and crystallization processes that followed have been studied by DTA, XRD and SEM. Hexagonal cordierite was precipitated in the residual amorphous phase and high mechanical properties were recorded such as moduli of rupture above 150 MNm<sup>-2</sup> and compressive strength greater than 1000MNm<sup>-2</sup>.

KoKubo (1990) developed bioactive glass-ceramics for bone replacement in human medicine. He used the technique of surface nucleation to precipitate apatite and wollastonite as main phases assemblage from the glass-ceramics.

Holand and Beall (2002) reported that glass-ceramics with high mechanical strength was developed from SiO<sub>2</sub>-Li<sub>2</sub>O-P<sub>2</sub>O<sub>5</sub>-ZrO<sub>2</sub> base glass system by phase separation that involved using controlled nucleation and crystallization processes. Apatite and diopside were produced by the controlled crystallization of base glass to produce biomaterials for restorative dental applications.

Garza-Garcia *et al* (2007) studied the effect of mixed alkaline-earth on some properties of glasses of the CaO-MgO-Al<sub>2</sub>O<sub>3</sub>-SiO<sub>2</sub> system which was caused by a partial substitution of CaO by BaO mixtures. The glass properties considered in this study were density, glass molar volume, oxygen molar volume, packing fraction, glass transition temperature, compressive strength and chemical resistance in neutral, basic and acidic aqueous media. The phases identified include diopside as primary phase and wollastonite as secondary phase.

Al-Harbi and Khan (2008) studied the relationship between heat-treatment temperature, crystalline phases and thermal expansion coefficients of Li<sub>2</sub>O-MgO-Al<sub>2</sub>O<sub>3</sub>-SiO<sub>2</sub> base glass system. The crystalline phases were characterized by differential thermal analysis (DTA), X-ray diffraction (XRD), scanning electron microscope (SEM) and dilatometer (DIL), the effects of nucleating agents such as TiO<sub>2</sub>, Cr<sub>2</sub>O<sub>3</sub> and P<sub>2</sub>O<sub>5</sub> and heat treatment temperatures ( 800°C, 900°C, 1000°C and 1100° C) on crystallization and morphology were also investigated. Wollastonite (CaSiO<sub>3</sub>) and diopside (CaMgSi<sub>2</sub>O<sub>6</sub>) were two major phases assemblage identified after two-stage heat treatment process.

Salama *et al* (2002) and Khater and Hamzawy (2008) investigated the effect of different nucleating agents on the crystallization behaviour of multicomponent system within the Na<sub>2</sub>O-CaO-MgO-Al<sub>2</sub>O<sub>3</sub>-SiO<sub>2</sub> system. They found that glass-ceramics containing Cr<sub>2</sub>O<sub>3</sub>, CaF<sub>2</sub> and TiO<sub>2</sub> as nucleating agents are characterized by fine-grained textures, whereas glass-ceramics containing LiF is characterized by coarse grain texture. Also, adding less than 10 wt % TiO<sub>2</sub> slows down phase separation.

Mohammed *et al* (2003) studied the influence of local raw materials on phase crystallization of nepheline-pyroxene glass-ceramics in the system CaO-MgO-Al<sub>2</sub>O<sub>3</sub>-SiO<sub>2</sub> using titania (TiO<sub>2</sub>), chromium oxide (Cr<sub>2</sub>O<sub>3</sub>) and lithium fluoride (LiF) as nucleating agents and then heat-treated in the temperature range between 655°C to 715° C to induce nuclei formation and then crystallized at high temperature range between 850°C to 1050°C for 8 hours. Titania rapidly crystallized the base glass sample to nepheline and titanite phases, lithium fluoride (LiF) as nucleating agent precipitated wollastonite, akermanite and diopside in the residual glassy phase while chromium oxide being nucleation catalyst helped in the formation of diopside and nepheline.

Ren-Ping *et al* (2007) studied the crystallization of some base glasses in CaO-MgO-Al<sub>2</sub>O<sub>3</sub>-SiO<sub>2</sub> system using Cr<sub>2</sub>O<sub>3</sub> as nucleation agent. Diopside with excellent micro hardness was precipitated as the main phase assemblage. The obtained microstructure resulted in higher hardness, resistance to abrasive wear and high resistance to acid (Concentrated H<sub>2</sub>SO<sub>4</sub>) and base (Concentrated NaOH) attack.

Garkida (2007) used powder processing technique to study various types of waste glasses from different sources such as soda lime-silica glass, lead crystal glass and borosilicate glass by subjecting them to heat treatment slightly above their T<sub>g</sub> using sinter crystallization technique and new products with superior properties to their parent glasses were achieved.

Ali (2008) developed a low temperature glass-ceramics from local raw materials by sinter crystallization of glass particle compact using heat treatment technique and materials with improved mechanical properties were achieved.

Rezvani *et al* (2005) studied the effect of  $\text{Cr}_2\text{O}_3$ ,  $\text{Fe}_2\text{O}_3$  and  $\text{TiO}_2$  on the crystallization behaviour of glass composition in the system  $\text{CaO-MgO-Al}_2\text{O}_3\text{-SiO}_2$  ( $\text{R}_2\text{O}$ ) using DTA, XRD and SEM, the findings revealed that the concurrent addition of  $\text{Cr}_2\text{O}_3$ ,  $\text{Fe}_2\text{O}_3$  and  $\text{TiO}_2$  was more effective in inducing bulk crystallization in the base glasses. The best nucleation and crystallization temperatures were determined to be  $740^\circ\text{C}$  and  $885^\circ\text{C}$  respectively. The main crystalline phase detected after a two-stage 3 hours heat-treatment at  $740^\circ\text{C}$  and  $885^\circ\text{C}$  was diopside.

Carl and Hoche (2002) reported that glass ceramics based on the ternary system  $\text{SiO}_2\text{-Al}_2\text{O}_3\text{-MgO}$  when nucleated with Titania promoted a phase separation with the formation of various crystalline phases that have a wide range of applications in areas related to ultra high vacuum, high voltage, high thermal stability and good mechanical strength among others.

Partridge *et al* (1989) developed glass ceramics based on the ternary system  $\text{MgO-Al}_2\text{O}_3\text{-SiO}_2$  using zirconia as nucleating agent. After heat treatment, the glass ceramics contained enstatite and tetragonal zirconia as the primary phases assemblage with superior mechanical properties being used as substrates in the electronics industry.

Similarly, Wada and Nimomiya (1995) and Tashiro, (1985) have pointed out that glass ceramics in the ternary system  $\text{SiO}_2\text{-Al}_2\text{O}_3\text{-CaO}$  using titania and zirconia as nucleating agents precipitated wollastonite as the main crystal phase being used as cladding in the building industry.

In a similar manner, Hussain *et al* (2010 ) studied the glass-ceramics in the system MgO-Al<sub>2</sub>O<sub>3</sub>-SiO<sub>2</sub> using magnesium fluoride (MgF<sub>2</sub>) as a nucleating agent and the development of phases assemblage was analyzed by X-ray diffraction (XRD), and the result revealed the precipitation of fluorophlogopite, nobergite and siliminite. Some surface porosity (3-4%) were detected using scanning electron microscope (SEM).

Hao *et al* (2010) studied the effects of replacement of MgO by CaO, on the characterization and crystallization behaviour of glass-ceramics in the CaO-MgO-SiO<sub>2</sub> base glass system. Investigations were conducted using DTA, XRD and FTIR techniques and by density measurements. The results show that the glass transition temperature (T<sub>g</sub>) and crystallization temperature (T<sub>C</sub>) increased and glassy network structure became denser with increasing CaO/MgO weight ratio. After some heat-treatment procedure, the dominant phase assemblage changes from diopside to wollastonite at the replacement of MgO by CaO. Studying the density measurement shows that, the density of glass samples increase by increasing CaO content at the expense of MgO.

Margha *et al* (2009) examined the crystallization behaviour of glass-ceramics rich in nanocrystals and ZrO<sub>2</sub> was incorporated as nucleating agent. The only observed crystal phases were tetragonal and monoclinic zirconia and hardness was found to increase with time and temperature increase.

Leszek (2005) has investigated the MgO-Al<sub>2</sub>O<sub>3</sub>-SiO<sub>2</sub> glass system using TiO<sub>2</sub> as nucleating agent. Disordered structure of glass near the transition temperature T<sub>g</sub>, cluster

nuclei formation and crystal growth were studied. A dendrite aggregate was formed alongside quartz. In addition, after replacement of  $\text{TiO}_2$  by  $\text{ZrO}_2$ , orthosilicate was precipitated.

Zanotto (1981) examined amorphous phase separation in crystal nucleation in spat cooled  $\text{Li}_2\text{O-SiO}_2$  glasses. It was revealed that the crystallization rate increases during the initial stages of primary and secondary phase separation which further emphasizes the role of diffusion zone around the amorphous droplets which act as nucleation sites.

Ping *et al* (2009) investigated the effect of  $\text{ZrO}_2$ ,  $\text{La}_2\text{O}_3$ ,  $\text{CeO}_2\text{Yb}_2\text{O}_3$  and  $\text{V}_2\text{O}_5$  on the crystallization kinetics, microstructure and mechanical properties of mica glass-ceramics using differential scanning calorimetry (DSC), X-ray diffractometry (XRD), scanning electron microscope (SEM) and microhardness. The results revealed that crystal growth was achieved through the incorporation of nucleating agents into the bulk glass and  $\text{ZrO}_2$  and  $\text{V}_2\text{O}_5$  were the best nucleating agents for mica base glass system because microstructure was interconnected which improved machinability and hardness.

Tulyaganov *et al* (2006) examined glass-ceramics based on the  $\text{CaO-MgO-SiO}_2$  system with some amount of additives such as  $\text{Na}_2\text{O}$ ,  $\text{CaF}_2$ ,  $\text{P}_2\text{O}_5$  and  $\text{B}_2\text{O}_3$ , the mixture was prepared and then melted at  $1400^\circ\text{C}$  for 1 hour and quenched in air or water to achieve a transparent bulk or frit glass. Raman spectroscopy revealed that the main constituents of the glass network structure were the silicates. Scanning electron microscopy (SEM) study confirmed liquid-liquid phase separation and that the glasses were prone to surface crystallization. Glass-ceramics were developed through sinter crystallization of glass

powder compacts made of milled glass frit of mean particle size 11-15  $\mu\text{m}$ . Thereafter, densification started at 620-625°C and was almost complete at 700°C. Crystallization occurs at temperature higher than 700°C. Highly dense phases assemblage, dominantly composed of diopside and wollastonite alongside akermanite and residual glassy phase were achieved after heat treatment at 750°C and 800°C. The glass-ceramics prepared at 800°C exhibited bending strength of 116-141 MPa. Vickers microhardness of 4.53-4.65 GPa and thermal expansion coefficient at 100-5.00°C° of  $9.4-10.8 \times 10^{-6} \text{ K}^{-1}$ .

Bing *et al* (2003) studied the effect of the microstructure on the mechanical properties of CaO-P<sub>2</sub>O<sub>5</sub>-SiO<sub>2</sub>-MgO-F<sup>-</sup> glass-ceramics which contains apatite and mica phases assemblage. The resultant glass-ceramics can be used for dental restoration and bone implant due to their biocompatibility and bioactivity respectively. Mechanical properties of glass-ceramics depends on their microstructure. The study in this paper focused on the relationship between the microstructure and the mechanical properties of CaO-MgO-P<sub>2</sub>O<sub>5</sub>-SiO<sub>2</sub> glass-ceramics containing fluorapatite and fluorophlogopite crystalline phases. They were analyzed using DTA, SEM, XRD techniques and some mechanical testing techniques, and the findings revealed that the sample heat treated at 810°C for 4 hours precipitated fluorapatite. The major crystalline phase had smaller crystal size and less volume fraction of fluorophlogopite with higher bending strength and crack toughness of 190 MPa and 2.63 MPa respectively.

Naruporn *et al* (2013) examined SiO<sub>2</sub>-Li<sub>2</sub>O-K<sub>2</sub>O-Al<sub>2</sub>O<sub>3</sub> base glass system to ascertain the effect of glass composition on their crystal formations and properties using P<sub>2</sub>O<sub>5</sub> and CaF<sub>2</sub> as nucleating agents. The findings revealed that P<sub>2</sub>O<sub>5</sub> and CaF<sub>2</sub> served as nucleating sites

for lithium phosphate and fluorapatite to encourage heterogeneous nucleation and produce fine-grained interlocking microstructure of lithium disilicate glass-ceramics.

Hooda *et al* (2012) studied zinc bismuth silicate glasses using conventional melt-quench technique. Density was measured using Archimedes' principle. The findings revealed that when ZnO addition increases progressively in the samples, molar volume and density were found to decrease. Glass transition temperature ( $T_g$ ) as determined by DSC was observed to increase as ZnO addition was increase. Similarly, Raman and FTIR spectra recorded at room temperature showed that in all the glass compositions, asymmetric and symmetric stretched vibrations of Si-O-bonds in  $\text{SiO}_4$  tetrahedral units exist with decrease in  $\text{Bi}_2\text{O}_3$  and this increased glass network connectivity of structure.

Bahman and Behzad (2012b) investigated the effect of  $\text{Al}_2\text{O}_3$  on the crystallization behavior of glass compositions in the  $\text{Na}_2\text{O}$ - $\text{CaO}$ - $\text{P}_2\text{O}_5$ - $\text{SiO}_2$  base glass system. DTA, XRD and SEM were used in the investigation. The density of the glass ceramics samples was measured using Archimedes' principle. It was revealed that the glass-ceramics containing 2 molar percent  $\text{Al}_2\text{O}_3$  had desirable sintering behaviour and reached an acceptable density. Similarly phase investigation and microstructural study were performed using XRD and SEM respectively.

Durrani *et al* (2010) fabricated magnesium alumino silicates glass-ceramics using three stage heat treatment which constitutes calcination, nucleation and crystallization through the incorporation of magnesium fluoride ( $\text{MgF}_2$ ) as nucleating agent. The thermal stability of MAS was measured by thermogravimetry (TG) and Differential thermal analysis (DTA).

Result revealed that the powder exists as MgO-Al<sub>2</sub>O<sub>3</sub>-SiO<sub>2</sub>-H<sub>2</sub>O in solid state and then it transformed to MgO-Al<sub>2</sub>O<sub>3</sub>-SiO<sub>2</sub> through some metastable intermediates above 300°C. The phases assemblage which were analyzed using XRD revealed the presence of wide variety of phases such as nobergite, siliminite, magnesium silicate and fluorophlogopite achieved at various heat treatment temperatures.

## **2.2 Previous Studies**

Since Stookey's discovery of the controlled and catalytic crystallization of base glass, a large volume of works have been undertaken in the area. Researches in this branch have been mainly restricted to glass in systems such as MgO-CaO-SiO<sub>2</sub>-P<sub>2</sub>O<sub>5</sub> (Kokubo *et al.*, 1986), Li<sub>2</sub>O-Al<sub>2</sub>O-SiO<sub>2</sub> (Holand and Beall, 2002), CaO-Al<sub>2</sub>O<sub>3</sub>-SiO<sub>2</sub> (Khater, 2010), CaO-MgO-Al<sub>2</sub>O<sub>3</sub>-SiO<sub>2</sub> (R<sub>2</sub>O) (Rezvani *et al.*, 2005 and Al-Harbi and Khan, 2007) among others. To avoid uncontrolled crystallization, controlled surface crystallization was carried out on these types of glass for systems MgO-Al<sub>2</sub>O<sub>3</sub>-SiO<sub>2</sub> (Mahdavi *et al.*, 2011 and McMillan, 1979). The main phases assemblage present were wollastonite, anorthite, cordierite, spinel, forsterite and monticellite (Khater, 2010). The choice of raw materials for production of glass-ceramic materials is vital. A wide variety of local raw materials are being increasingly utilized for the production of glass-ceramic materials (Khater, 2012). Therefore, local raw materials such as feldspar, limestone and magnesite have the potentials for used successfully in the production of glass-ceramics by controlled nucleation and crystallization processes.

## **2.3 Starting Materials for Making Glass**

The starting materials for the manufacture of base glass come from mined minerals and rocks that are selected for their purity or stable composition, or those that may be beneficiated to a suitable product. The relatively low cost of glass as a material is based on the fact that raw materials are plentiful, easy to obtain and low in cost. Typical compositions of some glass making raw materials and their oxides are as follows; Silica sand ( $\text{SiO}_2$ ), limestone ( $\text{CaO}$ ), Soda ash ( $\text{Na}_2\text{O}$ ), feldspar ( $\text{Na}_2\text{O}-\text{Al}_2\text{O}_3-6\text{SiO}_2$ ,  $\text{CaO}-\text{Al}_2\text{O}_3-2\text{SiO}_2$  and  $\text{K}_2\text{O}-\text{Al}_2\text{O}_3-6\text{SiO}_2$ ), Dolomite  $\text{CaCO}_3-\text{MgCO}_3$ , Borax ( $\text{B}_2\text{O}_3$ ) and Salt cake ( $\text{Na}_2\text{SO}_4$ ) among others (Alexis and David, 1979).

### **2.3.1 Silica sand ( $\text{SiO}_2$ )**

Silica makes up about three-fifths of the rocks of the earth. Great amounts of silica exist in combined state in the form of silicates taken from feldspar and talc or free silica in the form of quartz, sand and flint. Other vast quantities of quartz may be found in the sands of the seashore, or of sandy soils, or river beds mingled with other minerals and its so impure that no amount of beneficiation could ever separate pure silica from impurities (Alexis and David, 1979). The free silica has a much greater thermal expansion than combined silica. The three principal crystalline forms of silica include; quartz, tridymite and cristobalite and the highest amount of silica is found in the reacted form in alumino silicates (El-Meliegy and Richard, 2012).

Pure silica is sourced generally from quartz sands and frequently occurs in a glassy fused form which is preferable to fused silica. It has a very low thermal expansion coefficient. Thus, fused glassy silica has a high thermal shock resistance compared with crystalline silica. The three forms of silica namely quartz, tridymite and cristobalite have the same chemical formula ( $\text{SiO}_2$ ), but differ in their crystal structures. Silicon and oxygen atoms are

less closely packed in tridymite and cristobalite than in quartz. Therefore, tridymite and cristobalite show a lower specific gravity of 2.32 and 2.28 respectively when compared to 2.65 for quartz (El- Meliegy and Richard, 2012). In addition, cristobalite and tridymite phases are formed at higher temperatures. Quartz is a stable phase form up to 870° C. Tridymite is a stable phase between 870°C and 1,479°C, while cristobalite is stable phase between 1470°C and 1710°C, above 1710°C, silica is exposed to fusion resulting in glassy fused silica form. The changes occurring from one crystalline form to another form are very slow and reversible and the formation of tridymite from quartz or cristobalite may not occur in the absence of fluxing agents like oxides of lithium, sodium, or calcium in conjunction with aluminium (Alexis and David, 1979). Silica is a major glass former in commercial oxide glasses because the vast bulk of commercial glasses are based on silica, which will readily form single component glass (Shelby, 2005). Number one glass sand should have not less than 99.5 percent silica, not more than 0.3 percent alumina ( $Al_2O_3$ ), less than 0.1 per cent lime ( $CaO$ ) and magnesia ( $MgO$ ), and less than 0.025 percent iron (III) oxide ( $Fe_2O_3$ ). Moisture will be negligible, and any other oxides not mentioned above will be found only in traces. Similarly, the grains size distribution will be sufficient to pass through a 20-mesh screen (Alexis and David, 1979; Samuel, 1991 and Shelby, 2005).

### **2.3.2 Feldspar**

Feldspars are the most abundant rock-forming minerals that make up 60% of the earth's crust, and all the rock-forming feldspars are alumino-silicate minerals but oxides of Potassium, sodium and calcium are also present and one of these oxides is usually dominant. Infact, it is the proportion of these three oxides that help determine which specific feldspar is Formed (Michael, 2002). The common feldspars include potash

feldspar ( $K_2O-Al_2O_3-6SiO_2$ ), which is characterized by straight fracture and a variety of crossed, hatched, twinned orthoclase known as microcline ( $K_2O-Al_2O_3-6SiO_2$ ). Similarly, soda feldspar ( $Na_2O-Al_2O_3-6SiO_2$ ) is called albite and lime feldspar ( $CaO-Al_2O_3-2SiO_2$ ) is known as anorthite or plagioclase and this type of feldspar exhibits oblique fracture (James, 2006).

These three feldspar groups are named on the basis of K, Na and Ca content in each case. Potash and soda feldspars occur as major constituents of common igneous rocks as pegmatite, granite, syenite and feldspar porphyry among others (Immo, 1998). These feldspars crystallize from magma as intrusive and extrusive igneous rocks and they are present in many types of metamorphic and sedimentary rocks. Plagioclase feldspars lack potassium, they are light colour and are usually striated but potash feldspar has three polymorphs as follows; Microcline, orthoclase and Sanidine (Michael, 2006). The three polymorphs are almost identical in physical properties and chemical composition and sometimes it is impossible to distinguish one from another without X-ray analysis. They only differ in crystal arrangement as the key difference is between structures and the randomness of the aluminium and silicon atoms. In microcline, the ions are ordered and this produces the lower symmetry of triclinic. At high temperatures, the position of the aluminium and silicon become more ordered and produce the monoclinic symmetry of orthoclase and Sanidine. Microcline is a stable structure at very low temperature of about  $400^\circ C$  which crystallizes into triclinic system and exhibits lamellar twinning as its common feature (Hassan *et al.*, 2012).

Similarly, orthoclase is stable between 500°C and 900°C, it crystallizes into monoclinic and demonstrates striation as its common feature. Sanidine also being the polymorph of potash feldspar is stable above 900°C. Commercial feldspars are group minerals sourced from pegmatite which include; albite or soda feldspar ( $\text{Na}_2\text{O}-\text{Al}_2\text{O}_3-6\text{SiO}_2$ ), orthoclase or potash feldspar ( $\text{K}_2\text{O}-\text{Al}_2\text{O}_3-6\text{SiO}_2$ ). Although, lime feldspars ( $\text{CaO}-\text{Al}_2\text{O}_3-2\text{SiO}_2$ ) or anorthite or plagioclase are not common in pegmatite and do not constitute source of commercial feldspars (Hassan *et al.*, 2012). Commercially, the most important members of the feldspar family are the potash feldspars such as microcline, orthoclase and soda feldspars.

35% of the World feldspar production is used in glass industry, 60% in ceramics industry and 5% in rubber, paint, plastic, welding electrodes filling material (Hassan *et al.*, 2012). The total reserve of the World is  $1.740 \times 10^6$  metric tons and the bulk of this reserve is found in Asia. Turkey has a reserve of 14% of the World feldspar reserves and it has the largest sodium feldspar reserves among other countries in the World (Ali *et al.*, 2010). Feldspar is a vital ingredient for use in the manufacture of all types of glassware. The mineral is composed of silica, alumina, potash, soda and small quantities of lime, all of which are essential compounds used in the production of glass. Alumina is the important component of feldspar and the best medium for introducing alumina to glass batches is by the use of feldspar which is the most economical and efficient method.

In glass industry, feldspar is the major source of silica sand and alumina. Feldspar is used in varying proportions containing 10 to 15 % of the batch. It valued for two purposes in

glass making, it acts as a fluxing material which prompts faster melting and energy savings and the alumina content aids in eliminating non bridging oxygen formation caused by modifying oxide such as CaO, Na<sub>2</sub>O among others (El-Meliegy and Richard, 2012). Alumina promotes network connectivity of glass structure by increasing viscosity and elastic modulus of melt and this result in lowering of thermal expansion coefficient, improves mechanical properties such as hardness and strength, provides excellent chemical durability, prevents devitrification, scum and weathering, greater transparency, chemically stable against most environments except hydrofluoric acid and some molten salts in oxide glasses (Shelby, 2005).

In the manufacture of high quality colourless glass, feldspar should have a maximum of 0.03% Fe<sub>2</sub>O<sub>3</sub>, although up to 0.1% iron oxide is tolerable (Alexis and David, 1979). The presence of iron oxide in the batch composition is very objectionable because its presence even in minute quantity tends to colour the glass (Michael, 2002; Shelby, 2005 and El-Meliegy and Richard, 2012). Therefore, feldspar must be carefully watched to avoid contamination of other oxides.

### **2.3.3 Magnesite**

Magnesite is a natural ore known as magnesium carbonate with a chemical formula (MgCO<sub>3</sub>) and occurring as primary mineral in igneous and sedimentary rocks (Bron *et al.*, 1962). Magnesite is a vital industrial material composed of 47.8 percent magnesia (MgO) and 52.2 percent carbon dioxide (Aslani *et al.*, 2010). It occurs in hydrothermal veins and sea deposit. Furthermore, it has been estimated that 6 percent to 8 percent of the earth's

crust is magnesite and is the third most abundant mineral found in sea water (Abali *et al.*, 2006). Magnesite has the same crystal structure as calcite and also many properties of magnesite are similar to those of calcite. However, the best means of distinguishing magnesite from calcite is that the carbonate ion in magnesite does not react with cold acids; it occurs predominantly as cryptocrystalline particles 1-5  $\mu\text{m}$  in size and occurs commonly in rhombohedra crystals (Yehia and Al-Wakeel, 2013).

Magnesite is the most common source of magnesia and serves a wide spectrum of applications such as high temperature liners for glass, iron- steel, ceramics kilns, fertilizer, binder in flooring material, catalyst and fillers in synthetic rubber production, it is the basic raw material for the manufacture of alkaline refractory, paper industry, paint and ink, pharmaceutical as an anti acid and in the production of numerous magnesium chemicals (Abdel-a'al *et al.*, 1994; Abali *et al.*, 2006 and Amer, 2010).

In glass industry, magnesite is used in varying proportions ranging from 2.0 -12.0 wt% of the batch compositions (Doyle, 1979). The principal functions of magnesite in glass production are as follows; chemical durability and temperature stability, brilliancy and smoothness to glass, lowers thermal expansion coefficient, improves strength and decreases dimensional changes among others (Shelby, 2005). In addition, Magnesite contains varying amounts of impurities including silica, iron, aluminum, manganese, and calcium, usually present in the form of various minerals, for example, quartz, talc, mica and magnetite.

#### **2.3.4 Barium carbonate ( $\text{BaCO}_3$ )**

Baryte ( $\text{BaCO}_3$ ) is a white powder and a form of earthy base available for use in glass making. It can be used to replace lime and lead oxide with similar results. Barium carbonate is a very powerful flux in glass at high temperature because it has the lowest melting point of all alkaline earth metals. It gives increased brilliancy and little coloration. For this reason, it is useful in the manufacture of pressed glassware, giving a glass better gloss or luster than is found to be the case with lime glasses and lead crystal glasses and also imparts better translucency in glass-ceramics (El-Meliegy and Richard, 2012).

### **2.3.5 Limestone ( $\text{CaCO}_3$ )**

Limestone is a sedimentary rock which is formed through accumulation of sediments in air or water. Calcite ( $\text{CaCO}_3$ ) has been the dominant mineral alongside quartz ( $\text{SiO}_2$ ) present in limestone. In addition, the primary oxide present in limestone is calcium oxide ( $\text{CaO}$ ) alongside other impurities like iron ( $\text{Fe}_2\text{O}_3$ ) among others (Ryemshak *et al.*, 2012). Limestone majorly serves as source of  $\text{CaO}$  in glass. The function of lime in the glass is to act as a stabilizing material, to provide chemical stability and in conjunction with soda ash it forms glass by uniting with sand. In addition, lime imparts smoothness and brilliancy to glass and increases its power of resistance to chemical attack. The role of lime in glass is to render it more insoluble so that it can be used in contact with water or materials containing water. It also increases melt ability and hardness as well as prevents cords formation (Alexis and David, 1979).

## **2.4 Crystallites**

Polycrystalline materials are solids that are composed of a wide range of crystallites of varying size and orientation. Crystallites are also known as grains and they are microscopic crystals formed during the cooling of numerous materials. Their orientation can be

random with no preferred direction, known as random texture possibly due to growth and processing conditions. The areas where crystallite grains meet are called grain boundaries. Most inorganic solids are polycrystalline including ceramics, metals among others. Structure of a monocrystalline crystal is highly ordered and its lattice is continuous and unbroken. Amorphous material such as glass is noncrystalline and do not exhibit any structures as their constituents are not arranged in an ordered manner. Polycrystalline material contains crystals but there is no relationship between neighbouring crystal grains.

## **2.5 Nature of Glass**

Glass is an amorphous solid completely lacking long range, periodic atomic arrangement and exhibits a region of time dependent glass transformation behaviour (Shelby, 2005). Glass structure is not at equilibrium because it is obtained when a liquid is cooled down in such a way that on passing the melting temperature or liquidus temperature ( $T_L$ ), freezing occurs in lieu of crystallization (Rappensberger, 1996). Glass has a frozen liquid-like structure showing only short-range orders which distinguish it from crystalline structure that exhibits long-range order, a periodic atomic arrangement with repetition of a unit cell. Upon reheating, glassy material slowly and continuously decreases in viscosity and revert to its former mobile state in the absence of definite melting point (Mahmud, 2007).

Therefore, the final temperature must be so slow that molecules or atoms move too slowly to rearrange to the more stable crystalline form (Eric, 2008). Glassy material is frozen in structure exhibiting short range order which makes its characterization quite difficult when compared to crystalline structure that exhibits long-range order. Molten glass has the ability to slowly adjust the structure upon cooling to rigid condition without crystallizing. However, upon reheating, they gradually decrease in viscosity and revert to the former

mobile state without any defined melting point. Thus, they can be formed using high-speed manufacturing techniques such as blowing, casting, rolling, pressing, drawing, spinning and can be manipulated to a wide range of shapes using traditional flame, sagging and fire-polishing techniques (Casasola and Rincon, 2002; Mahmud, 2007; Park, 2008; Daniela *et al.*, 2010 and Rezvani, 2011). Inorganic glasses can be made from a wide variety of composition like silicates, borates, aluminates, phosphates, halides, chalcogenide among others. However, the vast bulk of glasses used in commerce are oxide glasses. It is assessed that 95% are silica-based glasses (Casasola and Rincon, 2002; Mahmud, 2007 and Park, 2008).

Oxides that can form glass on their own are known as glass formers example include;  $\text{SiO}_2$ ,  $\text{GeO}_2$ ,  $\text{B}_2\text{O}_3$  among others, and those oxides that practically lack the ability to form glass include;  $\text{MgO}$ ,  $\text{CaO}$ ,  $\text{BaO}$ ,  $\text{K}_2\text{O}$ ,  $\text{Na}_2\text{O}$ ,  $\text{Li}_2\text{O}$  and they are described as modifying oxides. On one hand modifying oxides introduce non bridging oxygen to the glass network structure which become increasingly destabilized but on the other hand, they are useful modifying components because they are useful in improving nucleation and crystal growth in the course of crystallization process (Shelby, 2005 and El-Meliegy and Richard, 2012). Oxides such as  $\text{CaO}$ ,  $\text{MgO}$ ,  $\text{BaO}$  are known as alkaline earth oxides or stabilizing agents, they impart to the glass excellent chemical durability and transparency among others. Alkali oxides like  $\text{Li}_2\text{O}$ ,  $\text{Na}_2\text{O}$  and  $\text{K}_2\text{O}$  are important fluxing agents because they help in reducing the melting temperature of glass forming melts (Rappensberger, 1996 and El-Meliegy and Richard, 2012). Generally, silicate glasses are inexpensive and naturally occurring, they have excellent transparency and high chemical resistance. Silicate glasses

are elastic and exhibit brittle failure as no plastic deformation occurs before fracture and the material can be reassembled to the original shape (Case *et al.*, 1999 and Shelby, 2005).

### **2.5.1 Glass Forming Melts**

Inorganic glasses are made through the incorporation of a wide range of starting materials chiefly oxides, chalcogenides, metallic, halides among others (Lewis, 1989 and Shelby, 2005). Zachariasen (Shelby, 2005) proposed that the structure of glass was similar to that of a crystal, but with a larger lattice energy resulting from the disordered arrangements of polyhedral units, to possess a random network lacking long-range periodic order, he listed four conditions for a structure to favour the formation of glassy material, as follows; an oxygen or anion must not be linked to more than two cations; the number of oxygen or anions coordinated to the cations must be small, typically three or four; the cation-anion polyhedral must share corners rather than edges or faces; and at least three corners must be shared in order to form three dimensional network (Mahmud, 2007). These conditions result in the formation of open structures that can accommodate a distribution of interpolyhedral bond angles that are associated with the loss of long-range structural order when a crystal form a glass. In addition, X-ray diffraction studies confirms that glasses and crystals possess similar short-range polyhedral structures but different long-range polyhedral arrangements. Oxides that do not possess the open network structures of the glass-forming oxides are classified as network modifiers or intermediate oxides, depending on their structural roles. In addition, oxides with large coordination numbers and relatively weak bonds are known as network modifiers and they alter the glass-forming network by replacing stronger bridging oxygen (BO) bonds between glass-forming polyhedral with weaker, non bridging oxygen (NBO) bonds to modifying polyhedral. The network

modifiers are vital constituents to glassy materials because they decrease the melting temperature and control many useful properties. The intermediate oxides have coordination numbers and bond strengths between the network formers and network modifiers and tend to have an intermediate effect on glass properties (Rappensberger, 1996; Salama *et al.*, 2002 and Mahmud, 2007).

### **2.5.2 Structure of silicate glass**

Goldschmidt's radius ratio criterion and Zachariasen's random network theory are the two main theories on glass formation, both of which have been thoroughly investigated and for both of which a great deal of information is known. Regarding Goldschmidt's, in the early 1920's he proposed a rule for the formation of glass based on the knowledge about glass forming oxides such as  $\text{SiO}_2$ . He stated that if an oxide is expressed as  $X_mY_n$ , the ratio of the ionic radii of the atom X and the atom Y,  $r_X/r_Y$  needs to be between 0.2 and 0.4 for glass formation. This implies the tetrahedral coordination of the glass forming cation.

Zachariasen on the other hand defined a glass as a substance that can form an extended three-dimensional network that is lacking periodicity with energy content comparable with that of the corresponding crystal network and summarized the basic rules (1,2,3 and 4) for glass formation in simple oxides as well as modified rules (5,6 and 7) for complex glasses respectively, which have been developed during extensive utilization of forming a continuous 3-dimensional glass network. These rules are as follows:

1. Each oxygen atom is linked to no more than two cations.
2. The oxygen coordination number of the network cation is small.
3. Oxygen polyhedral share only corners and not edges or faces.

4. At least three corners of each oxygen polyhedron must be shared in order to form 3D network.
5. The sample must contain a high percentage of network cations which are surrounded by oxygen tetrahedral triangles.
6. The tetrahedra or triangles share only corners with each other.
7. Some oxygens are linked only to two network cations and do not form further bonds with any other cation.

The structure of silica glass contains a well-defined  $\text{SiO}_4$  tetrahedra connected to another neighbouring tetrahedron through each corner. Figure 2.1 shows structures of silica tetrahedron ( $\text{SiO}_4$ ) versus its corresponding crystalline form. Figure 2.2 displays Schematic two-dimensional (2D) representation of the silica random network built by  $\text{SiO}_4$  tetrahedra: (a) crystalline structure (or long-range order), (b) random network or glass. Figure 2.3 presents the structure of vitreous silica which is composed of (a) basic building block, the  $\text{SiO}_4$  tetrahedron (corner spheres denote Oxygen and the central sphere silicon), which forms (b) a 3D noncrystalline network of fully connected tetrahedra. Figure 2.4 demonstrates that the basic unit is a silicon atom (small circle) surrounded by four oxygens (large circles), bridging oxygens are open circles and non-bridging oxygens are filled circles. Figure 2.5 has revealed the neutron diffraction studies which indicated that the Si-O distance in the  $\text{SiO}_4$  tetrahedron is 0.162 nm and that the shortest O-O distance is 0.265 nm, the same dimensions are found in crystalline silica (Mahmud, 2007). The intertetrahedral Si-O-Si bond angle distribution is centered near  $144^\circ$ , but is broader than that found for crystalline silica, producing the loss in long-range order. Similarly, the O-

Si-O bond angle distribution is centered around  $109.5^\circ$ . Figure 2.5 depicts the basic tetrahedral units in silicate glasses .

## **2.6 Preparation of Glass**

Glasses are made by fusion of raw materials termed batch at sufficiently high temperature to allow stable reaction and escape of gas bubbles from the molten glass. Most glass batches melt homogeneously at higher temperature between  $1450^\circ\text{C}$  and  $1600^\circ\text{C}$  and homogeneity is achieved when the starting materials are pure since small amount of impurity could largely affect the crystallization kinetic of the base glass (Shelby, 2005). Glass-based systems are made from materials that contains mainly silica with varying quantity of alumina. Naturally occurring alumino silicates contain varying proportions of alkali oxides such as sodium oxide ( $\text{Na}_2\text{O}$ ), calcium oxide ( $\text{CaO}$ ) potassium oxide and are termed feldspar ( $\text{K}_2\text{O}$ ) (Russell and Edward, 2010).

### **2.6.1 Shaping of Glass**

When melting is completed, there is need to cool molten glass to the working range at relatively higher viscosity. At this temperature, a wide range of forming techniques can be employed such as blowing, casting, pressing, drawing, rolling to shape the glassy material to a desired shape (Lewis, 1989 and Mahmud, 2007).

### **2.6.2 Transition Temperature ( $T_g$ ) of Glass Samples.**

Thermal analysis is a powerful tool utilized for detecting and analyzing the glass transition temperature of glasses (Shelby, 2005). Glass transition temperature can be defined as an approximate temperature where the supercooled molten glass converts to a solid or rigid

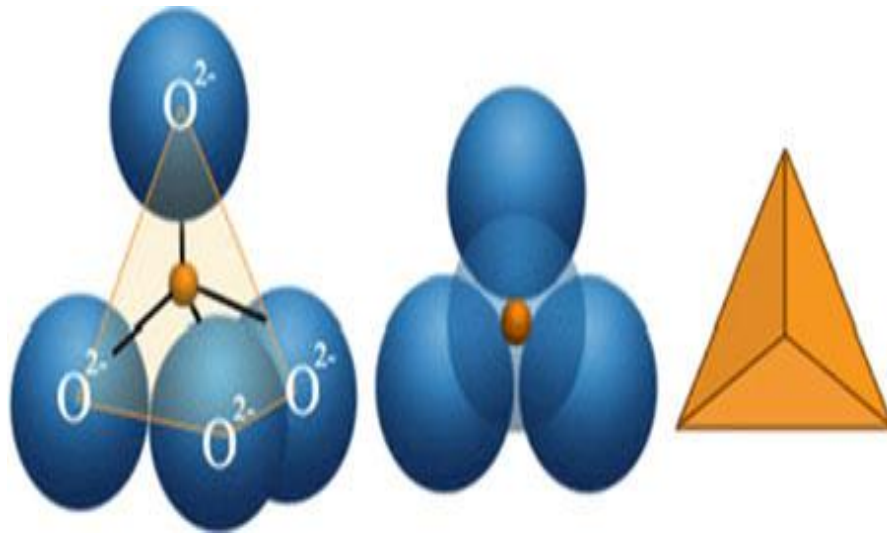
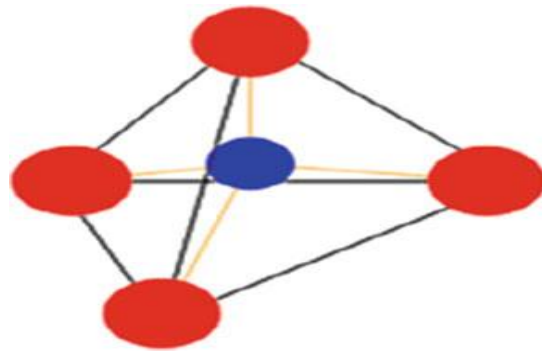
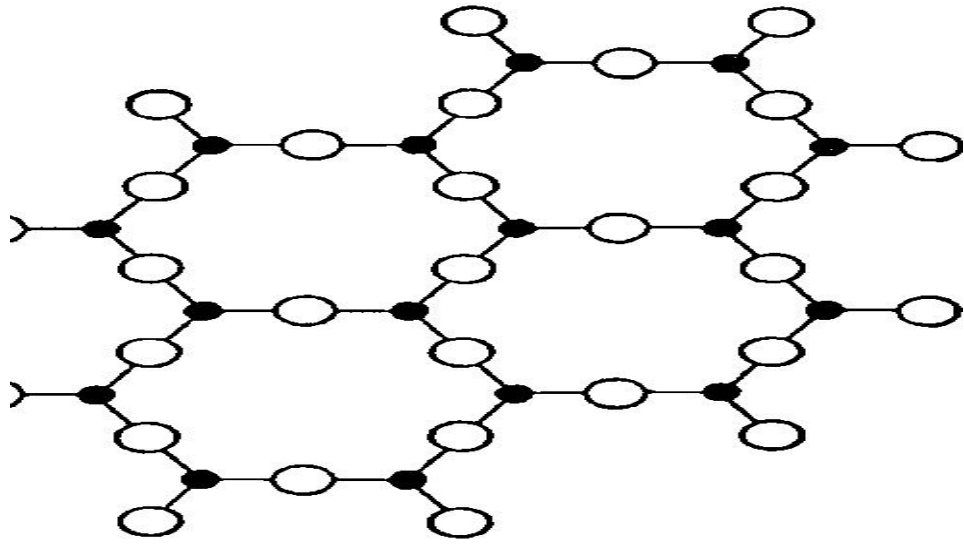
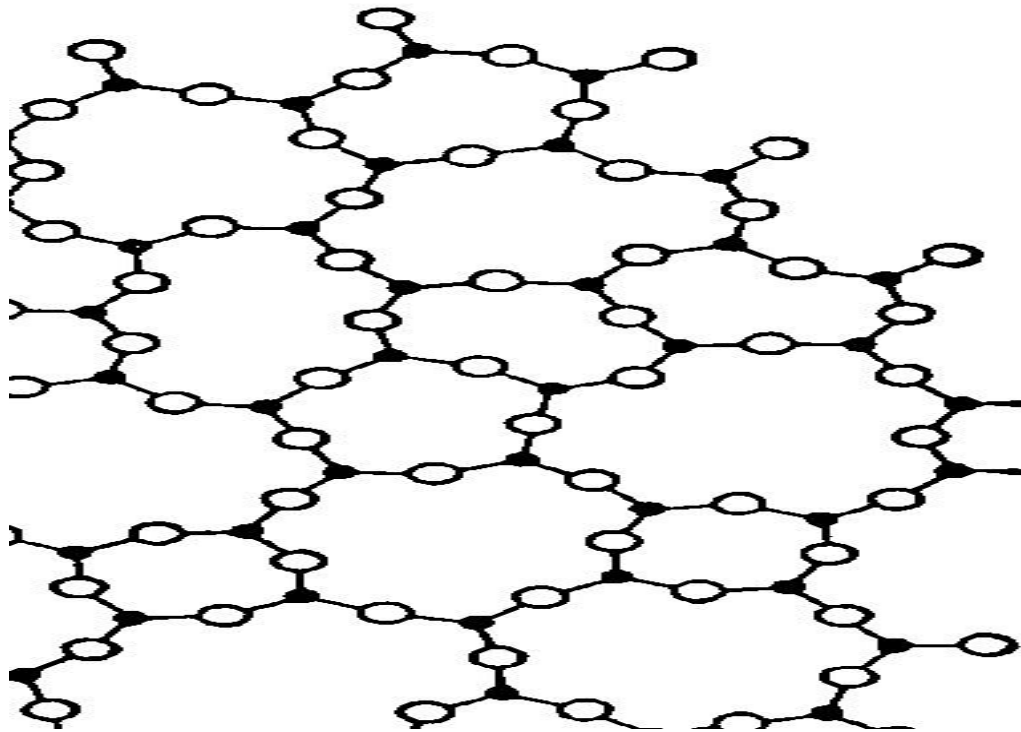


Figure 2.1: Structure of Silica Tetrahedron ( El-Meliegy and Richard, 2012)

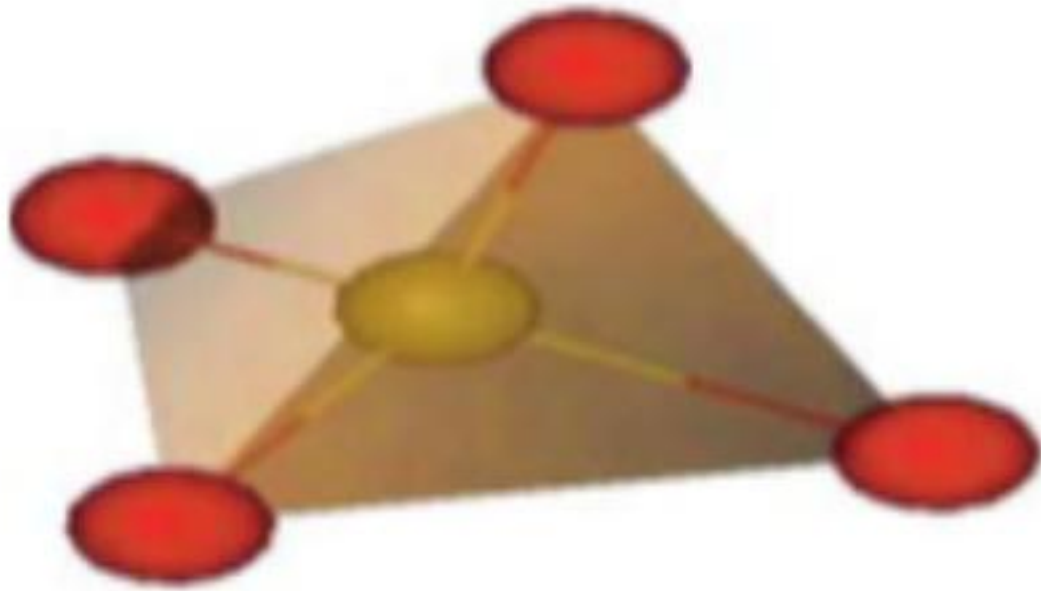


(a)

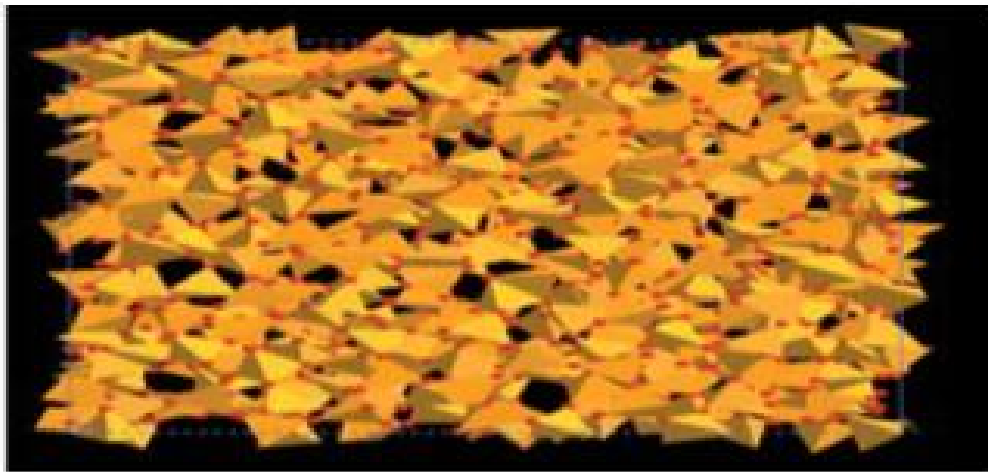


(b)

Figure 2.2: Schematic two- dimensional (2D) representation of the silica random network built by  $\text{SiO}_4$  tetrahedra: (a) crystalline structure (long-range order), (b) random network (glass) ( Harper, 2001).



(a)



(b)

Figure 2.3: The structure of vitreous silica is composed of a (a) basic building block, the  $\text{SiO}_4$  tetrahedron (corner spheres denote Oxygen and the central sphere silicon), which forms (b) a 3D noncrystalline network of fully connected tetrahedral (Shackleford and Doremus, 2008).

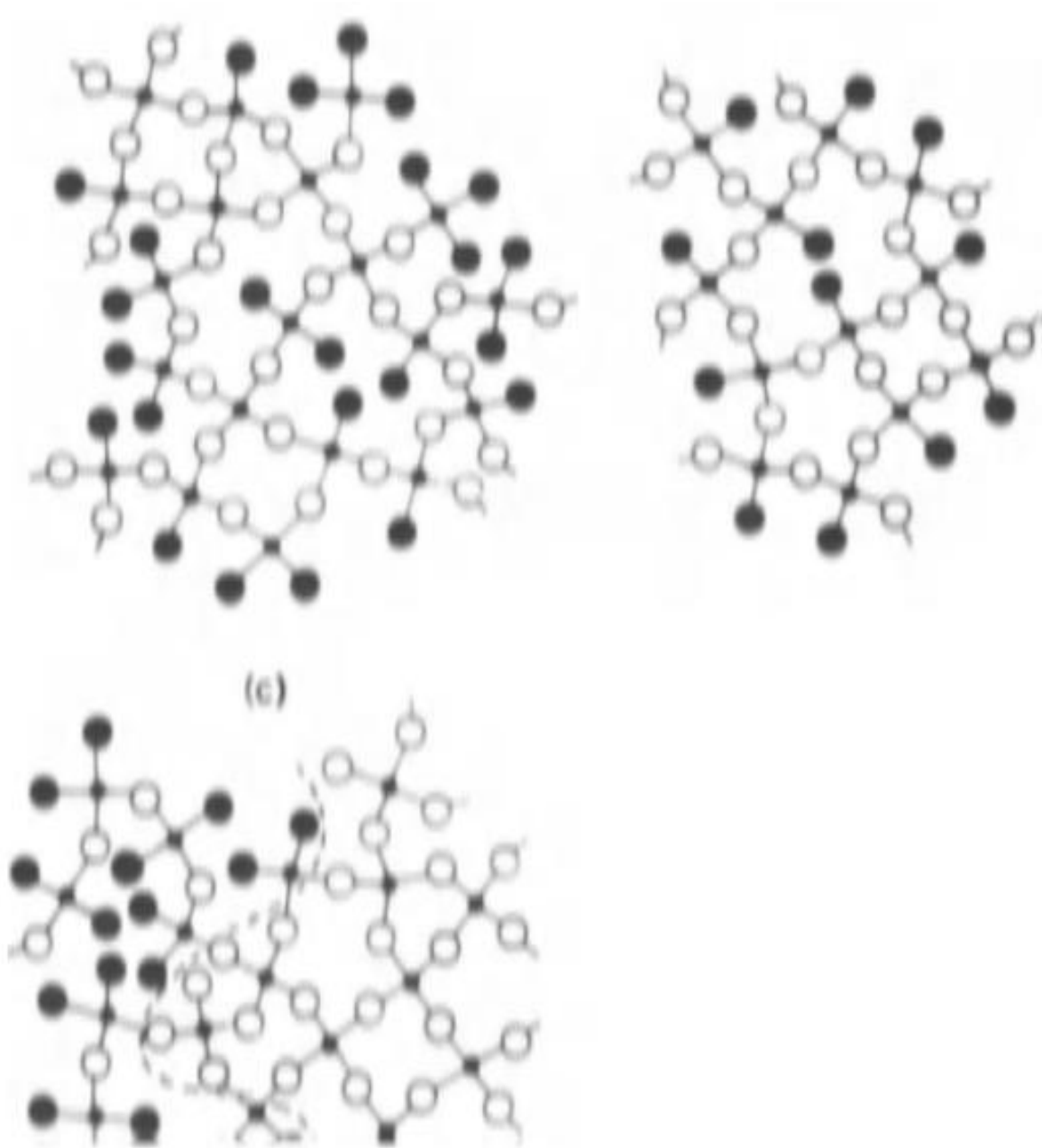


Figure 2.4: The basic unit is a silicon atom (small circle) surrounded by four oxygens (large circles) Bridging oxygens are open circles and non-bridging oxygens filled circles. (Lewis, 1989)

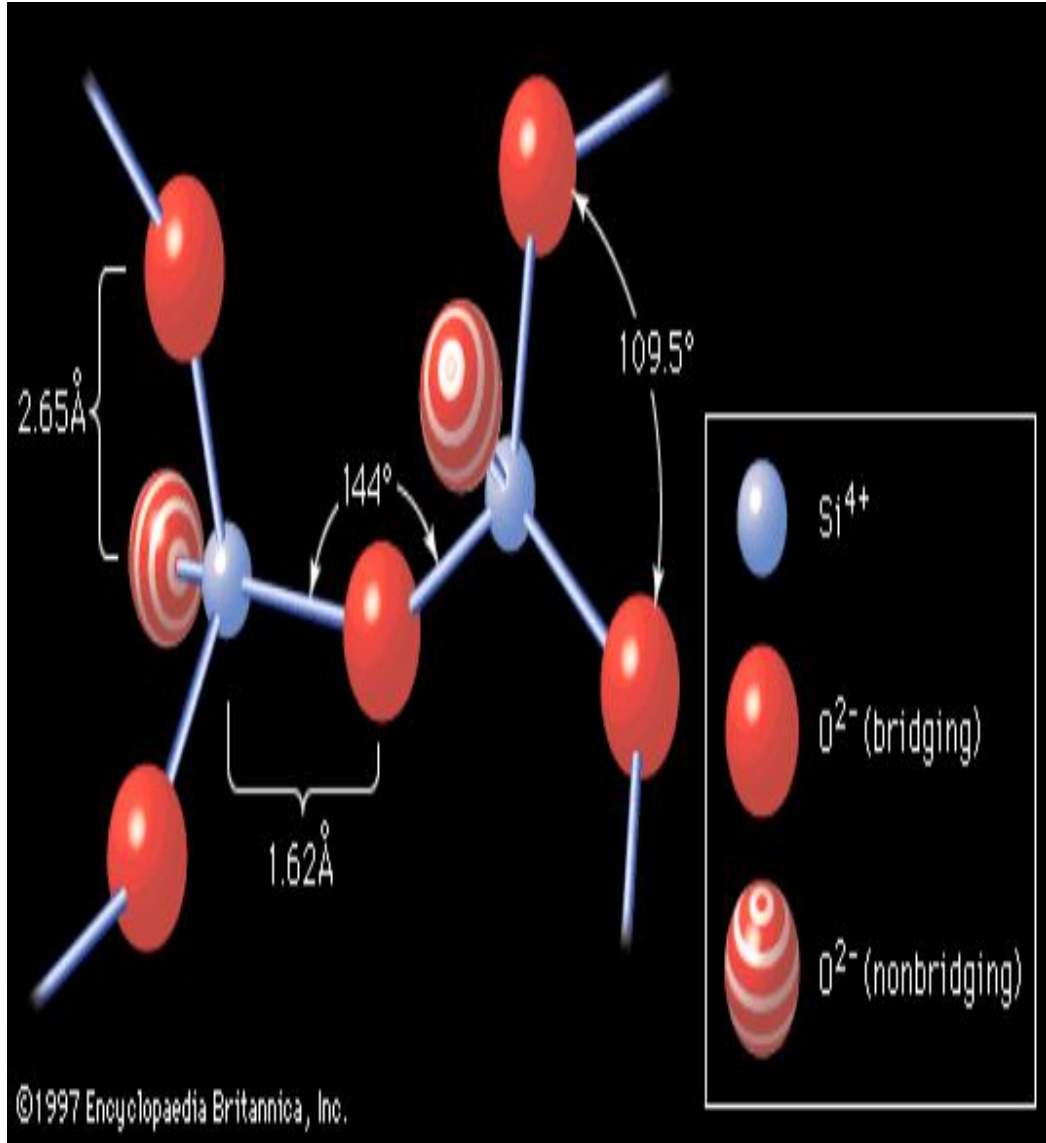


Figure 2.5: Basic Tetrahedral Units in Silicate Glasses (Kartalia, 2010)

glass on cooling or where the solid glass begins to behave as viscoelastic solid on reheating (Mahmud, 2007).

## 2.7 Base Glass Composition and Crystallization

The findings of great deal of researchers have revealed that there are considerable chemical and mineralogical compositions that could be made into glasses and subsequently heat treated and then transformed into crystalline materials (Mahmud, 2007). It has been observed that glass-ceramics are either alkali or alkaline earth alumino silicates, notable among which are lithium-alumino- silicates ( $\text{Li}_2\text{O}-\text{Al}_2\text{O}_3-\text{SiO}_2$ ). This category of glass-ceramics have zero coefficient of thermal expansion and high thermal shock resistance as well as excellent chemical durability and is a potential candidate for household applications particularly cookware. Conversely, Sodium- alumino-silicates ( $\text{Na}_2\text{O}-\text{Al}_2\text{O}_3-\text{SiO}_2$ ), potassium-alumino-silicates ( $\text{K}_2\text{O}-\text{Al}_2\text{O}_3-\text{SiO}_2$ ) and Barium-sodium-alumino-silicates ( $\text{BaO}-\text{Na}_2\text{O}-\text{Al}_2\text{O}_3-\text{SiO}_2$ ) have high coefficient of thermal expansion and low mechanical properties, although such can be strengthened through surface compression techniques (Kon *et al.*, 1994). In addition, magnesium-alumino-silicates ( $\text{MgO}-\text{Al}_2\text{O}_3-\text{SiO}_2$ ) have high bending strength, high resistance to abrasion and surface hardness, and low coefficient of thermal expansion (Leszek, 2005 and Khater, 2010). Glass-ceramics based on the calcium-magnesium-alumino-silicate ( $\text{CaO}-\text{MgO}-\text{Al}_2\text{O}_3-\text{SiO}_2$ ) base glass system that is developed from alkaline-earth alumino silicate which use natural rocks and slags as starting materials has been painstakingly investigated. Crystalline phases such as diopside, wollastonite, cordierite, anorthite and mellite among others have been crystallized from the base glasses using controlled heat treatment resulting in glass-ceramics with attractive

mechanical properties, high abrasive-wear and surface hardness as well as high chemical durability which are the most valuable characteristics of such pyroxenic glass-ceramic. (Carl and Hoche, 2002; Tulyaganov *et al.*, 2002; Mohammed *et al.*, 2003; Tomohiro *et al.*, 2004; Alexander and Mario, 2006; Mahmud, 2007; Khater, 2010; Daniela *et al.*, 2010; Kaya *et al.*, 2011 and Bahman and Behzad, 2012a).

## **2.8 Basic Principles of Crystallization**

Crystallization is the precipitation of crystals from a melt in which nuclei are formed and then grow with time (El-Meliegy and Richard, 2012). In glass, crystallization commences from a distinct site and crystal growth occurs through deposition of material upon the tiny particles termed nuclei (El-Meliegy and Richard, 2012). The crystallization process involves nuclei formation and subsequent crystal growth. The crystallization of glass is controlled by the rate of these processes namely the nucleation rate that is the number of nuclei formed in a unit volume per unit time, and the rate of crystal growth which is the velocity of the crystalline interface in the glassy mass (Holand and Beall, 2002).

Crystallization can be on the surface or bulk (volume) depending on the mechanisms of formation. In the case of surface crystallization, the crystals would nucleate at the glassy interface initiated by surface heterogeneities such as surface flaws, dust particles among others. As a result of the low density of nuclei formed on the surface, coarse-grained large crystalline microstructure might result, which often compromises the mechanical properties of the resultant glass-ceramics (Rappensberger, 1996; El-Meliegy and Richard, 2012). However, a wide range of glass-ceramic products have been crystallized using surface crystallization, these products include glass-ceramics matrix composites developed by sinter-crystallization of large specific surface area glass frits (Gadkaree, 1991;

Wadsworth and Stevens, 1992; Lewis, *et al.*, 1993 and Salama *et al.*, 2002) as well as multilayer packaging (Knickerbocker *et al.*, 1993). Furthermore, surface crystallization improves glass strength by making the surface flaws inoperative through the provision of a surface compressive layer (Antti, 2012). In the case of bulk (volume) crystallization, the crystal growth initiates from nucleation sites within the molten glass. When crystallization is started by foreign materials onto the bulk of glass, such nucleation is termed heterogeneous nucleation whereas homogeneous nucleation occurs when the constituents of the nuclei are the same as the bulk of the glass (Mohammed *et al.*, 2003).

## **2.9 Heat Treatment of Glass**

The nucleation and crystal growth which are pertinent for the conversion of base glass into glass-ceramics are induced by thermal treatment schedule. The rates of nuclei formation and crystal growth are usually controlled in the course of heat treatment (Holand and Beall, 2002).

The crystallization of glass into glass-ceramics is usually guided by thermal analysis data. The heat treatment transforms the glassy material into uniform crystalline glass ceramics with properties that are superior to the base glass and the development of uniform microstructural configuration which results in improving the strength that tailored a wide variety of desirable properties (Mahdavi *et al.*, 2011 and Khater, 2012). The central idea behind a favourable heat treatment schedule is the development of a given nuclei population from their initial size to their final size as rapidly as possible (Michael, 1992; El-Meliegy and Richard, 2012).

Efficient nucleation causes the formation of dense small crystals rather than small numbers of large crystals which is the main target of glass-ceramics (El-Meliegy and Richard, 2012). For this reason, there is need to raise the temperature of the glass nuclei so as to allow crystal growth on the developed nuclei. This is achieved at a carefully controlled heating rate in order to avoid glass-ceramics deformation during crystallization (El-Meliegy and Richard, 2012). If the rate of heating is too high, the rate of crystal growth may not be sufficiently rapid and this could result in glass deformation. In contrast, if the rate of heating is low, deformation may not occur as the residual glassy phase decreases progressively on temperature increase (Lewis, 1989 and Garza-Garcia *et al.*, 2007).

The transition temperature ( $T_g$ ) is the temperature in which molten glass (supercooled glass) transforms into an amorphous solid. The optimum nucleation temperature is estimated to be close to the annealing point of a glass. Therefore, glass should be nucleated by heat treating the glass to a temperature slightly higher than the glass transition temperature (Holand and Beall, 2002). The most favourable nucleation temperature generally exists at temperature range between the transition temperature ( $T_g$ ) and a temperature somewhat 100°C above  $T_g$ , and this range corresponds to the glass viscosities of  $10^{12} - 10^{14}$  poises (Shelby, 2005). The crystal growth should immediately follow the nuclei formation. During nuclei formation, the temperature of the glass should increase at a heating rate sufficiently slow to allow crystallization process. The slow heating rates ensures safe maturing without forming undesirable deformation. Therefore, the heating rate should not exceed 5°C/min so as to avoid deformation of glassy material (El-Meliegy and Richard, 2012).

The crystal growth of some glasses can be achieved slightly above the nucleation temperature, and to achieve crystal growth, the temperature may be elevated by more than 300°C above the nucleation temperature. The crystal growth temperature for glass-ceramics is selected such that maximum crystallization can be achieved without deformation. The temperature at which glass-ceramics starts to deform corresponds to the melting temperature (liquidus) of the dominant phase assemblage (El-Meliegy and Richard, 2012).

### **2.10 Nucleation and Crystal Growth**

The scientific basis of the supercooled liquids was discovered by Tammann in 1903 (Holand and Beall, 2002), but it was in the 1950s that the general theories of nucleation and crystal growth in glasses were well established. Since then glass-ceramics have played a significant role in a wide range of scientific and technological developments (Lewis, 1989).

The crystallization of a glassy material to develop glass-ceramics consists of a nucleation stage, in which small seeds or nuclei develop within the glass, followed by heating to a higher temperature to induce crystal growth which facilitates the enlargement of crystals until they reach the desired size. The nucleation of crystalline phases can occur in two different ways as follows; homogeneous nucleation, when the nuclei arise from their own melt composition in the absence of foreign boundaries and heterogeneous nucleation occurs when the crystalline phases develop from foreign boundaries like grain boundaries or interfaces or even nucleation catalysts (Daniela *et al.*, 2010).

From the thermodynamic point of view, the nucleation of a glassy material below its liquidus temperature commences when an ordered molecular arrangement is feasible, resulting in nuclei formation (seed or germ). Nucleation entails a decrease in the free energy of the system, and the more favoured the nucleation process, the higher the energy released in the formation of stable nuclei. Kinetically, the nucleation rate depends on both the probability of formation of stable nuclei and the diffusion of atoms necessary for the development of the nuclei. The lower the nucleation temperature (higher undercooling), the greater the energy released during nuclei formation and the greater the nuclei achieved and then nucleation rate decrease as developed nuclei generate strong increase in melt viscosity hence the rate of diffusion decreases (Rusell, 2008). The crystal growth stage commences once stable nuclei are formed within the glass, and the crystallization rate will depend on the ability to transport atoms from the glass network towards the crystalline phase in development. The temperature dependence of the nucleation rate exhibits a maximum usually at temperatures slightly above  $T_g$ . As shown in Figure 2.6, the crystal growth velocity also exhibits a maximum which, however is observed at far higher temperature. Therefore, Figure 2.6 demonstrates the temperature dependencies of the nucleation rate and the crystal growth velocity. There are two principal routes for making glass-ceramics as follows; Bulk (volume) crystallization from a bulk glass and sinter-crystallization from a glass powder compact (Manfredini *et al.*, 1997). In bulk crystallization, the nuclei developed in the nucleation stage are homogeneously and randomly distributed throughout the whole volume of the glass. Thus, the stage of crystal growth results in a closely interlocking microstructure with mean crystal in the region of one micro ( $1\mu$ ) or smaller (50-100nm) (Casasola and Rincon, 2012).

To successfully achieve a glass-ceramics from a bulk glass, controlled crystallization conditions are required to attain a uniform material, free from defects such as micro cracks, voids or surface roughness (El-Meliegy and Richard, 2012).

Usually, the chemical composition of glasses formulated to develop glass-ceramics by bulk crystallization include the incorporation of nucleating agents which speeds up the phase separation giving rise to discontinuities in the glassy lattice when they are introduced into the melt (Holand and Beall, 2002). Common nucleating agents are oxides and metallic colloids. Oxides operate by either a valence change mechanism (e.g. metal oxides such as  $\text{TiO}_2$ ,  $\text{ZrO}_2$ ,  $\text{Cr}_2\text{O}_3$ ,  $\text{MnO}_2$ ,  $\text{MoO}_3$ ,  $\text{V}_2\text{O}_5$ ) or an imbalance charge mechanism (e.g. non-metal oxides such as  $\text{P}_2\text{O}_5$ ). Metallic colloids can be introduced in the glass composition as oxides or chlorides and can precipitate metal species by redox or photosensitive reactions (e.g. Ag, Cu, Au, Rh, Ru, Pb, Pt). Another common nucleating agent in glass-ceramics manufacturing is the  $\text{F}^-$  ion with an ionic radius similar to that of oxygen that can be introduced into the glass network connectivity of structure and lead to the segregation of  $\text{CaF}_2$  crystals, which act as nucleating sites (Holand and Beall, 2002; Casasola and Rincon, 2012).

Volume (bulk) crystallization can be produced without the influence of external agents. In this case, a second liquid phase is segregated in the glass matrix and the liquid-liquid immiscibility would be responsible for homogeneous nucleation. In addition, it has been observed that phase separation in glasses does not always lead to homogeneous nucleation, as the droplet-matrix interfaces could act as heterogeneous nucleation sites. There are three main aspects concerning the relationship between phase separation and nucleation. Bulk crystallization can be achieved at earlier stages or delayed by changing the composition of

glass matrix. As a result, surface crystallization or uncontrolled bulk crystallization can be controlled. A second aspect is that phase separation can form a highly mobile phase that leads to homogeneous crystallization, while the glass matrix crystallizes heterogeneously, either in parallel or later. Finally, phase separation processes can result in interface that can exhibit optimum crystallization (Lewis, 1989; Holand and Beall, 2002).

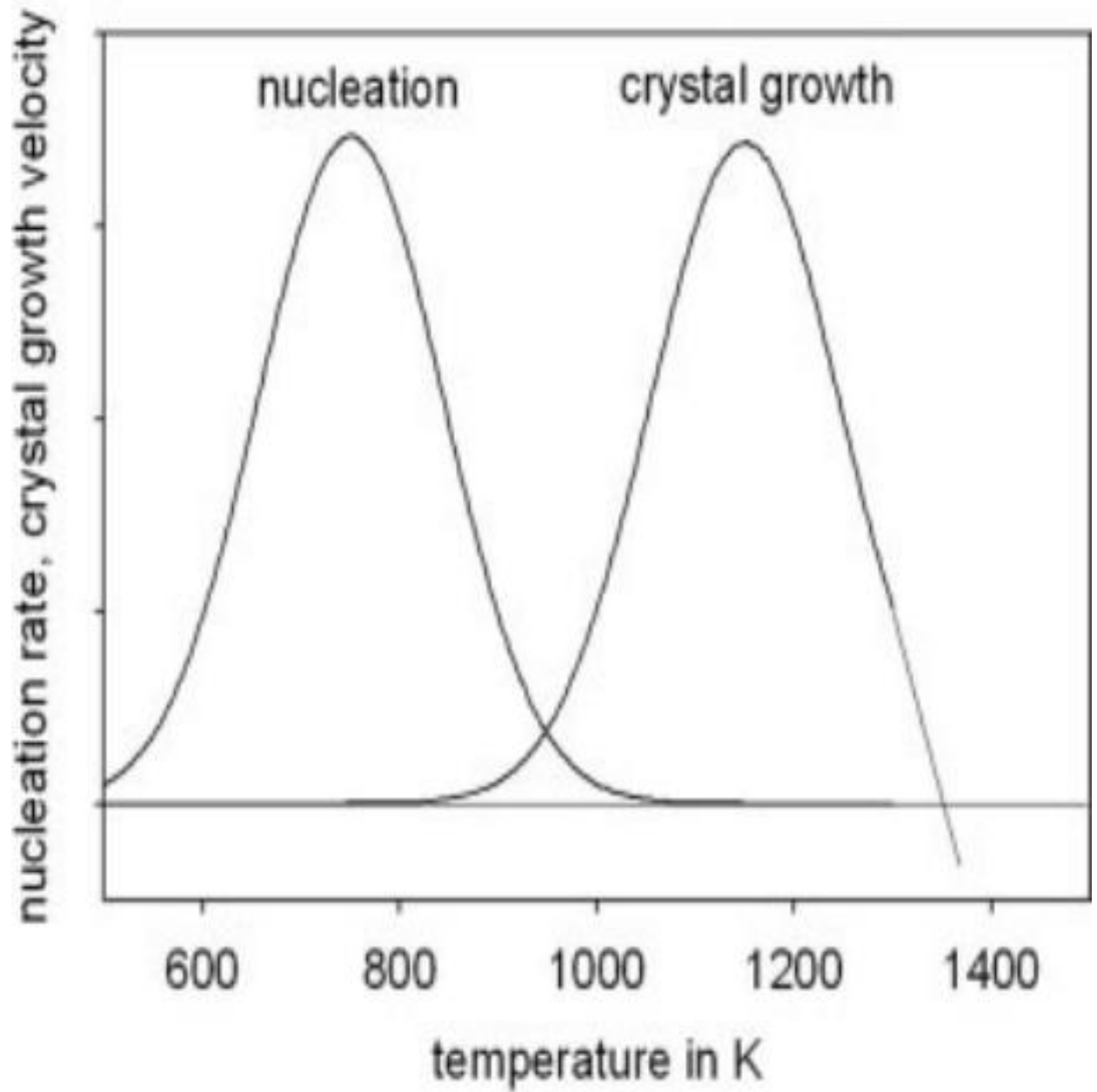
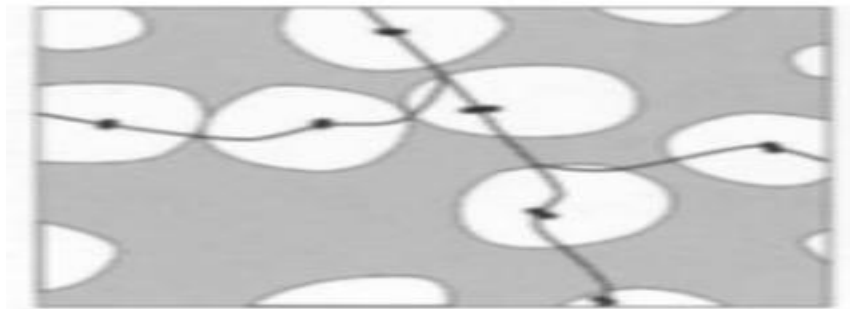


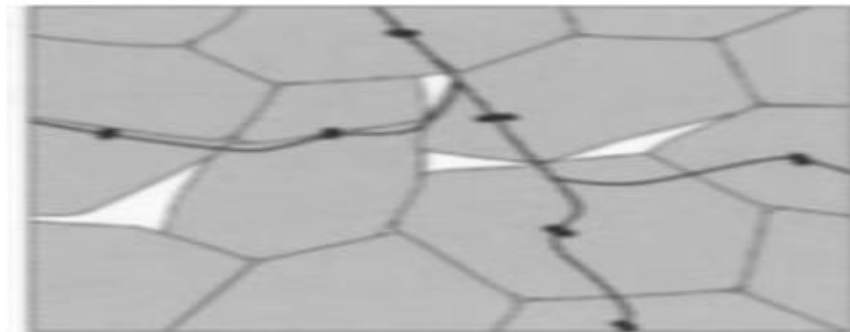
Figure 2.6: Shows the Nucleation Rate and Crystal Growth Rate as Function of temperature (Russell, 2008)



(a)



(b)



(c)

Figure 2.7: Glass-ceramics from powdered glass: (a) Powdered glass compact (b) Densification and sinter-crystallization (c) Frit-derived glass-ceramics (Holand and Beall, 2002)

Most glass-ceramics are manufactured through controlled nucleation in the bulk of the base glass, but there are also glasses in which this route is ineffective simply because bulk

nucleation cannot be initiated, and controlled crystallization can only be achieved through surface crystallization (Chen, 2007). Therefore, the most efficient route for making such type of glass-ceramics involves sinter-crystallization of glass powders in which glass powders or frits (3-15  $\mu\text{m}$ ) particle diameter are compacted using conventional ceramming techniques known as forming techniques such as slip casting, extrusion, pressing among others. The subsequent heat treatment involves sintering for densification prior to crystallization. The final microstructural configuration of the resultant glass-ceramics achieved using both routes (bulk and sinter-crystallization) is similar (Rappensberger, 1996; Holand and Beall, 2002; Mahmud, 2007). Figure 2.7 shows the development stages for making glass-ceramic via sinter-crystallization in the absence of nucleating agent. (a) displays transformation of a powdered glass compact (b) shows dense sintered glass with some surface nucleation site and (c) depicts highly crystalline powder-derived glass-ceramics.

## **2.11 Nucleation**

Controlled crystallization of glasses is a vital requirement for development of glass-ceramics. In the absence of controlled crystallization, glass-ceramics with superior properties could not be achieved. The term crystallization actually refers to a combination of two processes namely; nucleation and crystal growth. Nucleation is a decisive factor for controlled crystallization, as crystallization of a base glass generally occurs in two stages as follows: formation of submicroscopic nuclei, and their growth into macroscopic crystals. These two stages are known as nucleation and crystal growth. The nuclei may be either homogeneous or heterogeneous. Holand and Beall (2002) described the temperature dependence of nucleation and crystallization of glasses and then utilized this function to

develop glass-ceramics and thus expanded the theory of nucleation and crystal growth (Holand and Beall, 2002). Nucleation is assumed to be influenced by two factors as follows: appropriate selection of the chemical composition of the base glass, with the usual addition of a nucleating agent. Controlled heat treatment of the base glass, with time and temperature as process variables.

### **2.11.1 Homogeneous nucleation**

This type of nucleation occurs spontaneously within the melt in the absence of preferential nucleation sites for nuclei formation and the nuclei are chemically of the same materials as the growing crystal (El-Meliegy and Richard, 2012). The favourable conditions for homogeneous nucleation to take place are the structural, chemical and energetic homogeneity of the base glass without defects.

Generally, glasses contain defects such as particle of dust on the melt surface , fragments of refractory, incomplete melted material among others. For this reason, homogeneous nucleation of most glasses is difficult and tends to be impossible (Rawson, 1980). In homogeneous nucleation, the tiny seeds termed embryos are accomplished through local fluctuations in the structural configuration of the glassy phase. They are thermodynamically unstable because of their tiny radii which are smaller than the critical one and this lowers the free energy of the system. To become thermodynamically stable, their radii must be equal to the critical radii. This type of nucleation can only be achieved at higher degrees of super saturation or supercooling (Patridge, 1994).

In addition, the rate of nucleation depends solely on thermodynamics and kinetic energy. The thermodynamic factor is zero at liquidus temperature ( $T_L$ ) and increases as the supercooling further increases progressively. However, at higher supercooling, the kinetic

factor becomes dominant and the nucleation rate decreases with further cooling after attaining a maximum (Rappensberger, 1996). Figure 2.8 represents the various stages of homogeneous nucleation in the absence of nucleation site for achieving nuclei formation.

### **2.11.2 Heterogeneous nucleation**

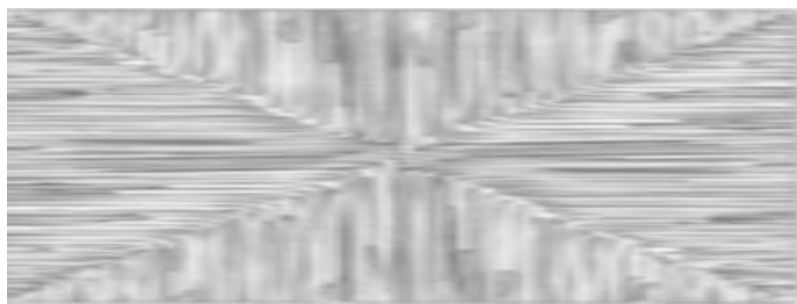
Heterogeneous nucleation involves nuclei formation on the surface of an already existing phase (substrate). Heterogeneous nucleation are formed at a pre-existing surfaces such as that due to an impurity, crucible wall etc, or through the incorporation of nucleation catalysts (Holand and Beall, 2002). The parent glass composition is quite different chemically from the developed crystals in which case, the nucleation can commence from within the bulk of the glass or from the surface (Rappensberger, 1996; El-Meliegy and Richard, 2012). The presence of substrate decreases the thermodynamic barrier for nucleation. In glass compositions where homogeneous nucleation is hindered or the nucleation rate is small, bulk crystallization with high nucleation rate can be obtained through the incorporation of nucleation catalysts. In addition, photo nucleation is a special type of heterogeneous nucleation within which photosensitive glass is irradiated by ultraviolet (UV) radiation of about 300-400 nm followed by subsequent heat treatment that results in the separation of colloidal metal particles distributed throughout the bulk of the base glass. However, the metal particles act as heterogeneous nucleation sites for the dominant phase assemblage in the second heat treatment that transforms the base glass into resultant glass-ceramics (Rappensberger, 1996 and Daniel *et al.*, 2010). Figure 2.9 presents the various stages of transforming base glass to glass ceramics through the incorporation of nucleation catalysts.



(a)

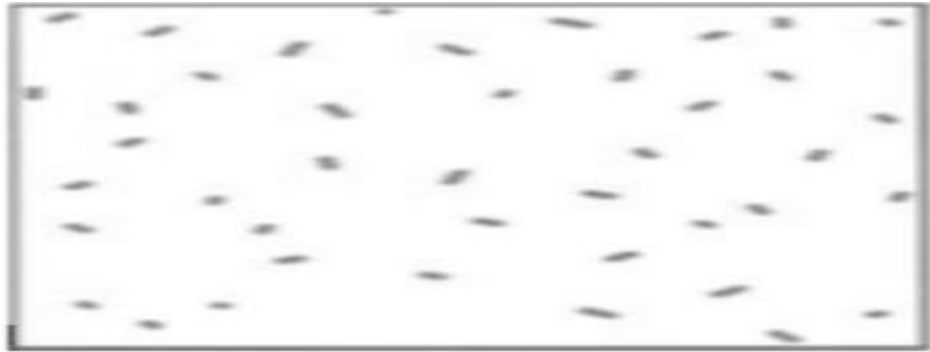


(b)

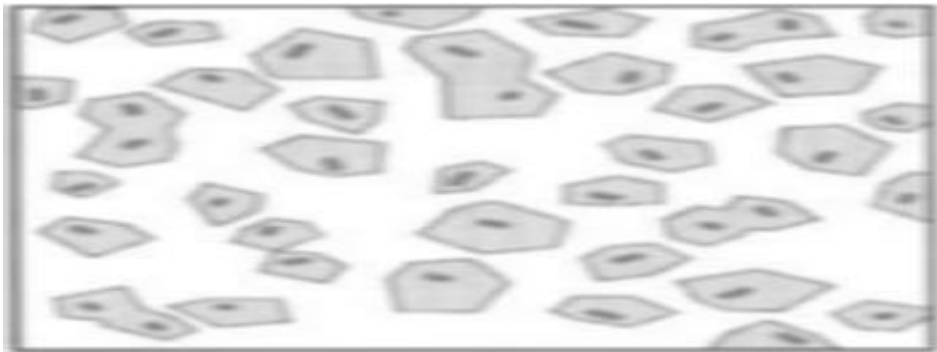


(c)

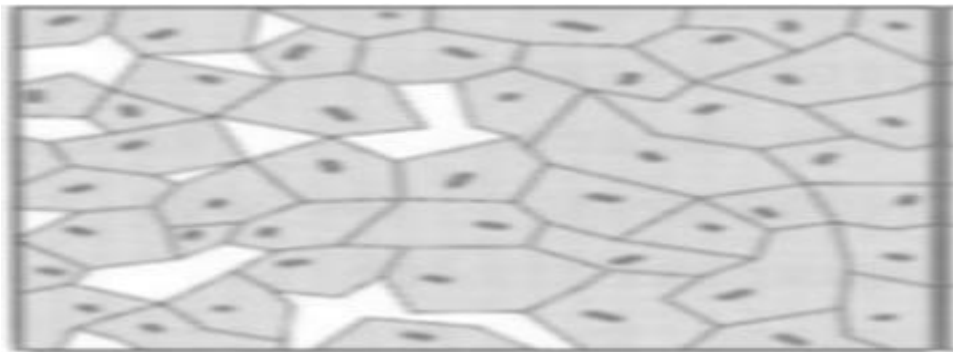
Figure 2.8: Crystallization of glass without internal nucleation (Holand and Beall, 2002).



(a)



(b)



(c)

Figure 2.9: From Glass to Glass-ceramics: (a) Nuclei formation (b) Crystal growth (c) Glass-ceramics microstructure (Holand and Beall, 2002)

### **2.11.3 The nucleation temperature**

The nucleation temperature of a glassy material is best determined from the DTA curve, and this is achieved by heating the glassy material to a temperature above the glass transition temperature ( $T_g$ ) for enough time to assure good nuclei formation (Lewis, 1989). In other words, the best nucleation temperature happens between the transition temperature ( $T_g$ ) and a temperature some 50-100° C above  $T_g$ . Also, the nucleation temperature appreciably corresponds to the endothermic peak within the DTA curve (El-Meliegy and Richard, 2012). The Differential Thermal Analysis (DTA) refers to the technique in which the difference in temperature between the sample and a reference material is monitored against time or temperature while the temperature of the sample, in a specified atmosphere is programmed. Matters that are inert or do not change in the measurement temperature range (usually  $\alpha$ -alumina) are used as reference (Lewis, 1989).

### **2.11.4 Nuclei formation**

For crystallization to occur, nuclei must be present. Nucleation involves the initiation of regions of longer-range atomic order termed embryo. If no nuclei are present, crystal growth cannot occur and the material will form a glass and even if some nuclei are present, but no growth has happened, the extremely small size and low volume fraction of the nuclei inhibits their detection, such material is still a glass (Lewis, 1989 and Shelby, 2005). When these embryos achieved a critical minimum size capable of developing into particles of stable phase, they are termed nuclei. The growth rate of nuclei (homogeneously or heterogeneously produced) is a function of nuclei size (El-Meliegy and Richard, 2012). For any given nuclei size, there exists a temperature which generates a maximum growth rate. Therefore, as the nuclei grows, the maximum growth rate temperature also increases.

For small nuclei, the temperature for maximum growth rate is low and the growth rate is low. This corresponds to a relatively flat sloping portion on a time/temperature heating schedule (Salama *et al.*, 2002). For a larger nuclei, for example that which is generated from a heterogeneous material, the temperature for maximum growth is high and the growth rate is high, and this is equivalent to a relatively steeply sloped portion on the time/temperature heating schedule. Therefore, the expected form of favourable heat treatment schedule should be a smooth curve of increasing slope (Mukherjee *et al.*, 2012).

On heating a glassy material, the main bulk of the glass would crystallize internally and uniformly upon these tiny nuclei instead of crystallization from the surface of the glassy material. Once stable nuclei are formed, the crystal growth stage commences. Growth entails the movement of atoms/molecules from the residual glass across the glass-crystalline interface, and into the crystal. The driving force for this process is the difference in volume or free energy,  $\Delta G$  between the residual glassy phase and phase assemblage (Holand and Beall, 2002).

Starting from these nuclei, the dominant phase assemblage would grow until it impinges on neighbouring silicate crystals, creating a phase assemblage with residual glassy phase. Without the internal nucleation, as a precursor of crystallization, devitrification is initiated at lower energy surface sites (Christain *et al.*, 2015). Flow of the uncrystallized core glass in response to change in bulk density during crystallization commonly forces the original shape to undergo certain deformations. However, efficient internal nucleation and crystal growth in a viscous glassy medium would generate an exceptionally uniform and fine-grained microstructure that simply cannot be found in conventional ceramics, metal, polymer, glass or natural rocks (Bahman and Behzad, 2012a). Nucleation may occur either

homogeneously that is freely in the volume of the original glassy phase or heterogeneously on surfaces of the container, foreign particles or on the structural imperfection (El-Meliegy and Richard, 2012). In homogeneous nucleation, the composition of the major nuclei do not differ from that of the main phase assemblage. The nuclei are chemically of the same materials as the growing crystals. Homogeneous nucleation is difficult and tends to be impossible due to the risk of uncontrolled crystallization which is termed devitrification, whereas, in heterogeneous nucleation, the nuclei are quite different chemically from the developed crystals and are created through the incorporation of nucleation catalysts such as titania or zirconia (Holand and Beall, 2002). The crystallization of the base glass is caused through incorporating foreign nuclei, the nucleating agent, which is generally a metal, oxide or fluoride and is usually incorporated in the batch and becomes the integral part of the base glass during melting (Lewis, 1989). The nucleation can commence from the surface of the glass or from within the bulk of the glass (El-Meliegy and Richard, 2012).

A generalized way in which nucleating agents induced nuclei formation and subsequent crystal growth can not be developed since the role of the nucleating agents in catalyzing the formation of nuclei and the dominant phase assemblage undoubtedly differs from one nucleating agent to another. Therefore, nucleating agent introduces sites of lower thermodynamic stability in the base glass (Daniela *et al.*, 2010).

Oxides that are commonly utilized to enhance phase separation in glass system are  $\text{Cr}_2\text{O}_3$ ,  $\text{ZrO}_2$ ,  $\text{V}_2\text{O}_5$ ,  $\text{P}_2\text{O}_5$ ,  $\text{TiO}_2$  among others. It was suggested that the interfacial energy between two glassy phases is less than that between amorphous phase and a crystal phase thereby reducing the limit for nuclei formation (Mahmud, 2007).

### 2.11.5 The nucleation rate

Nuclei formation occur when atoms are constantly vibrating and in motion due to thermal energy. If the atomic vibration of each atom is allowed to link to the nucleus, the nucleation rate would be expressed as follows;

$$I = nv$$

Where;

$n$  = number of atoms per unit volume

$v$  = atomic vibration frequency per second

There are two barriers to nuclei formation; a thermodynamic barrier and a kinetic barrier. The thermodynamic barrier denoted by  $W$  is the net free energy change of the system after nuclei have been formed. The kinetic barrier designated by  $\Delta E$  is the activation energy needed for an atom to cross the liquid-nucleus boundary, which involved breaking bond strength with neighbouring atoms and reorientation into more ordered structure within the surface of the nucleus (Russell, 2008).

### 2.11.6 Volume nucleation

Volume nucleation otherwise known as bulk crystallization is the most desirable crystallization process and is utilized in the manufacture of almost all commercial glass-ceramics as it assures a uniform microstructure with high crystallinity content because nuclei are formed within the bulk of the glass (Russell and Edward, 2010). This indicates that the material can be achieved in its desirable final glass shape and then transformed into glass-ceramics through thermal treatment schedule. Bulk crystallization involves converting the base glass into microcrystalline glass-ceramics using two-step process

which requires the use of a nucleating agent. The technique involves nuclei formation achievable at low temperature somewhat 100°C above the transition temperature ( $T_g$ ) and held within that transition range for sufficient period of time to induce nucleation (Casasola and Rincon, 2012). The nucleated material is heated further to temperature within the crystallization range for a time sufficient to form crystal growth. The presence of nucleation catalyst is a powerful driving force for nucleation and crystal growth of glass-ceramics developed using bulk crystallization (Kartelia, 2010). The following are some of the nucleating agents used for glass ceramics production by bulk crystallization mechanism; Calcium fluoride, zirconia, gold, silver and titania among others (Holand and Beall, 2002).

The rate of crystal growth depends on the temperature. At temperatures slightly above transition range, crystal growth is being retarded which result in deformation of the material. Therefore, the rate of heating for base glass at temperatures above the transition range should be sufficiently slow to give enough time to achieve substantial crystal growth, sufficient to support the material against deformation. For this reason, heating rate of 10°C/min and higher can be employed successfully. Equally important, a heating rate range between 3-5°C/min can also produce glass-ceramics (Holand and Beall, 2002).

### **2.11.7 The crystallization temperature**

After nucleation stage, the nucleated glass would be subjected to secondary heat treatment temperatures higher than the glass transition temperature ( $T_g$ ), the crystallization process commences. The crystal growth temperatures can be ascertained from the differential thermal analysis (DTA) peak which corresponds to exothermic peak. One or more phases assemblage can precipitate from the glassy phase through exothermic reactions. The nucleated material should be heated to temperature somewhat higher than the crystal

growth temperature for enough time to ensure crystal growth without deformation of the dominant phase assemblage (Russell, 2008).

### **2.11.8 Crystal growth**

The growth rate of crystal nucleus depends on the rate at which atoms get attached to the surface of the nucleus. The rate of crystal growth as a function of temperature exhibits close similarities to that of the nucleation rate, since the two major factors such as thermodynamic and kinetic factor which determines the rate of crystal growth are similar to those determining the nucleation rate (El-Meliegy and Richard, 2012). Usually, controlled crystal growth results in diverse crystals rather than a single crystal phase, thereby giving the glass-ceramics material superior properties. The crystalline phases also display a superior microstructural arrangement in the glassy matrix.

### **2.12 Phase separation**

Glass-in-glass phase separation is often encountered during the development of glass-ceramics. However, liquid phase separation is the separation and growth of non-crystalline phases having different composition from the original glass (Shelby, 2005). The driving force for phase separation is the attainable decrease in the overall free energy of the system.

The Gibbs type free energy ( $\Delta G$ ) of the system is as follows;

$$\Delta G = \Delta H - T\Delta S$$

Where;

T = The temperature

$\Delta H$  = Enthalpy and

$\Delta S = \text{Entropy}$

The compositional fluctuation has high probability at negative or small positive values of the free energy's second derivative. When the derivative is negative, the separation of the glass into two phases is accompanied by a simultaneous decrease of free energy, and the process is called spinodal decomposition (Mahmud, 2007). When the derivative has a small positive value, the early stage of the phase separation causes an increase of free energy, therefore the separation will occur by nucleation and growth (Rusell, 2008). The above processes are easily seen by the "immiscibility dome" which is the limiting phase composition of immiscibility as a function of temperature. The inner dome is known as "spinodal", referring to spinodal decomposition. Within this dome, the glass forming melt will spontaneously separate and the separation process is only limited by the diffusion of the components. In the outer dome, which is known as the "binodal", the phase separation has an energy barrier, therefore it requires nuclei formation (Rusell *et al.*, 2010). Plate I represents liquid-liquid phase separation of glassy mass.

Introducing glass-glass controlled phase separation before crystallization can be used to achieve bulk nucleation and fine-grained microstructure glass-ceramics. In addition, phase separation can trigger subsequent crystal growth through the provision of nucleation sites at the newly formed glass-glass interfaces (Garza-Garcia *et al.*, 2007).

### **2.13 Nucleating Agents**

Nucleating agents are substances which when added to glass form nuclei for the growth of crystals in glass-ceramics, their addition to the melt promotes rapid nucleation at low temperature and subsequent crystallization at higher temperature (Salama *et al.*, 2002). On addition of nucleating agent either causes volume/bulk crystallization (after suitable heat

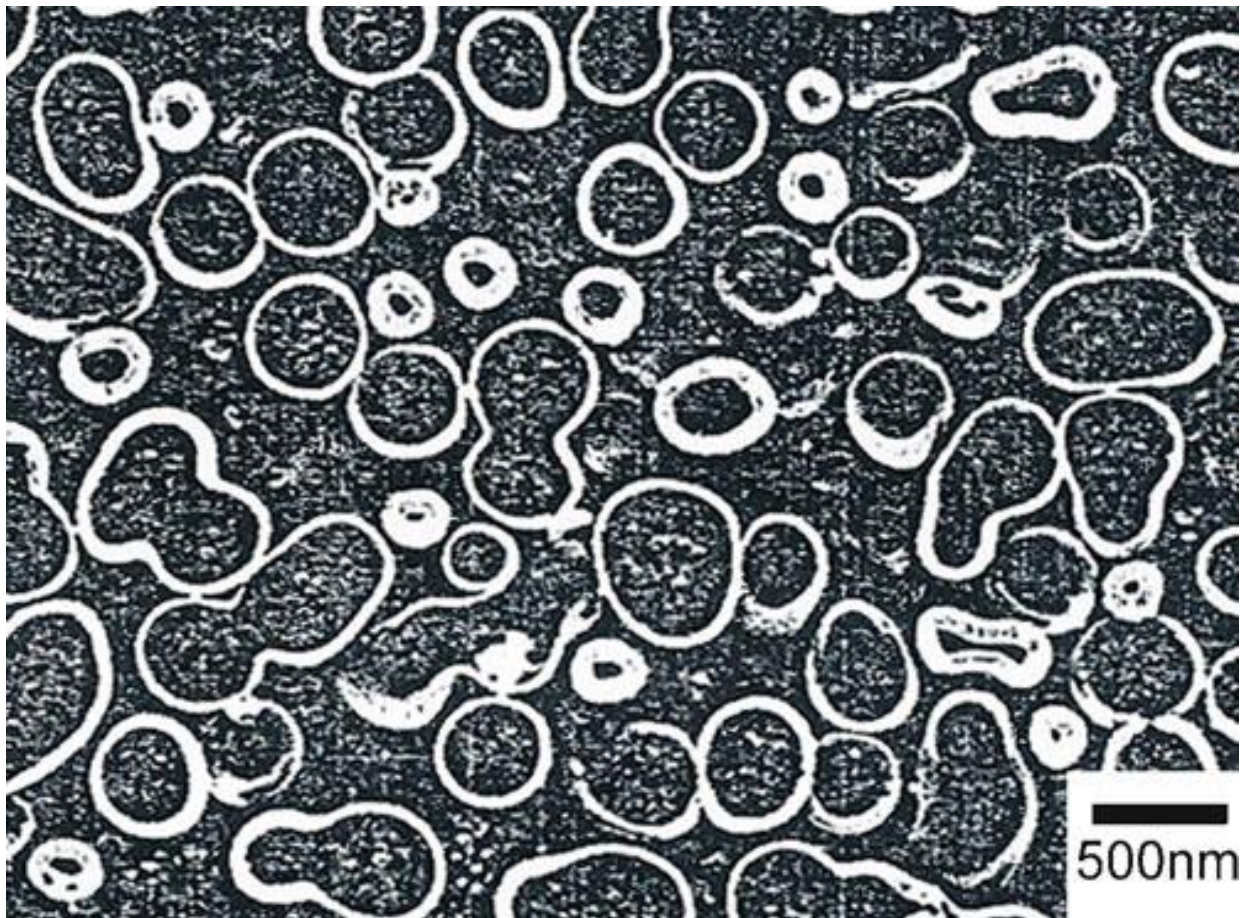


Plate I: Liquid-Liquid Phase Separation ( El-Meliegy and Richard, 2012)

treatment) of a composition or if the composition already exhibits low volume nucleation, increases it. The most important nucleating agents, vital in the preparation of practical glass-ceramics are oxides such as  $\text{TiO}_2$ ,  $\text{P}_2\text{O}_5$  and  $\text{ZrO}_2$  and various fluorides and sulphides (McMillan, 1974).

Nucleating agents are agents of heterogeneous nucleation and are widely utilized to modify the properties of the resultant glass-ceramics. They play a key role in glass-ceramic making because altering the concentration and or mixing it with another changes the morphology, crystal size as well as the physical appearance of the resultant glass-ceramics (Mahmud, 2007).

Two groups of nucleating agents are identified as follows; Firstly, the use of metallic ions as nucleating agents such as; Ag, Au, Pd, Pt and Rh among others. These metallic ions are incorporated in very small quantity to the base glass (0.01- 1.0 wt%) usually in the form of chlorides or nitrates (Rappensberger, 1996). In ionic form they are soluble in the glass melt but they can be easily reduced to the metallic state, which would lead to their precipitation, since the solubility of their metallic forms in base glasses is very low. Therefore, suitable heat treatment schedule of the base glass either by controlled cooling from the molten glass or by reheating the room-temperature glass that might result in the precipitation of tiny aggregates of colloidal dispersion of metal atoms. These aggregates act as heterogeneous nucleation sites for the dominant phases assemblage in the course of the heat treatment (Kartelia, 2010).

Metallic oxides (such as  $\text{TiO}_2$ ,  $\text{ZrO}_2$ ,  $\text{Cr}_2\text{O}_3$ ,  $\text{P}_2\text{O}_5$ ). Fluorides (like;  $\text{CaF}_2$ ,  $\text{NaF}$ ,  $\text{Na}_3\text{AlF}_6$ ), sulphides ( $\text{CdS}$ ) and selenides ( $\text{CdSe}$ ) (Rappensberger, 1996; Salama *et al.*, 2002 and Mohammed *et al.*, 2003) are also used as nucleation catalysts for accomplishment of desirable nuclei and crystal growth. Nucleating agents that are metallic oxides are soluble in silicate glasses, and are usually incorporated in larger quantity (1-20 wt%). The

nucleation abilities of sulphides, fluorides and selenides are similar to those of metallic ions. They precipitate as colloidal dispersion of fine crystals during heat treatment schedule and serve as heterogeneous nucleation sites for the dominant phase assemblage at higher temperatures (El-Meliegy and Richard, 2012). In contrast, the nucleation process induced by metallic oxides is more complex and generally depends on the nucleation catalysts, upon the base glass composition, the applied heat treatment schedule and the thermal history of the base glass. Some of the metallic oxides acting as nucleating agents can generate liquid-phase separation before nuclei formation, since most of them form prevalent immiscibility region with silica (Casasola and Rincon, 2012). The phase-separation can be followed by the crystallization of the separated phases as fine crystals, which in turn speeds up further growth. Other metallic oxides nucleating agents can precipitate in form of simple compounds formed with some constituents of the base glass, for example  $\text{MgO.TiO}_2$  (magnesium titanate) and then heterogeneously nucleate the dominant phase assemblage (Salama *et al.*, 2002). Metallic oxides nucleating agents such as  $\text{TiO}_2$ ,  $\text{ZrO}_2$  and  $\text{P}_2\text{O}_5$  are well known nucleants in various aluminosilicate based glass systems, they have been found to decrease nucleation rates when added to the  $\text{Na}_2\text{O-2CaO-3SiO}_2$  glass composition. Similarly, small additions of  $\text{TiO}_2$  to the  $\text{BaO.2SiO}_2$  composition reduce nucleation significantly. Oxides nucleating agent such as  $\text{TiO}_2$ , is used in amounts ranging typically from 2 to 20 wt% (McMillan, 1974).

In the mid 1950s S.D. Stookey tried incorporating titania as nucleating agent in aluminosilicate glasses and discovered it to be amazingly effective, thereafter, strong and thermal shock resistant glass-ceramics were then developed commercially within a year or two of this work as well-known products such as cooktops, cookware, bakeware, nose cones of

rockets, among others ( Holand and Beall, 2002). In addition, Hummel (1951) and Smoke (1951) both worked extensively on the lithium aluminosilicate (LAS) base glass system using  $ZrO_2$  combined with  $TiO_2$  and the dominant phase assemblage obtained was a high-quartz solid solution. The most interesting properties of LAS glass-ceramics are their thermomechanical properties, which suggests that such glass-ceramics are mechanically stronger and can sustain repeated and quick temperature changes up to 800-1000°C (McMillan,1974).

In  $\beta$ -quartz crystal phase for example, a high degree of crystallinity and more uniform microstructure is obtained by incorporating a nucleating agent such as titania (Holand and Beall, 2002). Different varieties of nucleating agents greatly promote the crystallization process of the base glass and enhance the formation of fine-grained microstructure (Bahman and Behzad, 2012a). The most suitable nucleation temperature was determined as 740°C for most promising specimens and when heat treated further at 885°C, it exhibits the sharpest peak in DTA analysis (Rezvani *et al.*, 2005).

## **2.14 Types of Nucleating Agents**

### **2.14.1 Effect of titania ( $TiO_2$ ) on glass-ceramics**

Titania ( $TiO_2$ ) is commonly used as nucleating agent. Infact it is one of the most vital nucleating agent in the preparation of practical glass-ceramics. Its addition can have a remarkable influence on the crystallization behaviour of base glasses in the quaternary system  $CaO-MgO-Al_2O_3-SiO_2$  (Mohammed *et al.*, 2003). Liquid phase separation occurs first in glass ceramic with titania ( $TiO_2$ ) added as nucleating agent, then crystalline compounds will be formed or  $TiO_2$  itself precipitates as fine crystals (titanate) of high

density. Consequently, these crystals act as surface active agents and increase the nucleation rate. Addition of alumina ( $\text{Al}_2\text{O}_3$ ) in combination with titania ( $\text{TiO}_2$ ) and silica ( $\text{SiO}_2$ ) promote achieving high density nuclei formation and fine-grained crystal growth (Barsoum, 1994). The incorporation of titania as nucleating agent in the glass batches lower the melting point and increases the homogenization of the melt. It also decreases the melting temperature by nearly 50-100°C. This is in agreement with findings of (Khater,2012) when he studied the role of  $\text{TiO}_2$  in the crystallization of glass-ceramics from Egyptian clays, titania has an intermediate effect in the glass structure implying that  $\text{Ti}^{+4}$  ion occupies tetrahedral network-forming sites. These ions tend to attract non-bridging oxygen ions which led to the lowering of crystallization temperature (Mohammad *et al.*, 2003). Titania is very effective as nucleating agent because of its high ionic field strength that enhances the phase separation and as well improve the heterogeneous nucleation rate (Rezvani, 2011).

The addition of titania ( $\text{TiO}_2$ ) improves both the nucleation and growth rates by decreasing the viscosity and the surface energy between crystal and glass (Khater, 2012). In addition, the incorporation of titania ( $\text{TiO}_2$ ) as nucleating agent to the base glass decreases the glass transition temperature and increases the homogeneity of the melt (Salama *et al.*, 2002 and Mohammed *et al.*, 2003). Further increase of titania in the melt might resulted in  $T_g$  decrease. This is attributable to the formation of non bridging oxygen bond in the glass network structure , and this result in decrease of viscosity as well as glass transition (Aykut, 2005). For base glasses where the titania ( $\text{TiO}_2$ ) concentration is less than 7%, crystallization commences from the surface but once this limit is exceeded, bulk or volume crystallization becomes the predominant way (Mahdavi *et al.*, 2011).Similarly, less

addition of titania slows down nuclei formation and increase addition of titania promotes high density nucleation and formation of crystals of uniform size (Holand and Beall, 2002). In addition, titania allows the formation of nucleating phase  $MgTi_2O_5$  by reducing high melting conditions in the development of high-strength glass ceramics (Daniela *et al.*, 2010). Titania is used in amounts ranging typically from 2 to 20 wt%. As pointed out, when the larger concentrations are employed, use of the term nucleating agent is questionable since the addition becomes a major component in the glass (Lewis, 1989). These crystals then act as heterogeneous sites for crystallization of the glass (Lewis, 1989). In addition, glass-ceramics based on the mineral codierite have good mechanical and thermal properties. They can be prepared from CaO-MgO- $Al_2O_3$ - $SiO_2$  based glass system when 5% CaO is incorporated to precipitate codierite crystalline phase. Addition of 10-12 wt % titania ( $TiO_2$ ) is considered to be suitable for quaternary system, and during controlled heat treatment of these glasses extensive phase separation occurs ( De Vekey and Majumdar, 1970).

#### **2.14.2 Advantages of titania ( $TiO_2$ ) on glass-ceramics**

1. It enhances amorphous phase separation and the appearance of nucleant phase.
2. It is responsible for the uniformity and fineness of the microstructure.
3.  $T^{4+}$  ion can be accommodated in the glass structure either as network former or as network modifier.
4. The titanium ion occupancy of  $Si^{4+}$  sites in the glass structure introduces a Ti-O bond that is weaker than the Si-O bond, and this improves batch melting and crystallization of the glass.

5. The addition of TiO<sub>2</sub> in the glass enhances the crystallization of anorthite, diopside plagioclase and titanate beside wollastonite (Salama *et al.*, 2002).
6. Addition of titania reduces the viscosity of the glass during crystallization and consequently increases the diffusion rate of ions and ionic complexes forming glass, thereby facilitating the formation of the structurally more complex phases like anorthitic plagioclase (Salama *et al.*, 2002).
7. It was found practically that the addition of 10 wt% titania to the base glass improved the batch melting and the crystallization of the glass through its bulk.
8. The presence of titania resulted in a decrease in the temperature of melting by about 100° C and modified the crystallization kinetics (Salama *et al.*, 2002).

#### **2.14.3 Effect of zirconia (ZrO<sub>2</sub>) on glass-ceramics**

Glass-ceramics nucleated by ZrO<sub>2</sub> are known in different chemical systems (Holand and Beall, 2002). A monoclinic ZrO<sub>2</sub> was used as nucleation catalyst with CaO-MgO-Al<sub>2</sub>O<sub>3</sub>-SiO<sub>2</sub> base glass system. The study revealed that zirconia not only aids in crystallization of glass-ceramics but also improve the mechanical properties of glass-ceramics. The produced glass-ceramics would have excellent strength, good chemical durability against acid and alkali and excellent wear resistance among others (Salman *et al.*, 2009). Zirconia has three different crystallographic forms; monoclinic, tetragonal and cubic. The monoclinic zirconia remains stable up to 1150°C when it transforms to tetragonal symmetry. At temperatures above 2300°C the cubic form exists. The transformation of tetragonal-to-monoclinic phase change is vital as this stress induced phase transformation at crack tip which makes the material resistance to crack propagation (Salman *et al.*, 2009).

Glass-ceramics that has a secondary phase of tetragonal zirconia dispersed in the residual glassy phase is suppose to have improved mechanical properties (Rehana and Madeeha, 2015). Similarly, glass-ceramics have been developed through incorporation of  $ZrO_2$  in the  $MgO-Al_2O_3-SiO_2$  base glass system , phase separation occurred in the temperature range of 800-900 °C and followed by rapid crystallization to precipitate enstatite as the main phase assemblage (Partridge *et al.*, 1989).

#### **2.14.4 Effect of Calcium fluoride ( $CaF_2$ ) on Glass-ceramics**

Calcium fluoride is often used as a nucleating agent for crystallization of glass ceramics. It has been reported that when glass samples are crystallized, the crystals of fluorides emanate first from the base glasses and become the site of heterogeneous nucleation of other crystals. According to (Bahman and Behzad, 2012a) who realized that fluoride improved the nucleation and growth of glass ceramics through fluoride ions and decrease the aggregate extent of the glass network. As the heat treatment commences in the base glass, a glass ceramics may be produced essentially with zero porosity (Mukherjee and Das, 2012). In silicate glasses, fluorine makes non bridging bond of Si-F resulting in the decrease of viscosity and promote phase separation resulting in the decrease of energy barrier necessary for crystallization (Salama *et al.*, 2002).

#### **2.14.5 Effect of metals on glass-ceramics**

Metals such as gold, silver and copper are used as nucleating agents to achieve bulk crystallization in base glasses. The metals are added to the base glass in ionic form, for example  $Au^+$ ,  $Ag^+$  . Metal nuclei for example  $Au^0$ ,  $Ag^0$ , in the presence of  $Ce^{3+}$  were

reduced in the glass with ultraviolet light and  $Ce^{3+}$  is oxidized to  $Ce^{4+}$  (Holand and Beall, 2002).

## **2.15 Glass-Ceramics**

Glass-ceramics differ from sintered ceramics by their techniques of production. The first step in the preparation procedure is the melting of a homogeneous glass using conventional melting techniques (Holand and Beall, 2002). In a second step, the cooled glass is heat treated which result in the crystallization of the glass. The thermal treatment is oftenly conducted as a two-step processes: In the first step, nucleation occurs while the second step is subsequent crystal growth. Glass-ceramics usually contain notable quantities of amorphous phase and two or more phases assemblage (El-Meliegy and Richard, 2012). The materials properties depend on the phases assemblage present and the microstructure, that is, the volume concentrations of the crystalline phases, the size and morphology of the crystals, and their arrangement and mutual orientation (Pinckney and Beall, 2008). Glass-ceramics are prepared from isotropic glasses and therefore are usually isotropic materials. Anitropic crystallization, however, is possible if a special driving force is applied or if nucleation occurs only in a small part of the volume. In principle, glass-ceramics can also be developed from powdered glass frit. In this case, the glass frit is being plastified using conventional processing, brought to the required shape and subsequently sinter-crystallized. Sinter-crystallization is attained through viscous flow thereafter either as a separate step at

a higher temperature or at the end of the sintering process, crystallization process is achieved (Khater *et al.*, 2013).

Glass-ceramics developed through this technique are known as sintered glass-ceramics. They have advantages if needed shape is more easily produced by ceramics technique than through glass-forming techniques from the viscous glassy state. Crystallization in glass can be achieved either by bulk or volume crystallization or via surface crystallization (Daniela *et al.*, 2010). In the later case, nucleation solely occurs at the surface. Also, in a system which usually only shows surface crystallization, volume crystallization can be attained through the incorporation of nucleating agents to the glass batch. For example, in many cases, 0.01% platinum incorporated to glass batch is enough to achieve volume crystallization (Holand and Beall, 2002). Other well known nucleating agents are titania, zirconia chromium oxide among others. Glass ceramics are versatile materials and have a wide variety of applications including: Glass-ceramics with zero thermal expansion coefficient, glass-ceramics with excellent strength, elastic modulus, hardness and toughness, machinable glass-ceramics as well as biocompatible glass ceramics (Russell, 2008). Additionally, glass-ceramics with high thermal shock resistance are frequently utilized as cook top panels or as telescope mirrors. In view of this, to avoid mechanical stresses, or even a change in geometry with temperature, the thermal expansion coefficient must be zero or near zero within a certain temperature range. This is achievable through crystallization of phases which exhibit a negative thermal expansion coefficient such as beta eucryptite or keatite (Holand and Beall, 2002).

Machinable glass-ceramics can be shaped for example by drilling with hard metal tools such as tungsten carbide. This is especially advantageous for rapid prototyping, and is

achieved by the crystallization of phases such as mica which exhibit strongly anisotropic properties such as fissionability along one crystallographic axis. Bioglass ceramics are used for bone replacement. In this case, biocompatible, bioactive and bioresorbable materials should be distinguished (El-Meliegy and Richard, 2012). Biocompatible glass-ceramics are often also machinable to enable rapid shaping technologies. Most resorbable bioglass ceramics are composed of phosphates. Among the bioglass ceramics, dental glass-ceramics for tooth replacement are the economically most important. Shaping this category of glass is possible for example by viscous flow or by milling. They should also possess high resistance against chemical attack (El-Meliegy and Richard, 2012). Glass-ceramics have a wide variety of applications in photonic technologies. These applications require a high transparency for light in the respective wavelength range which shows that scattering must not occur. This can only be attained, if crystals embedded in the glassy matrix are smaller than half of the wavelength of the light. Hence, the crystals must be sized in the nanometer range and distributed homogeneously in the volume (Daniela *et al.*, 2010). Among possible applications are up-conversion glasses, which transform light of long wavelength to light of shorter wavelength. In addition, glass-ceramics containing rare earth-doped fluoride crystals are potential candidates for laser applications.

### **2.15.1 Routes for making glass-ceramics**

Glass-ceramic materials may be produced via three techniques as follows:

- i. The heat treatment of solid glass (the conventional route)
- ii. The controlled cooling of molten glass known as peturgic method, and
- iii. The sintering and crystallization of glass powders (frits)

The first technique which is achieved on cooling molten glass or reheating solid glass involves basically precipitation of crystal from the melt in which nuclei are formed and then grow with time through the incorporation of nucleating agent. To achieve high density nucleation, it encompasses production of large numbers of small particles and this is the main target of glass-ceramics otherwise known as heterogeneous nucleation or without nucleating agent known as homogeneous nucleation. The nuclei are formed spontaneously due to fluctuation in density and kinetic energy and is not a common phenomenon and is known as devitrification (Tomohiro *et al.*, 2004; Mahmud, 2007 and El-Meliegy and Richard, 2012).

In the case of sintering, it involves simultaneous sinter crystallization of glass powdered compact in the absence of nucleating agent. Crystallization starts at glass particle interfaces or grain boundaries (Tulyaganov *et al.*, 2002). The glass powders are compacted and densified at relatively low temperature by exploiting a viscous flow sintering mechanism. After densification, the glass-ceramics material is subjected to crystallization via heat treatment to achieve the desired glass-ceramics microstructural configuration. Alternatively, both densification and crystallization can occur during a single sintering step. Considering the economic advantage of using relatively low processing temperatures, the powder technology technique is ideal for the production of a broad spectrum of advanced materials such as glass-ceramics with specified porosities in the glass-ceramics matrix.

The petrurgic route is the latest technology and it involves gradual cooling of molten glass to achieve concurrent nucleation and crystallization through the incorporation of nucleating agent. Using the petrurgic method, the slow cooling from the molten state induces nucleation and crystal growth of some phases assemblage. Thus, the final microstructure,

and the properties of the resultant glass-ceramics depend majorly on the composition and the cooling rate (Francis *et al.*, 2002).

### **2.15.2 Properties and applications of glass-ceramics**

The properties of glass-ceramics depend on composition, phase assemblage and microstructure (Pinckney and Beall, 2008). The composition and heat treatment determine the dominant phase assemblage formed and the phase assemblage controls physical, chemical durability, thermal and electrical properties (Holand and Beall, 2002). Similarly, the nature of the crystalline microstructure which constitute the crystal size and morphology, textural relationship among the crystals and glass controls mechanical and optical properties such as strength, hardness, toughness, machinability, transparency and opacity (Beall,1992). Also, the microstructural configuration can promote or diminish features of dominant phase assemblage. In addition, the glass composition controls the ability to form a glass and its degree of workability which involves viscosity, effectiveness of nucleation and crystal growth. A broad spectrum of microstructural configuration can result from tailoring both composition and thermal treatment (Rezvani *et al.*, 2005).The properties of glass-ceramics are superior to their corresponding base glasses because they have combination of physical, mechanical, chemical, thermal and biological properties and these properties can be tailored by changes in composition and heat treatment (Hans and Dieter, 2005; Mahmud, 2007; Shackleford and Doremus, 2008).

The phase assemblage generally has a volume part between 50-95% crystallinity and yield an array of materials with interesting properties such as zero or near zero thermal expansion coefficient, high strength, toughness, opacity, hardness, thermal, chemical,

dielectric and biological properties. The aforementioned properties are generally superior to conventional ceramics, metals and even polymers in broad spectrum of applications (Holand and Beall, 2002; Mahmud, 2007). The glass-ceramics material is biocompatible with human tissues; it demonstrated excellent chemical durability or resorb ability (El-Meliegy and Richard, 2012). In addition, glass-ceramics material exhibits good electrical properties such as high resistivity, low dielectric constant, superconductivity as well as high breakdown voltage among others (Kokubo *et al.*, 1986). In the field of medicine, they are used for dental restoration and bone implant because they are biocompatible with human tissues (El-Meliegy and Richard, 2012). In our homes, they are used as cookware and dinnerware simply because they have zero or near zero coefficient of thermal expansion and this has made it possible to transfer them directly from the refrigerator onto a burner or stove without breaking into pieces like glass. As vision ware for failing vision, floor and wall tiles (tilings) among others.

Numerous applications of glass-ceramics are based on their superior resistance to failure due to thermal shock. The phase assemblage in these materials should have a low or near zero coefficient of thermal expansion (Mihailova *et al.*, 2011). Good thermal shock resistance is achieved through a combination of a low expansion phase assemblage and a low residual glassy phase. The most common examples of these materials are vision and Corning ware such as cookware. These glass-ceramics are essentially the same composition, but have different thermal treatments to produce either a transparent or opaque material, respectively. The phase assemblage in these materials is a lithium aluminosilicate, which is either a  $\beta$ -quartz solid solution phase for vision ware or spodumene for Corning ware (Shelby, 2005). A mixture of  $\text{TiO}_2$  and  $\text{ZrO}_2$  in the batch

results in a very efficient nucleation process. Heat treatment below 900°C produces particles (< 100 nm) of  $\beta$ -quartz solid solution phase, which has a refractive index close to the residual glassy phase (very high silica concentration). The resulting material is transparent even though it is highly crystalline. Heat treating of the same material at a temperature above 1000 °C results in the transformation of the  $\beta$ -quartz solid solution phase into  $\beta$ -spodumene, accompanied by grain growth to produce crystals in the 1 to 2  $\mu\text{m}$  range (Shelby, 2005). These materials are opaque due to light scattering from the larger crystals, and are stronger than those based on the  $\beta$ -quartz solid solution.

Glass- ceramics are widely used because of their superior and desirable properties and they can be easily processed and machined using conventional tools. For this reason, they have a broad spectrum of applications as follows; in the field of technology; they are used as nose cones of aircrafts, spacecraft, telescope mirror, ring laser, heat resistant window among others (Garza-Garcia *et al.*, 2007).

### **2.15.3 Advantages of glass-ceramics**

Glass-ceramics have a wide variety of favourable properties like mechanical, chemical, thermal, biological, optical among others which are generally superior to corresponding base glass, conventional ceramics, metals and even organic polymers (Holand and Beall,2002). Glass-ceramics are placed between inorganic glasses and ceramics and the most important advantage of the glass-ceramic formation is the broad spectrum of special microstructures which cannot be produced in any other material (Holand and Beall, 2002). The glassy phase may show different structure and may be arranged in different morphologies, moreso, the phases assemblage posses even wider range of properties

(Holand and Beall, 2002; El-Meligiey and Richard, 2012). It is important to note that glass-ceramics have numerous advantages as follows:

Glass-ceramics can be mass produced and also have the ability to utilize high speed plastic forming techniques developed in glass industries such as blowing, casting, pressing, drawing, spinning, rolling among others to create complex shapes basically free of internal inhomogeneities, in this regard, the shape of the corresponding glass can be preserved even at high degree of crystallinity (Garza-Garcia *et al.*, 2007). It is possible to design their nanostructure or microstructural configuration for a given applications because their properties can be tailored by changes in composition and heat treatment schedule (Demirci and Gunay, 2011). Glass-ceramics have the ability to combine a wide variety of properties like zero or near zero coefficient of thermal expansion with transparency for cookware (Wang *et al.*, 2010). Another advantage is the combination of high strength, toughness with translucency, chemical durability, biocompatibility and relatively low hardness for dental restoration (El-Meliogy and Richard, 2012). In addition, glass-ceramics are stable at high temperature and they are one of the few materials that can be made to have zero coefficient of thermal expansion (Holand and Beall, 2002). Glass-ceramics are biocompatible with human tissues. Infact, human tissues can grow within glass-ceramics and form natural bond. Furthermore, glass-ceramics have superior aesthetics and their low thermal conductivity make them comfortable in the mouth as prostheses (Varshneya, 1994). Glass-ceramics can achieve flexural strength of up to 500 MPa and toughness of about 3MPa equally important no other material shows these properties alongside translucency and then allows itself to be pressed or cast without shrinkage or porosity other than glass-ceramics (Holand and Beall, 2002). Glass-ceramics have high strength and toughness

values compared to base glasses which are brittle materials, glass-ceramics exhibit these outstanding properties simply because of their reproducible, fine-grained and uniform microstructure without porosity. Glass-ceramics are few materials that can be cast or pressed without any dimensional change or shrinkage unlike conventional ceramics in which shrinkage occurs during drying or firing and is usually accompanied by distortion of shape (Bahman and Behzad, 2012a). Additionally, the more complex the composition of the base glass, the greater the diversity of the expected phases assemblage and the higher the probability of achieving a successful combination of properties of the resultant glass-ceramics (Salama *et al.*, 2002). Glass-ceramics are used as multilayer substrates for electronic packaging because of their low dielectric constant of 4-6 as compared to alumina which has a dielectric constant of 9. In view of this, glass-ceramics can be cofired below 1000°C and metallized with gold, silver or copper while alumina can only be cofired at above 1500°C using molybdenum or tungsten (Holand and Beall,2002). Finally, another advantage of glass-ceramics is the products (kitchenware) and this materials are produced on large scale for industrial, technological and household usages (Kaya *et al.*, 2011).

### **2.16 Crystallization Phases that Precipitate from CaO.MgO.Al<sub>2</sub>O<sub>3</sub>.SiO<sub>2</sub> Base Glass System**

The phases assemblage that will precipitate from calcium-magnesium-alumino-silicate base glass system are diopside as the primary phase. The microstructural configuration of diopside has excellent hardness and high chemical durability making it a potential candidate for wear resistance applications. Wollastonite, anorthite, cordierite and melilite are secondary phases suitable for building and coating applications (Carl and Hoche, 2002; Salama *et al.*,2002; Tulyaganov *et al.*, 2002; Mohammed *et al.*, 2003; Tomohiro *et al.*,

2004; Alexander and Mario, 2006; Mahmud, 2007; Daniela *et al.*, 2010; Kaya *et al.*, 2011; Khater, 2011; Bahman and Behzad, 2012a).

### **2.17 Nucleating Agents for CaO-MgO-Al<sub>2</sub>O<sub>3</sub>-SiO<sub>2</sub> Base Glass System**

The most effective nucleating agents for inducing nucleation and subsequent crystal growth (phase separation) for calcium magnesium alumino silicate base glass system to provide bulk crystallization are shown below; Titania (TiO<sub>2</sub>), Chromium (III) oxide (Cr<sub>2</sub>O<sub>3</sub>), Calcium fluoride (CaF<sub>2</sub>), Phosphorus pent oxide (P<sub>2</sub>O<sub>5</sub>) (Salama *et al.*, 2002 and Daniela *et al.*, 2010). But, the most frequently applied nucleating agents are titania (TiO<sub>2</sub>) and zirconia (ZrO<sub>2</sub>) (Rappensberger, 1996) Small amount(3-5 wt%) promote bulk crystallization which results in the precipitation of anorthite as primary phase (Rappensberger, 1996). However, high concentration of titania (10-18 wt %) result in the precipitation of fine-grained glass-ceramics that contains diopside as prevalent phase and anorthite and wollastonite as secondary phases (Rappensberger, 1996). Additionally, small amounts of calcium fluoride (CaF<sub>2</sub>) are effectively utilized as nucleation catalyst. It decreases the viscosity of the glassy melt and the crystallization temperature as well as extends the range of phase separation. Similarly, high percentages of calcium fluoride (CaF<sub>2</sub>) is used on calcium-magnesium-alumino-silicate base glass system and it is crystallized via liquid phase separation with the precipitation of anorthite in the residual glassy phase (Hill *et al.*, 1992).

### **2.18 Glass-Ceramics Microstructures and Phases Assemblage**

The microstructure of glass ceramics is a vital property influencing the other properties and the desired application. The microstructure of glass-ceramics is responsible for the most

valuable properties of the material. The microstructure is composed of fine-grained phases dispersed in the matrix of the residual glassy phase. However, small pores, voids or microcracks may be present in between grain boundaries as shown in Plate II below. The grains or crystals making up the glass-ceramics microstructure are the main phases assemblage or crystalline phases, and the grain boundaries represent the interface that separate two grains in which the orientation of the crystal lattice transforms from one grain to another. However, this contrast with the interphase boundary that represents the boundary between grains of different compositions (Holand and Beall, 2002 and El-Meliegy and Richard, 2012).

The morphology of the major phase grains describing the shape, size, and distribution of the crystals or grains dispersed in the residual glassy phase determines the glass-ceramics properties. Properties that can be tailored by optimizing the microstructure include mechanical properties such as strength, hardness, machinability, chemical resistance and optical properties. The most efficient and desirable microstructure has a fine-grained and uniform microstructure without voids, microcracks or other porosity (El-Meliegy and Richard, 2012). Microstructure being key to mechanical and optical properties, it can as well promote or diminish characteristics of dominant phase. However, microstructure is not an independent variable because it solely depends on the bulk composition and phase assemblage and more importantly, it can be modified through heat treatment to tailored desired properties. In addition, composition controls the phase assemblage which in turn controls the general, physical, chemical and thermal properties (Holand and Beall, 2002 and El-Meliegy and Richard, 2012).

## **2.19 Property Tests**

### **2.19.1 Hardness**

Hardness measures the ability of a material to resist penetration or indentation by means such as abrasion, cutting, bending, drilling, scratching and wear. Hardness is an intrinsic property, which refers to the materials resistance to localized plastic deformation under load (Rezvani, 2011). Resistance to wear by either friction, erosion generally increases with hardness. The greater the hardness of a material, the greater resistance it has to deformation. The hardness of glass-ceramic material depends on strength of the chemical bonds in the phases assemblage and the microstructural configuration which constitutes the size and morphology of crystals and the amount and distribution of the residual glassy phase (Holand and Beall, 2002). Hardness of glass-ceramic material depends on a number of factors as follows: the heat treatment schedule which determines the type and proportion of phases assemblage and the fine-grained and uniform microstructure of interlocking crystals. These promote achieving excellent hardness, as propagating micro cracks are diverted, hindered, slowed down or even inhibited as they cross glassy and phases assemblage grain boundaries. The surface conditions that has to do with edge chipping and coarse surface reduces hardness, the interfacial bond strength, the differences of the phases assemblage and the residual glassy phase, elastic modulus and thermal expansion coefficient mismatch gave rise to micro stresses at the boundaries of crystalline phases and the residual glassy phase as well as the sample dimension (Rappensberger,1996). Microhardness testing is a technique for determination of a material hardness. Important hardness measurement are: Scratch hardness; this measures how resistance a sample is to fracture or permanent plastic deformation due to friction from a sharp object. The Mohs scale is used to measure it. Indentation hardness measures the resistance of a sample to

material deformation due to compressive stress from a sharp object. Indentation hardness scales are Vickers, Rockwell, Knoop, Brinell among others (El-Meliegy and Richard, 2012). However, all these tests follow the same principle. An indenter is used to penetrate the sample. The indenter will apply load on the sample and the area in contact with the indenter will deform slightly. An indentation mark is achieved on the sample. The area of the indentation mark is measured. Hardness is proportional to the ratio of load applied by the indenter to the area of the mark

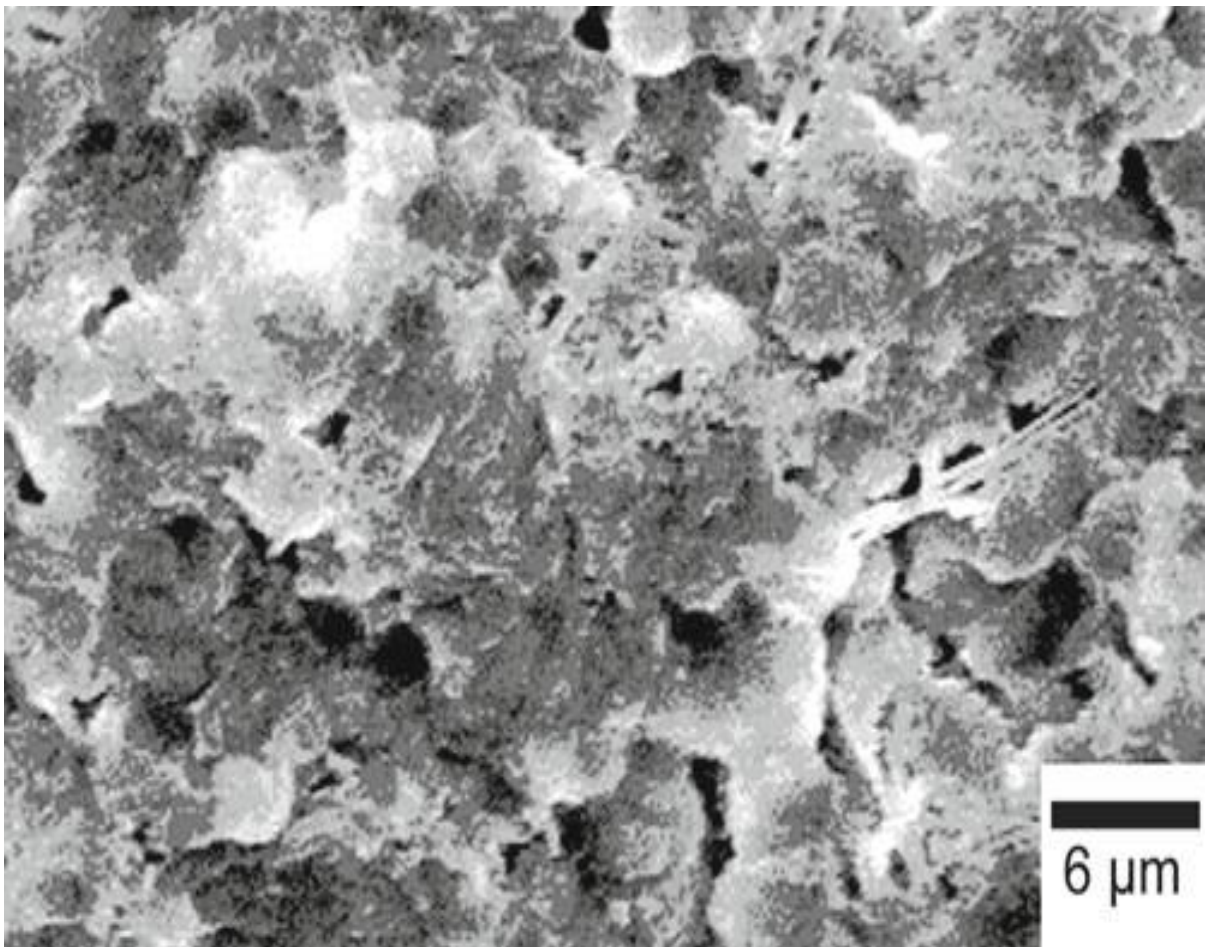


Plate II: Voids present in the microstructure between grain boundaries of glass-ceramic Material (El-Meliegy and Richard, 2012).

formed by the indenter. Micro in microhardness only indicates that the hardness measurements were made in a micro scale. The ability of a harder material to scratch a softer one is the basis for Moh's scale of hardness. However, Vickers and Knoop are the most widely used methods for glasses and ceramics which are based on the indentation method, and both techniques used a diamond pyramid indenter. For ceramics, its usually recorded using ASTM 1327 standard (George,1998). The unit of hardness include Vickers Pyramid Number (HV) or Diamond Pyramid Hardness (DPH).

### **2.19.2 Apparent Density Measurement**

Property tests for this study include; density measurement, porosity measurement, water absorption measurement in accordance to ASTM C 373-88 standard (Chinnam *et al.*, 2015). Apparent density is defined as the volume of a given material including all the pores within it (Amman, 2014). An increase in apparent density of a given glass ceramic increases its volume stability, heat capacity, mechanical and thermal properties as well as chemical stability. If the sample is free of bubbles, voids or other defects, the calculated density is known as true density of the material. If, however, the sample contains bubbles, the calculated density will be less than that of the true density and is called apparent

density (Shelby, 2005). The density of a glass-ceramic material is an additive function of the densities of the crystalline phases present and the residual glassy phase (their contribution is weighted according to their volume fraction). Glass-ceramics generally have higher density than their parent glass and the density difference according to Strnad is usually less than 3wt % (Strnad, 1986).

## **2.20 Differential Thermal Analysis (DTA)**

Differential Thermal Analysis (DTA) of powders involve measurement of temperature difference ( $\Delta T$ ) between the temperature at the center of a powder sample and the temperature at the center of standard which is inert powder as both samples are heated and cooled side-by-side through a standard firing programme. When the samples' temperature is compared to the standards' temperature, the resulting DTA curves exhibit exothermic reaction that releases energy and is shown as peaks and the endothermic reaction absorbs or take energy and is being displayed as valleys. They take place in the sample under study as it is heated from room temperature to the firing temperature and cooled back again to room temperature. Alumina is often utilized as the standard because it is inert over a broad spectrum of temperatures. Alumina is inert simply because it does not react with gases, decomposes or undergo phase changes over range of firing temperatures. DTA analysis requires small sample of dry powders which must be thoroughly dried before carrying out analyses

## **2.21 X-Ray Techniques**

### **2.21.1 X-Ray Fluorescence (XRF)**

X-Ray Fluorescence (XRF) is used to quantitatively measure the elemental and oxide composition of raw materials and bodies. XRF can be used to analyse the composition of a material, the percentage of iron impurities present in a sample. Also, it can be utilized to identify the alkalis present in a sample as well as their respective percentages. X-ray analysis is the method used to determine the chemical composition of an unknown substance as quickly as possible without much preparative effort as solid, powdered and liquid samples can be analysed. Although, achieving accuracy depends on sample preparation and on the quality of the standard utilized. The analysis range from the qualitative statements about the elemental concentration which is subdivided into major, minor and trace constituents and semi quantitative results with high relative error rates to fully quantitative analyses with small error rates. However, the range of detectable elements extend from boron ( $Z=5$ ) to uranium ( $Z=92$ ). The glass industry uses XRF for the following applications; quality control, identification of unknown glass types, raw material analysis, environmental analysis and tracking of trace elements among others (Bach and Krause, 1999 and Kaufmann, 2003). X-ray Fluorescence Measurement is carried out using powdered sample which must be pressed into pellets. In addition, slices of metals and other finished ware can be polished first and then analyzed. X-Ray Fluorescence (XRF) instrument can only measure the composition of material and cannot be used to measure mineralogical composition.

### **2.21.2 X-Ray Diffraction (XRD)**

Identification of mineralogical compositions present in sample powders as well as crystalline phases formed during heat treatment of glass samples are conducted using x-ray

diffraction (XRD) analysis. A scanning speed of 2 degree per min is used for the analysis. XRD of samples do not only identify the phases or mineral compositions but can be used to quantitatively determine the amount of each present. Additionally, it can be used to qualitatively identify the diffraction patterns or peaks of the sample under study as well as checking any crystalline contamination in the ground powdered sample. Some samples undergo several phase changes during firing. Each phase will have a slightly different crystal structure. XRD can be used to detect and identify each of the particular crystalline phases of materials. XRD cannot be conducted on vitreous sample as the technique is based on the distance between long-ranged order atomic planes in crystals and no such long-ranged order atomic planes exist in melts and amorphous materials. Additionally, XRD can be used to identify some minor impurities present in a sample as well as quantitatively determine the amount in each case. Fundamentally, XRF technique identifies oxide composition but XRD analysis determines crystal structures and mineralogical compositions.

## **2.22 Microscopy**

### **2.22.1 Scanning Electron Microscopy (SEM)**

Scanning Electron Microscope (SEM) is utilized to study morphologies, surfaces and structures of materials and this includes: grain shape, grain size, packing of grains, grain boundary, pore shape and size and new phases formed (Amman, 2014). SEM analyses are carried out in vacuum environments, and non conductive samples must be coated with electrically conductive coatings before they can be observed in the scanning electron microscopes (SEM). The technique allows assess to magnified image of particles, objects,

porosities, surface features, surfaces, morphologies, polished sections, fracture surfaces among others. Moreover, shapes and surface textures of grains, identification of impurities and sources of defects are all examples of information that can be studied using SEM. When energy dispersive sensors or spectrometer are incorporated in SEM system, the expected output encompasses maps showing densities and position of various elements present in the samples. SEM measurement is not limited to analysis of morphology and observation of structure and features, but the elemental compositions of the individual features of those structures can be determined as well. In addition, individual particles, grains, intergranular materials, impurities and phase compositions can be distinguished and identified using SEM-EDS analysis.

### **2.23 Energy Dispersive Spectroscopy (EDS)**

Energy Dispersive Spectroscopy (EDS) is used for identifying elemental compositions. When samples are studied using focused electron beams such as scanning electron microscope (SEM), a wide range of signals are emitted from the samples. SEMs are mainly designed to detect, amplify and display secondary electrons emitted when focused electron beams impact samples. But in addition to secondary electrons, focused electron beams also induced X-ray to be emitted from the samples. In SEM without EDS system, all emitted X-rays are simply ignored and lost. But when EDS system has been installed as part of the SEM, images of the samples can be produced using the secondary electron signals and elemental maps of those images can then be generated using the X-ray signals collected by the EDS system. A single EDS can concurrently identify a wide variety of elements. EDS sensors are excellent additions to SEMs and they are routinely utilized in X-ray Fluorescence systems as well.

## **2.24 Loss on Ignition (LOI)**

The loss on ignition (LOI) technique, often referred to as ashing, is a simple and relatively inexpensive method for determining organic matter present in the sample. Loss on ignition is a test designed to measure the amount of moisture or impurities lost on sample's ignition. It is a test used in inorganic analysis particularly in the analysis of minerals. It involves strong heating (igniting) of a sample at specified temperature, allowing volatile substances to escape until a constant mass is achieved. This can be carried out in reactive or inert atmosphere. The test involves placing a few grams of the material in pre-ignited crucible and determining its mass, placing it in a temperature-controlled furnace for a set time, cooling it in a controlled atmosphere and redetermining the mass (ASTM C 25 and ASTM C 114). It should be noted that if sample has lost weight, the loss is positive, if it gained weight, the loss is negative.

## **CHAPTER THREE**

### **3.0 MATERIALS AND METHODS**

#### **3.1 Materials**

The materials and reagents utilized in the course of this research are as follows; feldspar from Matari (Kaduna State), limestone from Kalambaina (Sokoto State), Magnesite from Tsakesimptah (Adamawa State), Chemical grade Titania ( $\text{TiO}_2$ ), Chemical grade sodium chloride ( $\text{NaCl}$ ), poly vinyl alcohol (PVA), lithium tetra borate flux, 1M HCl, 1M NaOH and Keller's reagent.

#### **3.2 Equipment**

The equipment used for this study are as follows; Thermo Fisher ARL 9400 XP + Sequential XRF with Win XRF software, PAN analytical X'Pert Pro powder diffractometer with X'celerator detector, FESEM-EDS model number JEOL JSM-7500F, Vega 3 Tescan SEM-EDS model, Mettler Toledo Differential Scanning Calorimetry (DSC), Small polythene bags, Crucibles, Electric Muffle Furnace Rigaku Model, Ovens, Stirrer,

Crusher, Ball miller, Sieve -105  $\mu\text{m}$  mesh, Shimadzu XRD Testing Machine 6,000 and Vickers Hardness Tester Model MV1-PC.

### **3.3 Methods**

The procedure for the crystallization of quaternary base glass system  $\text{CaO-MgO-Al}_2\text{O}_3\text{-SiO}_2$  to glass ceramics through a two-step heat treatment process from local raw materials involves using feldspar, limestone, magnesite as starting materials. Chemical grade titania ( $\text{TiO}_2$ ) and sodium chloride ( $\text{NaCl}$ ) were used as nucleating agent and fining agent respectively. In addition, it involves samples collection and Preparation, characterization of samples using instrumental analytical techniques, melting of glass batches, and crystallization of base glasses using bulk or a two-step process, characterization of the resultant glass-ceramics and determination of some properties of the resultant glass ceramics under study.

#### **3.3.1 Samples Collection and Preparation**

The samples for this study were sourced from their respective deposits in Nigeria as follows; feldspar sample was collected at random from Matari feldspar deposit in Soba LGA, Kaduna State. Limestone was obtained from Kalambaina limestone deposit in Wamakko LGA of Sokoto State and magnesite was sourced from Tsakesimptah magnesite deposit in Gombi LGA of Adamawa State. Each lump sample (feldspar, limestone and magnesite) was crushed, milled and sieved with Tyler mesh No.140 to desirable particle size distribution of -105  $\mu\text{m}$  and then stored in small polythene bag. Each powdered sample was characterized using instrumental analytical techniques to analyzed the oxides composition by X-ray fluorescence (XRF), mineralogical constituents using X-ray

diffraction (XRD), micro particles study by scanning elemental microscope (SEM), elemental distribution on SEM micrograph using energy dispersion spectroscopy (EDS). In addition, loss on ignition (LOI) was carried out in each case.

### **3.3.2 Determination of Loss on Ignition (LOI)**

Weight of each sample and crucible were recorded and then 1 gm of each sample powders was placed in a crucible and dried at 100°C. Each sample was roasted in a crucible at 1000°C in the furnace. The samples were removed from the furnace and placed in a desiccator as quickly as possible. The samples were allowed to cool to room temperature and then weighed. The loss on ignition was calculated using weight of sample before heating minus the weight of sample after heating is the “initial” loss on ignition. Loss on ignition was calculated using the expression: dividing “ initial loss “ by “initial weight” of sample and multiply by 100.

### **3.3.3 Analysis of samples by X- ray Fluorescence (XRF)**

1g powdered sample in each case was mixed with 6g lithium tetra borate flux and heated to 1050°C to make a stable formula for trace elements analysis. The Thermo Fisher ARL 9400 XP + Sequential XRF with Win XRF software was used for interpretation of results. Powdered samples in each case was mixed with a poly vinyl alcohol (PVA) binder and pressed into pellets using a 10 tons press as required by the machine standard for proper account and analysis. Each sample was placed in the machine for one hour thirty minutes for determination of major oxides constituent and then one hour for analysis of traces oxides in each case. A blank and certified reference material was analyzed with each sample. The three samples were analyzed for oxides of calcium, silicon, magnesium, sodium, potassium, chromium, phosphorus, vanadium, iron, nickel, copper among others.

### **3.3.4 X-ray Diffraction (XRD) analysis of sample powders**

Identification of mineral phases present in each sample was carried out using X-ray diffraction (XRD) analysis. The diffraction patterns were obtained using a PAN analytical X'Pert Pro powder diffractometer with X'celerator detector and variable divergence-and receiving slits with Fe filtered Co-K $\alpha$  radiation. A voltage of 40 kV and current of 30 mA were applied. A scanning speed of 2 degrees was used for analyses. The phases were identified using X'Pert high score software. The relative phases amounts (weights%) were estimated using Rietveld method (Autoquan Program).

### **3.3.5 Microstructural determination of sample powders using SEM-EDS**

Surface morphologies of Matari feldspar and Kalambaina limestone sample powders were carried out using Field Emission Scanning Electron Microscope equipped with Electron Dispersion Spectrometer (FESEM-EDS) model number JEOL JSM-7500F while SEM-EDS analysis of Tsakesimptah magnesite powders was done using Vega 3 Tescan SEM model equipped with Energy Dispersive Spectroscopy (EDS). 1gm of each sample was placed on sample holder of the machine which was then placed into the machine. Each sample was irradiated to generate emission that was translated on SEM micrographs. Also Energy Dispersive Spectrometry (EDS) was carried out for the powdered samples to determine the elemental composition of the different minerals present in each sample.

## **3.4 Batch Formulation**

Six (6) batch compositions of the quaternary base glass system CaO-MgO-Al<sub>2</sub>O<sub>3</sub>-SiO<sub>2</sub> in Table 3.1 were formulated from the starting materials (feldspar, limestone & magnesite). Chemical grade titania (TiO<sub>2</sub>) as nucleating agent was incorporated to the various batches

in varying quantity as follows; 0%, 2%, 4%, 6%, 8% and 10%. Furthermore, 0.3 wt% chemical grade sodium chloride (NaCl) was added as fining agent (Doyle, 1979). The sources of silica ( $\text{SiO}_2$ ), alumina ( $\text{Al}_2\text{O}_3$ ) and potash ( $\text{K}_2\text{O}$ ) was feldspar, the raw material for CaO and MgO were their carbonates sourced from limestone and magnesite respectively. The research adopted Whitney (2002) who reported that alkaline earth aluminosilicate base glass system should have less percentage of alkali oxides, 15-25 wt% alumina ( $\text{Al}_2\text{O}_3$ ), 52-60 wt% silica ( $\text{SiO}_2$ ) and 8-15 wt% alkaline earths. The six sets of batches were test-melted and DSC analysis was carried out on each case.

### **3.5 Production of Glasses**

The batches were thoroughly mixed and each batch was put into a crucible and then placed inside electric muffle furnace. The batches were melted at the temperature range of 1450- 1600°C for 3 hours. The homogeneity of the melt was achieved by frequent swirling the crucibles containing the melts severally at 20 minute intervals. Melting was carried out at normal laboratory condition without controlling the atmosphere. After melting was completed, all glass samples were annealed at 600°C for 1 hour and then cooled to room temperature. After cooling, the physical appearances of the produced glass samples were observed.

Glass No.	SiO <sub>2</sub>	Al <sub>2</sub> O <sub>3</sub>	CaO	MgO	K <sub>2</sub> O	TiO <sub>2</sub>	NaCl	Fe <sub>2</sub> O <sub>3</sub>	Trace(oxides)
Glass 1	52.00	16.00	18.00	8.00	2.00	0.00	0.30	2.50	1.2
Glass 2	52.00	16.00	16.00	8.00	2.00	2.00	0.30	2.50	1.2
Glass 3	52.00	16.00	14.00	8.00	2.00	4.00	0.30	2.50	1.2
Glass 4	52.00	16.00	12.00	8.00	2.00	6.00	0.30	2.50	1.2
Glass 5	52.00	16.00	10.00	8.00	2.00	8.00	0.30	2.50	1.2
Glass 6	52.00	16.00	8.00	8.00	2.00	10.00	0.30	2.50	1.2

Table 3.1: Chemical Composition of the Glass Batches in Oxide Form (wt%)

### **3.6 Differential Scanning Calorimetry(DSC) of Glass Samples produced**

Differential Thermal Analysis (DTA) of the glass powders were conducted using Differential Scanning Calorimeter (DSC) Mettler Toledo Model. Glass powders in the range 4.8000 to 5.9000 mg weight were used. Each sample alongside reference material  $\text{Al}_2\text{O}_3$  was heated from room temperature to 500°C at a heating rate of 10°C/min, and then cooled from 500°C to room temperature at the same heating rate. The DSC analysis was carried out to determine the transition temperature ( $T_g$ ) of each glass powders, and the results obtained were used as guide for determining the heat treatment temperatures required to induce nuclei formation and crystal growths.

### **3.7 Preparation of Glass-ceramics**

The glass samples were subjected to controlled thermal heat treatment schedule so as to promote the process of crystallization and the transformation of glass samples into glass-ceramics. For this reason, a two-stage (bulk) heat treatment schedule was adopted for this research. The heat treatment involves heating the glass samples to the nucleation temperature to achieve nuclei formation followed by subsequent crystal growth. Therefore,

the choice of the heat treatment temperatures was guided by the results of the differential scanning calorimetry (DSC) analysis. The heat treatment temperature of each glass sample was selected using the glass transition temperature ( $T_g$ ) determined by differential scanning calorimetry (DSC). To ensure adequate heterogeneous nucleation, the glass samples (GL1, GL2, GL3, GL4, GL5 and GL6) were heat treated conventionally to nucleation temperatures  $T_1$  (373°C, 367°C, 366°C, 363°C, 356°C and 321°C respectively) and then each glass sample was held (soaked) at varying time of (1, 2, 3 and 4 hours) for nuclei formation. After nucleation, each nucleated glass sample was heat treated further at temperature 300° C above their respective nucleation temperatures at varying time of (1, 2, 3 and 4 hours) for subsequent crystal growth onto the nuclei. Thus, transforming each sample into a glass-ceramics. A heating rate of 5°C/min was kept constant for both nucleation and crystal growth periods because the range of heating rate is 3°C to 10°C/min (El-Meliegy and Richard, 2012). Each sample was furnace cooled to room temperature at 5°C/min with the power of furnace being turned off. Figure 3.1 shows the heat treatment schedule for transformation of glass samples into glass-ceramics.

### **3.8 Property Tests**

A total of twenty four (24) heat treated glass samples were made available for each property test and ASTM standard was adopted all through as follows; Physical properties namely; apparent density, porosity and water absorption were carried out using the American Society for Testing and Materials (ASTM C 373- 88) standard (Chinnam *et al.*, 2015). Hardness test was performed using ASTM 1327 standard (George,1998) and chemical solubility was done using ASTM 6872 (Naruporn *et al.*, 2013).

## RESULT :Heat Treatment Schedule applied to Transform Glass Samples to Glass-ceramics

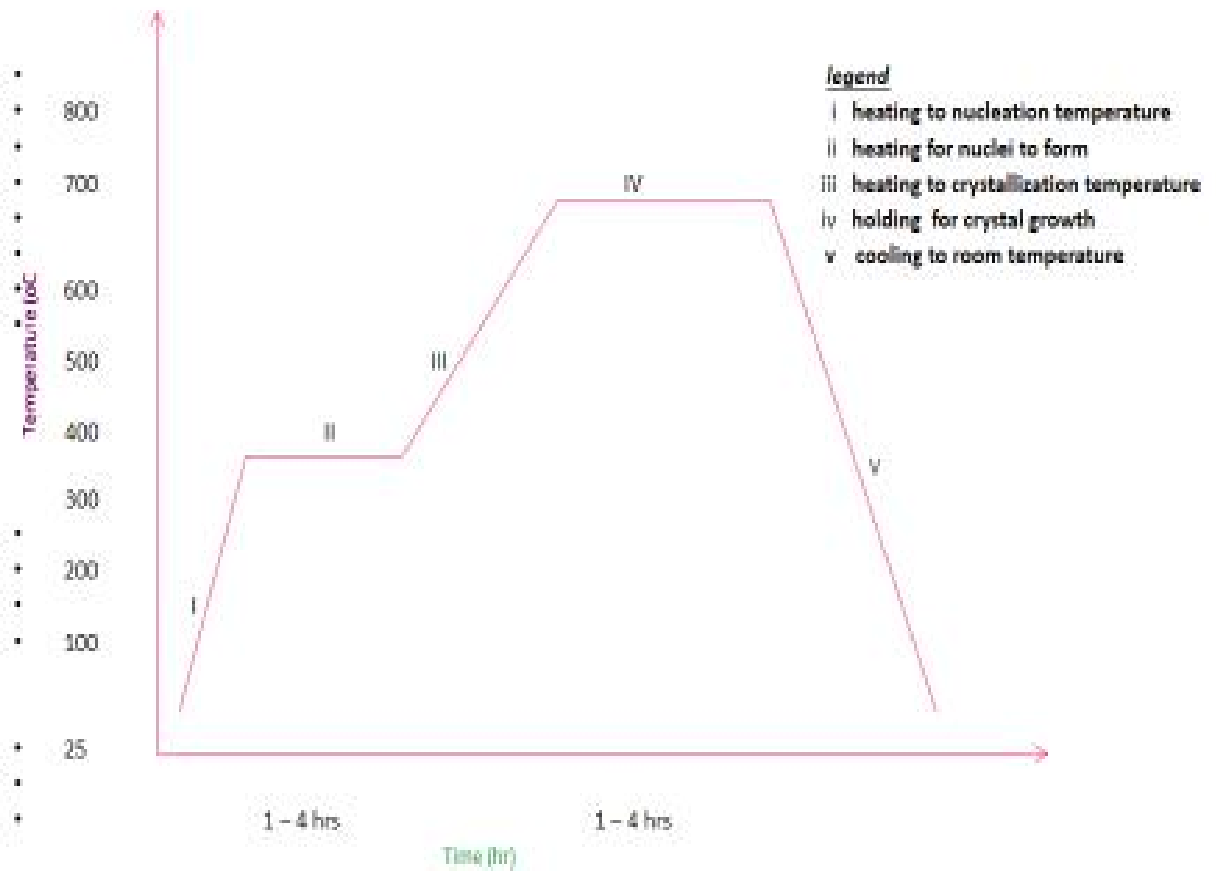


Figure 3.1: Heat treatment schedule applied to transform glass samples into glass-ceramics by controlled nucleation and crystallization processes.

### 3.8.1 Apparent Density Measurement

The measurement of density was conducted using Archimedes method which is in accordance with the ASTM C 373-88 standard. All the glass-ceramics samples under study were weighed in the air and recorded down, this is dry weight (D). The dried samples were transferred into a dessicator to get rid of trapped air. The samples were suspended in a beaker containing distilled water and suspended weight was taken in each case as (S). The samples were further boiled for 30 minutes, cooled and soaked for 24 hours. The test samples were dried using cloth and the soaked weight of each case was recorded as (W). Apparent density was calculated with the assumption that 1 cm<sup>3</sup> of water weighs 1g. The Apparent density of each sample was calculated using expression below:

$$\text{Apparent density} = \frac{D}{W-S} \text{ g/cm}^3$$

Where,

D = Weight of sample in the air (g).

W = Weight of sample soaked in distilled water (g).

S = weight of sample suspended in distilled water (g).

### 3.8.2 Determination of Porosity

Porosity of developed glass-ceramic materials was measured in accordance with ASTM C 373-88 standard (Chinnam *et al.*, 2015). The glass-ceramics samples were oven dried at 110°C for 30 minutes and weighed to obtain the dried weight (D). The test samples were immersed into a beaker of boiling water and allowed to soak for 30 minutes with continuous agitation regularly to assist in the released of trapped air bubbles. Thereafter, the hot water was replaced with cold water and the samples were allowed to soak for 24

hours and their soaked weight was taken as (W). The suspended weight (S) of the samples were recorded using a beaker containing water placed on top of a balance and their porosities were calculated using the relationship:

$$\text{Porosity} = \frac{W-D}{W-S} \times 100 \%$$

Where,

W = Dried weight of sample

D = Soaked weight of sample

S = Suspended weight of sample

P = percentage of porosity

### **3.8.3. Determination of water absorption**

The test was carried out in accordance with the ASTM C 373-88 standard test method for water absorption in glass-ceramic materials (Chinnam *et al.*, 2015). Each dry sample was oven dried at a temperature of 105°C until constant mass was attained. The sample was cooled to room temperature and its weight was recorded as  $M_1$ . The sample was completely immersed in clean water at a temperature of 30°C for 24 hours. The sample was removed from water, traces of water were removed with a damp clean cloth and reweighed as  $M_2$ . The percentage for water absorption of each sample was calculated using the following equation:

$$\text{Water Absorption} = \frac{M_2 - M_1}{M_1} \times 100 \%$$

Where;

$M_1$  = Dried weight of sample

$M_2$  = Saturated weight of sample

$W_a$  = Water absorption

### 3.8.4 Vickers hardness test

The microhardness measurement was performed to investigate the influence of particulate weight fraction on the matrix hardness of the glass-ceramics samples. The technique was based on the degree of penetration of a specified indenter forced into the sample. In this study, twenty four (24) samples were tested using a standard Vickers Hardness Tester Model MV1-PC. The load applied to each sample was 0.3 Kgf and indenter used was square based diamond pyramid. The test was conducted in accordance with ASTM 1327 standard (George,1998).

### 3.8.5 Determination of resistance to chemical attack

After two-stage heat-treatment, ASTM 6872 standard was adopted and the samples were polished to create parallel faces (Naruporn *et al.*, 2013). Samples were washed and oven dried at 100°C for 4 hours and then weighed to the nearest 0.1 mg ( $W_a$ ). The total surface area of the samples was determined to the nearest 0.1 cm<sup>3</sup>. Each sample was individually immersed in 50 ml glass bottle containing 1M HCl. The bottle was closed with its cap and then placed in the oven at 80° C for 12 hrs .Thereafter, each sample was washed and then oven dried at 100°C to achieve a constant mass. Finally, the sample was reweighed to obtain the mass after immersion ( $W_b$ ). Same procedure was applied using aqueous solution of sodium hydroxide (1M NaOH). The chemical solubility of each sample was determined using the following equation:

$$\text{Chemical solubility} = \frac{W_a - W_b}{\text{Surface area of the sample}} \quad \text{ASTM 6872 Standard}$$

Where,  $W_a$  = Initial weight of sample

$W_b$  = Final weight of sample

$C_s$  = Chemical Solubility

### **3.9 X-Ray Diffractometry (XRD)**

Powder XRD was carried out on six (6) pairs of samples and each pair of sample was heat treated for 2 and 4 hours respectively for detection of phases assemblage precipitated in each sample. Phases analyses of samples were done using a PAN analytical X'pert Pro powder diffractometer with X'celerator detector with Fe filtered Co- $K_\alpha$  radiation. Each sample was scanned from 10 to 80 degrees  $2\theta$  at 2 degrees per minute.

### **3.10 Scanning Electron Microscopy (SEM)**

The microscopy was carried out on six (6) pairs of samples and each pair of sample was heat treated for 2 and 4 hours respectively to study morphology using Scanning Electron Microscopy (SEM). Microstructural measurement was performed to examine the microstructural configuration. The surface of each sample under study was polished prior to examination. Characterization is done in etched conditions and etching was accomplished using Keller's reagent. The SEM micrographs of glass-ceramics samples were obtained using scanning electron microscope. Microscopic studies to examine the microstructure were done by Field Emission Scanning Electron Microscope (FESEM) model number JEOL JSM-7500F. Micrographs were taken at appropriate accelerating voltages for the best possible resolution using the secondary electron imaging. Thereafter, each sample was loaded into sample holder and then scanned by electron beam and the reflected beam of electrode was collected and then displayed on FESEM micrograph which represents the surface features of each glass-ceramics sample under investigation.

## CHAPTER FOUR

### 4.0 RESULTS

The characterization of sample powders was performed using instrumental analytical techniques such as XRF, XRD SEM and EDS to determine oxides composition, mineralogical constituents, micro particles and elemental distribution respectively. In addition, batch compositions of varying proportions of nucleating agent (0wt%, 2wt%, 4wt%, 6wt%, 8wt% & 10wt%) were formulated and then melted to form primary glasses. The as-formed glasses of varying amount of nucleating agent were transformed into glass-ceramics using controlled heat treatment scheduled. Thermal, structural morphology and phase analyses were carried out to understand the effects of small amount of progressively increasing  $\text{TiO}_2$  addition on the microstructural configuration of the resultant glass ceramics.

Data were gathered via direct observations and quantitative measurements. The prepared powdered samples of feldspar, limestone and magnesite respectively were for preliminary study. The preliminary study encompasses: XRF, XRD, SEM-EDS as one of the objectives of the study, followed by the conversion of glass samples to glass-ceramics via controlled nucleation and crystallization processes. Thereafter, the powdered glass ceramics were subjected to characterization using XRD and SEM to determine the effects of heat treatment time and titania ( $\text{TiO}_2$ ) addition on microstructure and the number of mineral phases that were formed. Also, properties such as hardness, chemical resistance, apparent density, water absorption and porosity of the produced glass ceramic samples were evaluated.

#### **4.1 Characterization of Matari feldspar powders**

Table 4.1 presents the oxides composition of Matari feldspar powders, Figure 4.1 displays the qualitative XRD patterns of Matari feldspar powders, Table 4.2 reveals the quantitative XRD result determined by Rietveld Method. Plates IIIa to Plate IIIe are the SEM micrographs of Matari feldspar powders at various magnifications and Figure 4.2 displays the Energy Dispersion Spectroscopy (EDS) points of Matari feldspar powders.

#### **4.2 Result for Loss on Ignition (LOI) of Matari feldspar powders**

It is clearly seen from Table 4.1 that the amount of loss on ignition (LOI) in the Matari feldspar sample was (0.14wt%). Loss on ignition (LOI) of Matari feldspar is very negligible (0.14 wt%) and is slightly above the tolerable level for industrial feldspar specifications which usually lacks organic content. The permissible level is 0 wt% LOI. (Alexis and David, 1979).

#### **4.3 Characterization of Kalambaina limestone powders**

Similarly, Table 4.3, Figure 4.3, Table 4.4, Plates IVa - Plate IVd and Figure 4.4 show oxides composition of Kalambaina limestone powders determined by XRF, qualitative XRD patterns of Kalambaina limestone powders, quantitative Rietveld result of Kalambaina limestone powders, Scanning Electron Microscope (SEM) mapping images of Kalambaina limestone powders as well as Energy Dispersion Spectroscopy(EDS) points of Kalambaina limestone powders.

Table 4.1: Chemical composition of Matari feldspar powders as determined by XRF

Oxide	K <sub>2</sub> O	Na <sub>2</sub> O	CaO	SiO <sub>2</sub>	Fe <sub>2</sub> O <sub>3</sub>	Al <sub>2</sub> O <sub>3</sub>	Cr <sub>2</sub> O <sub>3</sub>	P <sub>2</sub> O <sub>5</sub>
Wt. %	11.33	2.75	0.12	67.32	0.10	17.54	0.01	0.35

Oxide	ZrO <sub>2</sub>	MgO	V <sub>2</sub> O <sub>5</sub>	NiO <sub>2</sub>	Cu <sub>2</sub> O	MnO <sub>2</sub>	LOI	TOTAL
Wt. %	0.01	>0.01	<0.01	<0.01	<0.01	0.02	0.14	99.73

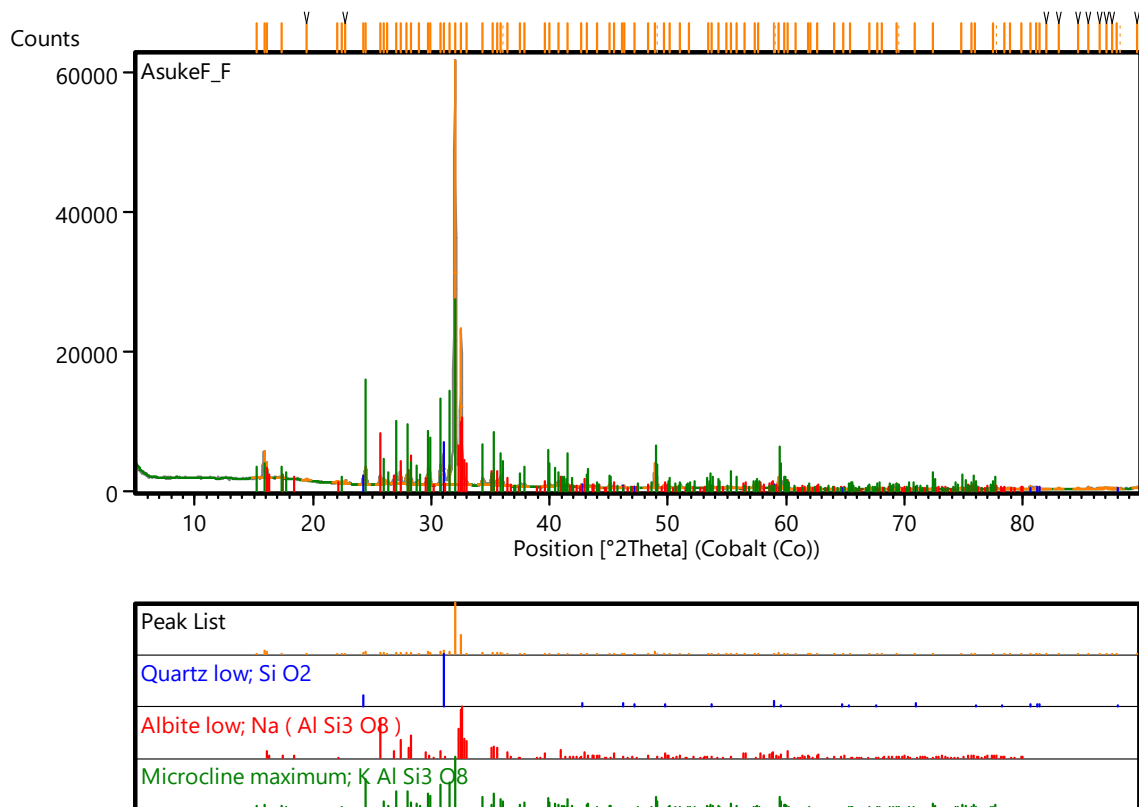


Figure 4.1: Qualitative XRD patterns of Matari feldspar powders showing the mineral phases

Table 4.2: The relative mineral phases assemblage of Matari feldspar powders amount in (wt%) estimated by the Rietveld Method.

Mineral	Weight %	3 $\sigma$ error
Microcline	59.6	2.04
Albite	34.7	2.1
Quartz	5.71	0.87

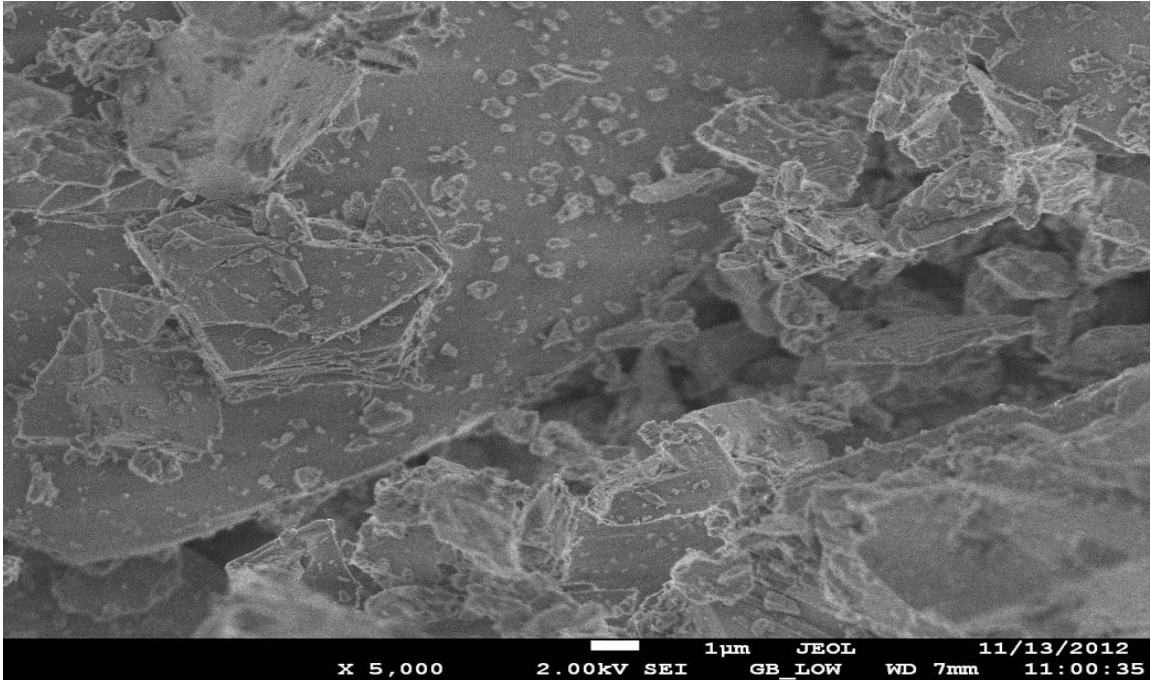


Plate IIIa: SEM micrograph of Matari feldspar powders at x 5000 showing lamellar patterns.

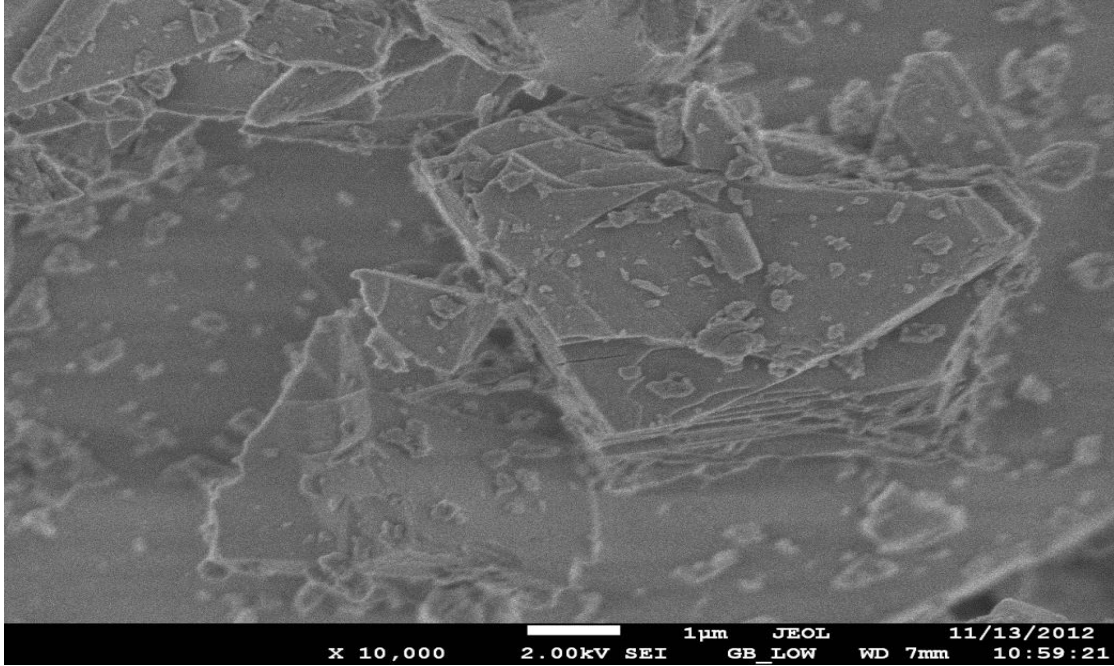


Plate IIIb: SEM image of Matari feldspar powders at x 10,000 demonstrating lamellar twinning.

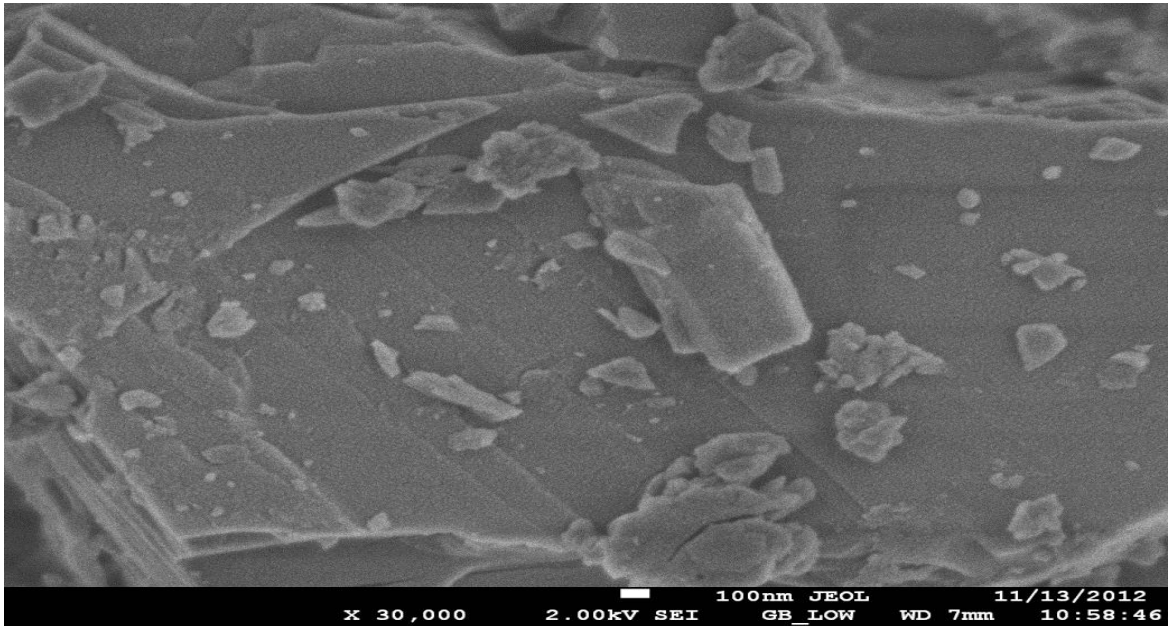


Plate IIIc: SEM photomicrograph of Matari feldspar powders at x 30,000 displaying lamellar twinning.

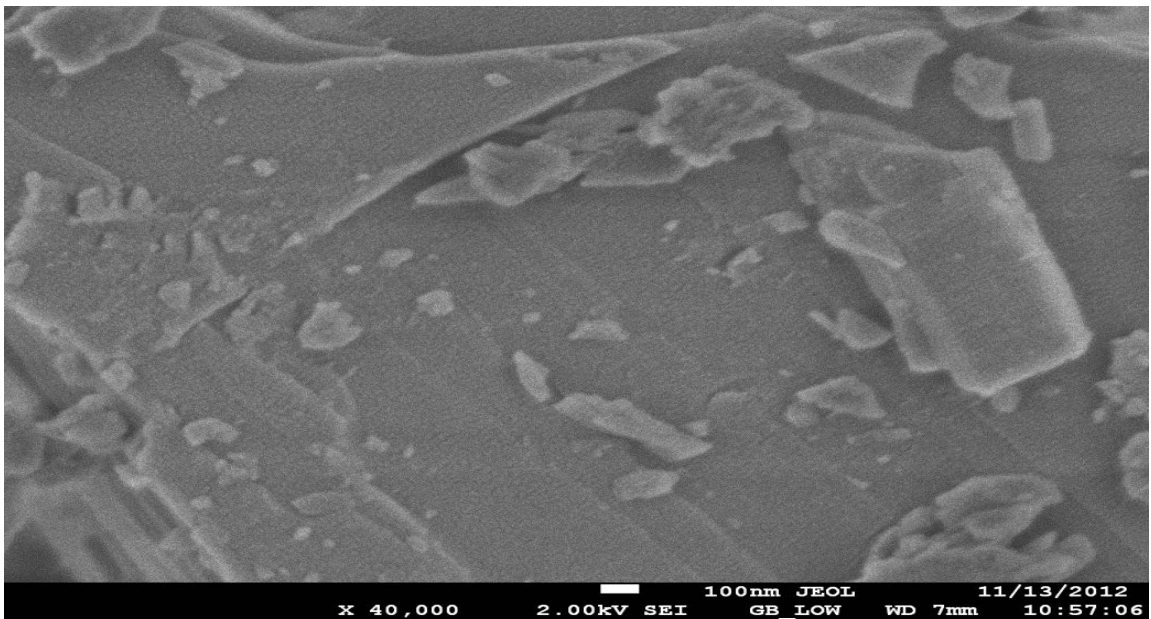


Plate IIIId: SEM mapping of Matari feldspar powders at x 40,000 exhibiting lamellar patterns.

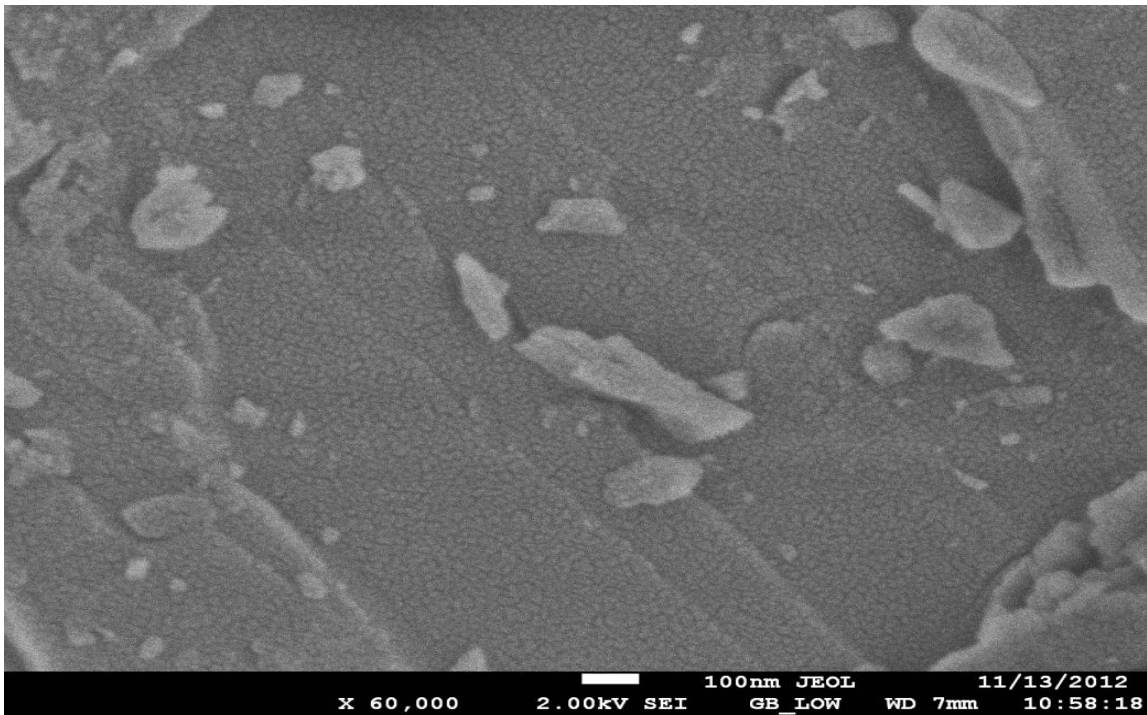


Plate IIIe: SEM micrograph of Matari feldspar powders at x 60,000 displaying lamellar patterns.

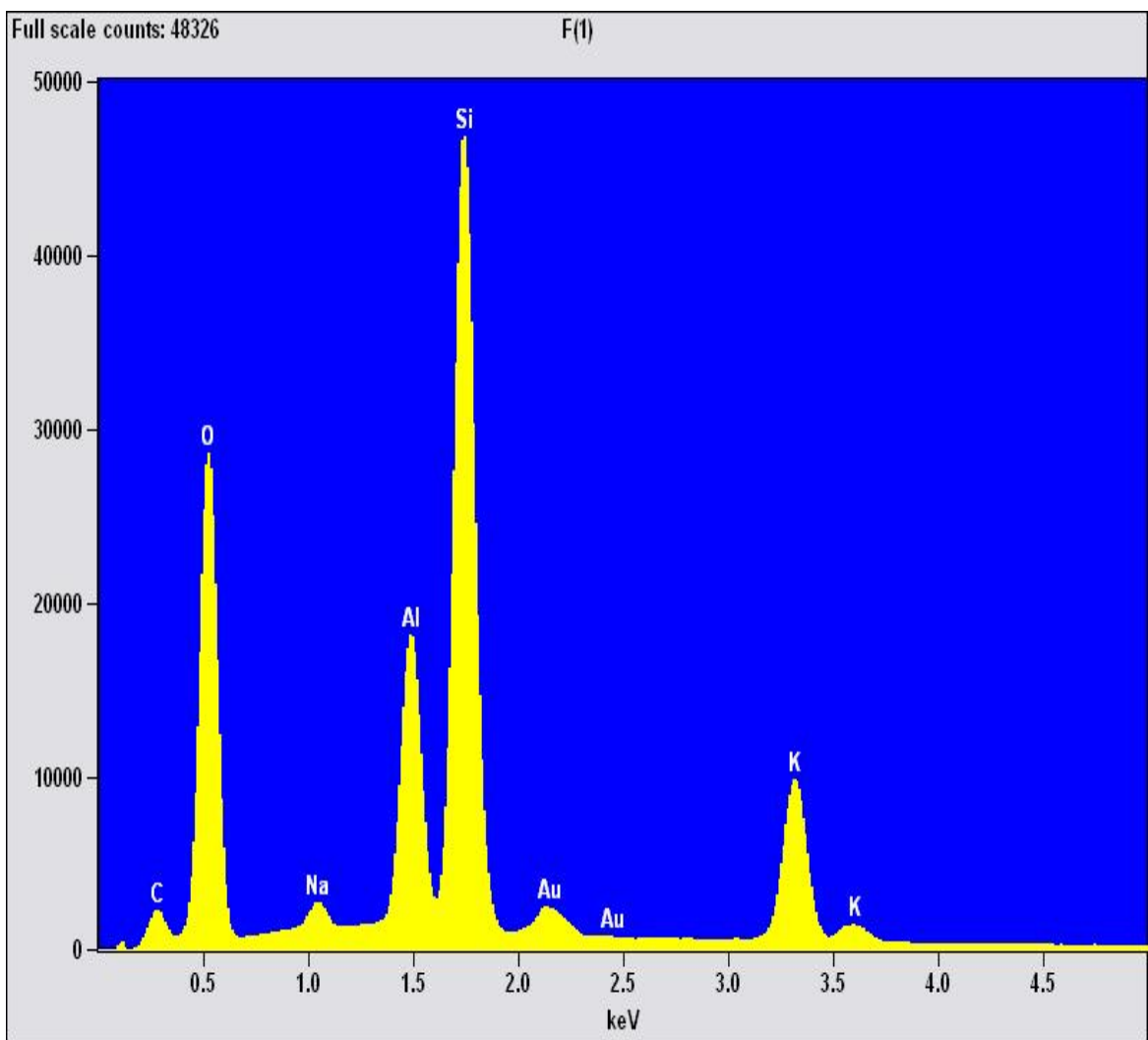


Figure 4.2: EDS of Matari feldspar powders on SEM micrograph showing the elemental composition (C, O, Si, Na, Al, Si, Au and K).

Table 4.3: Oxides composition of Kalambaina limestone powders determined using XRF.

Oxide	CaO	MgO	Fe <sub>2</sub> O <sub>3</sub>	Al <sub>2</sub> O <sub>3</sub>	MnO <sub>2</sub>	TiO <sub>2</sub>	P <sub>2</sub> O <sub>5</sub>	V <sub>2</sub> O <sub>5</sub>
Wt.%	53.08	0.73	0.55	0.75	0.03	0.04	0.11	<0.01

Oxide	ZrO <sub>2</sub>	NiO <sub>2</sub>	Cu <sub>2</sub> O	SiO <sub>2</sub>	Na <sub>2</sub> O	Cr <sub>2</sub> O <sub>3</sub>	LOI	TOTAL
Wt.%	<0.01	<0.01	<0.01	3.38	<0.01	<0.01	42.00	100.75

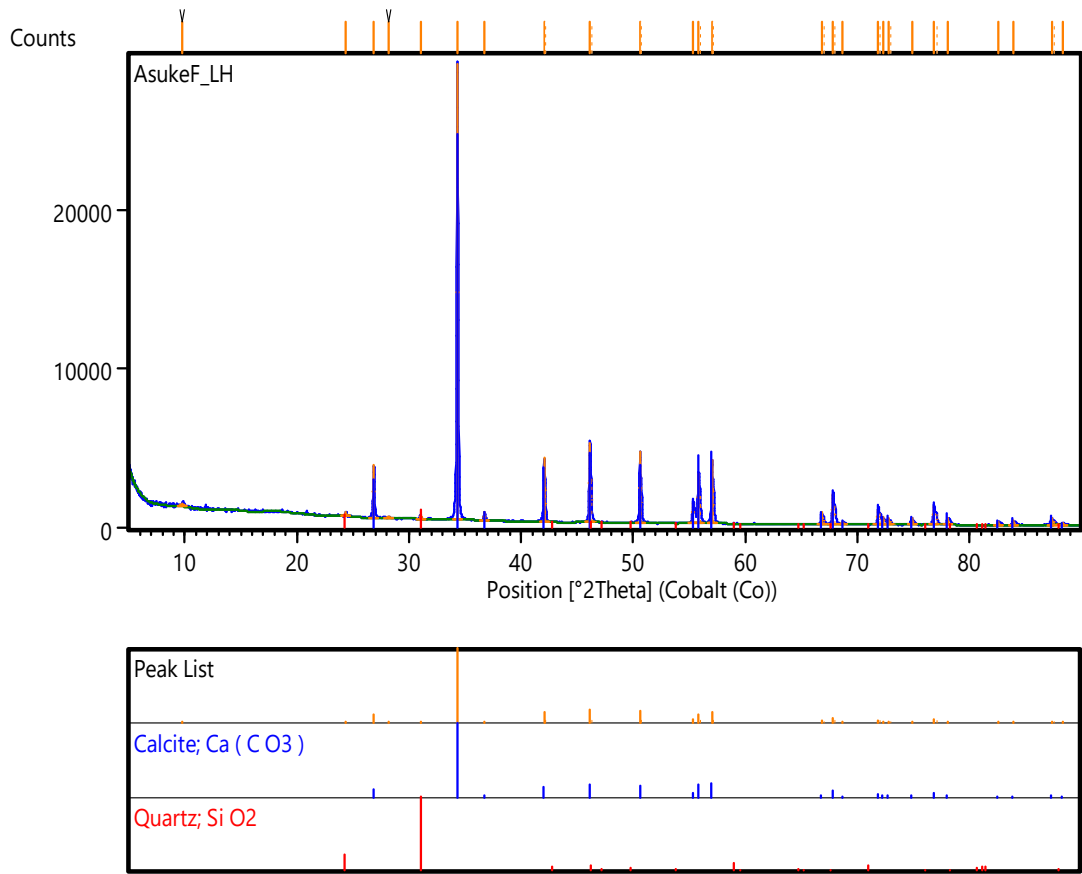


Figure 4.3: Qualitative XRD patterns of Kalambaina limestone powders

Table 4.4: Quantitative XRD results of Kalambaina limestone powders determined by Rietveld Method

Mineral	Weight %	$3 \sigma$ error
Calcite	99.5	0.14
Quartz	0.5	0.14

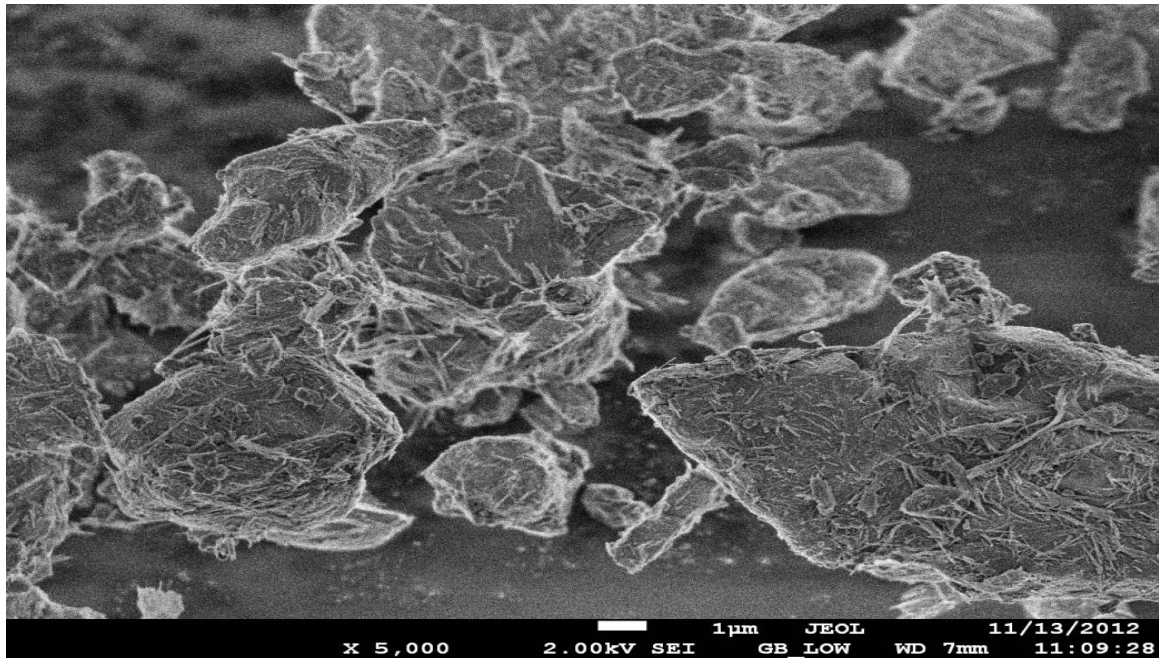


Plate IVa: FESEM micrograph of Kalambaina limestone powders at x 5,000 showing the distribution of mineral phases.

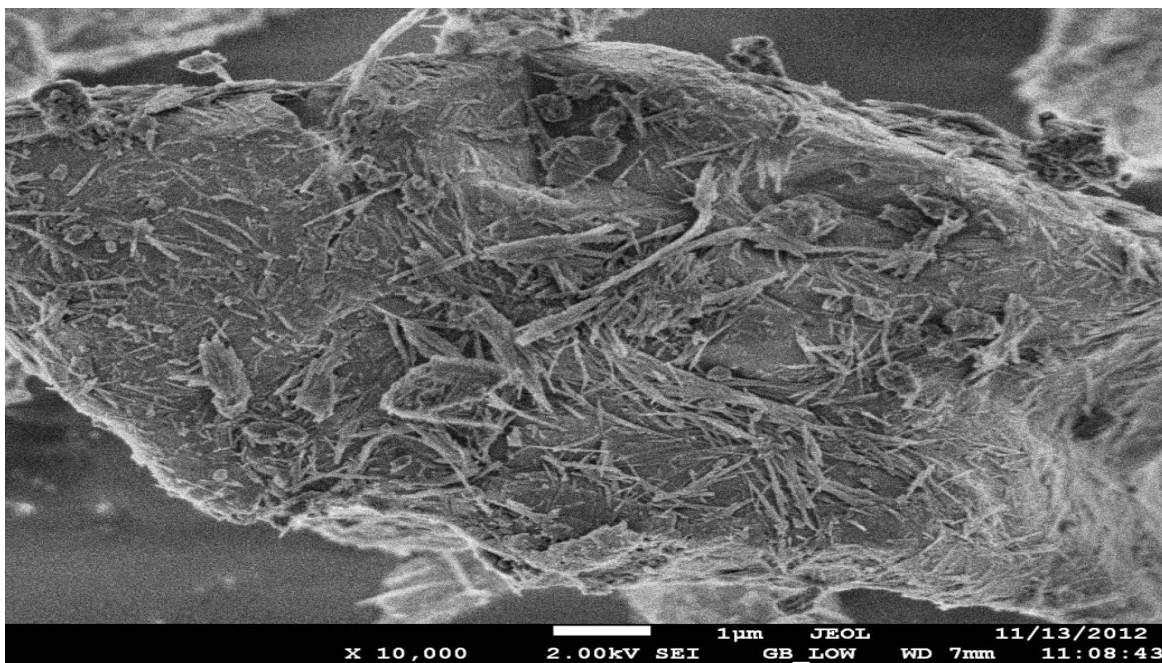


Plate IVb: FESEM micrograph of Kalambaina limestone powders at x 10,000 displaying the micro dusty particles in mass.

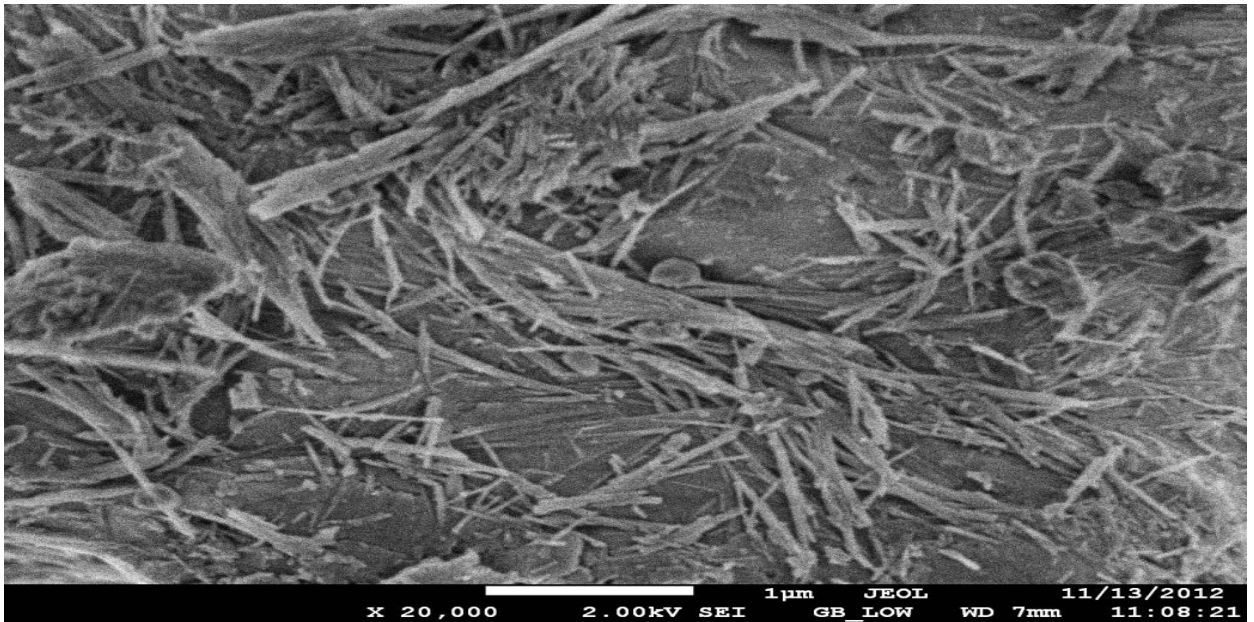


Plate IVc: FESEM image of Kalambaina limestone powders at x 20,000 exhibiting dusty microparticles.

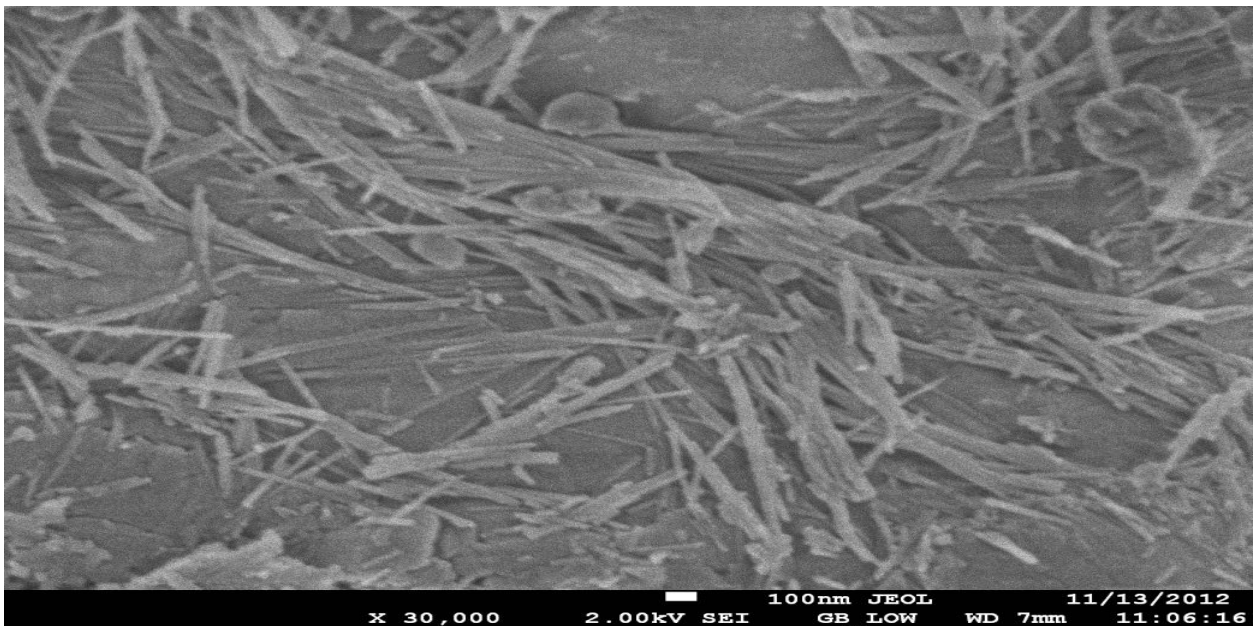


Plate IVd: FESEM micrograph of Kalambaina limestone powders at x 30,000 showing dusty microparticles.

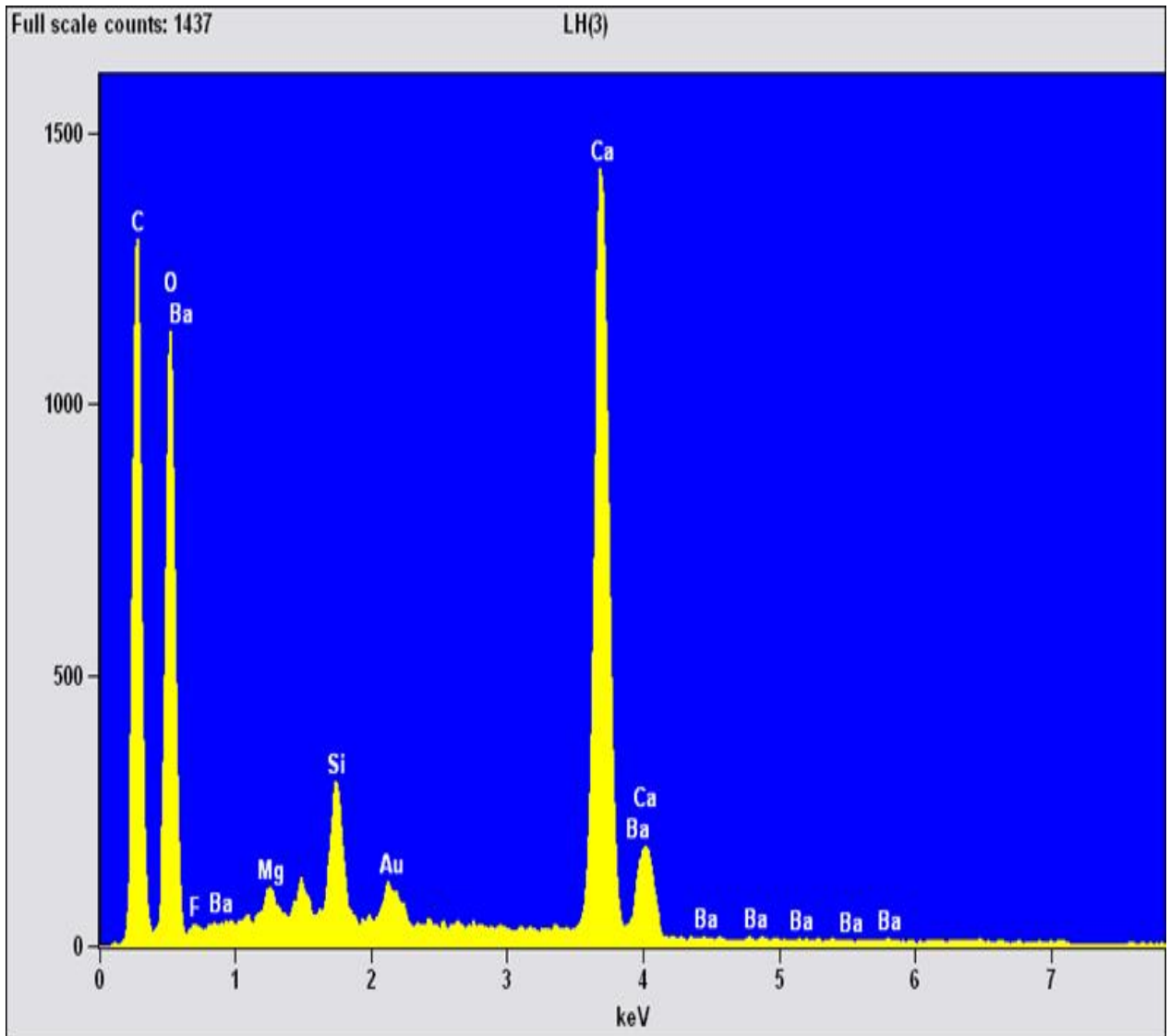


Figure 4.4: Energy dispersion spectroscopy (EDS) of Kalamaina limestone powders on SEM image displaying the elemental components (C,O, Ba, Mg, Si, Ca, Au ).

#### **4.4 Result for the Loss on Ignition (LOI) of Kalambaina Limestone Powders.**

The result for the loss on ignition (LOI) in Table 4.3 of the Kalambaina limestone powders was found to be (42.00wt%).

#### **4.5 Characterization of Tsakesimptah Magnesite Powders**

Table 4.5 displays the oxides composition of Tsakesimptah magnesite powders determined by X-Ray Florescent (XRF), Figure 4.5 shows the qualitative X-Ray Diffraction (XRD) pattern of Tsakesimptah magnesite powders, Table 4.6 presents the mineral details of the sample under study, Table 4.7 demonstrates the quantitative XRD results of Tsakesimptah magnesite powders, Figure 4.6 shows the weight percent of each of the two minerals present in Tsakesimptah magnesite powders, Table 4.8 reveals the crystallite size and lattice strain of Tsakesimptah magnesite powders as determined by Williamson Method, Plates Va to Plate Vb display SEM mapping of Tsakesimptah magnesite powders at various particles grain size distribution (20 $\mu$ m and 100 $\mu$ m respectively). Figure 4.5 shows the XRD patterns of Tsakesimptah magnesite powders at two theta degree indicating the sharpest peak as major mineral and the shorter peaks correspond to minor mineral. Table 4.6 shows XRD minerals detail of Tsakesimptah magnesite, and the findings of the Tsakesimptah magnesite powders revealed that the mineralogical constituents present are olivine HP and calcio-olivine. Figure 4.6 further displays the weight percent of each mineral constituent present in the Tsakesimptah magnesite powders. Figure 4.7 is the Energy Dispersion Spectroscopy (EDS) of Tsakesimptah magnesite powders on SEM micrograph showing the elemental distribution. Table 4.7 displayed the quantitative XRD result of Tsakesimptah magnesite powders displaying the primary mineral as calcio-olivine (80.8 wt%) and secondary minerals as olive HP (19.2 wt%).

Table 4.5 Oxides constituents of Tsakesimptah magnesite powders using XRF

Oxide	MgO	Al <sub>2</sub> O <sub>3</sub>	Na <sub>2</sub> O	P <sub>2</sub> O <sub>5</sub>	Fe <sub>2</sub> O <sub>3</sub>	K <sub>2</sub> O	TiO <sub>2</sub>
Wt.%	63.3	4.86	0.09	0.05	2.86	0.74	0.4

Oxide	CaO	MnO <sub>2</sub>	Rb <sub>2</sub> O	SO <sub>3</sub>	ZrO <sub>2</sub>	SrO	NiO <sub>2</sub>
Wt.%	9.77	0.08	0.083	0.08	0.013	0.05	0.015

Oxide	SiO <sub>2</sub>
Wt.%	17.7

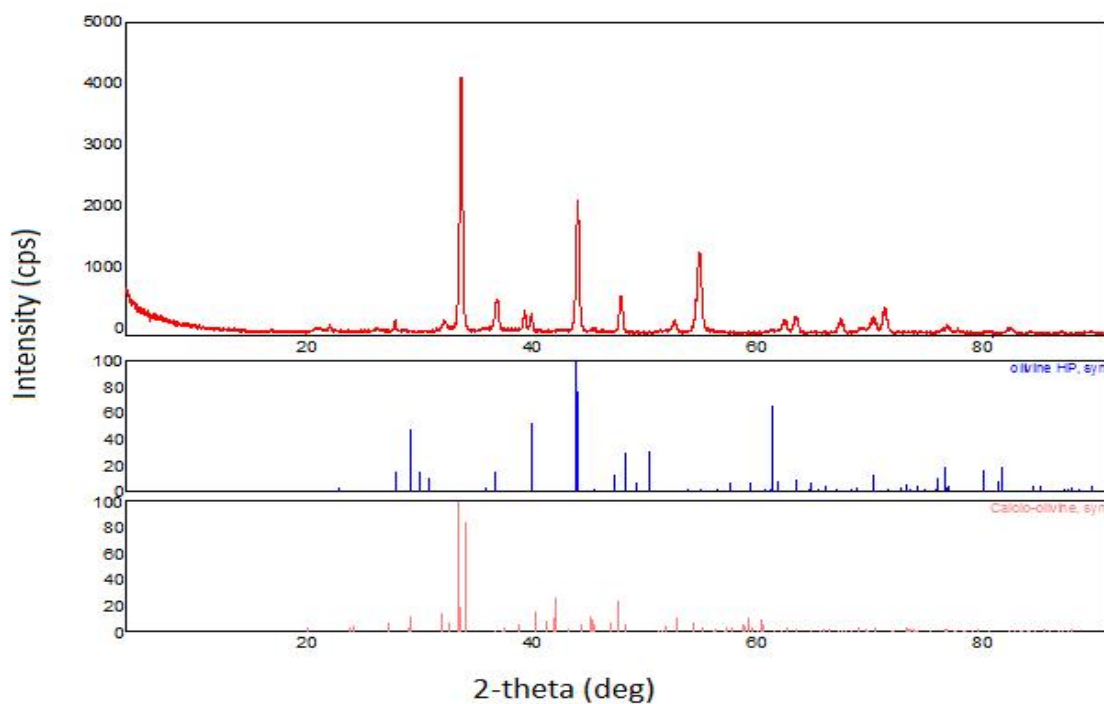


Figure 4.5: Qualitative XRD patterns of Tsakesimptah magnesite powders

Table 4.6: XRD results of Tsakesimptah magnesite powders indicating minerals detail

Phase name	Formula	Figure of merit	Phase reg. detail
Olivine HP, syn	$Mg_2 ( Si O_4 )$	1.851	ICDD (PDF2010)
Calcio-olivine, syn	$Ca_2 ( Si O_4 )$	1.446	ICDD (PDF2010)
Olivine HP, syn	$Mg_2 ( Si O_4 )$	62 : Pnma	ICDD (PDF2010)
Calcio-olivine, syn	$Ca_2 ( Si O_4 )$	62 : Pnma	ICDD (PDF2010)

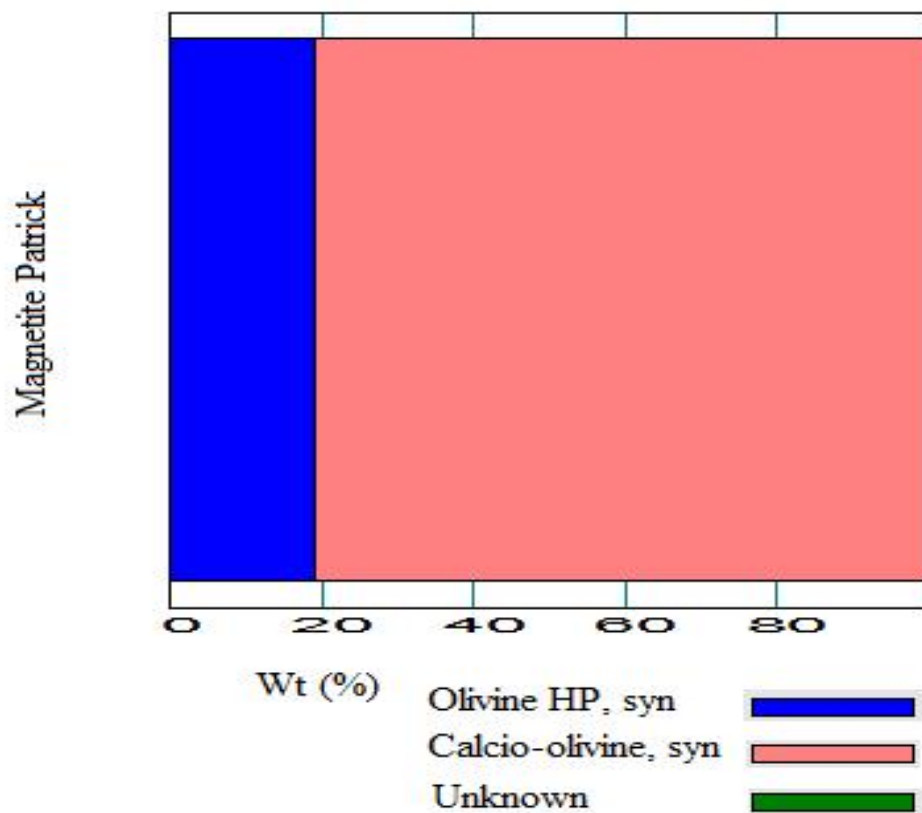


Figure 4.6: Wt.% of mineral phases in Tsakesimptah magnesite powders.

Table 4.7: Quantitative XRD analysis of Tsakesimptah magnesite powders displaying both dominant and lesser minerals.

Phase name	Content (%)
Olivine HP, syn	19.2 (3)
Calcio-olivine, syn	80.8(14)
Unknown	0.000000e+000

Table 4.8: Crystallite size and Lattice strain of Tsakesimptah magnesite determined by Williamson-Hall Technique.

File name	Crystallite size (A)	Strain (%)
Magnetite Patrick	194.01(10)	0.22(2)
Magnetite Patrick	184.95(8)	0.22(2)

Phase name	Crystallite size(A)	Strain (%)
olivine HP, syn	194.01(10)	0.22(2)
Calcio-olivine, syn	184.95(8)	0.22(2)

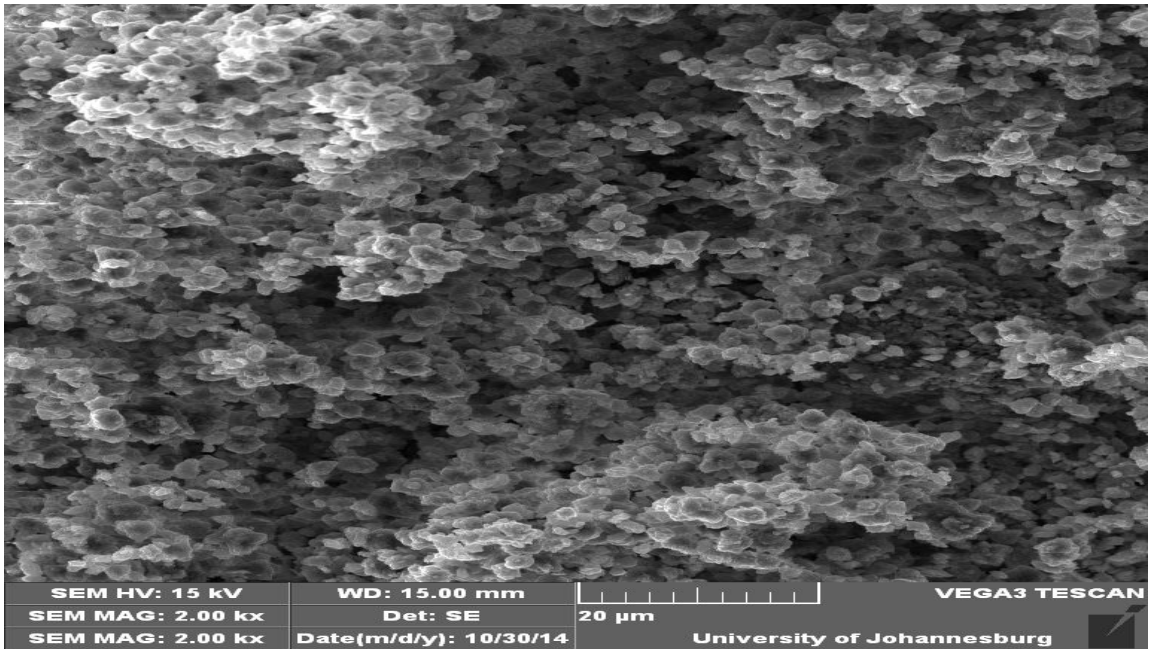


Plate Va: SEM micrograph of Tsakesimptah magnesite powders at  $20\ \mu\text{m}$  showing dusty micro particles.

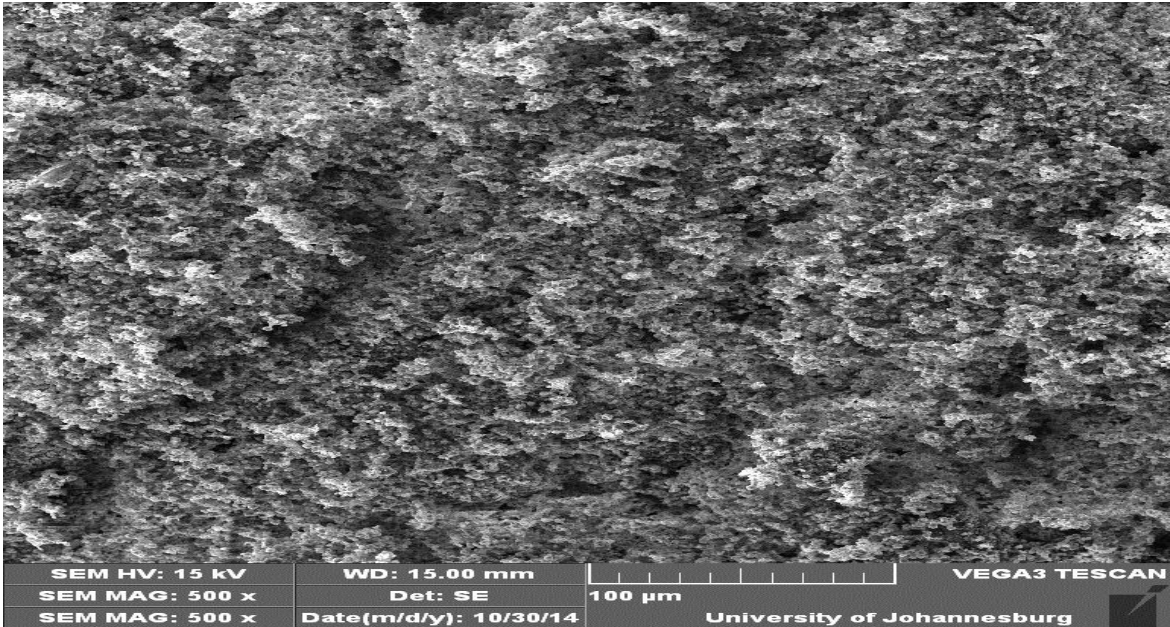


Plate Vb: SEM micrograph of Tsakesimptah magnesite powders at  $100\ \mu\text{m}$  showing dusty micro particles.

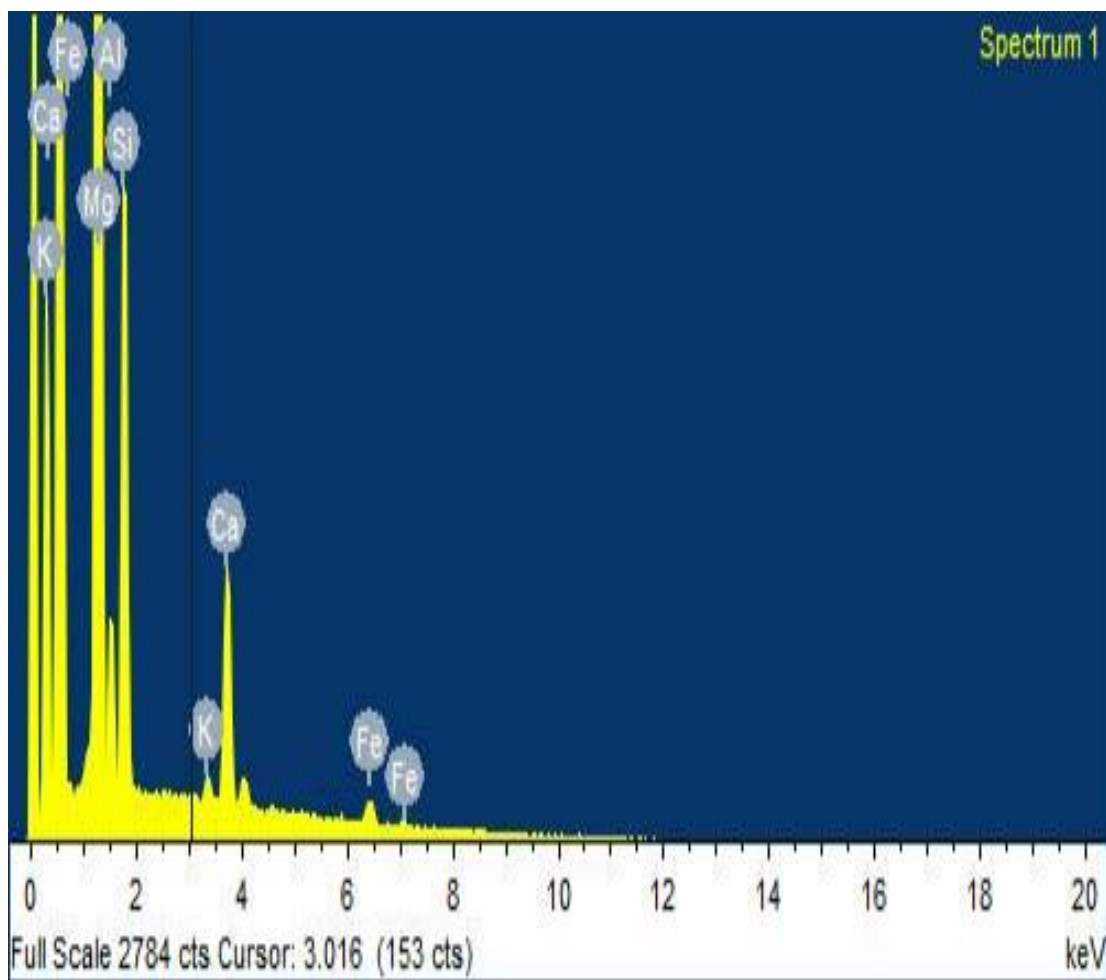


Figure 4.7: Energy Dispersion Spectroscopy (EDS) of Tsakesimptah magnesite powders on SEM micrograph displaying the elements present in the sample (K, Ca, Fe, Mg, Al, Si).

#### **4.6 Produced Glasses**

Each set of the produced glass as described in Section 3.5 yielded a brownish colouration due to large concentration of impurities present in the starting materials (feldspar, limestone and magnesite).

#### **4.7 Transition Temperatures( $T_g$ ) of Glass Samples.**

The glass transition temperature ( $T_g$ ) of the studied base glasses were determined by Differential Scanning Calorimetry (DSC) which was carried out according to the procedure described in section 3.6. Differential scanning calorimetry (DSC) analysis assisted in determining the proper heat treatment schedule to be applied to study the base glasses as heat treatment temperatures were guided by the results of the DSC analysis. Figures 4.8 to 4.13 represent the thermograms of the various glass batches produced as determined by differential scanning calorimetry (DSC).

#### **4.8 Glass-Ceramics Samples Produced**

The first set of produced glasses to which no titania was added were subjected to heat treatment at nucleation temperature ( $373^\circ\text{C}$ ), soaked for 1-4 hours, heat treated further to crystallization temperature ( $667^\circ\text{C}$ ) and then soaked for another 1-4 hours for crystals to grow onto the nuclei. The glass samples did not crystallize because nucleating agent ( $\text{TiO}_2$ ) was not incorporated. After heat treatment, the four samples were still glass. However, second to sixth sets of glass samples produced have various percentages of titania (2wt%, 4wt%, 6wt%, 8wt% and 10wt%) addition. They were heat treated and soaked at various heat treatment temperatures and heat treatment time (1, 2, 3 & 4 hours) for transformation into glass-ceramics via controlled nucleation and crystallization processes. All the samples

to which various amount of nucleating agent was incorporated were successfully transformed into glass-ceramics.

#### **4.9 Results of X-Ray Diffraction (XRD) Test on Glass-Ceramics Samples Produced**

This section was carried out in accordance with the procedure described in 3.9 section. The results of the findings showed that XRD did not identify any phase assemblage crystallized on glass samples to which no titania ( $\text{TiO}_2$ ) was incorporated in the batch composition. The result is expected because controlled crystallization cannot occur in the absence of nucleation catalyst (Holand and Beall, 2002). However, XRD has detected the presence of wider range of crystal phases dispersed within the matrix of heat treated (2 and 4 hours) samples to which various amount (2,4,6,8 & 10 wt%  $\text{TiO}_2$ ) of titania was added as nucleating agent. This result is expected because nucleating agents are generally potential candidates for promoting high density nucleation and crystal growth (Alekseev *et al.*, 2010 and Jing *et al.*, 2013). Also, gradual addition of  $\text{TiO}_2$  as nucleating agent promote achieving high density nucleation and formation of uniform crystals (Holand and Beall, 2002).

The XRD result of glass-ceramic sample that has 2 wt%  $\text{TiO}_2$  added and subjected to thermal treatment at 367/667°C for 2 hours suggested that the diffraction patterns correspond to the following crystalline phases: hematite ( $\text{Fe}_2\text{O}_3$ ) and quartz ( $\text{SiO}_2$ ). The aforementioned phases assemblage were precipitated within the matrix of residual glassy phase. The XRD peaks of the corresponding glass-ceramics sample heat treated at 367/667°C for 4 hours correspond to the following crystalline phases: hematite ( $\text{Fe}_2\text{O}_3$ ),

andradite ( $\text{CaO}\cdot\text{Fe}_2\text{O}_3\cdot 3\text{SiO}_2$ ), carbide ( $\text{Fe}_2\text{C}$ ) and cordierite ( $2\text{MgO}\cdot 2\text{Al}_2\text{O}_3\cdot 5\text{SiO}_2$ ) dispersed in the matrix of the residual glassy phase.

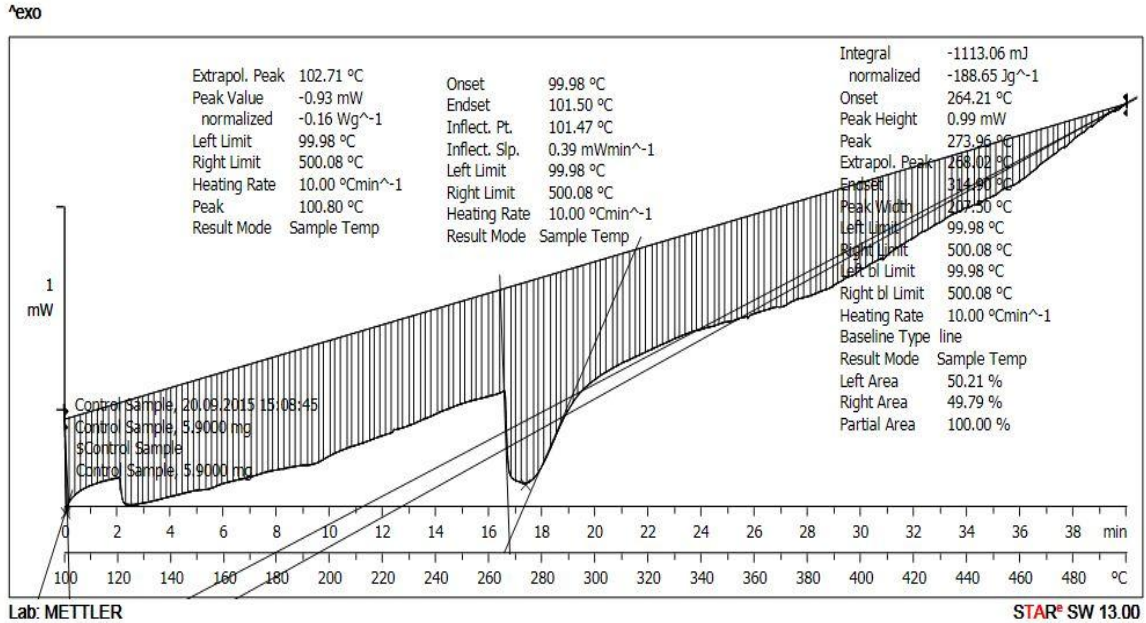


Figure 4.8: DSC Thermogram of Glass (GL1) to which 0wt% titania ( $\text{TiO}_2$ ) was added Exhibiting 273°C as Glass Transition( $T_g$ ) Temperature.

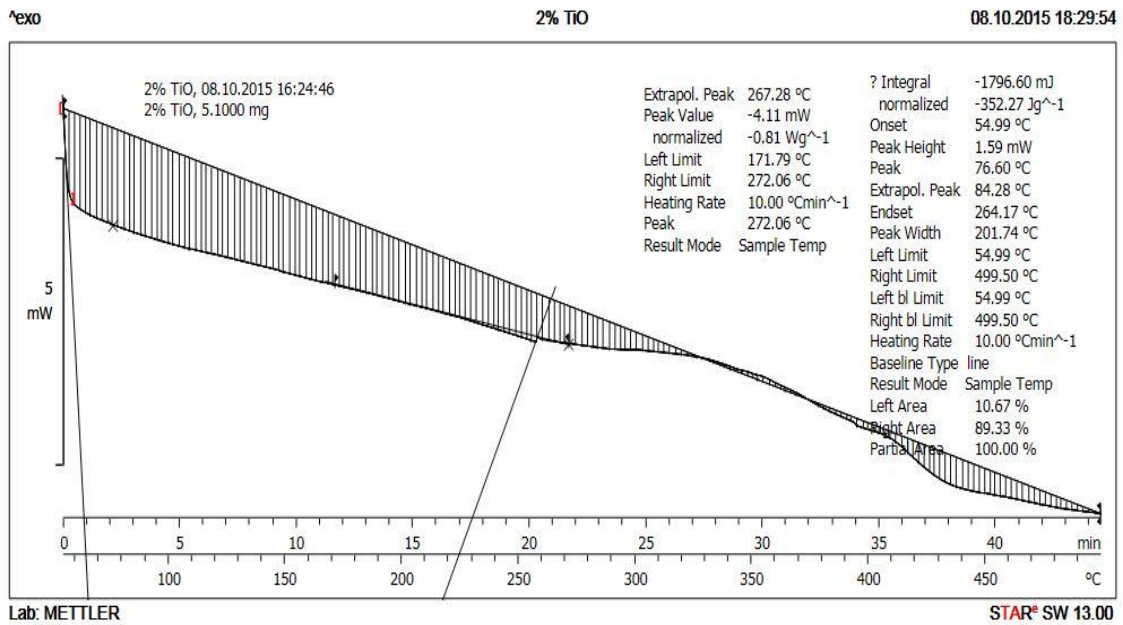


Figure 4.9: DSC Thermogram of Glass (GL2) containing 2wt% titania ( $\text{TiO}_2$ ) showing

267°C as Glass Transition( $T_g$ ) Temperature.

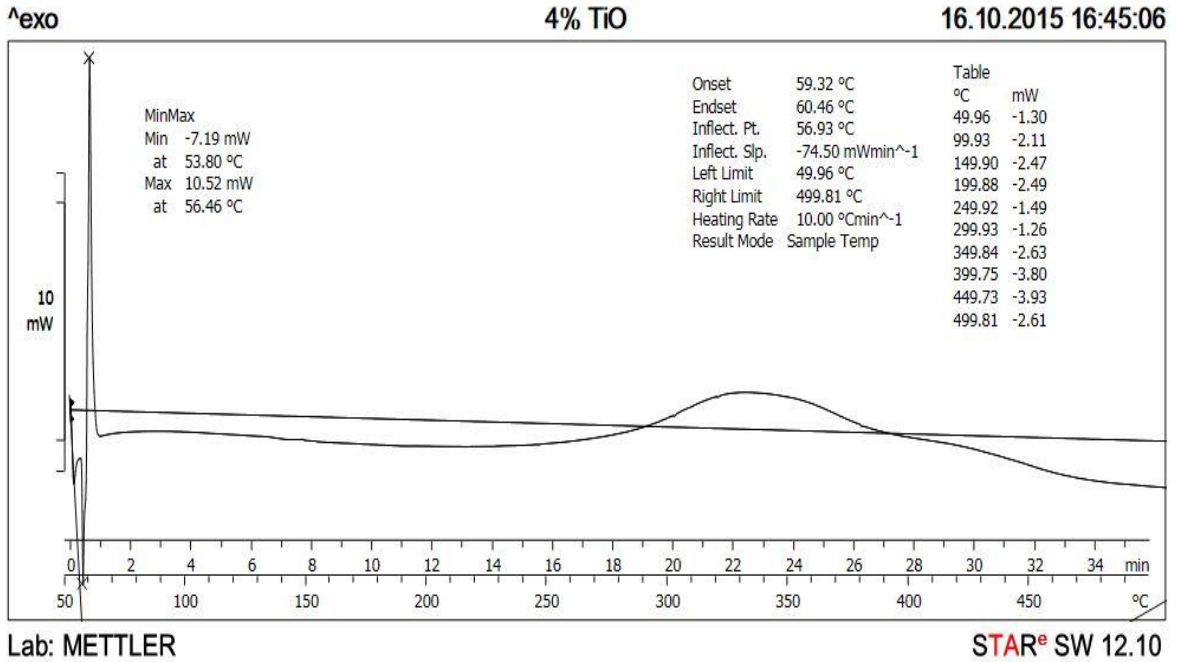


Figure 4.10: DSC Thermogram of Glass (GL3) containing 4wt% titania (TiO<sub>2</sub>) displaying 266°C as Glass Transition( $T_g$ ) Temperature.

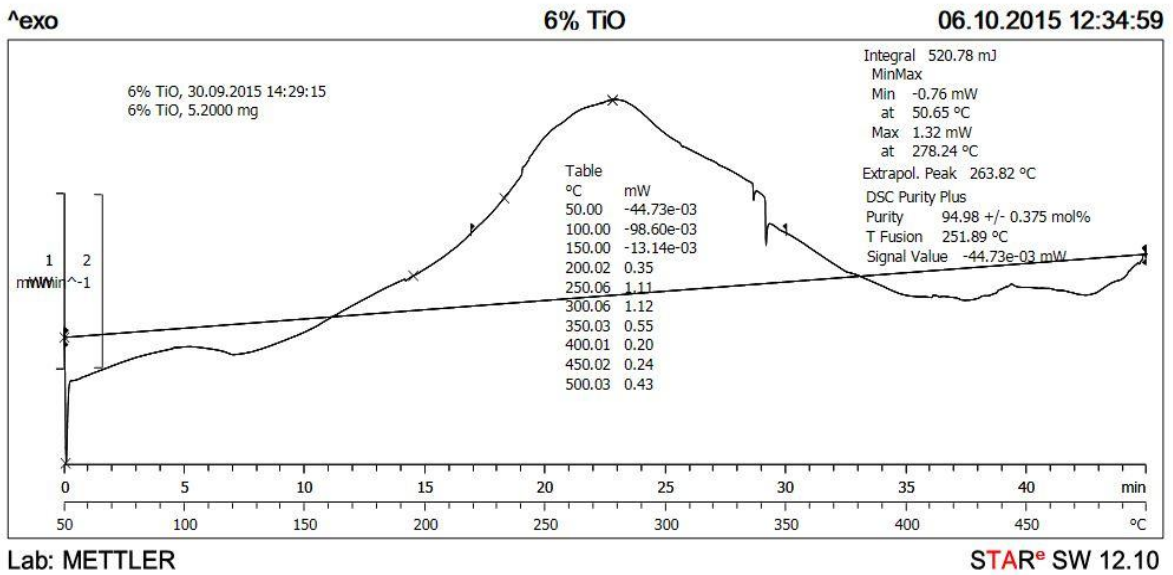


Figure 4.11: DSC Thermogram of Glass(GL4) containing 6wt% titania (TiO<sub>2</sub>) showing 263°C as Glass Transition( $T_g$ ) Temperature.

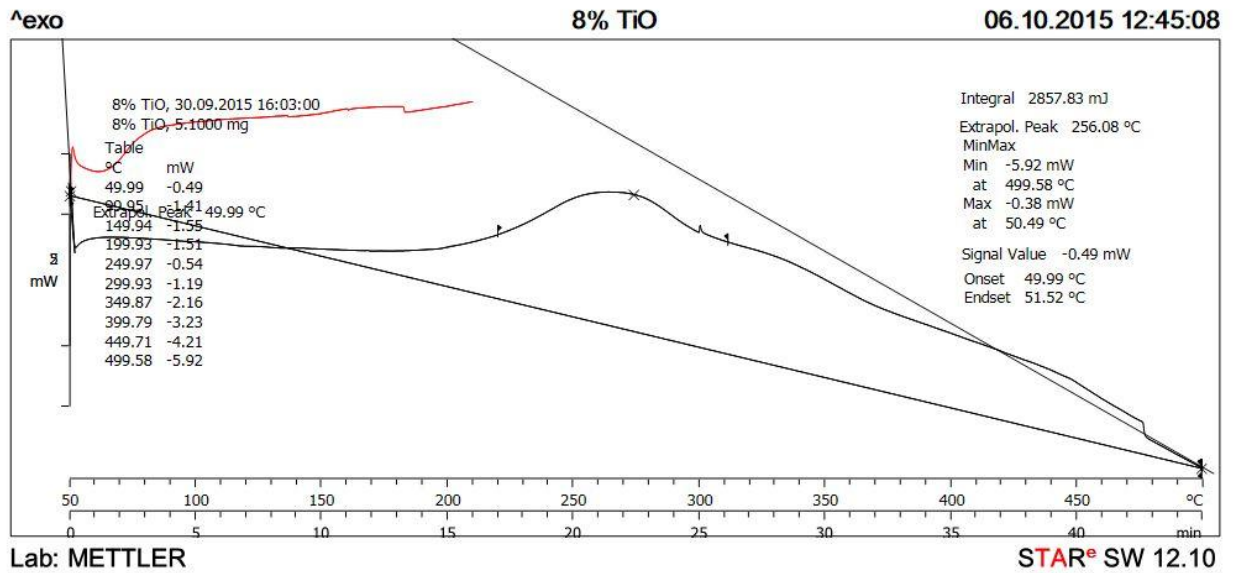


Figure 4.12: DSC Thermogram of Base glass(5) containing 8wt% titania (TiO<sub>2</sub>) displaying 256°C as Glass Transition(T<sub>g</sub>) Temperature.

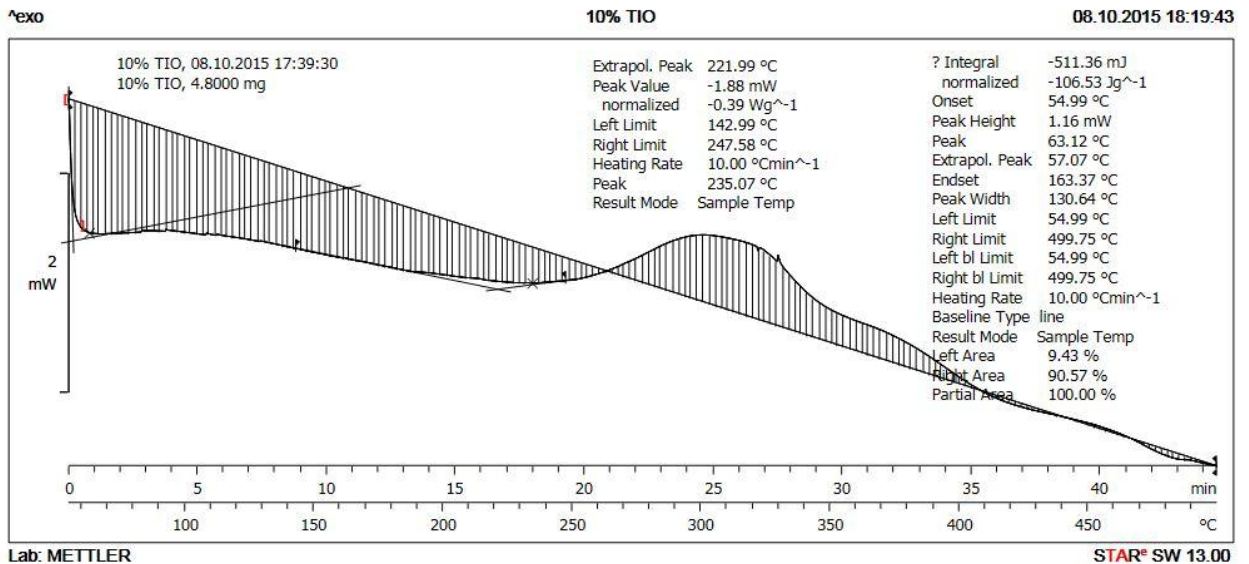


Figure 4.13: DSC Thermogram of Base glass(6) containing 10wt% titania (TiO<sub>2</sub>) showing 221°C as Glass Transition(T<sub>g</sub>) Temperature.

Similarly, the XRD of glass-ceramics sample to which 4 wt% TiO<sub>2</sub> was incorporated and exposed to heat treatment for 2 hours at 366/666 revealed that the XRD intensity peaks correspond to the following phases assemblage: albite (Na<sub>2</sub>O.Al<sub>2</sub>O<sub>3</sub>.3SiO<sub>2</sub>), monticellite (CaO.MgO.SiO<sub>2</sub>) and quartz (SiO<sub>2</sub>) and the phases are embedded in the residual glass. In addition, XRD result of the corresponding glass-ceramics sample heat treated at the same temperature for 4 hours has the following as crystal phases: albite (Na<sub>2</sub>O.Al<sub>2</sub>O<sub>3</sub>.3SiO<sub>2</sub>), monticellite (CaO.MgO.SiO<sub>2</sub>) quartz (SiO<sub>2</sub>) and witherite (BaCO<sub>3</sub>) dispersed in the residual glassy phase.

In a similar manner, the crystal phases dispersed in the residual glass as detected by XRD within the microstructure of glass-ceramic sample to which 6 wt% TiO<sub>2</sub> was incorporated and heat treated for 2 hours at 363/663°C are presented as follows: quartz (SiO<sub>2</sub>), dolomite (CaMg(CO<sub>3</sub>)<sub>2</sub>) and albite (Na<sub>2</sub>O.Al<sub>2</sub>O<sub>3</sub>.3SiO<sub>2</sub>). However, the XRD result of the corresponding glass-ceramics sample heat treated at the same temperature for 4 hours exhibited the following crystal phases: witherite (BaCO<sub>3</sub>), albite (Na<sub>2</sub>O.Al<sub>2</sub>O<sub>3</sub>.3SiO<sub>2</sub>), wollastonite (CaO.SiO<sub>2</sub>) and quartz (SiO<sub>2</sub>). The finding was in agreement with (Salama *et al.*, 2002) who disclosed that adding TiO<sub>2</sub> as nucleating agent augments the crystallization of wollastonite.

The XRD patterns of glass ceramics sample containing 8 wt% TiO<sub>2</sub> and subject to heat treatment for 2 hours at 356/656°C has the following crystalline phases dispersed in the matrix of the residual glassy phase: wollastonite (CaO.SiO<sub>2</sub>), calcite (CaCO<sub>3</sub>) and albite (Na<sub>2</sub>O.Al<sub>2</sub>O<sub>3</sub>.3SiO<sub>2</sub>). However, XRD result of the corresponding sample heat treated at the same temperature for 4 hours contained the following crystal phases dispersed in the matrix of residual glassy phase: hematite (Fe<sub>2</sub>O<sub>3</sub>), anorthite (CaO.Al<sub>2</sub>O<sub>3</sub>.2SiO<sub>2</sub>),

wollastonite ( $\text{CaO.SiO}_2$ ), cordierite ( $2\text{MgO.2CaO.5SiO}_2$ ) and andradite ( $3\text{CaO.Fe}_2\text{O}_3.3\text{SiO}_2$ ). According to Salama *et al* (2002) using  $\text{TiO}_2$  as nucleation catalyst leads to precipitation of anorthite and wollastonite.

The XRD patterns of glass-ceramics sample containing 10 wt%  $\text{TiO}_2$  and subjected to heat treatment at 321/621°C for 2 hours precipitated the following crystal phases: wollastonite ( $\text{CaO.SiO}_2$ ), monticellite ( $\text{CaO.MgO.SiO}_2$ ), quartz ( $\text{SiO}_2$ ), andradite ( $\text{CaO.Fe}_2\text{O}_3.3\text{SiO}_2$ ) and cordierite ( $2\text{MgO.Al}_2\text{O}_3.5\text{SiO}_2$ ). This result is in agreement with (Salama *et al.*,2002) who stated that addition of  $\text{TiO}_2$  can crystallized wollastonite in the glassy phase.

The XRD patterns of glass-ceramic sample that has 10 wt%  $\text{TiO}_2$  and subjected to heat treatment to crystallized it at 321/621°C for 4 hours has the following phases assemblage within the residual glassy phase: albite ( $\text{NaO.Al}_2\text{O}_3.3\text{SiO}_2$ ), quartz ( $\text{SiO}_2$ ), wollastonite ( $\text{CaSiO}_3$ ), titanate ( $\text{CaO.TiO}_2.\text{SiO}_3$ ), microcline ( $\text{K}_2\text{O.Al}_2\text{O}_3.3\text{SiO}_2$ ), hematite ( $\text{Fe}_2\text{O}_3$ ), monticellite ( $\text{CaO.MgO.SiO}_2$ ), andradite ( $3\text{CaO.Fe}_2\text{O}_3.3\text{SiO}_2$ ), calcite ( $\text{CaCO}_3$ ) and cordierite ( $2\text{MgO.Al}_2\text{O}_3.5\text{SiO}_2$ ). The findings is in agreement with (Barsoum, 1994; Rappensberger, 1996 and Mahdavi, 2011) who reported that the incorporation of 10-18 wt%  $\text{TiO}_2$  to the base glass system promotes achieving high density nucleation and crystallization leading to the precipitation of considerable number of phases assemblage. In addition, according to Holand (1991), Rappensberger (1996), Salama *et al* (2002) and Daniela *et al* (2010) incorporation of  $\text{TiO}_2$  as nucleating agent allows the formation of nucleation phase such as titanate. Besides, microcline and wollastonite would be precipitated. Figures 4.14 – 4. 23 are the X-ray diffraction patterns of glass-ceramics

samples heat treated at various heat treatment temperatures between 2 and 4 hours heat treatment time.

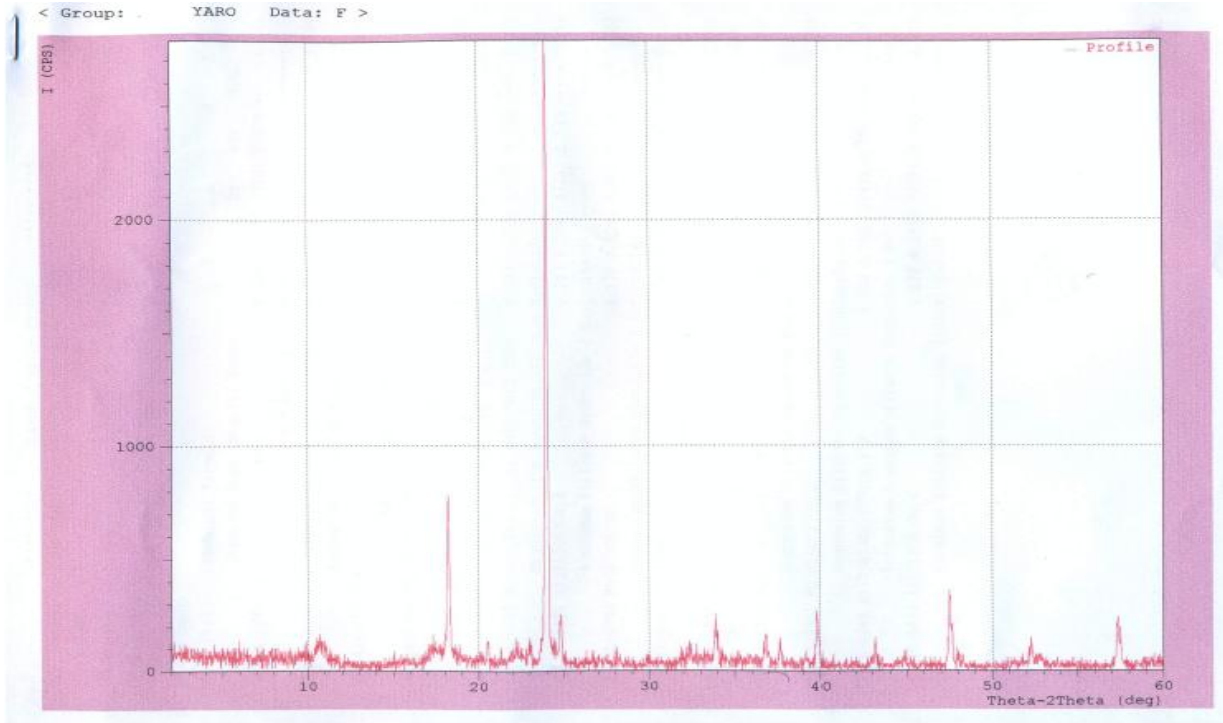


Figure 4. 14 : XRD patterns of glass-ceramics sample to which 2 wt% TiO<sub>2</sub> was added and then heat treated for 2 hours.

Table 4.9 : Mineral phases assemblage of glass-ceramics sample to which 2 wt% TiO<sub>2</sub> was added and heat treated for 2 hours.

Phase	Chemical name	Chemical formula
Hematite	Iron(III)Oxide	Fe <sub>2</sub> O <sub>3</sub>
Quartz	Silicon dioxide	SiO <sub>2</sub>

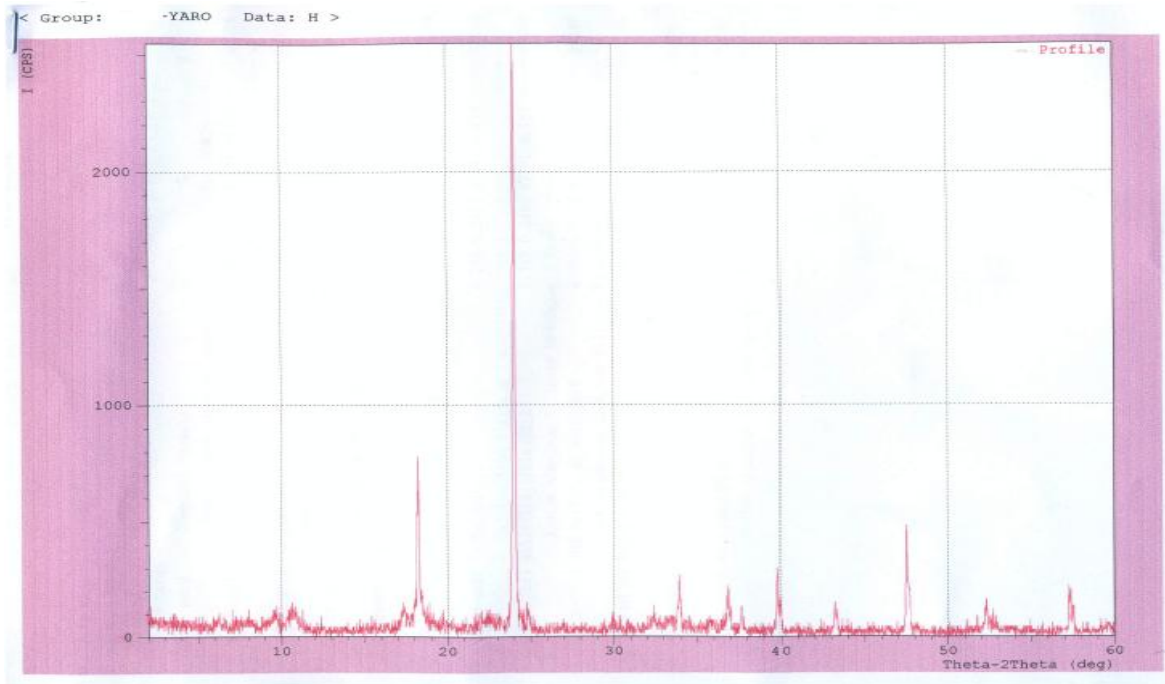


Figure 4.15 : XRD patterns of glass-ceramics sample to which 2 wt% TiO<sub>2</sub> was added and then heat treated for 4 hours.

Table 4.10 : Mineral phases assemblage of glass-ceramics sample containing 2 wt% TiO<sub>2</sub> and heat treated for 4 hours.

Mineral phase	Chemical name	Chemical formula
Hematite	Iron(III)Oxide	Fe <sub>2</sub> O <sub>3</sub>
Andradite	Calcium-iron-silicate	3CaO.Fe <sub>2</sub> O <sub>3</sub> .3SiO <sub>2</sub>
Cordierite	Magnesium-alumino-	2MgO.2Al <sub>2</sub> O <sub>3</sub> .5SiO <sub>2</sub>

	silicate	
--	----------	--

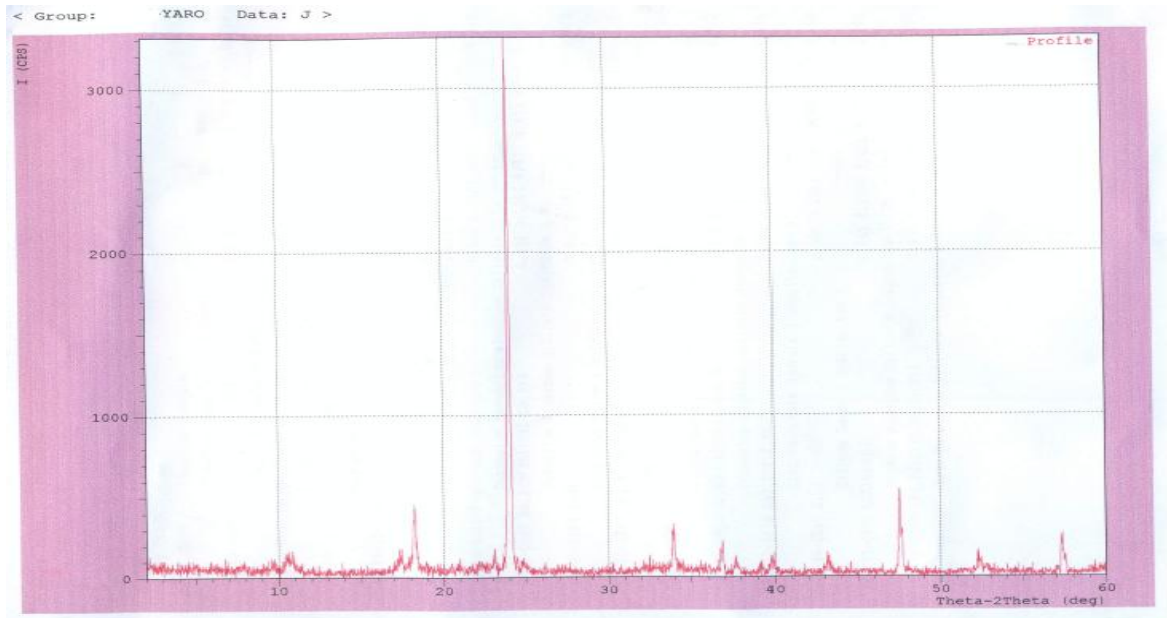


Figure 4.16 : XRD patterns of glass-ceramics sample that has 4 wt% TiO<sub>2</sub> and then heat treated for 2 hours.

Table 4.11 : Mineral phases assemblage of glass-ceramics sample that contains 4 wt% TiO<sub>2</sub> and then heat treated for 2 hours.

Mineral phase	Chemical name	Chemical formula
Albite	Sodium-alumino-silicate	Na <sub>2</sub> O.Al <sub>2</sub> O <sub>3</sub> .3SiO <sub>2</sub>
Monticellite	Calcium-magnesium-silicate	CaO.MgO.SiO <sub>2</sub>
Quartz	Silicon dioxide	SiO <sub>2</sub>



Figure 4.17: XRD patterns of glass-ceramics sample to which 4 wt% TiO<sub>2</sub> was added and then heat treated for 4 hours.

Table 4.12: Mineral phases assemblage of glass-ceramic sample to which 4 wt% TiO<sub>2</sub> was added and heat treated for 4 hours.

Mineral phase	Chemical name	Chemical formula
Albite	Sodium-alumino-silicate	Na <sub>2</sub> O.Al <sub>2</sub> O <sub>3</sub> .3SiO <sub>2</sub>
Monticellite	Calcium-magnesium-silicate	CaO.MgO.SiO <sub>2</sub>
Witherite	Barium carbonate	BaCO <sub>3</sub>

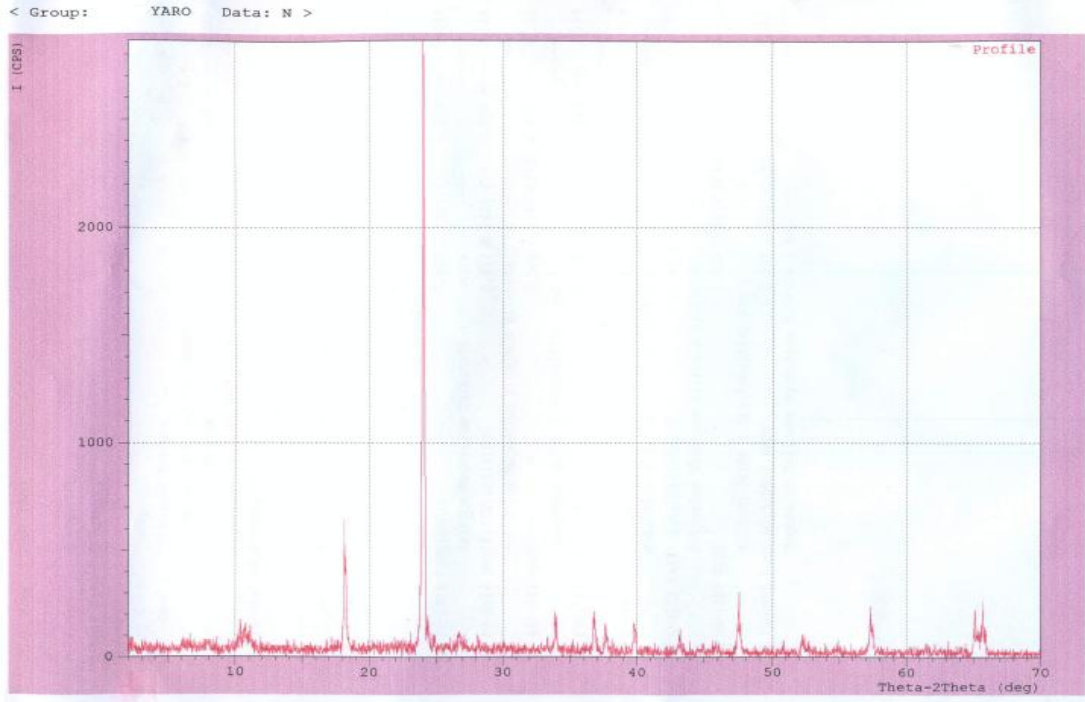


Figure 4.18: XRD patterns of glass-ceramics sample that has 6 wt%  $\text{TiO}_2$  and then heat treated for 2 hours.

Table 4.13: Mineral phases assemblage of glass-ceramics sample to which 6 wt%  $\text{TiO}_2$  was added and then heat treated for 2 hours.

Mineral phase	Chemical name	Chemical formula
Quartz	Silicon dioxide	$\text{SiO}_2$
Albite	Sodium-alumino-silicate	$\text{Na}_2\text{O} \cdot \text{Al}_2\text{O}_3 \cdot 3\text{SiO}_2$
Dolomite	Calcium-magnesium-carbonate	$\text{CaMg}(\text{CO}_3)_2$

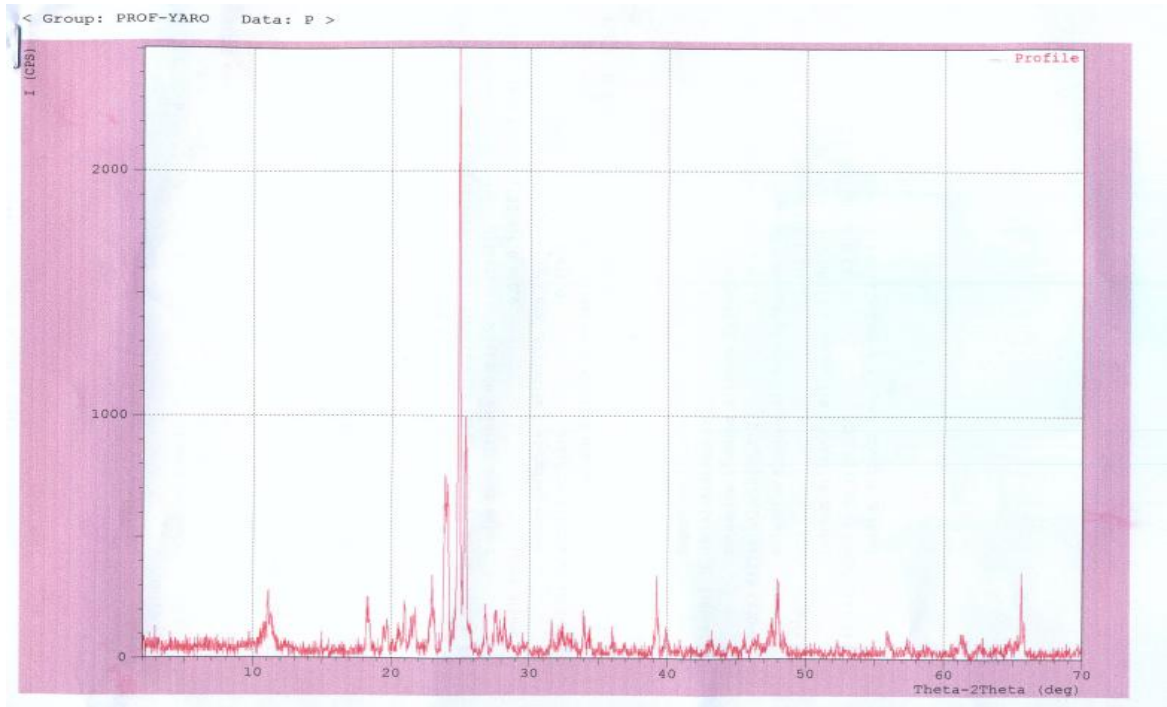


Figure 4.19 : XRD patterns of glass-ceramics sample to which 6 wt% TiO<sub>2</sub> was added and then heat treated for 4 hours.

Table 4.14: Mineral phases assemblage of glass-ceramics sample to which 6 wt% TiO<sub>2</sub> was added and heat treated for 4 hours.

Mineral phase	Chemical name	Chemical formula
Albite	Sodium-alumino-silicate	Na <sub>2</sub> O.Al <sub>2</sub> O <sub>3</sub> .3SiO <sub>2</sub>
Quartz	Silicon dioxide	SiO <sub>2</sub>
Witherite	Barium carbonate	BaCO <sub>3</sub>
Wollastonite	Calcium silicate	CaO.SiO <sub>2</sub>

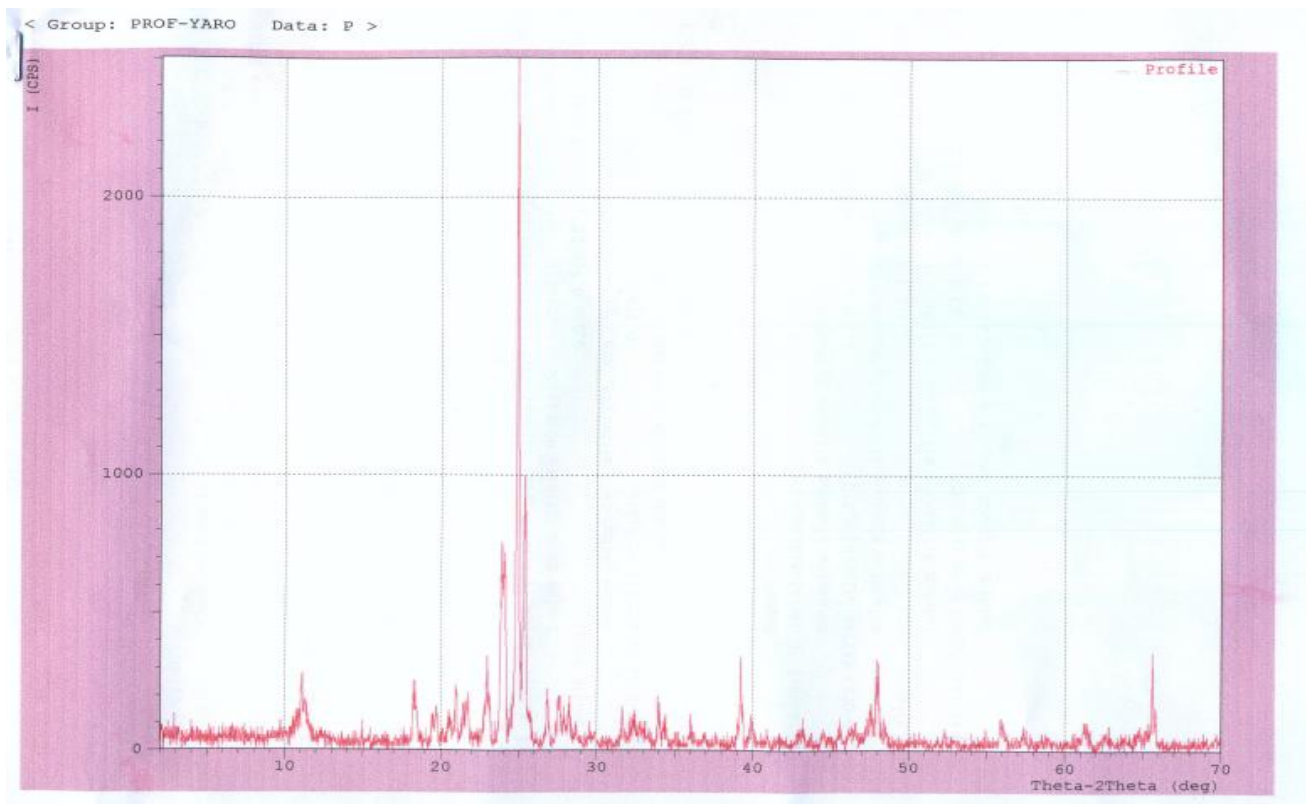


Figure 4.20 : XRD patterns of glass-ceramics sample to which 8 wt% TiO<sub>2</sub> was added and then heat treated for 2 hours.

Table 4.15: Mineral phases assemblage of glass-ceramics sample to which 8 wt% TiO<sub>2</sub> was added and heat treated for 2 hours.

Mineral phase	Chemical name	Chemical formula
Albite	Sodium-alumino-silicate	Na <sub>2</sub> O.Al <sub>2</sub> O <sub>3</sub> .3SiO <sub>2</sub>
Wollastonite	Calcium silicate	CaO.SiO <sub>2</sub>
Calcite	Calcium carbonate	CaCO <sub>3</sub>

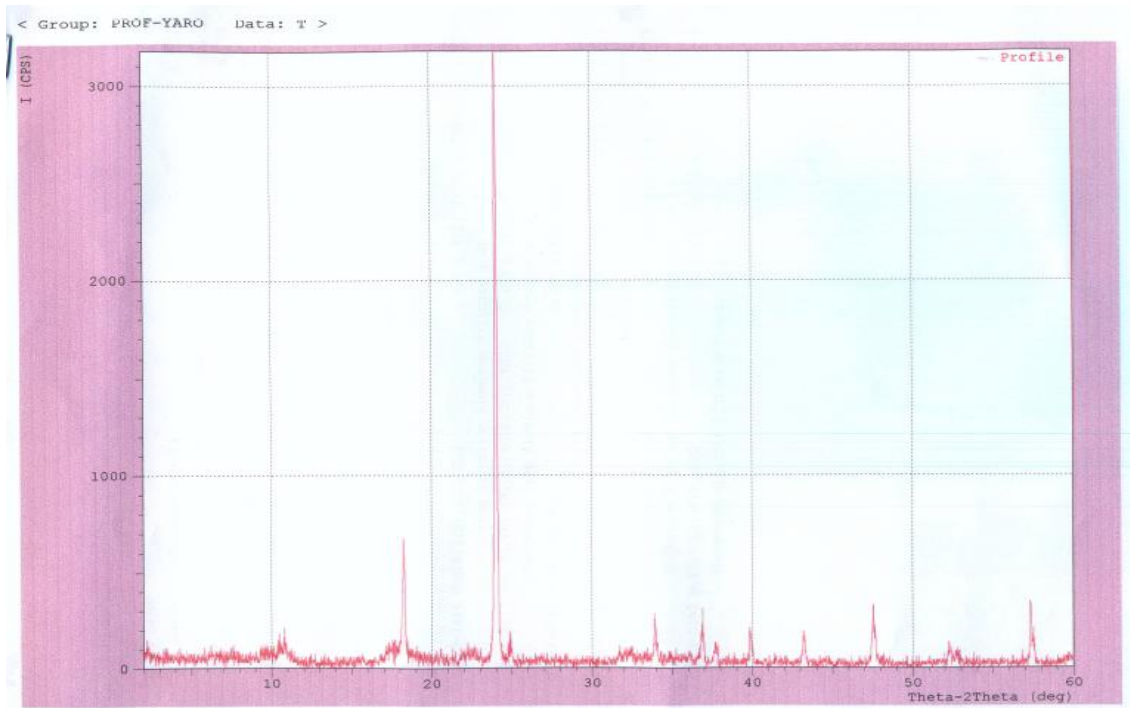


Figure 4.21 : XRD patterns of glass-ceramics sample to which 8 wt% TiO<sub>2</sub> was added and then heat treated for 4 hours.

Table 4.16: Mineral phases assemblage of glass-ceramics sample to which 8 wt% TiO<sub>2</sub> was added and heat treated for 4 hours.

Mineral phase	Chemical name	Chemical formula
Hematite	Iron(III)Oxide	Fe <sub>2</sub> O <sub>3</sub>
Anorthite	Calcium-alumino-silicate	CaO.Al <sub>2</sub> O <sub>3</sub> .2SiO <sub>2</sub>
Wollastonite	Calcium silicate	CaO.SiO <sub>2</sub>
Cordierite	Magnesium-alumino-silicate	2MgO.2Al <sub>2</sub> O <sub>3</sub> .5SiO <sub>2</sub>

Andradite	Calcium-iron-silicate	$3\text{CaO}\cdot\text{Fe}_2\text{O}_3\cdot 3\text{SiO}_2$
-----------	-----------------------	--

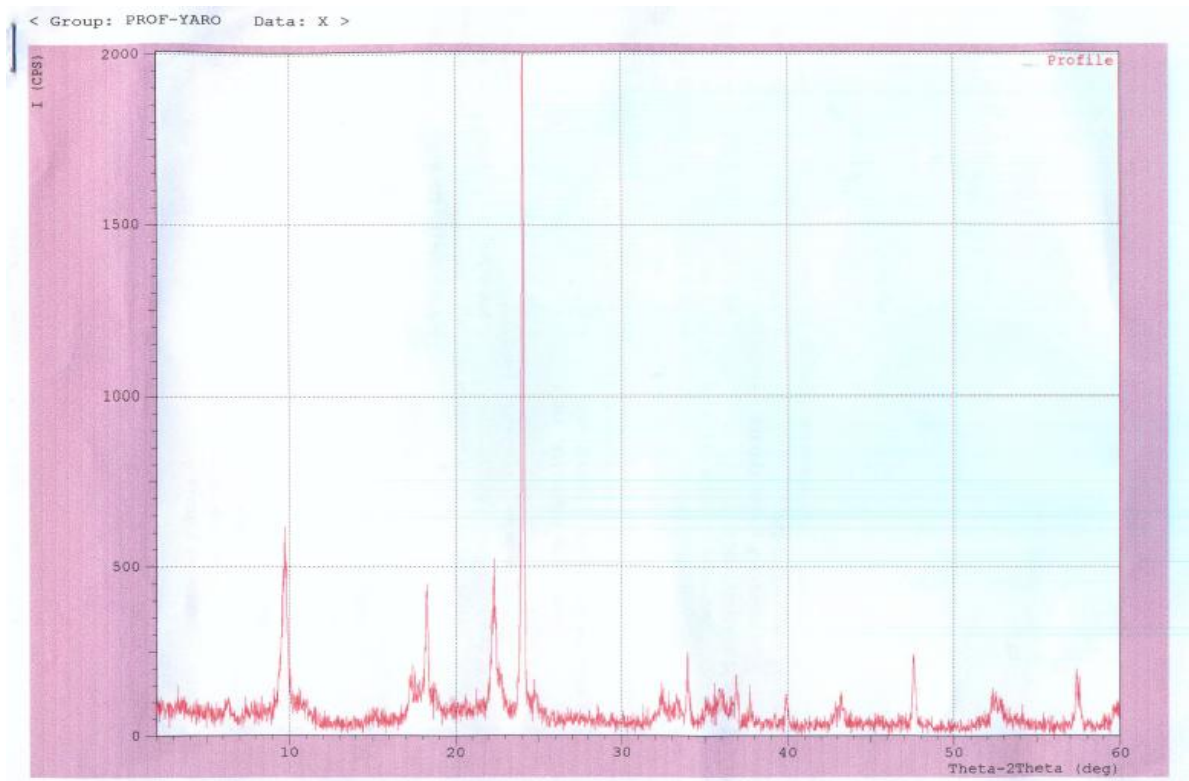


Figure 4.22 : XRD patterns of glass-ceramics sample to which 10 wt%  $\text{TiO}_2$  was added and then heat treated for 2 hours.

Table 4.17: Mineral phases assemblage of glass-ceramics sample to which 10 wt%  $\text{TiO}_2$  was added and heat treated for 2 hours.

Mineral phase	Chemical name	Chemical formula
Quartz	Silicon dioxide	$\text{SiO}_2$
Andradite	Calcium-iron-silicate	$3\text{CaO}\cdot\text{Fe}_2\text{O}_3\cdot 3\text{SiO}_2$
Cordierite	Magnesium-alumino-silicate	$2\text{MgO}\cdot 2\text{Al}_2\text{O}_3\cdot 5\text{SiO}_2$

Monticellite	Calcium-magnesium-silicate	CaO.MgO.SiO <sub>2</sub>
Wollastonite	Calcium silicate	CaO.SiO <sub>2</sub>

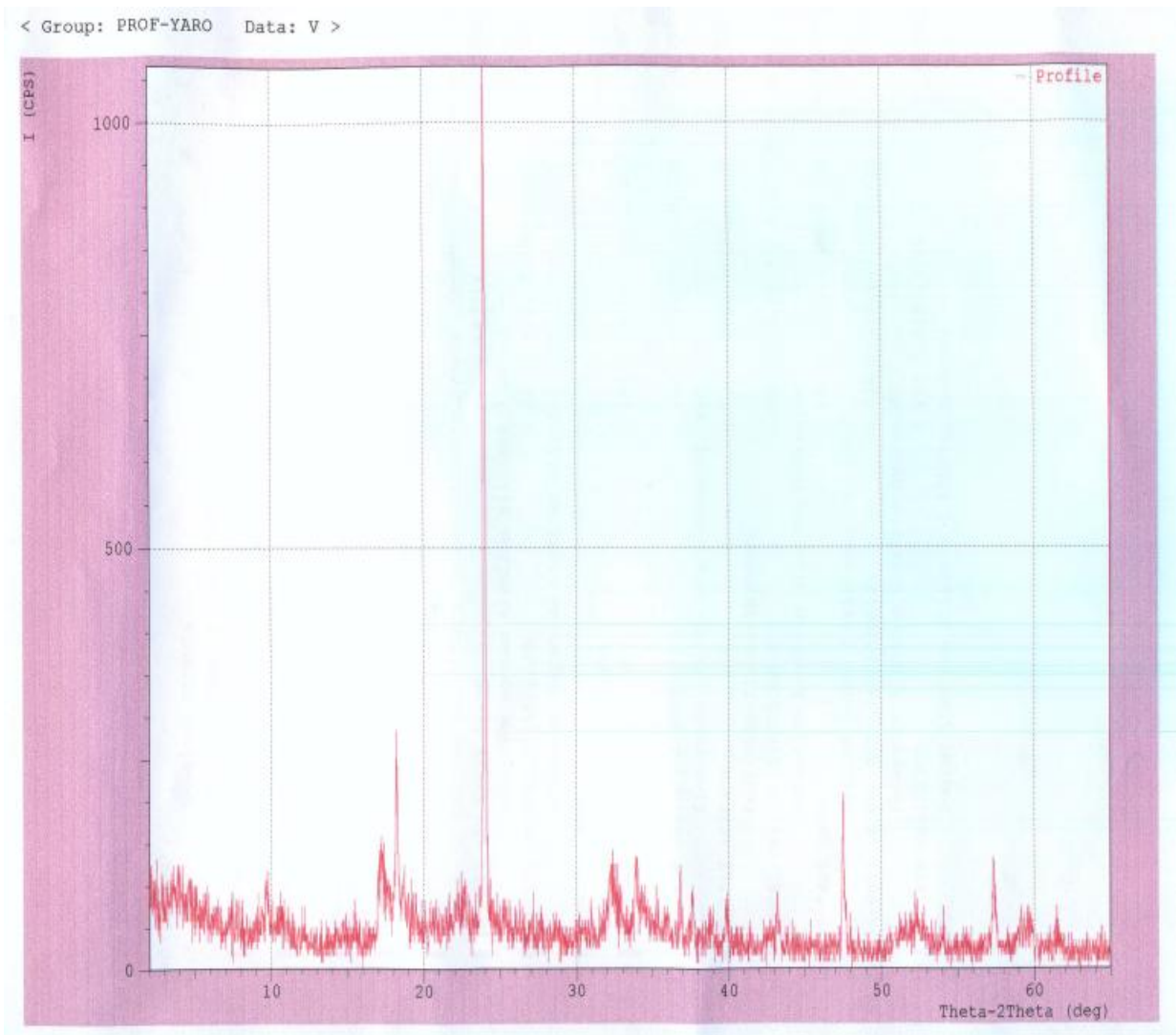


Figure 4.23: X-Ray Diffractograms of glass-ceramic sample to which 10 wt% TiO<sub>2</sub> was added and then heat treated for 4 hours.

Table 4.18: Mineral phases assemblage of glass-ceramic sample to which 10 wt% TiO<sub>2</sub> was added and heat treated for 4 hours

SMineral phase	Chemical name	Chemical formula
Albite	Sodium-alumino-silicate	Na <sub>2</sub> O.Al <sub>2</sub> O <sub>3</sub> .3SiO <sub>2</sub>
Quartz	Silicon dioxide	SiO <sub>2</sub>
Titanate	Calcium-titanium-silicate	CaO.TiO <sub>2</sub> .SiO <sub>2</sub>
Hematite	Iron(III)Oxide	Fe <sub>2</sub> O <sub>3</sub>
Calcite	Calcium carbonate	CaCO <sub>3</sub>
Wollastonite	Calcium silicate	CaO.SiO <sub>2</sub>
Microcline	Potassium-alumino-silicate	K <sub>2</sub> O.Al <sub>2</sub> O <sub>3</sub> .6SiO <sub>2</sub>
Andradite	Calcium-iron-silicate	3CaO.Fe <sub>2</sub> O <sub>3</sub> .3SiO <sub>2</sub>
Cordierite	Magnesium-alumino-silicate	2MgO.2Al <sub>2</sub> O <sub>3</sub> .5SiO <sub>2</sub>
Monticellite	Calcium-magnesium-silicate	CaO.MgO.SiO <sub>2</sub>

#### **4.10 Results of Scanning Electron Microscopy (SEM) of Glass-Ceramics Samples produced**

The Scanning electron micrograph (FESEM) of each sample under investigation is identified according to the procedure described in Section 3.10. The FESEM images are as follows:

The control sample (0wt% TiO<sub>2</sub>) after being subjected to heat treatment temperatures 373/673°C for 2 hours, the FESEM image was presented in Plates VIa at 1000 X magnifications while Plate VIb presents the FESEM image of the corresponding sample heat treated at 373/673°C for 4 hours at 2000 X magnifications.

Similarly, Plate VIIa presents the FESEM micrograph of glass-ceramic sample to which 2wt% titania was added and heat treated at 367/667°C for 2 hours at 500X magnifications while Plate VIIb presents the FESEM micrograph of the corresponding sample heat treated at same heat treatment temperatures for duration of 4 hours at 1000 X magnifications.

In a similar manner, Plate VIIIa presents the FESEM micrograph of glass-ceramics sample containing 4 wt% TiO<sub>2</sub> and heat treated at 366/666°C for 2 hours at 500X magnifications while Plate VIIIb presents the corresponding sample heat treated at the same heat treatment temperatures for duration of 4 hours at 380X magnifications.

Plate IXa shows the FESEM micrograph of fully crystallized sample that contains 6 wt% TiO<sub>2</sub> and heat treated at 363/663°C for 2 hours at 2000X magnifications while Plate IXb

presents the FESEM image of the corresponding sample subjected to heat treatment temperatures 363/663°C for 4 hours at 500X magnifications.

Plate Xa presents the FESEM image of glass-ceramic sample to which 8 wt% TiO<sub>2</sub> was added and heat treated at 356/656°C for 2 hours at 500X magnifications while Plate Xb presents the FESEM micrograph of the corresponding sample heat treated at the same heat treatment temperature for 4 hours at 500X magnifications.

Finally, Plate XIa presents the FESEM image of glass-ceramics sample to which 10 wt% TiO<sub>2</sub> was incorporated and heat treated at 321/6521°C for 2 hours at 500X magnifications while Plate XIb presents the FESEM of the corresponding sample subjected to the same heat treatment temperatures for duration of 4 hours at 3000 X magnifications.

#### **4.11 Property Tests of Samples**

Figure 4.24 presents the hardness values of 24 samples at varying heat treatment time (1-4 hours) and TiO<sub>2</sub> addition (0, 2, 4, 6, 8, 10 wt%).

Figure 4.25 shows chemical solubility values of 24 samples in 1M HCl acid that were heat treated at varying heat treatment time (1-4 hours) and TiO<sub>2</sub> incorporation (0,2,4,6,8,10 wt%).

Figure 4.26 displays chemical solubility values of 24 samples in 1M NaOH solution that were subjected to varying heat treatment time (1-4 hours) and TiO<sub>2</sub> incorporation (0, 2, 4, 6, 8, 10 wt%).

Figure 4.27 presents apparent density results of 24 samples that were subjected to various heat treatment time (1-4 hours) and TiO<sub>2</sub> addition (0, 2, 4, 6, 8, 10 wt%).

Figure 4.28 depicts porosity results of 24 samples that contain varying  $\text{TiO}_2$  incorporation and subjected to heat treatment time of 1 to 4 hours.

Figure 4.29 presents water absorption results of 24 samples heat treated at varying heat treatment time (1-4 hours) and  $\text{TiO}_2$  addition (0, 2, 4, 6, 8, 10 wt%).

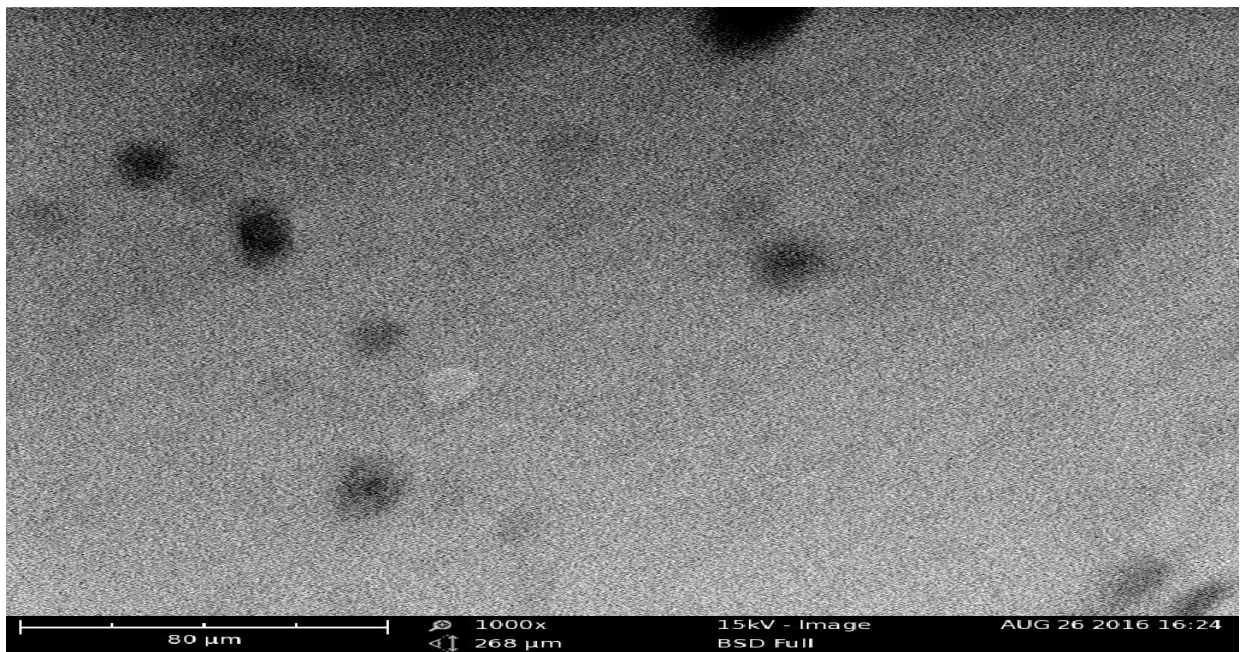


Plate VIa: FESEM image of 0wt%  $\text{TiO}_2$  : 2 hours at 1000 X

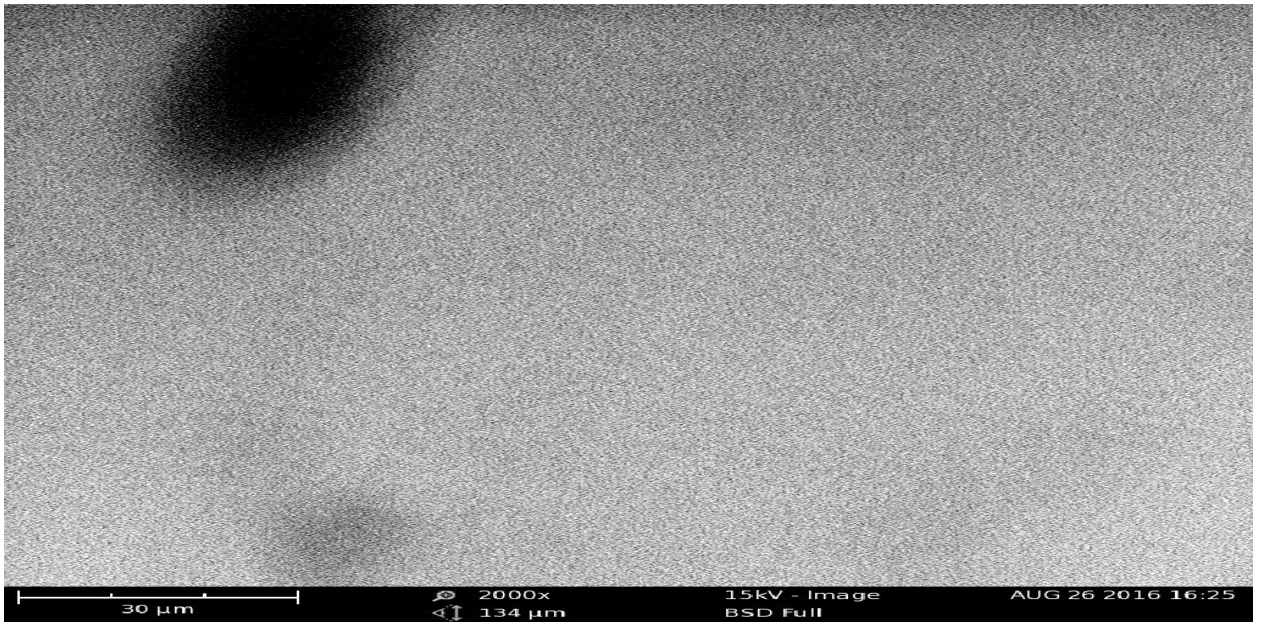


Plate VIb: FESEM image of 0 wt% TiO<sub>2</sub> : 4 hours at 2000 X

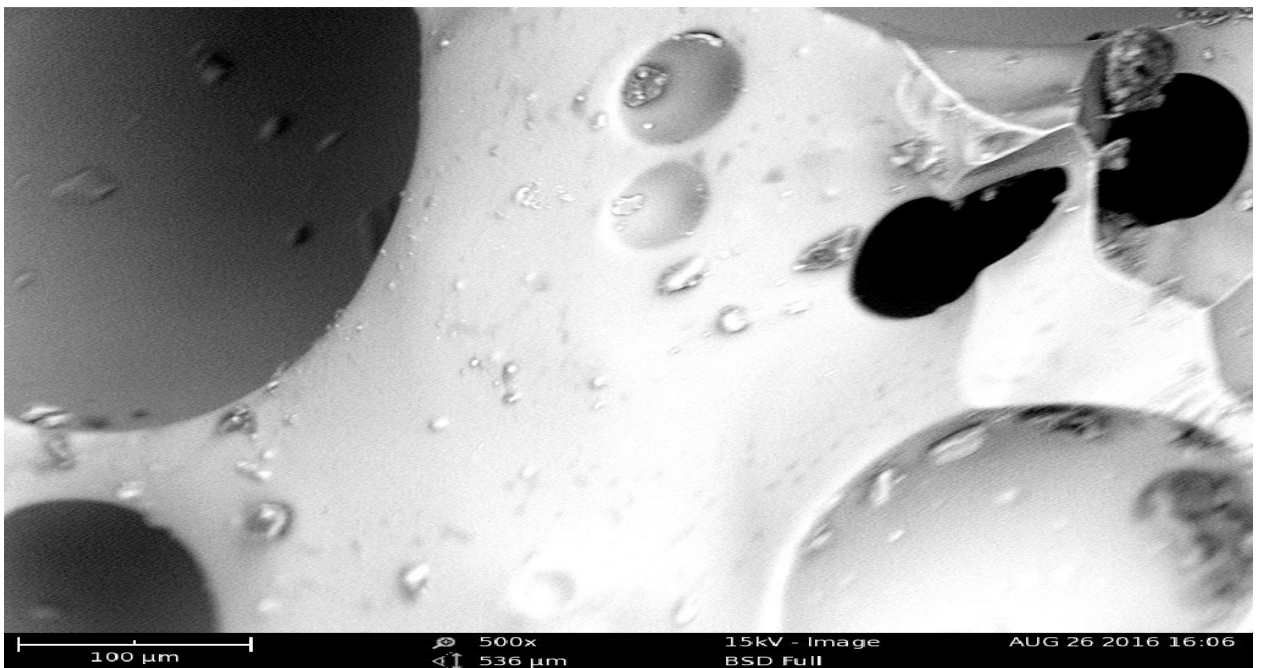


Plate VIIa: FESEM image of 2 wt% TiO<sub>2</sub> : 2 hours at 500 X

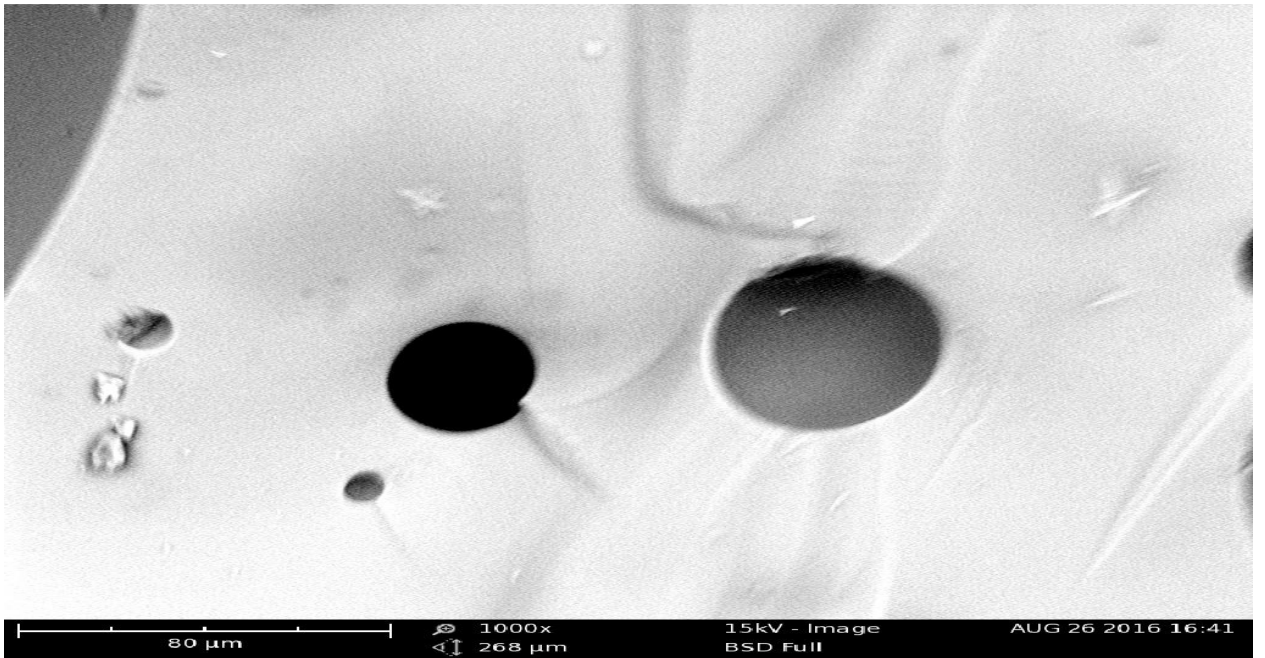


Plate VIIb: FESEM image of 2 wt% TiO<sub>2</sub> : 4 hours at 1000 X

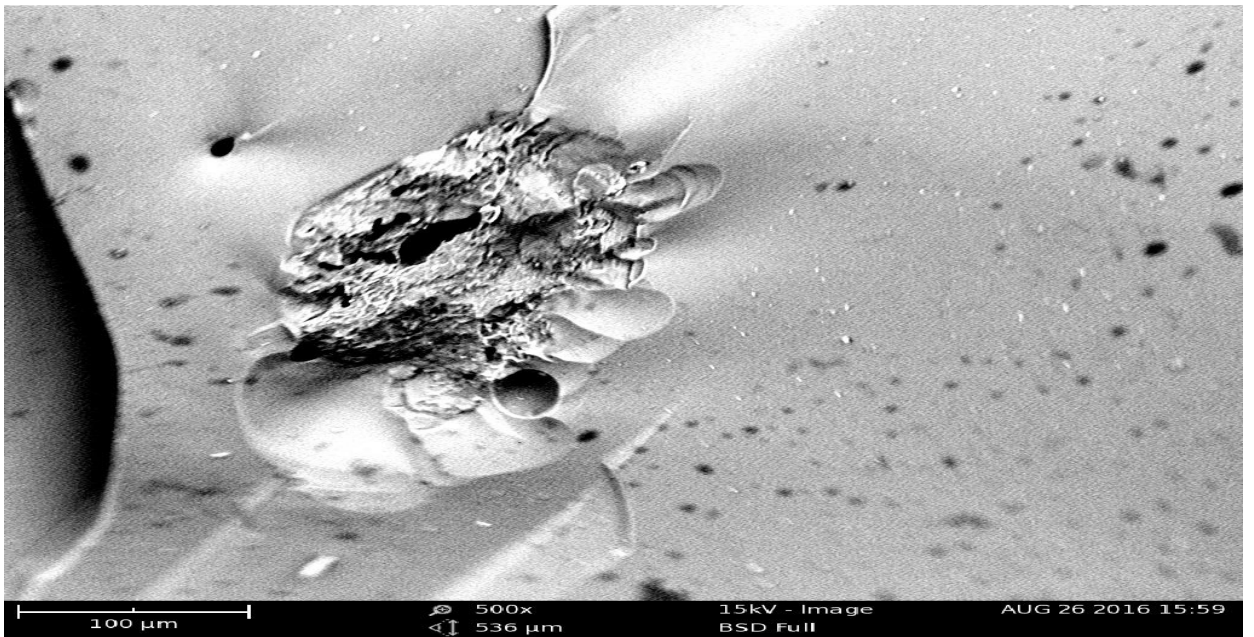


Plate VIIIa: FESEM image of 4 wt% TiO<sub>2</sub> : 2 hours at 500 X

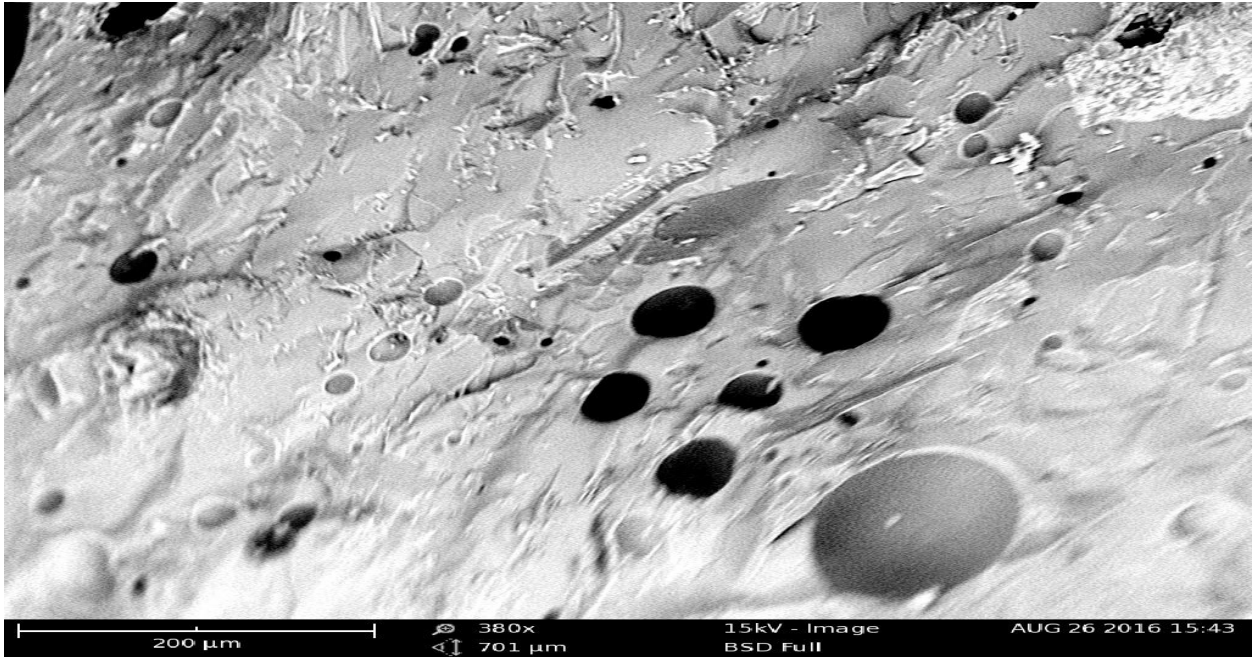


Plate VIIIb: FESEM of image of 4 wt% TiO<sub>2</sub> : 4 hours at 380 X

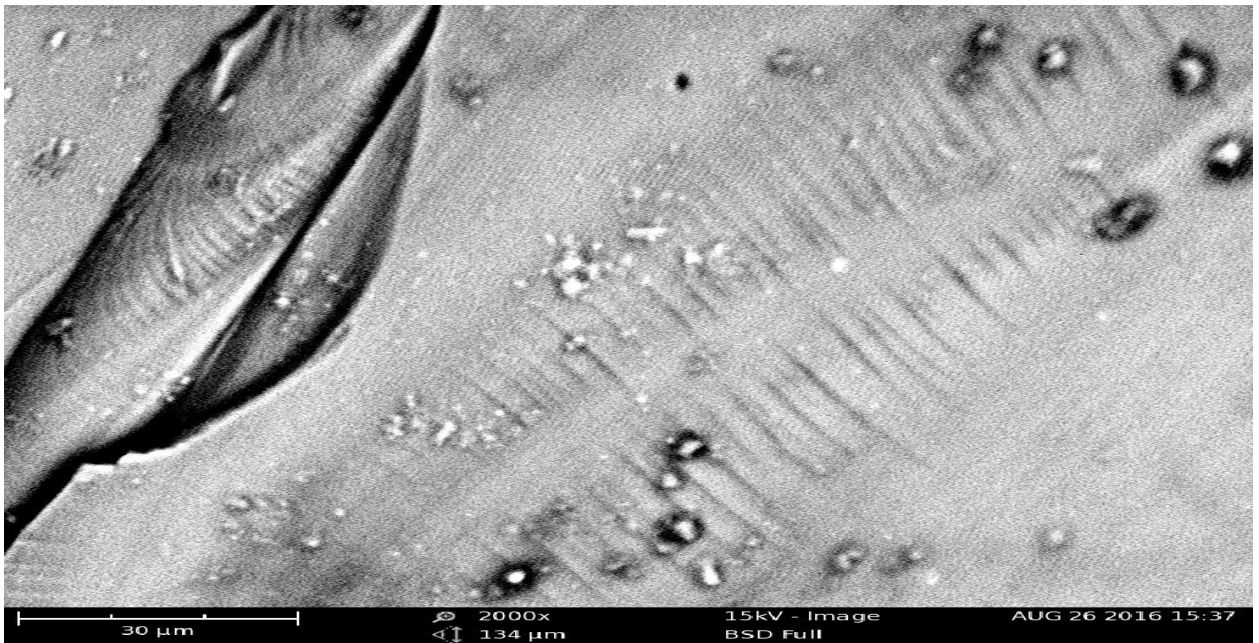


Plate IXa: FESEM micrograph of 6 wt% TiO<sub>2</sub> : 2 hours at 2000 X

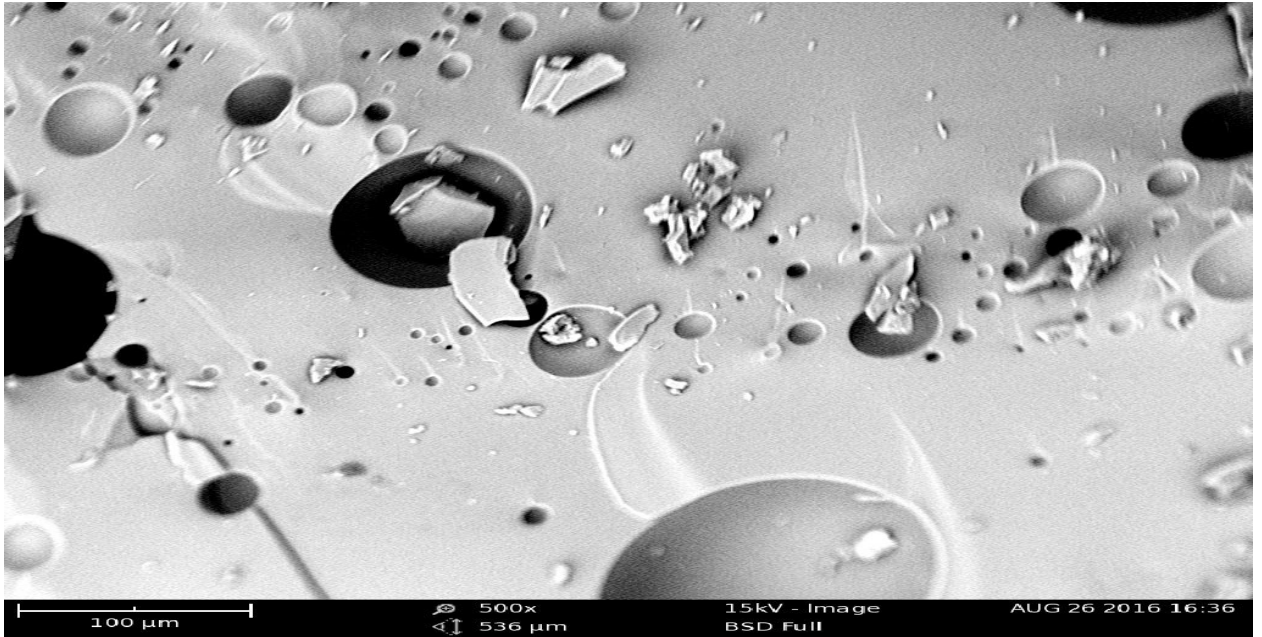


Plate IXb : FESEM image of 6 wt% TiO<sub>2</sub> : 4 hours at 500 X

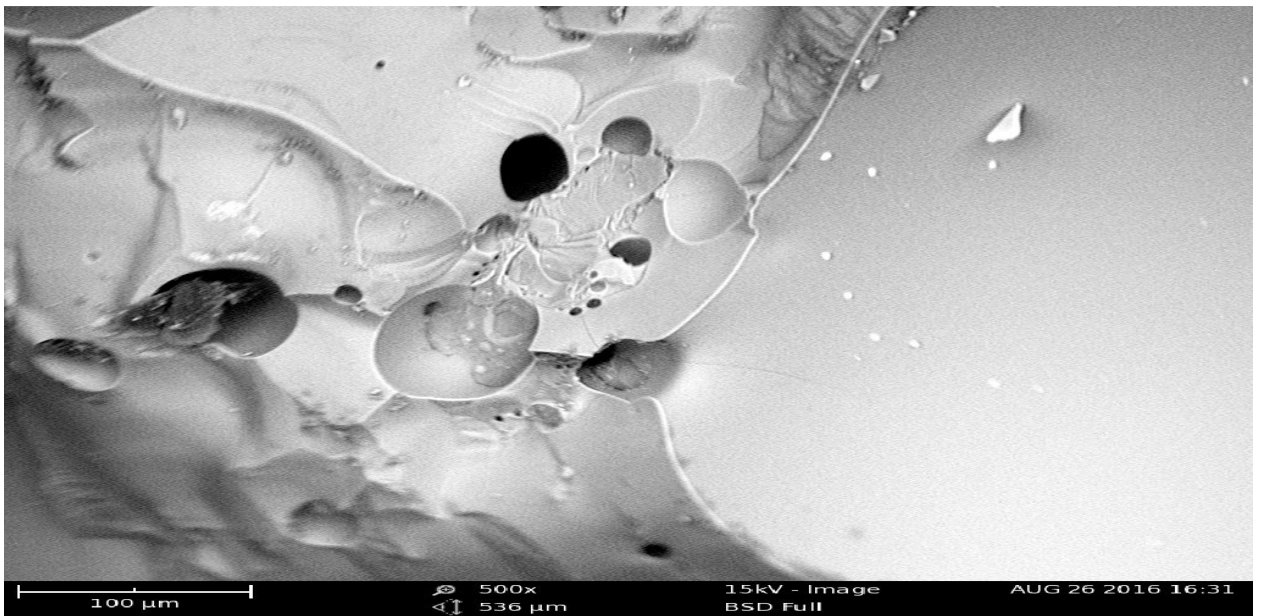


Plate Xa: FESEM image of 8 wt% TiO<sub>2</sub> : 2 hours at 500 X

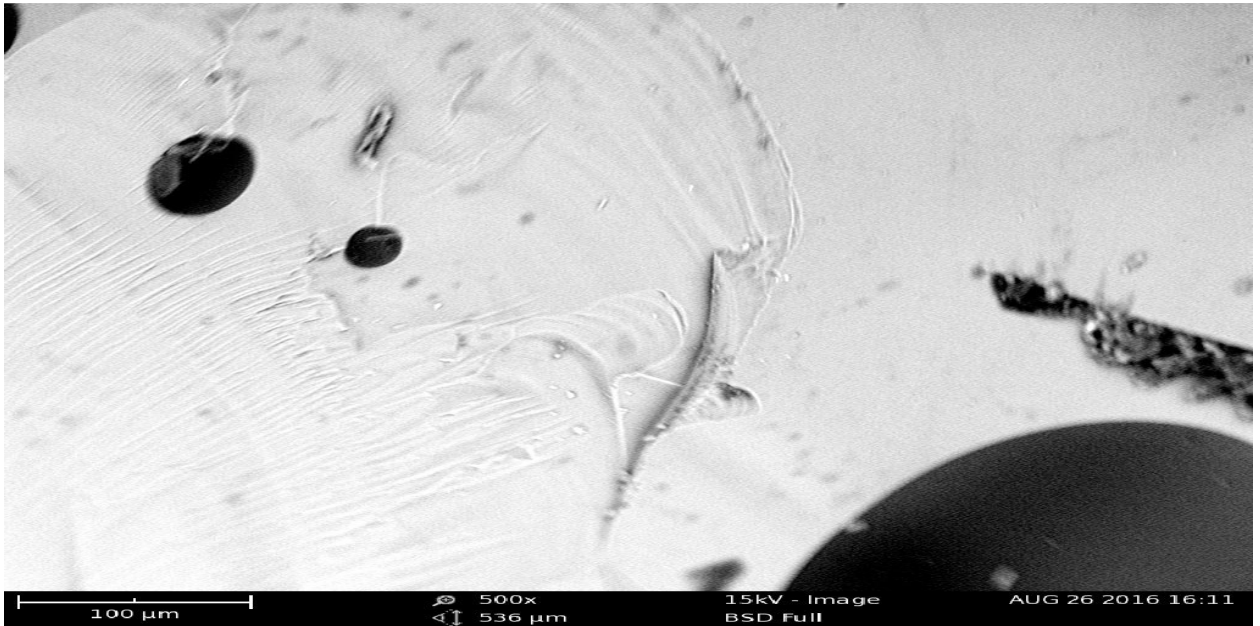


Plate Xb: FESEM image of 8 wt% TiO<sub>2</sub> : 4 hours at 500 X

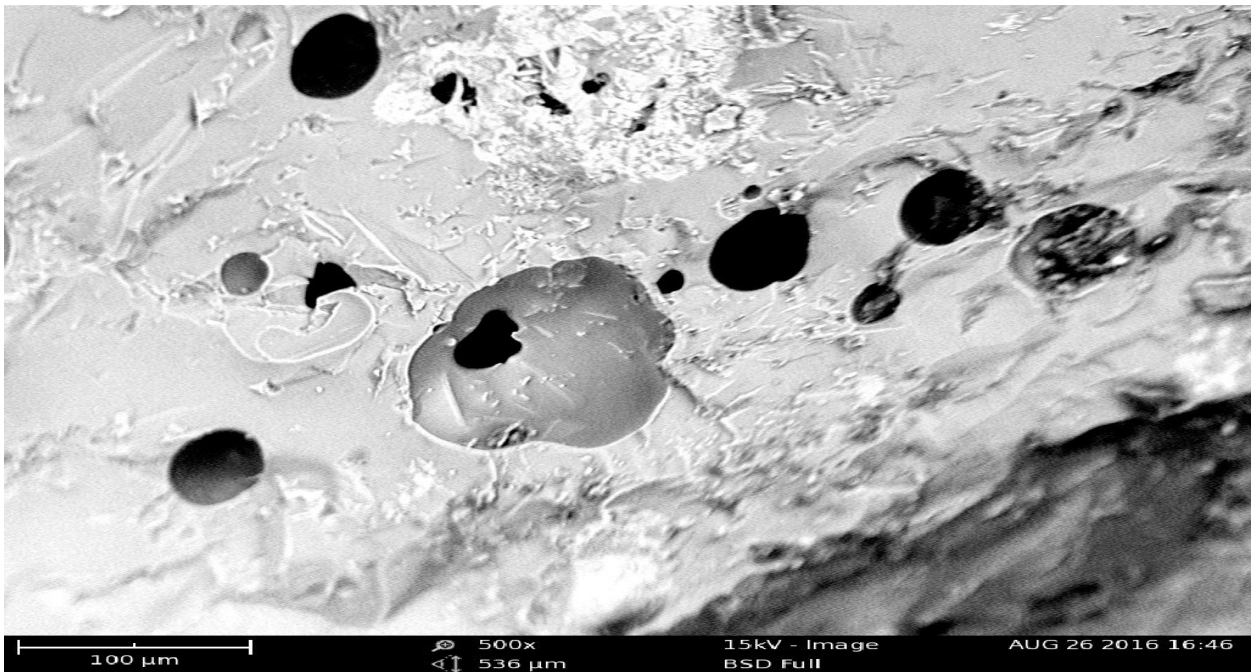


Plate XIa: FESEM image of 10 wt% TiO<sub>2</sub> : 2 hours at 500 X

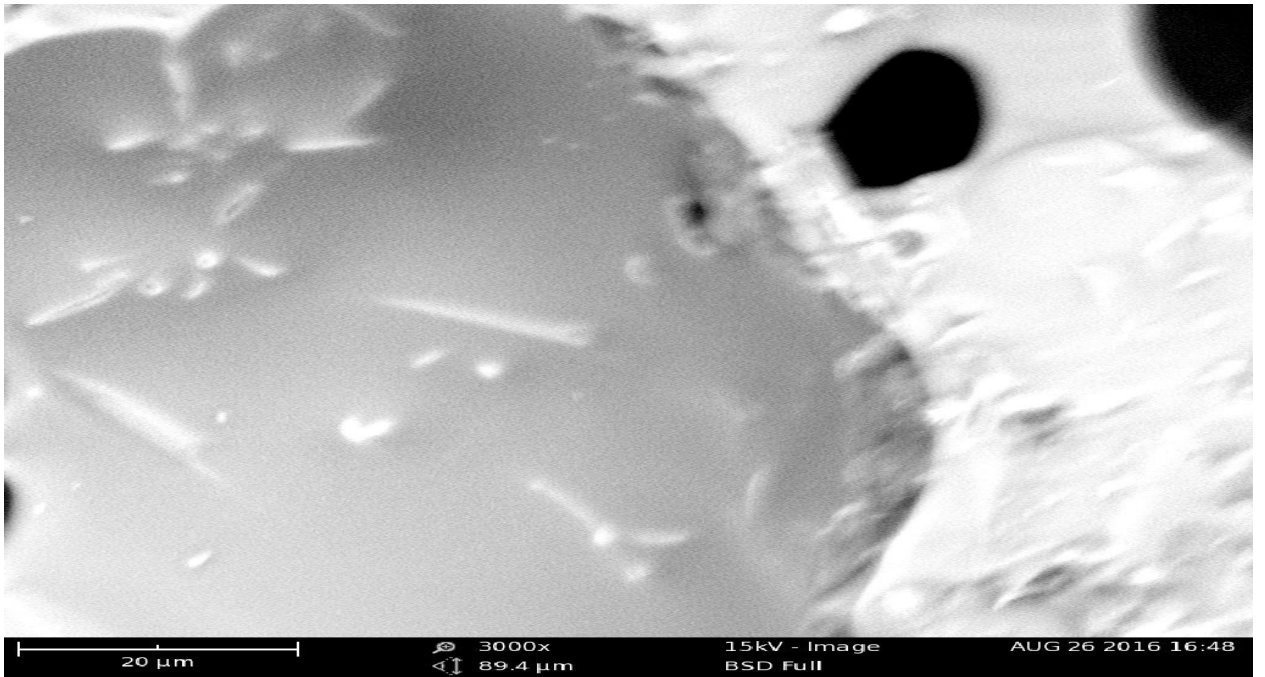


Plate XIb: FESEM image of 10 wt% TiO<sub>2</sub> : 4 hours at 3000 X

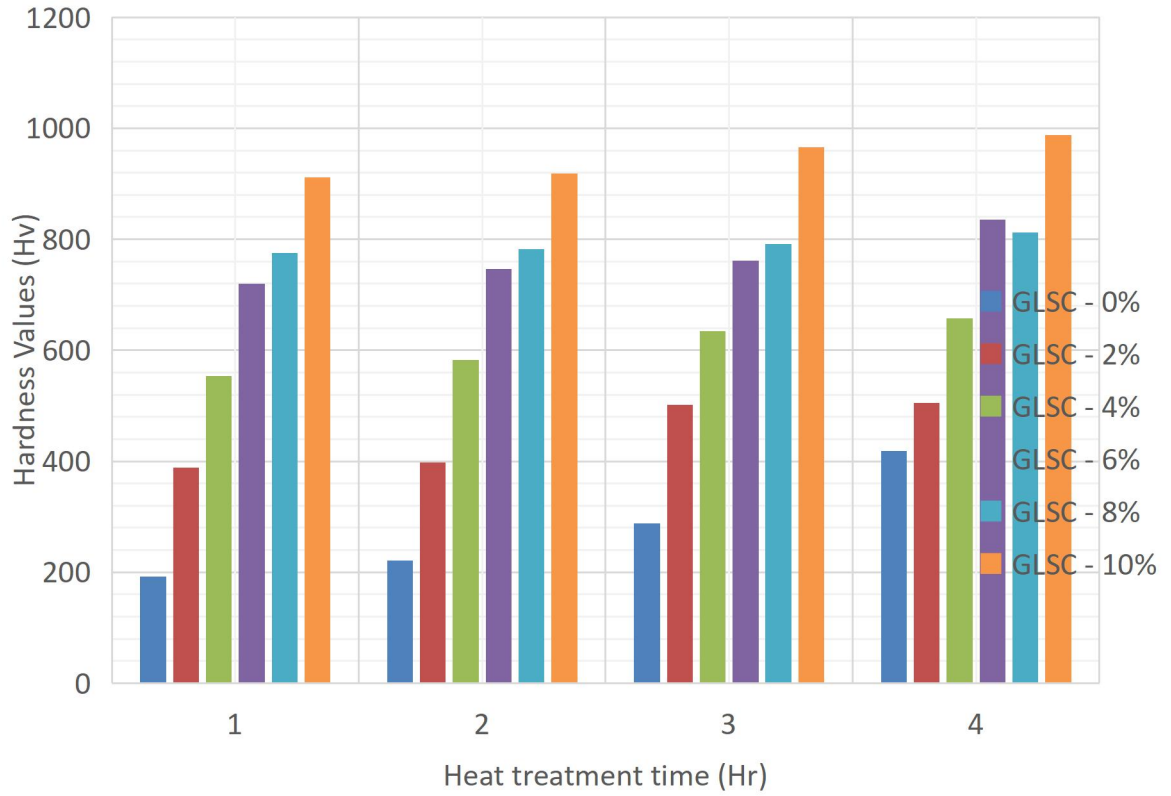


Figure 4.24: Effect of heat treatment time and TiO<sub>2</sub> addition on hardness for the various glass ceramic samples.

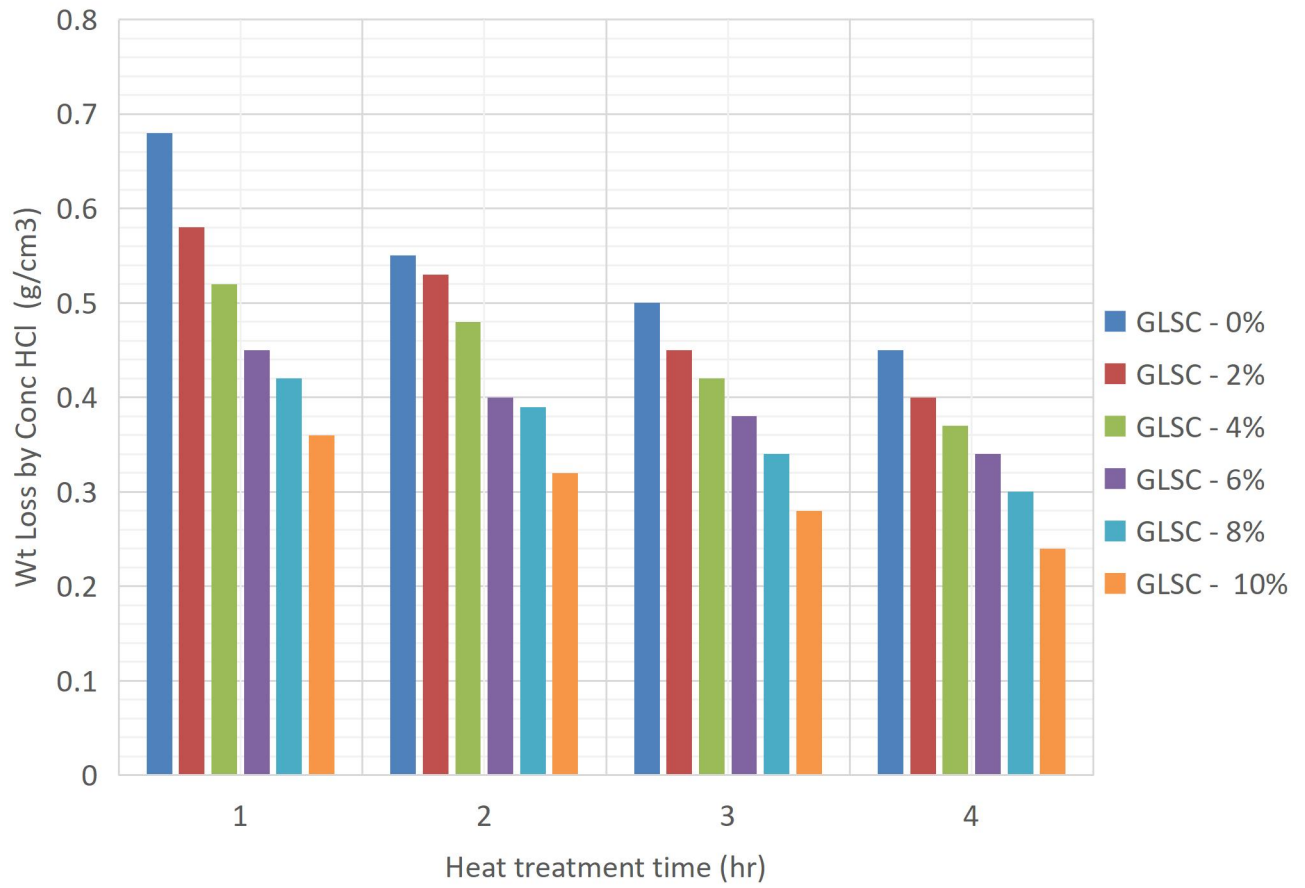


Figure 4.25: Effect of Heat treatment time and TiO<sub>2</sub> incorporation on weight loss using 1M HCl solution for the various glass ceramic samples.

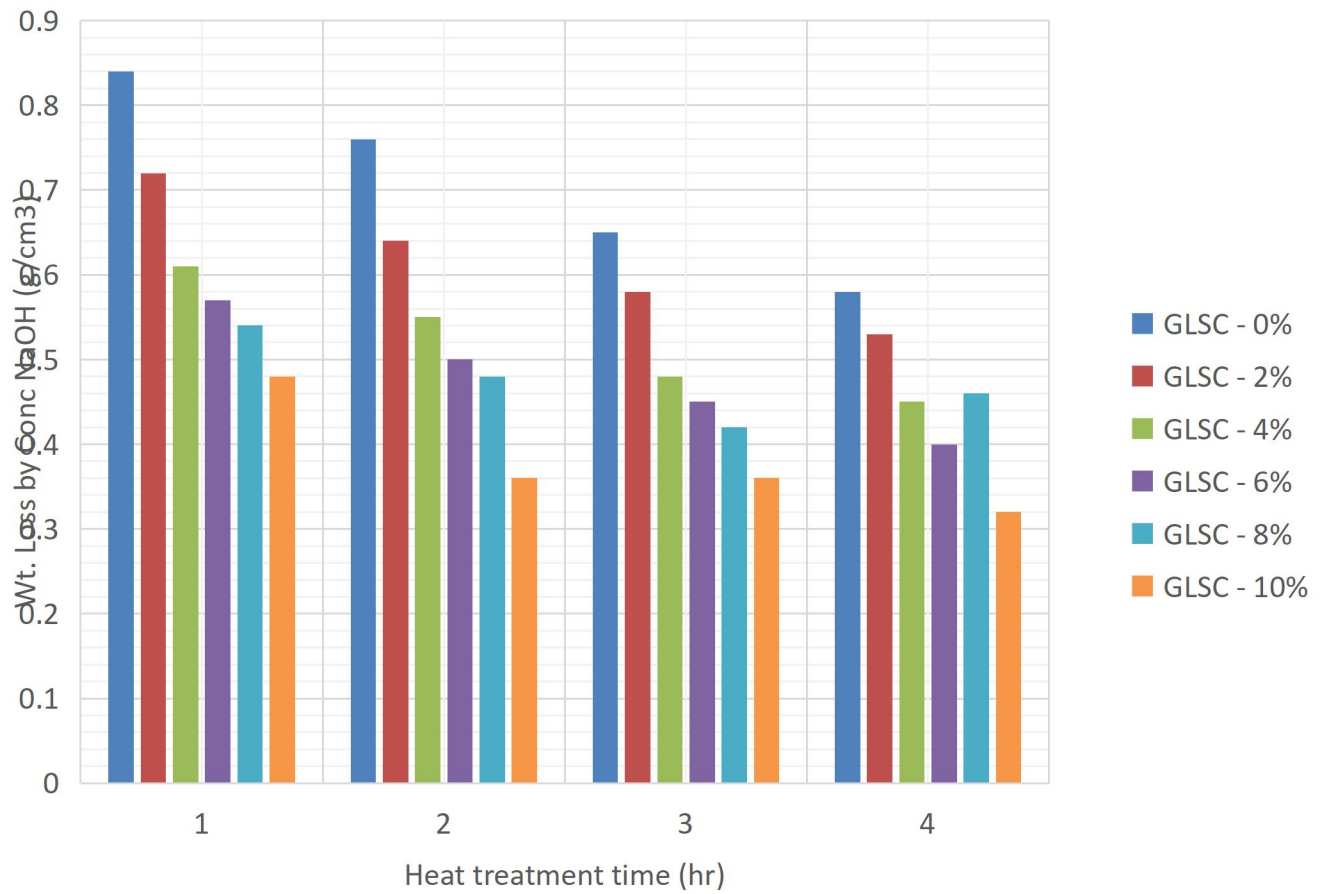


Figure 4.26: Effect of heat treatment time and TiO<sub>2</sub> incorporation on weight loss using 1M NaOH solution for the various glass-ceramic samples.

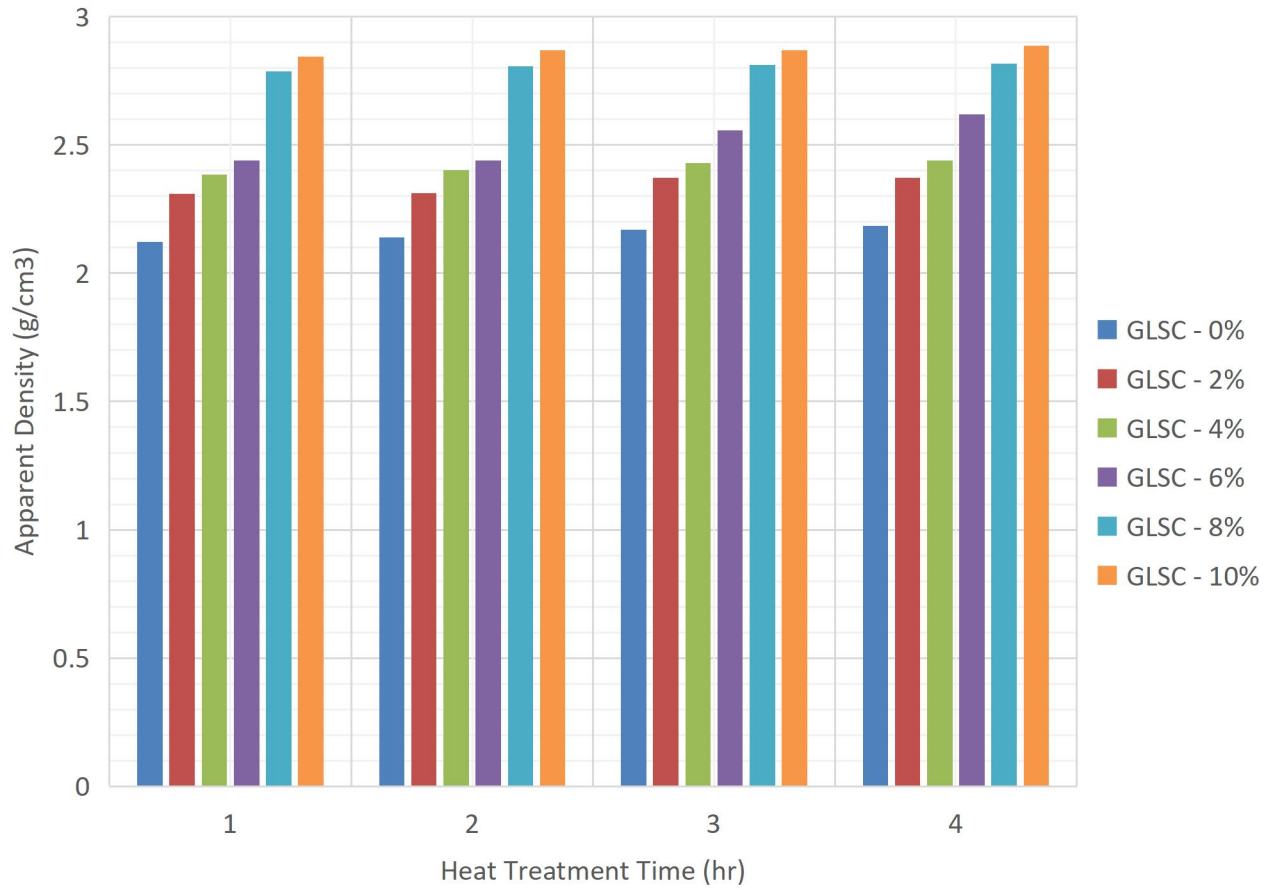


Figure 4.27: Effect of heat treatment time and TiO<sub>2</sub> addition on apparent density of various glass-ceramic samples under study.

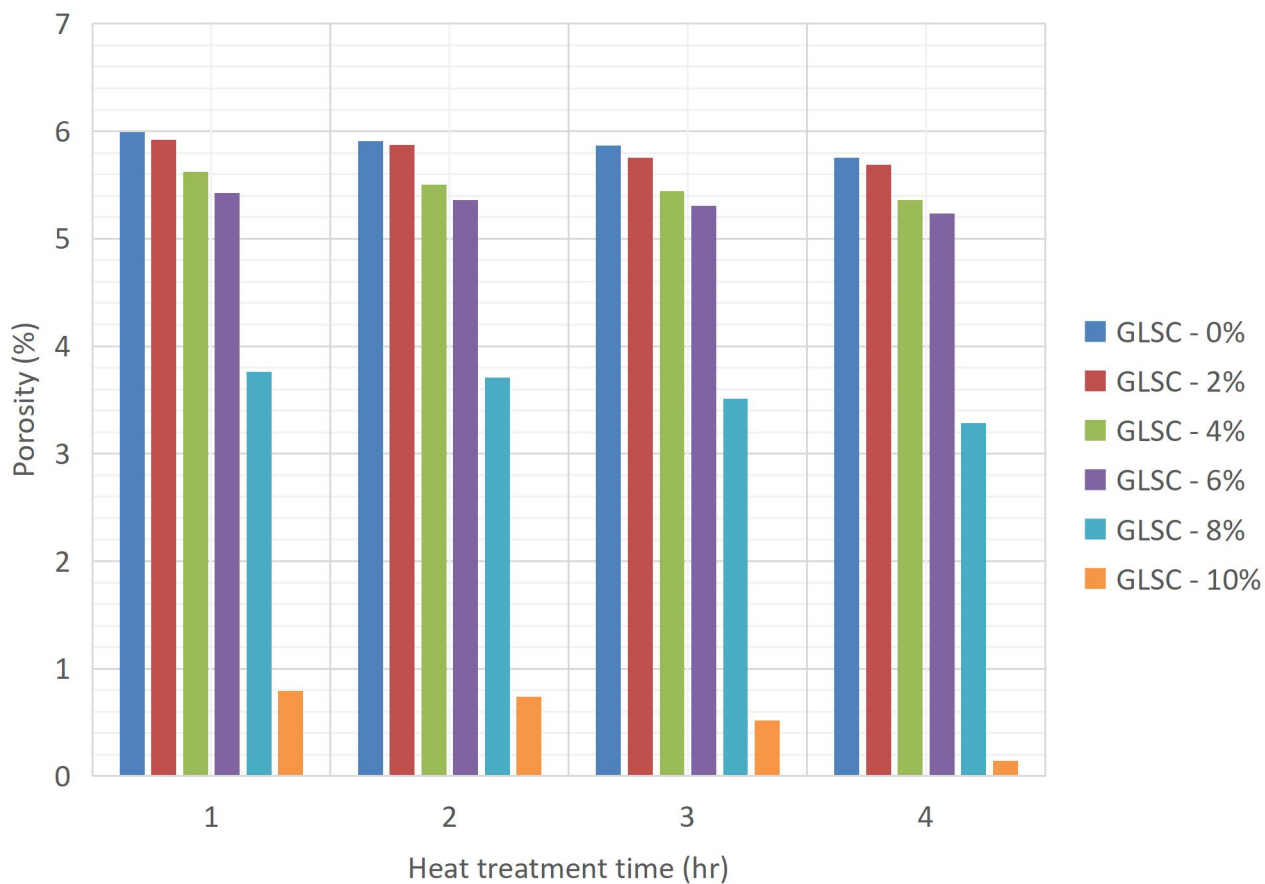


Figure 4.28: Effect of Heat Treatment Time and TiO<sub>2</sub> incorporation on Porosity of various glass-ceramic samples under study.

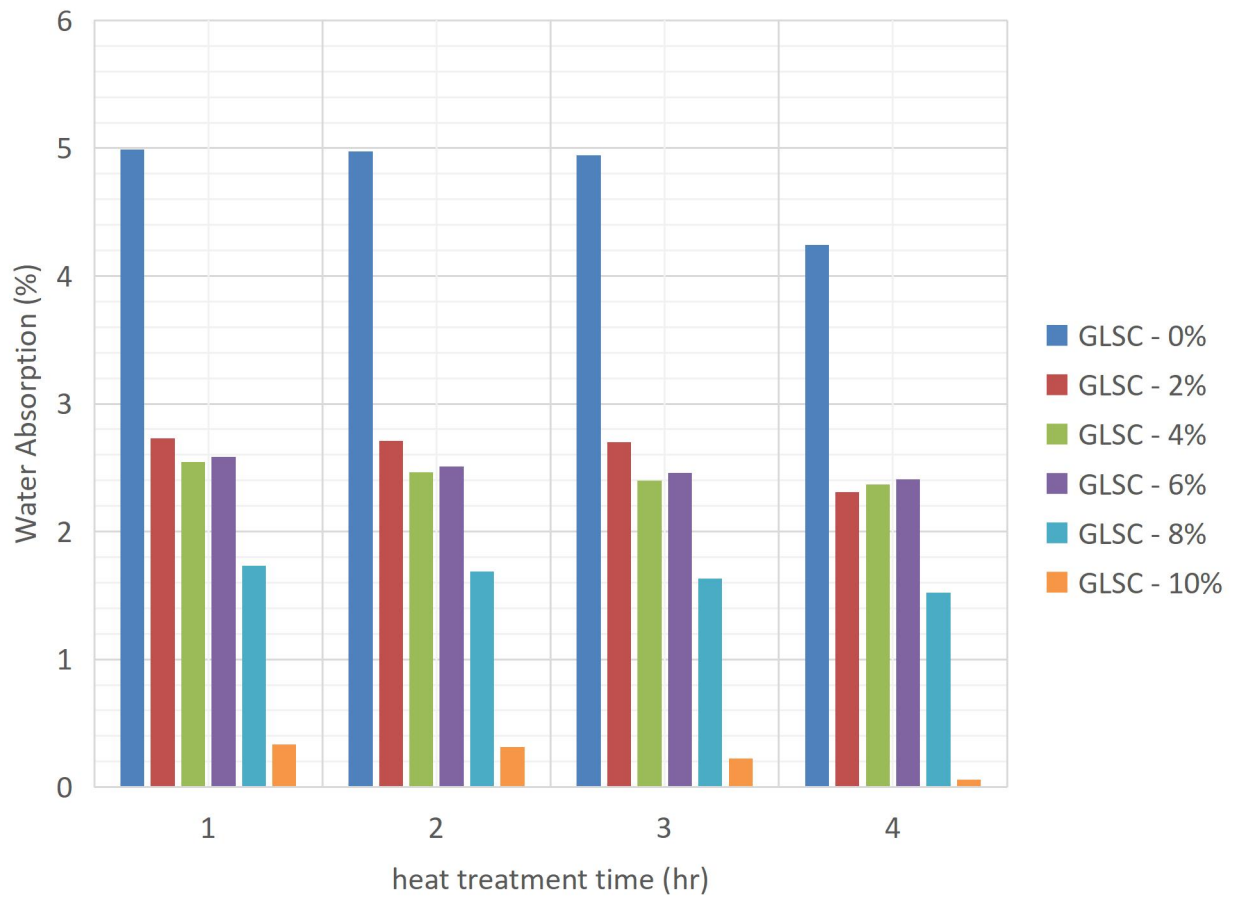


Figure 4.29: Effect of heat treatment time and TiO<sub>2</sub> addition on water absorption of various glass-ceramics samples under study.

## CHAPTER FIVE

### 5.0 DISCUSSION OF RESULTS

## 5.1 CHARACTERIZATION OF MATARI FELDSPAR POWDERS

### 5.1.1 X-Ray Fluorescence (XRF) analysis of Matari feldspar powders

Table 4.1 has revealed the chemical composition of the representative sample of the Matari feldspar deposit . It is composed of 11.33 wt% potash ( $K_2O$ ) which falls within the range of 10-15 wt% for potash feldspar needed in the glass industry (Gulsory *et al.*,2005). Since potash is the major alkali oxide in the composition, it can be deduced that Matari is potash form of feldspar (Immo, 1981).The potash content of Matari feldspar is higher than Richifa feldspar (Ali *et al.*,2010) and Turkish (Gulsory *et al.*,2005) as each case contains 8.95 wt% and 5.94 wt% respectively. Apart from high percentage of potash, XRD analysis detected that the sample is composed of 0.1 wt% iron oxide ( $Fe_2O_3$ ) an undesirable oxide in glass making due to its colouring effect on glass. However, in the manufacture of high quality colourless glass, feldspar should have a maximum of 0.1 w% iron oxide. Although, up to 0.3 wt% is permissible (Hassan *et al.*,2012). The rest of the other oxides such as  $Cr_2O_3$ ,  $MnO_2$ ,  $ZrO_2$ ,  $TiO_2$  among others present in trace in the sample are either used as colourants or opallizing agents in glass making. However, Matari feldspar should undergo beneficiation to enhance the quality of the resultant glass. In view of this, Matari feldspar deposit has met the common feldspar specifications and the requirement for the production of high quality colourless glass. In addition, Matari feldspar being rich in potash, suggests that its suitable as fluxing agent for fast melting and energy saving as well as promotes crystallization processes in glass-ceramics (El-Meliegy and Richard, 2012). The feldspar deposit has high percentage of silica and alumina content 67.32 wt% and 17.54 wt% respectively. Therefore, Matari feldspar deposit is a good source of potash, alumina and

silica for making alumino silicate glasses and soda lime-silica glasses (Alexis and David, 1979 and Shelby, 2005).

### **5.1.2 Result for loss on ignition (LOI) of Matari feldspar powders**

Loss on ignition (LOI) of Matari feldspar powders is very negligible (0.14 wt%) and is slightly above the permissible level (0.00 wt%) for industrial feldspar specifications which usually lacks volatile materials (Alexis and David, 1979). The implication of LOI above the tolerable level is detrimental because the presence of high volatile matters concentration in a material cause reduction of quality.

### **5.1.3 X-Ray Diffraction (XRD) Patterns of Matari feldspar powders.**

Figure 4.1 indicates the qualitative X-Ray Diffraction (XRD) patterns of Matari feldspar powders as determined by PAN analytical pro powder diffractometer equipped with iron filtered Co-K $\alpha$  radiation. The highest diffraction pattern corresponds to dominant mineral (microcline) and the shorter patterns are equivalent to the lesser minerals which are albite and quartz.

### **5.1.4 Quantitative XRD analysis of Matari feldspar powders using Rietveld Method.**

The quantitative XRD analysis as determined by Rietveld method in Table 4.2 further reveals that the dominant mineral present in Matari feldspar powders was microcline (59.6 w %) while albite and quartz account for the lesser phases (34.7wt% and 5.71 wt%) respectively.

### **5.1.5 Scanning Electron Microscope (SEM) images of Matari feldspar powders.**

Plates IIIa-IIIe displayed a wide variety of scanning electron microscope (SEM) micrographs of the representative powdered samples of the Matari feldspar sample at numerous magnifications and grain sizes exhibiting lamellar twinning as their

characteristic features. In addition, the images revealed the distribution of majorly microcline, albite and quartz.

#### **5.1.6 Energy Dispersion Spectroscopy (EDS) of Matari feldspar powders.**

Figure 4.2 shows raw output (counts) versus X-ray energies measured in (keV) of Matari feldspar powders. The prominent peaks in the output data are identified and X-ray in the 0.00- 10.00 keV energy range were detected by the EDS detector on the powdered sample. The prevalent alkali element present in the sample powders as determined by EDS is potassium (K). In addition, the energy spectrum shows other elements which are present in lower concentrations at the analysis point. The elements present include; Carbon (C), Oxygen (O), sodium (Na) and Gold (Au). However, silicon (Si), aluminium (Al) and potassium (K) were present in higher concentration simply because Matari feldspar is aluminosilicate material.

### **5.2 CHARACTERIZATION OF KALAMBAINA LIMESTONE POWDERS**

#### **5.2.1 X-Ray Fluorescent(XRF) analysis of Kalambaina limestone powders**

The result in Table 4.3 shows that Kalambaina limestone contains 53.08 w% CaO which is close to 54-56 wt% required as standard for making plate and window glasses (Alexis and David, 1979). Apart from high lime (CaO), it contains little or no magnesia (0.73 wt%). Usually, CaO rich limestone is almost free of magnesia when compared with standard of less than 3.0 wt% (Ryemshak *et al.*,2012). However, it worth noting that the lime (CaO) content of the Kalambaina limestone is higher than Ubo limestone (Ryemshak *et al.*,2012) and that of Indian Shahabad as each contains 52.84 and 43.2 wt% calcium oxide (lime) respectively, both are presently used in glass making. Iron oxide in glass making is

undesirable due to its colouring effect, the concentration of iron oxide (0.55 wt%) in Kalambaina limestone is far above the permissible level for making quality colourless glasses (0.1-0.3 wt%) (Alexis and David, 1979). Therefore, beneficiation is required for its removal. Loss on ignition (42.00wt%) is within the permissible range (41.0-44.0 wt%) for making a quality colourless glass as well as industrial limestone specifications (Alexis and David, 1979). The rest of the other oxides present in Kalambaina limestone powders such as ( $\text{Cu}_2\text{O}$ ,  $\text{Cr}_2\text{O}_3$ ,  $\text{NiO}_2$ ,  $\text{MnO}_2$ ,  $\text{ZrO}_2$ ,  $\text{TiO}_2$ ) are specifically used as colourants or opacifiers when transparency is not a requirement (Harper, 2001). Similarly, lime ( $\text{CaO}$ ) as the dominant oxide in Kalambaina limestone plays the role of stabilizing amorphous glass as well as improves achieving nucleation and subsequent crystallization during glass-ceramics making (El-Meliegy and Richard, 2012).

### **5.2.2 Result for loss on ignition of Kalambaina limestone powders**

Loss on ignition (LOI) is prescribed to be determined with a view to getting an idea of the nature of the material. This also helps in verifying the correctness of the total analysis result. Loss on ignition (42.0 wt%) for Kalambaina limestone powders is even below the tolerable level for industrial limestone specification (Alexis and David, 1979).

### **5.2.3 X-Ray Diffraction (XRD) patterns of Kalambaina limestone powders**

In a similar manner, the qualitative x-ray diffraction peaks of Kalambaina limestone powders are shown in Figure 4.3 as follows; the highest diffraction peak in Kalambaina limestone powders corresponds to the major mineral and the shorter peak belong to the minor mineral.

#### **5.2.4 Quantitative XRD analysis of Kalambaina limestone powders using Rietveld Method**

The Quantitative XRD result is further confirmed in Table 4.4 which reveals the quantitative results as follows; calcite constitutes 99.5 wt% and the mineral quartz accounts for the balance (0.5%).

#### **5.2.5 Scanning Electron Microscope (SEM) images of Kalambaina limestone Powders.**

Similarly, Plates IVa-IVd displayed the Field Emission Scanning Electron Microscope (FESEM) of Kalambaina limestone powders at a wide variety of magnifications with 1 $\mu$ m particle grain size displaying the distribution of calcite as prevalent mineral and quartz constitutes the lesser mineral phase.

#### **5.2.6 Energy Dispersion Spectroscopy (EDS) of Kalambaina limestone Powders.**

Figure 4.4 further displayed the corresponding EDS of powdered Kalambaina limestone linked to SEM image showing the elemental constituents of different minerals in the sample as follows: C, O, Ba, F, Mg, Si, Au and Ca. The EDS result indicates that Ca (calcium) is the major element as it possesses the highest peak.

### **5.3 CHARACTERIZATION OF TSAKESIMPTAH MAGNESITE POWDERS**

#### **5.3.1 X-Ray Fluorescence (XRF) Analysis of Tsakesimptah Magnesite powders**

Table 4.5 presents the oxides component of Tsakesimptah magnesite powders. The sample has 63.3 wt% magnesia (MgO). The range of magnesia (MgO) present in magnesite is from 47.8 wt% (Aslani *et al.*, 2010), but Tsakesimptah magnesite powders contains 63.3wt.% MgO higher than the acceptable range. The findings showed that Tsakesimptah magnesite is rich in magnesia (63.3 wt %), and magnesia induces stability and also improves resistant to chemical dissolution in glasses. Furthermore, magnesia (MgO) being a modifying oxide, plays vital role in filling up the interstitial spaces in fused silica glass

and making it less permeable to gases (Shelby, 2005). In a similar vein, magnesia (MgO) which is the major oxide in Tsakesimptah magnesite composition and a member of alkaline earth oxides, functions as stabilizing agent that stabilizes the network connectivity of amorphous glass structure as well as promotes ceramization process (Salama *et al.*,2002). The high concentration of magnesia (MgO) in the sample has made it suitable as one of the starting materials for making soda-lime-silica glasses. However, Tsakesimptah magnesite contains high percentage of iron oxide (2.86 wt %) above the tolerable level (0.25 wt%) for making standard colourless glass (Doyle, 19179). The concentration of iron oxide present in Tsakesimptah magnesite is higher than the amount required for making amber and green bottles (0.22-0.96 wt%) respectively, (Doyle, 1979). Also, Tsakesimptah magnesite deposit contains traces of other oxides such as titanium oxide, manganese oxides among others which act as opallizing agent and colourant respectively in glass manufacture (Le-bourhis, 2008). The implication of high iron oxide concentration and other impurities in the Tsakesimptah magnesite would only make it suitable for the production of low grade green glasses due to its undesirably colouring effect. On beneficiation using magnetic separation to remove impurities present therein, Tsakesimptah magnesite is highly suitable and would be recommended as one of the starting materials for making high quality soda-lime silica glass due to its high concentration of magnesia.

### **5.3.2 X-Ray Diffraction (XRD) analysis of Tsakesimptah magnesite powders**

Figure 4.5 shows the XRD patterns of Tsakesimptah magnesite at two theta degree indicating the sharpest peak as major mineral and the shorter peaks correspond to minor mineral. Table 4.6 shows XRD mineral details of Tsakesimptah magnesite powders, and

the findings of the Tsakesimptah magnesite powders revealed that the mineralogical constituents present are olivine HP and calcio-olivine. Figure 4.6 further displays the weight percent of each mineral constituent present in the Tsakesimptah magnesite powders, and Table 4.7 displayed the quantitative XRD result of Tsakesimptah magnesite powders displaying the primary mineral as calcio- olivine (80.8 wt%) and secondary minerals as olivine HP (19.2 wt%). Table 4.8 indicates the crystallite size and strain recorded by Williamson Hall method indicating the crystallite size and lattice strain of dominant material as 184.95 (8) and 0.22 (2)% respectively and lesser phase 194.01(10)and 0.22(2) % for calcio-olivine and olivine HP respectively.

### **5.3.3 Scanning Electron Microscope (SEM) of Tsakesimptah magnesite powders**

Plates Va-Vb show the surface morphology of Tsakesimptah magnesite powders as determined by scanning electron microscopy (SEM) showing the dusty micro particles dark background of calico-olivine and white patches of olivine HP.

### **5.3.4 Energy Dispersion Spectroscopy (EDS) of Tsakesimptah magnesite powders.**

Figure 4.7 further displayed the corresponding EDS of Tsakesimptah magnesite powders in the SEM image showing the elemental distribution of various minerals present in the sample powders under investigation as follows; Ca, Fe, Al, Si, Mg and K. The EDS findings demonstrates that magnesium (Mg) is the major element present as it possesses the highest peak.

## **5.4 Glass Samples produced**

The test-melted batches yielded undesirably brownish glasses, and this was due to the presence of huge amount of impurities present in the starting materials such as iron oxide

( $\text{Fe}_2\text{O}_3$ ), Chromium oxide ( $\text{Cr}_2\text{O}_3$ ), Manganese oxide ( $\text{MnO}_2$ ) copper oxide ( $\text{CuO}$ ) and vanadium pentoxide ( $\text{V}_2\text{O}_5$ ) among others, which are often used as colourant in glass making (Doyle, 1979). Their presence alongside opallizing agents such as titania ( $\text{TiO}_2$ ) and zirconia ( $\text{ZrO}_2$ ) in the glass compositions definitely colourized the resultant glasses. However, physical appearance of the glass samples has suggested that the products were totally glasses, for they did not show any evidence of crystallinity.

### **5.5 Transition Temperatures ( $T_g$ ) of Glass Samples produced**

Alumina ( $\text{Al}_2\text{O}_3$ ) and silica ( $\text{SiO}_2$ ) are effective in increasing the viscosity and transition temperature of base glass due to the formation of building block units such as  $\text{SiO}_4$  tetrahedron and  $\text{AlO}_4$  group which have an effect on the strength of the glass network connectivity of structure. It was a known fact that the ions would form highly stable triangular or tetrahedral structural building units and the glass viscosity would depend on the strength of the bridging oxygen linkages at the corners of adjoining units (Salama *et al.*, 2002).  $\text{CaO}$  and  $\text{MgO}$  are very effective in decreasing glass viscosity and transition temperature ( $T_g$ ) through the introduction of non bridging oxygen. Therefore, the presence of  $\text{Al}_2\text{O}_3$  in base glass compositions under investigation eliminates non bridging oxygen present in the melt which disrupt network structure and thus restore the network connectivity structure of glasses which result in increase of viscosity and glass transition ( $T_g$ ) temperature.

It has been observed that the glass transition temperature of each sample decreases on titania ( $\text{TiO}_2$ ) addition indicating stability and network homogeneity in the glass systems. In addition,  $\text{T}^{4+}$  ion can be accommodated in the glass structure either as network former or as network modifier. The titanium ion occupancy of  $\text{Si}^{4+}$  sites in the glass structure

introduces a Ti-O bond that is weaker than the Si-O bond, and this improves batch melting and crystallization of the glass. The incorporation of titania as nucleating agent in the glass batches decrease both melting temperature, viscosity, glass transition temperature as well as enhance homogeneity of the melt (Salama *et al.*, 2002, Muhammed *et al.*, 2003 and Daniela *et al.*, 2010).

The findings revealed that the control sample or the sample containing zero percent (0wt%) titania exhibited 273°C as its glass transition temperature ( $T_g$ ). However, it has been observed that on gradual addition of titania as nucleating agent all through, the glass transition temperature of glass samples containing 2wt% , 4wt%, 6wt%, 8wt% and 10wt% decreased progressively from 267°C , 266°C, 263°C, 256°C and 221°C respectively. The decrease in the glass transition temperature in each sample was as a result of increase in titania incorporation. Titania ions occupancy of  $Si^{4+}$  sites in the glass structure introduces a Ti-O bond that is weaker than the Si-O bond, and this improves batch melting due to the formation of non bridging oxygen bond in the glass structure ( Salama *et al.*, 2002; Mohammed *et al.*, 2003 and Al-Harbi and Khan, 2008). Incorporating 10wt% titania into the batch brought down the transition temperature ( $T_g$ ) to 221°C. The result of the findings was in accordance with the works by Salama *et al* (2002) and Mohammed *et al* (2003) who reported that incorporation of  $TiO_2$  to glass batch decreases both melting temperature and glass transition temperature ( $T_g$ ). The value of glass transition temperatures ( $T_g$ ) achieved in each case would be used as guide for determining the heat-treatment temperature that might result in nuclei formation and subsequent crystals growth, and the expected nucleation temperature and crystal growth were 100°C and 300°C respectively above glass

transition temperature ( $T_g$ ) of each glass sample under study (El-Meliegy and Richard,2012).

### **5.6 Preparation of Glass-Ceramics and the Significant Changes Occurring.**

There was significant changes in the appearance observed after heat treatment of base glass samples. After heat treatment at a wide range of temperatures and various holding time. It was observed that ,there was change in appearance of the glass-ceramic samples. Glass samples have lost their brownish colour and became greyish opaque due to crystallization. The translucency observed in the samples was due to light scattering occurring (El-Meliegy ans Richard, 2012). After heat treatment, It was evident that, there were nucleation and subsequent crystallization due to the presence of nucleating agent ( $TiO_2$ ) in the glass matrix.

It was observed from the appearance of the heat treated samples that phase separation has occurred and two or more phases assemblage were precipitated during crystallization of the glass samples or as-formed glasses. Crystalline phases precipitated during crystallization of the base glass were identified using powder XRD analysis. The formation of new interfaces within the glass matrix gave sites for scattering of light. Therefore, heterogeneous nucleation has occurred at lower temperatures which was followed by subsequent crystal growth at higher temperatures (Salama *et al.*, 2002). Heterogeneous nucleation has been completed and crystal growth has taken control over the glass matrix.

This has shown that crystal phases have been precipitated throughout the residual glass matrix thus transforming the material completely opaque.

### **5.7 Identification of Crystalline Phases by XRD**

The samples to which no titania is added and then heat treated at various heat treatment time (2 and 4 hrs) did not crystallize to glass-ceramics due to lack of nuclei formation upon which crystals grow. On subjecting them to XRD analysis for detection of phases assemblage, there was no any crystal phase detected. In addition, the SEM images of the two glass samples heat treated for 2 and 4 hours exhibited the presence of single glassy phase which suggested absence of crystallization due to lack of TiO<sub>2</sub> incorporation into the sample composition. The result is expected as titania is a driving force for nuclei formation and subsequent crystallization (Salama *et al.*, 2002; Muhammed *et al.*, 2003 and Daniela *et al.*, 2010).

The XRD analysis has identified the presence of hematite (Fe<sub>2</sub>O<sub>3</sub>) and quartz (SiO<sub>2</sub>) dispersed in the matrix of the residual glassy phase of glass-ceramics sample to which 2 wt%TiO<sub>2</sub> was incorporated and heat treated at 367/667°C for 2 hours. However, the XRD peaks of the corresponding glass-ceramics sample heat treated at the same heat treatment temperatures for 4 hours has the following phases assemblage precipitated within the residual glassy phase: hematite (Fe<sub>2</sub>O<sub>3</sub>), andradite (3CaO.Fe<sub>2</sub>O<sub>3</sub>.3SiO<sub>2</sub>), carbide(Fe<sub>2</sub>C) and cordierite (2MgO.2Al<sub>2</sub>O<sub>3</sub>.5SiO<sub>2</sub>). Prolong heat treatment time of 4 hours strongly influenced the precipitation of more phases assemblage and crystallinity in the residual glassy phase as can be seen in Plate VIIIb as revealed by SEM the micrograph. According

to Daniela *et al* (2010); Rezvani (2011) and Salama *et al* (2002), glass-ceramics must contain two or more crystalline phases dispersed in the matrix of residual glass.

Similarly, the XRD of glass-ceramics sample to which 4 wt% TiO<sub>2</sub> was added and exposed to heat treatment for 2 hours at 366/666 revealed that the XRD intensity peaks correspond to the following phases assemblage: albite (Na<sub>2</sub>O.Al<sub>2</sub>O<sub>3</sub>.3SiO<sub>2</sub>), monticellite (CaO.MgO.SiO<sub>2</sub>) and quartz (SiO<sub>2</sub>) and the phases are embedded in the residual glass. In addition, XRD result of the corresponding glass-ceramics sample heat treated at the same temperature for 4 hours has the following as crystal phases: albite (Na<sub>2</sub>O.Al<sub>2</sub>O<sub>3</sub>.3SiO<sub>2</sub>), quartz (SiO<sub>2</sub>), witherite (BaCO<sub>3</sub>) and monticellite (CaO.MgO.SiO<sub>2</sub>). The SEM image in plate VIIIb shows that crystals are seen clearly in the microstructure suggesting that the proportion of crystallinity is enough in the residual glassy phases.

In a similar manner, the crystal phases dispersed in the residual glass as detected by XRD within the microstructure of glass-ceramic sample containing 6 wt% TiO<sub>2</sub> that was subjected to heat treatment for 2 hours at 363/663°C are presented as follows: quartz (SiO<sub>2</sub>), dolomite (CaMg(CO<sub>3</sub>)<sub>2</sub>) and albite (Na<sub>2</sub>O.Al<sub>2</sub>O<sub>3</sub>.3SiO<sub>2</sub>). The SEM micrograph in Plate IXa, shows that the crystals dispersed in the residual glassy phase were collected in mass. XRD result of the corresponding glass-ceramics sample heat treated at the same heat treatment temperature for 4 hours exhibited the following crystal phases: witherite (BaCO<sub>3</sub>), albite (Na<sub>2</sub>O.Al<sub>2</sub>O<sub>3</sub>.3SiO<sub>2</sub>), wollastonite (CaO.SiO<sub>2</sub>) and quartz (SiO<sub>2</sub>). The SEM mapping in Plate IXb displays the precipitation of crystal phases embedded in the residual amorphous phase. The finding was in agreement with Salama *et al* (2002) who disclosed that adding TiO<sub>2</sub> as nucleating agent augments the crystallization of wollastonite.

The XRD patterns of glass ceramics sample to which 8 wt% TiO<sub>2</sub> was added and subject to heat treatment for 2 hours at 356/656°C has the following crystalline phases dispersed in the matrix of the residual glassy phase: wollastonite (CaSiO<sub>3</sub>), calcite (CaCO<sub>3</sub>) and albite (Na<sub>2</sub>O.Al<sub>2</sub>O<sub>3</sub>.3SiO<sub>2</sub>).

The SEM micrographs in Plate Xa shows the various crystal phases dispersed in the residual glassy phase. However, XRD result of the corresponding sample heat treated at the same temperature for 4 hours contained the following crystal phases dispersed in the matrix of residual glassy phase: hematite (Fe<sub>2</sub>O<sub>3</sub>), anorthite (CaO.Al<sub>2</sub>O<sub>3</sub>.2SiO<sub>2</sub>), wollastonite (CaO.SiO<sub>2</sub>), cordierite (2MgO.2CaO.5SiO<sub>2</sub>) and andradite (3CaO.Fe<sub>2</sub>O<sub>3</sub>.3SiO<sub>2</sub>). The SEM image in Plate Xb shows the precipitation of crystalline phases in the residual glassy phase. According to Salama *et al* (2002), using TiO<sub>2</sub> as nucleation catalyst leads to precipitation of anorthite and wollastonite.

The XRD patterns of glass-ceramics sample to which 10 wt% TiO<sub>2</sub> was incorporated and subjected to thermal treatment at 321/621°C for 2 hours precipitated the following crystal phases: wollastonite (CaO.SiO<sub>2</sub>), monticellite (CaO.MgO.SiO<sub>2</sub>), quartz (SiO<sub>2</sub>), andradite (CaO.Fe<sub>2</sub>O<sub>3</sub>.3SiO<sub>2</sub>) and cordierite (2MgO.Al<sub>2</sub>O<sub>3</sub>.5SiO<sub>2</sub>). The SEM image in plate XIa shows that crystals are seen clearly in the microstructure suggesting that there is high proportion of crystallinity in the residual glassy phases. This result is in agreement with (Salama *et al.*, 2002) who stated that addition of TiO<sub>2</sub> can crystallized wollastonite in the glassy phase. However, the XRD patterns of glass-ceramics sample that has 10 wt% TiO<sub>2</sub> and subjected to heat treatment to crystallized it at 321/621°C for 4 hours has the following phases assemblage within the residual glassy phase: albite, quartz, wollastonite, titanate, microcline, hematite, monticellite, andradite, calcite and cordierite. Prolong heat treatment

time of 4 hours strongly influenced the precipitation of more crystalline phases dispersed in the residual glassy phase as can be seen in Plate XIb as revealed by SEM micrograph. The findings is in agreement with (Barsoum, 1994; Rappensberger, 1996 and Mahdavi, 2011) who reported that the incorporation of 10 wt% TiO<sub>2</sub> to the base glass system promotes achieving high density nucleation and crystallization leading to the precipitation of considerable number of phases assemblage. In addition, according to Holand (1991); Rappensberger (1996); Salama *et al* (2002) and Daniela *et al* (2010) incorporation of TiO<sub>2</sub> as nucleating agent allows the formation of nucleation phase such as titanate. Besides, anorthite, microcline and wollastonite would be precipitated.

### **5.8 Scanning Electron Microscope (SEM) of Glass-Ceramics Samples**

The FESEM micrographs of heat treated sample that has 0wt% TiO<sub>2</sub> heat treated for 2hrs is presented in Plates VIa at 1000X magnifications and the SEM image of the corresponding sample heat treated for 4 hours is shown in Plate VIb. The SEM micrograph of each case has exhibited a single glassy phase which suggested absence of crystallization due to lack of TiO<sub>2</sub> incorporation into the sample composition. The result is expected as titania is a driving force for nuclei formation and subsequent crystallization (Salama *et al.*, 2002; Muhammed *et al.*, 2003 and Daniela *et al.*, 2010). However, microsized bubbles were observed in the glassy phase. This could be due to the presence of residual soluble gases in the amorphous melt (Nemec and Tonarova, 2008). The concentration of soluble gases in the melt depends on heat treatment temperature, glass composition and the concentration of fining agents which facilitate bubble shrinkage (Nemec and Tonarova, 2008). However, it has been observed that there are crystal phases dispersed within the matrix of heat treated samples that has gradual addition of titania due to crystallization.

Plates VIIa presents SEM micrograph of glass-ceramics sample to which 2 wt% TiO<sub>2</sub> was incorporated and then subjected to heat treatment at 367/667°C for 2 hours. The image is shown at 500X magnifications. The resulting microstructure is characterized by dense, uniform and consist of randomly distributed crystal which are circular-like alongside micro-sized voids between grain boundaries, all dispersed in the matrix of the residual amorphous phase.

However, Plate VIIb presents the SEM micrograph of the corresponding glass-ceramics sample at 2000 X magnifications heat treated at the same temperature for 4 hours. It can be observed that the microstructures had swallowed the amorphous phase because they agglomerated in mass. The microstructure is characterized by dense, needle-like and ellipsoid-like microstructures alongside tiny micro-sized voids randomly dispersed in the residual glass. The image micrograph of the resultant glass-ceramic have changed. This result is expected simply because altering the heat treatment time changes morphology, crystal size as well as physical appearance of the resultant glass-ceramic (Mahmud, 2007). The crystal phases precipitated according to XRD are as follows: hematite, andradite and cordierite. This confirmed that the material produced was glass-ceramics due to the presence of crystalline phases in the residual glass (Holand and Beall, 2002; Daniela, *et al.*, 2010; Rezvani, 2011).

In a similar vein, the microstructural studies of Plate VIIIa is SEM mapping of glass-ceramics sample to which 4 wt% titania was added and heat treated at 366/666°C for 2 hours. The SEM image is displayed at 500 X magnifications. The microstructure is characterized by dense, flake-like shaped crystals along side tiny micro-sized pores distributed in the matrix of the residual glassy phase. The phases assemblage precipitated

in the matrix of the amorphous phase include: albite, monticellite and quartz. However, Plate VIIIb displayed the SEM mapping of the corresponding glass-ceramics sample heat treated at the same temperature for 4 hours. The SEM image is shown at 380X magnifications. It can be observed that the growth of the crystalline phases had eventually consumed the residual glassy phase surrounding them. In addition, the microstructure is composed of dense, circular like crystals which are randomly distributed. The precipitated crystalline phases as identified by the XRD are: albite, monticellite, witherite and small amount of microsized voids dispersed in the matrix of residual glass.

Similarly, SEM micrograph of glass-ceramics sample with 6 wt% TiO<sub>2</sub> thermally treated at 363/663°C for 2 hours is shown in Plate IXa at 2000 X magnifications. The crystals in the residual glassy phase had swallowed the glassy phase because they were collected into mass. The crystals are characterized by dense, needle-like and clustered-like crystals alongside microsized bubbles embedded between crystals while the SEM mapping of the corresponding glass-ceramics sample heat treated for 4 hours is depicted in Plate IXb at 500 X magnifications. The microstructure is characterized by heap, circular-like, flake-like and needle-like clusters alongside microsized voids between crystals. The crystalline phases identified by the XRD include: albite, wollastonite, witherite and quartz dispersed in the residual amorphous phase.

The SEM microstructural mapping of glass-ceramics sample to which 8 wt% TiO<sub>2</sub> is added and heat treated at 356 /656°C for 2 hours is depicted in Plate Xa at 500X magnifications. The microstructure is projected as mass, ellipsoid-like layered structure alongside fewer microsized inclusions embedded in the residual glass matrix. The XRD translated the crystalline phases present in the glass-ceramics sample as follows: Wollastonite, calcite and

Albite. Glass-ceramics must contain at least two or more crystal phases dispersed in the residual glassy phase (Daniela *et al.*, 2010 and Rezvani, 2011). However, the SEM micrograph of the corresponding glass-ceramics sample heat treated at the same temperature for 4 hours is exhibited in Plate Xb at 500 X magnifications. The microstructure is characterized by dense and collection of randomly distributed flake-like crystals alongside fewer microsized pores. The XRD result revealed that the following crystal phases are present in the residual glass (hematite, anorthite, wollastonite, cordierite and andradite). This is in line with Salama *et al* (2002); Garza Garcia *et al* (2007); Daniela *et al* (2010); Russell and Edward (2010); Rezvani (2011) and Khater (2012) who reported that glass-ceramic must contain two or more crystalline phases dispersed in the glass matrix. In addition, according to Alizadeh and Marghussian (2000) and Abdulhamid *et al* (2003) numerous phases assemblage can be crystallized from the CaO-MgO-Al<sub>2</sub>O<sub>3</sub>-SiO<sub>2</sub> base glass system.

SEM micrograph mapping of glass-ceramics sample to which 10 wt% TiO<sub>2</sub> was incorporated and subjected to thermal treatment at 321/621°C for 2 hours is visualized on Plate XIa at 500X magnifications. The microstructure displayed dense, circular, ellipsoidal, needle and lamellar twinning-like crystals dispersed in the matrix of residual glass. The microstructural behaviour may be due to the presence of the following crystalline phases as identified by the XRD: albite, orthoclase, wollastonite, rutile and quartz. In addition, fewer microsized bubbles were also identified between grains. The microsized bubbles might result from soluble gases in the glassy melt (Nemec and Tonarova, 2008). This result is also in line with the findings of the following Holand and Beall (2002); Daniela *et al*

(2010); Rezvani (2011) and Mohammed *et al* (2003) who indicated that high density nucleation yield a great deal of crystal phases.

SEM micrograph of the corresponding glass-ceramics sample heat treated at the same temperature for 4 hours are exhibited on Plate XIb at 3000 X magnifications. The microstructure is characterized by dense, needle, circular, ellipsoidal, flake and lamellar twinning-like crystals dispersed in the amorphous phase. This might result from the presence of the following phases assemblage: microcline, wollastonite, albite, monticellite, quartz, andradite, hematite, titanate, cordierite and calcite. Furthermore, according to XRD result, fewer microsized pores were detected between grains. The findings is in agreement with the following Holand (1991); Holand and Beall (2002); Salama *et al* (2002); Daniela *et al* (2010) and Rezvani (2011) who pointed out that a great deal of crystalline phases would be precipitated when 10 wt% TiO<sub>2</sub> is incorporated into the base glass system and subjected to prolong heat treatment. Also, incorporating 10-18 wt% TiO<sub>2</sub> is sufficient to promote achieving extensive phase separation which enhances the precipitation of wollastonite, anorthite and cordierite (De Vekey and Majumdar, 1970 and Salama *et al.*, 2002).

In this research, formation of porosity has been observed among crystals. However, according to literature, when a glass-ceramics material is heat treated at higher temperatures, the formation of viscous flow is sufficient to eliminate the persisted microsized pores that were formed (Bahman and Behzad, 2012a).

In addition, the summary of crystalline phases precipitated in this research are as follows: orthoclase, wollastonite, anorthite, albite, cordierite, monticellite, andradite, witherite, calcite, hematite, titanate, quartz and microcline. This is also in accordance with the XRD

results of the preliminary studies in which the sample powders of the starting materials (feldspar & limestone) revealed the presence of the following: microcline, albite, quartz and calcite. Furthermore, each mineral phase detected has a beneficial application. Example, wollastonite is used for cladding in the building industry (Holand and Beall, 2002), wollastonite serves as flux for welding and as additive in paint among others. Calcite being the most stable polymorph of calcium carbonate ( $\text{CaCO}_3$ ) has been a source for lime ( $\text{CaO}$ ) which is essentially used as stabilizing agent in glass making (Doyle, 1979 and Shelby, 2005). Albite is another source for soda ( $\text{Na}_2\text{O}$ ) and soda is used as fluxing agent in glass making. Quartz is another source for silica ( $\text{SiO}_2$ ), and silica is a glass former in glass making (Shelby, 2005).

## **5.9 Property Tests**

### **5.9.1 Hardness of Glass-Ceramic samples produced**

The hardness of glass-ceramics depends on bond strength of its composition and the packing density of ions in its structure (Rappensberger, 1996). The findings on variation of heat treatment time and Titania ( $\text{TiO}_2$ ) addition against hardness of glass-ceramic samples are displayed in Figure 4.24. The result revealed that all glass samples (0wt%  $\text{TiO}_2$ ) heat treated at various time (1, 4 hrs) show low hardness values due to the presence of modifying oxides ( $\text{CaO}$ ,  $\text{MgO}$ ,  $\text{Na}_2\text{O}$ ,  $\text{K}_2\text{O}$ ) which weaken glass mechanical properties such as hardness. Increase in hardness from (192 HV to 418 HV) was noticeable as heat treatment time increases. The increase in hardness was due to viscous flow formation induced by prolonged heat treatment time. It is likely that hardness changes with prolonged heat treatment time (Martin *et al.*, 2010). Minimum hardness value (192 HV) was recorded on glass sample (0wt%  $\text{TiO}_2$ ) heat treated for 1 hour. However, the result shows

significant improvement in hardness because hardness values increased progressively as heat treatment time and TiO<sub>2</sub> addition were increasing simultaneously. This trend is expected because when converting glass into glass-ceramics, hardness usually increases and this was brought about by the formation of a wide range of crystalline phases precipitated in the matrix of residual glasses (Rappensberger, 1996; Salama *et al.*, 2002 and Margha *et al.*, 2009). The glass-ceramics under study must possess fine-grained microstructures in the residual glassy phase which also influenced increase in hardness. Also, Hasan *et al.* (2009) revealed that the hardness of silicate glass-ceramics increased due to the fine-grained microstructure in which the crystal size plays a key role in preventing the propagation of the cracks in the material structure.

Maximum hardness value (988HV) was recorded on glass-ceramic sample to which 10wt% TiO<sub>2</sub> was added and subjected to heat treatment time of 4 hours. The finding is in consonant with the result of the following researchers (Rappensberger, 1996; Salama *et al.*, 2002; Mohammed *et al.*, 2003; Daniela *et al.*, 2010 and Mahdavi *et al.*, 2011) who indicated that incorporation of 10-18 wt% TiO<sub>2</sub> as nucleating agent is sufficient to promote achieving excellent hardness as propagating micro cracks are hindered as they cross grain boundaries, thus creating stronger bond which boost hardness.

### **5.9.2 Chemical solubility of Glass-Ceramic samples using 1M HCl solution**

Chemical solubility directly affects the strength and hardness of glass-ceramic sample which significantly influences abrasion (Naruporn *et al.*, 2013). Acids generally attack the fluxing agents (Na<sub>2</sub>O, K<sub>2</sub>O) in the glass dissolving them by substituting H<sup>+</sup> ions for the alkali ions thus opening up the silica skeletal structure (Salah, 2016). Figure 4.25 presents the chemical solubility results of 24 samples that were subjected to varying heat treatment

time (1-4 hrs) and titania (TiO<sub>2</sub>) incorporation (0, 2,4, 6,8 and 10 wt%) in 1 M HCl. It has been observed that the glass samples (0 wt% TiO<sub>2</sub>) suffered dissolution in 1 M HCl due to leaching. The acid attacks the mobile alkali ions (Na<sup>+</sup>, K<sup>+</sup> ions) in the glass interstices gradually dissolving them in the network structure by substituting H<sup>+</sup> ion for the alkali thus leaving a porous surface and exposing the Si-O network structure (Harper, 2001 and Salah, 2016).

However, progressive decrease in weight loss was noticeable as heat treatment time (1-4 hours) increases across the glass samples. The decrease in weight loss was induced by prolong heat treatment time. 0.6831 g/cm<sup>3</sup> weight loss was recorded on glass sample (0 wt% TiO<sub>2</sub>) that was heat treated for 1 hour. The sample suffered greater dissolution than its corresponding sample (0.4253 g/cm<sup>3</sup>) heat treated for 4 hours due to leaching induced by ion exchange.

Decreases in weight loss was recorded on glass-ceramic samples to which varying amounts of titania (TiO<sub>2</sub>) were incorporated (2,4, 6,8 and 10 wt%) and heat treated at various heat treatment time (1-4 hours). The resistance to acid attack was due to the presence of large volume of phases assemblage dispersed in the matrix of residual glassy phase (Shelby, 2005; El-Meliegy and Richard, 2012). Minimum weight loss (0.2443 g/cm<sup>3</sup>) was recorded on glass-ceramic sample to which 10 wt% TiO<sub>2</sub> was added and heat treated for 4 hours. Generally, lack of resistance to acid attack was brought about by the presence of modifying oxides such as (K<sub>2</sub>O, Na<sub>2</sub>O, CaO, MgO) in batch composition and insufficient heat treatment time which promotes dissolution of glass sample in the acid (De Vekey and Majumdar 1970; Naruporn *et al.*, 2013 and Salah, 2016).

### **5.9.3 Chemical solubility of Glass-Ceramic samples using 1M NaOH solution**

Figure 4.26 shows chemical solubility of 24 glass-ceramic samples using 1M NaOH solution at different heat treatment times and TiO<sub>2</sub> incorporation. Alkali solutions generally attack silicon-oxygen (Si-O) bond in the glassy structure, although, titania ions if present in the batch composition can inhibit the attack more effectively than alumina in alkali silicate glasses (Naruporn *et al.*, 2013).

It has been observed that the chemical solubility of all the glass-ceramic samples to which varying concentration of TiO<sub>2</sub> was incorporated into the batch composition and heat treated at various heat treatment time inhibit alkali attack using 1M NaOH aqueous solution. This result was expected because the presence of Ti<sup>4+</sup> ions which serves as driving forces for inhibition of alkali attack as well as the presence of large volume of phases assemblage dispersed in the matrix of residual glassy phases are hindrance factors for alkali attack.

However, minimum weight loss (0.3211g/cm<sup>3</sup>) was recorded on glass-ceramic sample to which 10 wt% TiO<sub>2</sub> was added and heat treated for 4 hours. The result was expected and it suggested that a broad spectrum of crystalline phases were precipitated within the residual glassy phase as indicated by the XRD and they served as inhibition factors for dissolution of the sample in 1M NaOH solution (Naruporn *et al.*, 2013 and Salah, 2016). However, it was observed that all the glass samples (0wt% TiO<sub>2</sub>) suffered dissolution in 1M NaOH solution due to degeneration of network structure (Si-O). However, slight decrease of alkali attack was noticeable as heat treatment time increases progressively from 1-4 hours (0.84-0.58g/cm<sup>3</sup>) respectively. The slight decrease in alkali attack (1M NaOH) resulted from the prolong heat treatment time as well as the presence of Al<sup>3+</sup>, Ca<sup>2+</sup>, Mg<sup>2+</sup> among other variables which increase chemical resistance and hinders alkali dissolution (Salah, 2016). However, maximum alkali attack (0.84 g/cm<sup>3</sup>) was recorded on the

corresponding sample that was subjected to heat treatment for 1 hour. The sample had suffered considerably alkali attack than its corresponding sample (0.58 g/cm<sup>3</sup>) heated treated for 4 hrs. Generally, weight loss was induced by modifying oxides present in the amorphous samples (Naruporn *et al.*, 2013 and Salah, 2016). The results showed that heat treatment time and TiO<sub>2</sub> incorporation have greatly influenced weight loss because, as heat treatment time and TiO<sub>2</sub> addition increase, weight loss decreases progressively.

#### **5.9.4 Apparent density of Glass-Ceramics samples produced.**

Figure 4.27 displayed the results of 24 samples on the effect of heat treatment time and TiO<sub>2</sub> incorporation against apparent density. All density values had shown a gradual increase as heat treatment time and titania addition increase progressively. Minimum density values were recorded on glass samples (0 wt% TiO<sub>2</sub>) that were subjected to heat treatment for 1-4 hours. This was due to the absence of crystalline phases in the glass matrix and the presence of micro-sized bubbles as detected by SEM in the glassy phases, which grossly lower the density values (Shelby, 2005 and Salah, 2016). However, density values of glass samples (0 wt% TiO<sub>2</sub>) heat treated at a wide range of time (1-4 hrs) increased slightly as heat treatment time increases progressively. The slight increase in density was due to viscous flow formation resulting from prolonged heat treatment which eliminates or lowers the concentration of inclusions, thereby increasing the density values (Shelby, 2005; Pye *et al.*, 2005 and Bahman and Behzad, 2012a). However, the minimum density value (2.1233 g/cm<sup>3</sup>) was recorded on a sample to which 0 wt% TiO<sub>2</sub> was incorporated and subjected to

heat treatment time of 1 hour. Maximum density value (2.8873 g/cm<sup>3</sup>) was recorded on glass-ceramic sample to which 10 wt% TiO<sub>2</sub> was incorporated and heat treated for duration of 4 hours. The high density value was expected simply because the density of glass-ceramic sample is always larger than the density of its corresponding glass sample (Strnad, 1986). The difference in density was due to the presence of large volume of crystalline phases dispersed in the residual glassy phase (Strnad, 1986 and Rappensberger, 1996). Also, Chinnam *et al* (2015) reported that increase in hardness of a given glass-ceramic increases apparent density. Therefore, in conclusion, results revealed that apparent density is strongly influenced by heat treatment time and TiO<sub>2</sub> addition, because, as heat treatment time and TiO<sub>2</sub> addition increase, apparent density increases.

#### **5.9.5 The Porosity of Glass-Ceramic Samples.**

Porosity of glass-ceramic samples was measured as a percentage relationship of the volume of the open pores to its exterior volume. Figure 4.28 presents the porosity values of all the 24 samples under study at different heat treatment time and titania incorporation. The result shows that porosity decreases as heat treatment time and titania addition increased on all the samples. This is expected because glass-ceramics are non porous materials as grains of crystalline phases were able to block up the pores present thereby decreasing the porosity.

However, maximum porosity values were recorded on glass samples (0 wt% TiO<sub>2</sub>) that were subjected to heat treatment time from 1-4 hours. Although, a slight decrease in porosity was noticeable. This results from the closure of some microsized pores due to prolong heat treatment time brought about by viscous flow formation as well as absence of

phases assemblage (Bahman and Behzad, 2012a). However, minimum porosity value (0.1422%) was recorded on glass ceramic sample to which 10 wt% TiO<sub>2</sub> was incorporated and subjected to heat treatment of 4 hours. This results from the presence of large volume of phases assemblage precipitated in the sample. In conclusion, maximum porosity value (5.9886%) was observed on glass sample (0wt% TiO<sub>2</sub>) that was heat treated for 1 hour. Conversely, minimum porosity value (0.1422%) was recorded on glass-ceramic sample to which 10 wt% TiO<sub>2</sub> was added and heat treated for 4 hours.

#### **5.9.6 Water absorption of Glass-Ceramic samples**

Figure 4.29 displayed water absorption values of 24 samples at a wide range of heat treatment time and TiO<sub>2</sub> addition. All water absorption values had shown gradual decrease as heat treatment time and titania addition were increasing progressively. Low water absorption values were recorded on glass-ceramic samples (10 wt% TiO<sub>2</sub>) heat treated from 1- 4 hours. This was due to the presence of large volume of phases assemblage dispersed in the matrix of the residual glassy phase. Minimum water absorption value (0.0598%) was recorded on the corresponding glass-ceramic sample heat treated for 4 hours. This result is expected because the microstructure of glass-ceramics always consists of fine-grained phases assemblage dispersed in the matrix of residual glass which hindered propagating micro cracks as they cross grain boundaries (Rappensberger,1996). Maximum water absorption value was recorded on glass samples (0 wt% TiO<sub>2</sub>) heat treated from 1-4 hours. This is expected because of microsized pores dispersed in the matrix of the glassy phase. However, water absorption values decreased progressively

from 1-4 hours. This results from the closure of some microsized voids due to prolonged heat treatment time inducing viscous flow formation thereby eliminating the persistent inclusions (Bahman and Behzad, 2012a). The highest water absorption value (4.9876%) was recorded on the corresponding glass sample heat treated for 1 hour. This might result from insufficient heat treatment time and lack of crystal phases in the residual glass. Therefore, the result shows that prolonged heat treatment time has a significant effect on water absorption even though the sample does not contain TiO<sub>2</sub> but water absorption values have decreased considerably.

In conclusion, the effect of heat treatment time and titania (TiO<sub>2</sub>) addition produced different microstructural configuration, crystalline phases, physical properties, chemical stability and mechanical properties. The optimum condition that produced glass ceramics with excellent properties was 10wt% TiO<sub>2</sub> content at 4 hours heat treatment time. The sample has the best result all through in terms of hardness (988HV), weight loss using 1M HCl (0.2443g/cm<sup>3</sup>), weight loss using 1M NaOH solution (0.3211 g/cm<sup>3</sup>), density (2.8873g/cm<sup>3</sup>), porosity (0.1422%) and water absorption (0.0598%) than the corresponding amorphous sample heat treated at the same temperature and time. The sample is characterized by dense, needle-like, dendritic, lamellar twinning, flake-like and circular-like crystals embedded in the matrix of the residual glassy phase. The sample contains the following as crystalline phases: calcite

wollastonite, cordierite, titanate, hematite, microcline, monticellite, albite, andradite and quartz. Generally, heat treatment time and TiO<sub>2</sub> incorporation have greatly influenced the properties under study because as the two parameters were increasing, the property values were increasing progressively, except for chemical solubility, porosity and water

absorption in which weight loss values, porosity and water absorption values were decreasing. The findings concided with Salama *et al* (2002) and Mahdavi *et al* ( 2011) who reported that incorporating 10 wt% TiO<sub>2</sub> to the base glass system CaO-MgO-Al<sub>2</sub>O<sub>3</sub>-SiO<sub>2</sub> promotes achieving high density nucleation and subsequent crystallization which results in the formation of improved properties. Therefore, the relation between crystal phases of glass-ceramics and mineral phases of chemical composition has been established.

## CHAPTER SIX

### 6.0 SUMMARY, CONCLUSIONS AND RECOMMENDATIONS

#### 6.1 Summary

The research focuses attention on collection of samples locally as follows: feldspar was sourced at Matari feldspar deposit, limestone was collected at Kalambaina limestone deposit and magnesite was acquired from Tsakesimptah magnesite deposit. The samples were subjected to crushing, grinding and sieving to -105µm particle size distribution. Each sample was characterized using instrumental analytical techniques such as X-ray fluorescence (XRF), X-ray diffraction (XRD), Scanning electron microscope/ energy dispersion spectroscopy (SEM-EDS) to determine oxides composition, mineralogical compositions, morphological study and elemental compositions respectively The various analyses were carried out with a view to finding out their respective suitability in making

glass and the resultant glass-ceramics. The finding of each sample has revealed that it is suitable for making glass-ceramics. Chemical grade Titania ( $\text{TiO}_2$ ) was incorporated in varying quantity (2wt%, 4wt%, 6wt%, 8 wt% & 10wt%) to speed up nucleation and crystallization processes. Moreso, sodium chloride ( $\text{NaCl}$ ) was added as fining agent to remove both the small bubbles (seeds) and larger bubbles (blisters). Batches were formulated and glass samples were produced, followed by conversion of glass samples into glass-ceramics using controlled nucleation and crystallization processes. Furthermore, only glass-ceramic samples heat treated for duration of 2 and 4 hours were considered to be subjected to characterization using X-ray diffraction (XRD) and field emission scanning electron microscope (FESEM) analyses. The FESEM results revealed that the glass-ceramic samples were characterized by flake, a circular, semi circular or lamellar twinning crystals dispersed in the various residual glassy phases. In a similar vein, the XRD analysis of the six sets of glass-ceramic samples detected the following crystalline phases: wollastonite, anorthite, albite, cordierite, witherite, titanate, microcline, quartz, calcite, andradite, monticellite and hematite. This is in accordance with the XRD results of the preliminary studies which revealed the presence of as follows: microcline, albite, quartz and calcite in the samples powders (feldspar and limestone). Besides, determination of some property tests (hardness, apparent density, chemical solubility, porosity and water absorption) were carried out on each sample using standard procedures. Glass ceramic sample to which 10%  $\text{TiO}_2$  was added and subjected to heat treatment time of 4 hours has the best combination of microstructures and properties: Vis-à-vis hardness (988HV), apparent density ( $2.8873 \text{ g/cm}^3$ ), porosity (0.1222%), water absorption (0.0598%), chemical resistance to 1M HCl ( $0.2443 \text{ g/cm}^3$ ), and chemical resistance to 1M NaOH

(0.3211 g/cm<sup>3</sup>). Therefore, the relation between crystal phases of glass-ceramics and mineral phases of chemical composition has been established.

## 6.2 Conclusions

The study place emphasis on development of glass-ceramics by controlled nucleation and crystallization of glass samples produced from local raw materials (feldspar, limestone & magnesite). From the analyses and discussions of results, the following conclusions could be drawn:

1. That glass samples could be produced from locally available raw materials (Feldspar, limestone and magnesite).
2. That the produced glass samples could be transformed into glass-ceramics by controlled nucleation and crystallization processes.
3. That the microstructures of the glass ceramics samples are characterized by dense, flake, circular, semi circular or lamellar twinning crystals. The crystalline phases dispersed in the residual glass samples include: wollastonite, anorthite, albite, cordierite, witherite, titanate, microcline, quartz, calcite, andradite, monticellite and hematite.
4. Variation of heat treatment times and incorporation of the TiO<sub>2</sub> produced glass ceramics with different microstructures, crystalline phases, physical, mechanical and chemical properties.

5. Glass ceramic sample with 10% TiO<sub>2</sub> addition and heat treatment of 4 hrs has the best combination of microstructures and properties.
6. That the produced glass ceramics with optimal properties could be used for: cladding due to the presence of crystalline phase (wollastonite), tiling due to absence of porosity, and abrasive wear-resistance applications due to its excellent hardness.

### **6.3 Recommendations**

To further increase the development of glass-ceramics by controlled nucleation and crystallization of glass samples from locally available raw materials, the following recommendation for future work and improvement are given:

1. The starting materials (feldspar, limestone and magnesite) should undergo beneficiation for removal of impurities (Fe<sub>2</sub>O<sub>3</sub>, Cr<sub>2</sub>O<sub>3</sub>, MnO<sub>2</sub>, Cu<sub>2</sub>O) so as to improve the quality of the corresponding glass samples.
2. Further study should be carried out at higher percentage of TiO<sub>2</sub> addition.
3. Properties such as flexural strength, toughness and thermal shock resistance should be investigated.

### **6.4 Contributions to Knowledge**

The study has established:

1. the suitability of three (3) starting materials (feldspar, limestone and magnesite) for glass-ceramics production using controlled nucleation and crystallization processes.
2. that glass-ceramics with 10 wt% TiO<sub>2</sub> addition and heat treatment time of 4 hours has the best combination of microstructures and properties: Vis-à-vis hardness (988HV), apparent

density (2.8873 g/cm<sup>3</sup>), porosity (0.1222%), water absorption (0.0598%), chemical resistance to 1M HCl (0.2443 g/cm<sup>3</sup>), and chemical resistance to 1M NaOH (0.3211 g/cm<sup>3</sup>).

3.that variation of TiO<sub>2</sub> addition and heat treatment time produced glass-ceramics with different microstructures, crystalline phases, physical, mechanical and chemical properties.

4.that the glass ceramics sample produced with optimal properties could be used for tiling, cladding and abrasive-wear resistance conditions based on their microstructures, chemical, mechanical and physical properties.

## REFERENCES

Abali, Y., Copur, M. and Yavuz, M. (2006).Determination of the Optimum Conditions for Dissolution of Magnesite with Sulphuric Acid Solution. *Indian Journal of Chemical Technology*. 391-396.

Abdel-aal, E.A., Ibrahim, L.A., Rasha, M.M. and Ismail, A.K. (1994). Hydrometallurgical Processing of Egyptian Magnesite Ore for Production of Magnesium sulphate. *Journal of Physicochemical Problems of Metallurgy*.28, 165-175.

Aitken, B., and Beall, G. (1994). *Material Science and Technology Series. Vol.11*. Academic Press Publishers . New York.

Alekseev, O., Dymshits, M., Tsenter, A., Zhilin, V., Denisov, N., Skoptsov, A. Malyarevich, Yumasheve, K. (2010). *Journal of Non-crystalline Solid*.356,52-54 Elsevier.

Alexis, G. P and David, H. D. (1979). *Raw Materials in the Glass Industry*. Part one. Major Ingredients. Ashlee Publishing Co. INC.

- Alexander, K. and Mario, P.(2006). Sinter-Crystallization in the Diopside-Albite System Part II. Kinetics of Crystallization and Sintering. *Journal of the European Ceramic Society*. 26, 2519-2526.
- Al-Harbi, O. A. and Khan, M. M. (2008). Relationship between Heat-Treatment Temperature, Crystallized Phases and Thermal Expansion Coefficient of LiO<sub>2</sub>-MgO-Al<sub>2</sub>O<sub>3</sub>-SiO<sub>2</sub> System. *Emirates Journal for Engineering Research*. 13(1), 53-59.
- Ali, E. A. (2008). *Development of Low Temperature Glass Ceramics from Local raw Materials*. Unpublished PhD Thesis, Department of Industrial Design. Ahmadu Bello University, Zaria. Nigeria.
- Ali, E.A., Abdulkarim, F. and Magaji, S. (2010). Chemical Analysis of Feldspar from Richifa –Soba and its Suitability as a Glass Making Raw Material. *Ashakwu Journal of Ceramics*. 7, 1-8.
- Aliyu, Z. S., Garkida, A. D., Ali, E. A. and M. Dauda (2014). “Matari-Soba Feldspar Deposit for Glass Making.” *Proceedings of the Nigeria Engineering Conference held at Ahmadu Bello University, Zaria between 15<sup>th</sup> -18<sup>th</sup> September, with Theme: Engineering and Technology for Economic Transformation. 745-755.*
- Aliyu, Z. S., Garkida, A. D., Ali, E. A. and Dauda M. ( 2013). Characterization of Kalambaina (Sokoto State) Limestone Deposit for Glass Making. *Nigerian Journal of Engineering*. Faculty of Engineering. Ahmadu Bello University, Zaria, Kaduna-Nigeria. 19( 2), 44-50.
- Aliyu, Zainab Shehu; Garkida, Adele Dzikwi; Ali, Edwin Adoyi and Dauda, Muhammad (2015). Characterization of Feldspar by Instrumental Analytical Techniques. ” *Proceedings of a Symposium Sponsored by the Materials, Characterization Committee of the Extraction and Proceeding Division of The Minerals, Metals & Materials Society (TMS) held during TMS 2015 144<sup>th</sup> Annual Meeting &*

Exhibition, March 15-19, 2015 Walt Disney World- Orlando, Florida , USA.

- Alizadeh, P. and Marghussian, V. K. (2000). Effect of Compositional Charges on the Crystallization Behaviour and Mechanical Properties of Diopside, Wollastonite Glass- Ceramics in the CaO.MgO.SiO<sub>2</sub>. (Na<sub>2</sub>O) System. *Journal of the European Ceramic Society*. 20, 765-773.
- Alizadeh, P. and Marghussian, V. K. (2000). Effect of Nucleating Agents on the Crystallization Behaviour and Microstructure of SiO<sub>2</sub>-CaO-MgO(Na<sub>2</sub>O) Glass- Ceramics. *Journal of European Ceramic Society*.20, 775-782.
- Amman, S. K. (2014). *Development of Glass-Ceramics from Blast Furnace Slag*. Unpublished Undergraduate Thesis. Department of Ceramics Engineering. National Institute of Technology, Rourkela.
- Amer, A. M. (2010). Hydrometallurgical Processing of Low Grade Egyptian Magnesite. *Journal of Physico-chemical Problems of Mineral Processing*. 44, 5-12.
- Antti, A. (2012). *Modelling of Deformations and Stresses in Glass Tempering*. Unpublished PhD Thesis. Tampere University of Technology.
- Aslani, S., Samim, H.R. and Arianpour, F. (2010). Beneficiation of Iranian Magnesite Ores By Reverse Flotation Process and its Effect on Shaped and Unshaped Refractories. *Buletin Material Science*. 33(6),697-705.
- ASTM C 25-11 e2 *Standard Test Methods for Chemical Analysis of limestone, quicklime and Hydrated Lime*, ASTM International, West Conshohocken., PA, 2011, [www.astm.org](http://www.astm.org).
- ASTM C 114 *Standard Test Methods for Chemical Analysis of Hydraulic Cement*.
- Aykut, H. (2005). *Influence of B<sub>2</sub>O<sub>3</sub> Addition on the Microstructure of Mica based Glass-Ceramics*. Unpublished Masters Thesis, Middle East Technical University.

- Bach, H. and Krause, D.(1999). *Analysis of the Composition and Structure of Glass and Glass ceramics*. Springer-Verlag Berlin Heidelberg publishers.56-58.
- Bahman, M. and Behzad, M. 1a. (2012a). Effects of calcium fluoride on Sintering Behaviour of CaO-SiO<sub>2</sub>.Na<sub>2</sub>O.MgO Glass-Ceramics. *Journal of Processing and Applications of Ceramics*.6( 3), 159-164.
- Bahman, M. and Behzad, M. 1b. (2012b). Investigation of Crystallization and Microstructure of Na<sub>2</sub>O.CaO.P<sub>2</sub>O<sub>5</sub>.SiO<sub>2</sub>.Al<sub>2</sub>O<sub>3</sub> Bio Glass-ceramics System. *New Journal of Glass and Ceramics*. 2,1-6.
- Baldi, G., Generlli, E. and Leonelli, C. (1995). Effects of Nucleating Agents on Diopside Crystallization in New Glass- ceramics for Tile Glaze Application. *Journal of Material Science* . 30, 3251-3255.
- Barsoum, M. (1994). *Fundamental of Ceramics*. MCCrew-Hill Publishers, Singapore.
- Beall, G. H. (1985). Glass-ceramics: Current Propblems and Prospects. *Journal of Non Crystalline Solids* .73, 413-419.
- Beall, A.H. (1992). Design and Properties of Glass-Ceramics. *Annual Review Material Science*. 22, 91-119.
- Beall, G. H. 1993).Glass-Ceramics:“Recent Development and Applications”. *Journal of Ceramics Transactions*. 30, 241-266.
- Beall, G. H. (2008). Refractory Glass ceramics based on Alkaline Earth Aluminosilicates. *Journals of the European Ceramic Society* .Elsevier.
- Bing, Y., Kaiming, L. and Shouren, G. (2003). Effect of Microstructure on the Mechanical Properties of CaO-P<sub>2</sub>O<sub>5</sub>.SiO<sub>2</sub>-MgO-F<sup>-</sup> Glass-Ceramics. *Journal of Ceramics International*. 29,695-698.

- Bron, V. A., Simono, K.V., Chikunon, I.F. and Uzberg, A.I. (1962). *Spinel-bonded Magnesite Bricks for High Tonnage Electrical Arc Furnaces*. *Refractories*. 3, 267-271.
- Carl, G. and Hoche, T. (2002). Crystallization Behaviour of a MgO.Al<sub>2</sub>O<sub>3</sub>.SiO<sub>2</sub> Glass Proceedings XIX International Congress for Glass. *Journal of Physics and Chemistry of Glasses*. 43C, 256-258.
- Casasola, R., Ma, J. and Rincon, M.R. (2012). Glass-ceramics Glazes for Ceramics Tiles: A Review. *Journal of Material Science*. 47, 553-582.
- Case, J., Chilver, A.H. and Ross, C.T.F. (1999). *Strength of Materials and Structures*. John Wiley & Sons Publishers.
- Chen, G. H. (2007). Effect of Replacement of MgO by CaO on Sintering, Crystallization and Properties of MgO.Al<sub>2</sub>O<sub>3</sub>.SiO<sub>2</sub> System Glass-Ceramics. *Journal of Material Science*. 42, 7239-7244.
- Chinnam, R. K., Bernardo, E., Will, J. and Boccaccini, A. R. (2015). Processing of Porous Glass-ceramics from Highly Crystallisable Industrial Wastes. *Advance in Applied Ceramics Structure, Functional and Bioceramics*. 114(1)11-16.
- Christian, R. Christian, B. and Martina, S. Katrin, T. and Askan, K. (2015). News From Glass Crystallization. *journal of Chemical Technology and Metallurgy*. 50(40),357-366.
- Daniela, H., Tomasz, O. and Wieslaw, W. (2010). Wear Resistance Glass-ceramics with a Gahnite obtained in CaO-MgO-Al<sub>2</sub>O<sub>3</sub>-SiO<sub>2</sub>-B<sub>2</sub>O<sub>3</sub>-ZnO System. *Journal of the European Ceramic Society*. 31, 485-492.
- De Vekey, R. C. and Majumdar, A. J. (1970). Nucleation and Crystallization Studies of some Glasses in the CaO-MgO-Al<sub>2</sub>O<sub>3</sub>-SiO<sub>2</sub>. *System Journal of Mineralogical Magazine* 37(291), 771-779.
- Doyle, P.J. (1979). *Glass Making Today. An Introduction to Current Practice in Glass*

*Manufacture.* Portcullis Press Red hill.

Demirci, Y. and Gunay, E. (2011). Crystallization Behaviour and properties of Cordierite Glass-Ceramics with added Boron Oxide. *Journal of Ceramic Processing Research.* 12(3),352-356.

Durrani,S.K., Hussaini M.A. , Hussaini J.A. , Saeed, a, Hussaini, N. and Ahmed, N. (2010). Fabrication of Magnesium Alumino Silicate Glass-ceramics by Sintering Route. *Journal of Material Science-Poland.* 28(2),459-466.

Edgar, D. Z.and Peter, F.J. (DK 666.113.2.34.28=548.517=123.012.5) The Compositional Dependence of Crystal Nucleation in Li<sub>2</sub>O-SiO<sub>2</sub> Glasses. Department of Ceramics, Glass and Polymers, University of Shieffied, UK.

El-Meliegy,E. and Richard, V.(2012). *Glasses & Glass-Ceramics for Medical Applications.* Springer, New York, NY, USA.

El-Shennawi, A.W.A., Hamzawy, E.M.A, Khater, G.A. and Omar, A.A.(2001). Crystallization of some Aluminosilicate Glasses. *Journal of Ceramics International.* 27(7),725-730.

Eric Le Bourhis(2008). *Glass: Mechanics and Technology.* Wiley-Vch Verlag GmbH & Co. KGaA, Weinheim Publishers.

Francis, A. A., Rawlings, R. D., Sweeney, R., Boccaccini, A. R. (2004). Crystallization Kinetic of Glass Particle Prepared from Mixture of Fly- ash and Soda-lime Cullet Glass. *Journal of Non Crystalline Solid.* 333, 187-197.

Francis,A. A.,Rawlings, R. D.and Boccaccini, A. R. (2002). Glass-ceramics from Mixtures of Coal Ash and Soda-Lime Glass by the Petrurgic Method. *Journal of Material Science Letters.* 21,975-978.

Gadkaree, K. P.(1991). Whisker Reinforcement of Glass-Ceramics. *Journal of Material Science.*26, 4845-4854.

Garkida, A. D.(2007). *Glass Recycling in Waste Management.* Unpublished PhD Thesis.

Department of Industrial Design . Ahmadu Bello University, Zaria-  
Nigeria

Garza-Garcia, M., Lopez-Cuevas, J., Gutierrez-Chavarria, C. A., Rendon-Angeles, J. C.  
and

Valle-Fuentes, J. F.(2007). Study of a Mixed Alkaline-Earth on Some  
Properties of Glasses of the CaO.MgO.Al<sub>2</sub>O<sub>3</sub>.SiO<sub>2</sub> System. *Boletin De La  
Sociedad Espanola De Ceramica y Vidrio Articulo*. 46(3),153-162.

George, D. Q. (1998). National Institute of Standards and Technologies. Vol. 154. No.2.  
2<sup>nd</sup>

Edition of ‘Advanced Materials and Processes ‘ Magazine.

Goharian, P., Nemati, A., Shabaniyan, M., and Afshar, A. (2010). Properties, Crystallization  
Mechanism and Microstructure of Lithium Disilicate Glass-ceramics.  
*Journal of Non Crystalline Solids*. 356(4-5), 208-214.

Gulsory, O.Y., Can, N. M. and Bayraktar, I. (2005).Production of Potassium Feldspar from  
A Low-Grade Pegmatite Ore in Turkey. *Journal of Mineral Processing  
and Extractive Metallurgy*. 114(2), 80-86.

Hans, B. and Dieter, K. (2005). *Low Thermal Expansion Glass-Ceramics*. Springer- Verlag  
Berlin Heidelberg.

HaO, l., Xitang, W., Baoguo, Z. and Zhoufu, W. (2010). Influence of Composition on the  
Characterization and crystallization of CaO.MgO.SiO<sub>2</sub> Glass-Ceramics.  
*Journal of Advanced Material Research*. Chinese  
Ceramic Communication. 105(106), 592-596.

Harper, C. A. (2001).*Handbook of Ceramics, Glasses and Diamonds*. McGraw-Hill  
Publishers.

Hasan, S., Salman, S.M., Darwish, H. and Mahdy, E.A. (2009). Effect of Na<sub>2</sub>O on the  
Crystallization Characteristics and Microstructure of Glass-ceramics Based  
on the CaO.MgO. P<sub>2</sub>O<sub>5</sub>.CaF<sub>2</sub>.SiO<sub>2</sub>System. *Journal of Ceramic Silikaty*  
53 (3) 165-170.

- Hassan, H., Iigin, K. and Mert, T. (2012). Beneficiation of Low –Grade Feldspar Ore using Cyclojet Flotation Cell, Conventional Cell and Magnetic Separator. *Journal of Physico-chemical Problems of Mineral Processing*. 48(4),381-392.
- Hill, R. G., Goat, C. and Wood, D. (1992). Thermal Analysis of a CaO-Al<sub>2</sub>O<sub>3</sub>-SiO<sub>2</sub>-CaF<sub>2</sub>.Glass System. *Journal of American Ceramic Society*.75(4), 778-785.
- Höland, W., Wange, P., Carl, G., Jana, C., and Götz, W.(1996). *Fundamentals of Controlled Formation of Glass-Ceramics*. Society of Glass Technology, Sheffield, England.
- Holand, W. and Beall, G. (2002). *Glass-Ceramics Technology*. The American Ceramic Society Publishers, Westerville.
- Hooda, J., Punia, R., Kundu, R.S., Dhankhar, S. and Kishore, N. (2012). Structural and Physical Properties of ZnO Modified Bismuth Silicate Glasses. *International Scholarly Research Network ISRN Spectroscopy*.1-5. Doi: 10.5402/2012/578405.
- Hummel, F.A.(1951). Thermal Expansion Properties of some Synthetic Lithia Minerals. *Journal of the American Ceramic Society*.34(8),235-239.
- Hussain, S. Z., Durrani, S. K., Saeed, K. Hussain, M. A., Hussain, N. and Ahmad, N. (2010). Phase and Thermal Analysis of Magnesium Aluminum Silicate Glass-Ceramics. *Journal of Pakistan Material Society*. 4(1), 39-45.
- Immo, H. R. (1981). Flotation of Feldspar, Spodumene, Quartz and Mica from Pegmatites. *A Paper presented at the 13<sup>th</sup> Canadian Mineral Processors Annual Meeting*. Pp 3-20.
- Rehana, Z. and Madeeha, R. (2015). Influence of ZrO<sub>2</sub> on the Physical Properties of CaO-MgO- Al<sub>2</sub>O<sub>3</sub>-SiO<sub>2</sub> Glass-ceramic System. *Journal of Innovative Science*. 1 (1), 23-27.

- Isah, H. (2016). *Development of Glass-ceramics using Kaolin Processing Waste Soda Lime and Borosilicate Glass Wastes*. Unpublished PhD Thesis. Department of Industrial Design. Ahmadu Bello University, Zaria- Nigeria.
- James, T. (2006). Classification and Specification of Feldspar for Use in Various Industries. *Journal of the American Ceramic Society*.
- Jing, W., Jinshu, C., Liying, T. and Peijing, T. (2013). Effect of Nucleating Agents and Heat Treatments on the Crystallization of Magnesium Aluminosilicate Transparent Glass-ceramics. *Journal of Wuhan University of Technology -Mater.Sci.Ed.* 28(1), 69-72.
- John, T. K. and Kejin, W. (2010). Investigation of Corn Ash as a Supplementary Cementitious Materials in Concrete. *Second International Conference on Sustainable Construction Material and Technologies*. ISBN -1-4507-1490-7.
- Juan, M.P., Silvio, R.T., Rincon, J.M. and Maximina, R. 2012). Understanding the Crystallization of a Wollastonite Base Glass using Isoconversional IKP Method and Master Plots. *Journal of American Ceramic Society*. DOI: 10.1111/j 1551-2916.2012.05415x.
- Kartelia, E.M. (2010). Thermal Characterization of Magnesium containing Ionomer Glasses. Unpublished Undergraduate Thesis. Department of Metallurgical and Materials Engineering . University of Birmingham.
- Kaufmann, E.N.(2003). *Characterization of Materials Volumes 1 & 2*. John Wiley Publishers
- Kaya, G., Karasu, B. and Cakir, A.(2011). *Journal of Ceramic Processing Research*. 12( 2), 135-139.
- Khater, G.A. (2001). Crystallizing Phases from Multi-component Silicate Glasses in the System  $K_2O$ - $CaO$ - $MgO$ - $Al_2O_3$ - $SiO_2$ . *Journal of Ceramics International*. 27(6)661-668.

- Khater, G.A.(2010). Glass-ceramics in the CaO-MgO-Al<sub>2</sub>O<sub>3</sub>-SiO<sub>2</sub> System based on Industrial Waste Materials. *Journal of Non-Crystalline Solids*. 356(52-54), 3066-3070.
- Khater G. A. (2012). Preparation of Glass- Ceramic Material from Granite Rock Waste. *Journal of Processing and Application of Ceramics (PAC)*: 6(2), 109-166.
- Khater, G.A., Hamzawy, E.M.A., Metwally, H.I. and El-Meliegy, E.(2013). Spodumene-Nepheline Glass-Ceramics for Dental Applications. *Journal of Applied Sciences Research*.9(1),821- 825.
- Khater, G.A. Hamzawy, E.M.A. (2008). Effect of Different Nucleation Catalysts on the Crystallization Behaviour within the CaO.MgO.Al<sub>2</sub>O<sub>3</sub>.SiO<sub>2</sub> System. *Journal of Non- Crystalline Solid*. 103-107.
- Knickerbocker, S.H., Kumar, A.H. and Herron, L.W. ( 1993). Cordierite Glass-Ceramics for  
MultilayerCeramic Packaging. *America Ceramic Society Bulletin*.72( 1), 90-95.
- Kon,M., Kawano, F., Asaoka, K. and Matsumoto, N.(1994). Effect of Leucite Crystals on The Strength of Glassy Porcelain. *Dental Material Journal*. 13(2), 138-147.
- Kokubo, T. (1990). Surface Chemistry of Bioactive Glass-ceramics. *Journal of Non-crystalline Solids*. 120, 138-151.
- Kokubo, T. Ito. , S., Sakka,S.and Yamamura, T. (1986). Formation of High-Strength Bioactive Glass-ceramics in the System MgO-CaO-SiO<sub>2</sub>-P<sub>2</sub>O<sub>5</sub>. *Journal of Material Science*.21, 536-540.
- Le Bourhis, E.(2008). *Glass Mechanics and Technology*. WILEY-VCH Verlag GmbH & Co. KGaA Weinheim.
- Leszek, S. (2005). Real Glass Crystallization High Resolution Electron Microscopy (HREM) Study and Classic Nucleation Theory Concept. *Optica*

*Applicata*. XXXV(4), 819-827.

Lewis, M.H., Daniel, A.M., Chamberlain, A., Pharoah, M.W., and Cain, M.G. (1993). Microstructure-Property Relationship in Silicate –Matrix Composites *Journal of Microscopy*. 169(2), 109-118.

Lewis, M.H. (1989). *Glasses and Glass-ceramics*. Chapman and Hall Publishers. ISBN-13: 978-94-010-6854-3e-ISBN-13:978-94-009-0817-8  
DOI:10.1007/978-94-009-0817-8.

Madhumita, G., T. Mirza, A. Sarkar, shobha, M. Sangeeta, S.L. Verma, K.R.Gurumurthy, V.K. Shrikhande and G.P. Kothiyal (2000). Preparartion and Characterizatiom of Magnesium-Alumino-Silicate Glass-ceramics. *Bulletin Material Science*. 23( 5),377-382

Mahdavi S., Madani, V., Samedani, V. and Rezie, H.R. (2011). Investigation of the Percentage Crystallization in Glass- Ceramics using an Image Analyzer Method. *Journal of Ceramic Processing Research*.12(1), 34-37.

Mahmud, M.M.(2007). *Crystallization of Lithium Disilicate Glass by Variable Frequency Microwave Processing*. Unpublished PhD Thesis.Faculty of the Virginia Polytechnic Institute and State University, Blacksburg-Virginia USA. <https://theses.lib.vt.edu/>.

Majumdar, A and Jana, S. (2001). Glass and Glass-ceramic Coatings, Versatile Materials for Industrial and Engineering Applications. *Bulletin Material Science*. 24(1),69-77.

Manfredini, T. Pellacani, G. C. and Rinco, J. M. (1997). *Glass-Ceramics: Fundamentals and Applications*. Mucchi Editore, Modena Publishers.

Margha, F., AbdelHameed, S.A.M., Ghonim, N.A. and Kojima, T.(2009). Crystallization

- Behaviour and Hardness of Glass-ceramics Rich in Nanocrystals of ZrO<sub>2</sub>  
Articles. *Journal of Ceramics International*. 35(3)1133-1137.
- Martin, J., Mattrup, S. M and Yuanzheng, Y. (2010). Effect of Crystallization Degree on Hardness of Basaltic Glass-ceramics. *Poster session presented at 22<sup>nd</sup> international Congress on Glass, Salvador, Brazil*.
- Marques, V. M. F., Tulyaganov, D. U., Agathopoulos, S. and Ferreira, J. M.F. (2006). Low  
Tem Temperature Synthesis of anorthite based Glaass-ceramics via  
Sintering and Crystallization of Glass-Powder Compacts.  
*Journal of European Ceramic Society*. 26, 2503-2510.
- McMillan, P.W. (1974). "The Phase in Glass-Ceramics". *Glass Technology*. 15 (1)5-15.
- Mehdikhani,B. and Borhani, G.H.(2013).Crystallization Behaviour and Microstructure of  
Bioglass-ceramic System. *International Letters of Chemistry, Physics  
and  
Astronomy*. 14,58-68.
- Michael, C.W.(1992).Ceramic Transactions Nucleation and Crystallization in Liquids and  
Glasses. Volume 30. *The American Ceramic Society*.
- Michael, J.P. (2002). *Feldspar And Nepheline Syenite*. U.S Geological Survey Minerals  
Yearbook. 26.1-26.6.
- Mihailova, I. K., Djambazki, P. R. and Mehandjiev, D. (2011). The Effect of the  
Composition on the Crystallization Behaviour of Sintered Glass-  
Ceramics  
from Blast Furnace Slag. *Bulgarian Chemical Communications*.  
43(2), 293-300.
- Mohammed, A. B., Maher, H. I. and Khan, M. M. (2003).The Influence of Local Raw  
Materials on Phase Crystallization of Nepheline-Pyroxene  
Glass-ceramics. *The Arabian Journal for Science and Engineering* .  
28( 2A), 109-122.
- Mukherjee, D.P and ,Das, S. K. ( 2012). Effect of CaF<sub>2</sub> on the Crystallization,  
microstructure

and properties of CaO-Al<sub>2</sub>O<sub>3</sub>-SiO<sub>2</sub> Glass Ceramics.  
*Journal of Ceramics International*. 39, 571-578.

Naruporn, M., Pornchanok, L. and Witoon, T. (2013). Characterization and Properties of Lithium Disilicate Glass-Ceramics in the SiO<sub>2</sub>-Li<sub>2</sub>O-K<sub>2</sub>O-Al<sub>2</sub>O<sub>3</sub> Base Glass System for Dental Application. *Journal of Advance in Materials Science and Engineering*. 2013(2013),763838,11.

Nemec, L. and Tonarova, V. (2008). Glass Melting and its Innovation Potential: Bubble Removal under the Effect of the Centrifugal Force. *Ceramic-Silikaty*. 52(4) 225-239.

Noves de Oliveira, A. P, Manfredini T., Leonellic and Pellacani, G. C. (1994). Physical Properties of Quenched Glasses in the LiO<sub>2</sub>-ZrO<sub>2</sub>-SiO<sub>2</sub> System. *Journal of American Ceramic Society*. 79, 1551-2916.

Park, J. (2008). *Development of a Glass-ceramics for Biomedical Applications*. An Unpublished PhD Thesis, Department of Metallurgical and Material Engineering, Middle East Technical University.

Partridge, G., Elyard, C.A. and Budd, M.J.(1989). Glass ceramics in Substrates Applications.  
Chap Man and Hall Publishers, London.

Partridge, C. (1994). An Overview of Glass-Ceramics, Part 1- Development and Principal Bulk Applications. *Glass Technol*. 35( 3), 116-127.

Perez, J. M., Casasola, R., Rincon Ma, J. and Romero, M.(2012). Nucleation and Crystallization of a Na-fluorrichterite Based-Glass by Differential Scanning Calorimetry. *Journal of Non-crystalline Solids*. 328, 2741-2748.

Pinckney, L.R. and Beall, G.H.( 2008). Microstructural Evolution in Some Silicate Glass Ceramics: A Review. *Journal of American Ceramic Society*. 91,773-779.

- Ping, W., Liping, Y., Hanning, X., Yin, C. and Shixun, L. (2009). Influence of Nucleating Agents on Crystallization and Machinability of Mica Glass-Ceramics. *Journal of Ceramics International*. 35, 2633-2638.
- Pye, L.D., Montenero, A. and Joseph, I. (2005). *Properties of Glass-Forming Melts*. Taylor and Francis Publishers. 193- 211.
- Rappensberger, C.F.(1996). *Novel Rare-Earth Aluminosilicate Glasses and Glass-ceramics*.  
Unpublished PhD. Dissertation. Department of Physics.  
Warwick university. books.google.co.ke.
- Rawlings, R.D., Wu, J.P. and Boccaccini, A.R. (2006). Glass-ceramics: Their Production from Wastes. A Review. *Journal of Material Science* . 41, 733-761.
- Raw Material, Research and Council. "Guide to the Non-Metallic Mineral Industrial Potentials of Nigeria"*. (1989).
- Raw Materials Research and Development Council. Raw Material Sourcing for Manufacturing i Nigeria: "A Synthesis of Reports of the Techno-Economic Survey of Ten Industrial Sectors in Nigeria"* (1990).
- Rawson, H. ( 1980 ). *Properties and Applications of Glass; Glass Science and Technology*. Elsevier Scientific Publishing Company.
- Raymond, T. (1984). *Crystalline Phase Development in Cordierite Glass-ceramics*.  
Unpublished PhD Dissertation. Department of Physics,  
University of Warwick.
- Ren-Ping, WU., yan, YU; ying- Yun., GU and Jin-Yu., GUO (2007). Influence of Nucleation Agents Concentration on Crystallization, Structure and Properties of Glass- Ceramics. *Chinese Journal of Structural ,Chemistry*. 26(5), 562-566.

Rezvani, M. (2011). Effect of various Nucleating Agents on Crystallization Kinetics of LAS

Glass-ceramics. *Iranian Journal of Material Science & Engineering*. 8(4), 41-49.

Rezvani, M., Eftekhar-Yektaei, B., Solati-Hashjin, M. and Marghussian, V. K. (2005). Effect

of Cr<sub>2</sub>O<sub>3</sub>, Fe<sub>2</sub>O<sub>3</sub> and TiO<sub>2</sub> nucleating agents on the Crystallization behaviour of CaO-MgO-Al<sub>2</sub>O<sub>3</sub>-SiO<sub>2</sub> (R<sub>2</sub>O) Glass-Ceramics. *Journal of Ceramic International*. 31, 75-80.

Russell, G. and Edward, A.M. (2010). Ceramics Overview: Classification by Microstructure

and Processing Methods. *Journal of Continuing Education*. 231 (9), 682-697.

Rusell, C. (2008). *Ceramic Science and Technology*. WILEY-VCH Verlag GmbH & Co. 1, 377-390.

RyemshaK, S.A., Adeleke, A.A. and Salami, S. (2012). Characterization of Ubo Limestone

for Direct Burnt Lime production. *The Pacific Journal of Science and Technology*. 13 (1), 661-668.

Salah, H.A. (2016). Production of Ceramics from Waste Glass and Jordanian Oil Shale Ash. *Journal of Estonian Academy Publishers*. 33(3), 260-271.

Salama, S. N., Darwish, H. and Abo-Mosallam, H.A. (2005) Crystallization and Properties of

Glasses Based on Diopside-Ca- Tschermak's- Fluorapatite System. *Journal of the European Ceramic Society*. 1133-1142.

Salama, S. N., Salman, S. M. and Darwish, H. (2002). The Effect of Nucleation Catalysts on Crystallization Characteristics of Aluminosilicate Glasses. *Ceramic-Silikat*. 46(1), 15-23.

Salman, S.M., Salama, S.N., Darwish, H. and Abo-Mosallam, H.A. (2009). In vitro Bioactivity of Glass-ceramics of the CaMgSi<sub>2</sub>O<sub>6</sub>-CaSiO<sub>3</sub>-Ca<sub>5</sub>(PO<sub>4</sub>)<sub>3</sub>F Na<sub>2</sub>SiO<sub>3</sub> Base Glass System with TiO<sub>2</sub>

or ZrO<sub>2</sub> Additives. 35, 1083-1093.

Samuel, J. S. (1991). *Engineered Materials Handbook. Ceramics and Glasses. The Materials*  
Information Society Publishers.

Shackelford, J. F. and Doremus, R. H. (2008). *Ceramic and Glass Materials, Structure, Properties and Processing*. Springer Science+Business Media, LLC Publishers.

Shelby, J. E. (2005). *Introduction to Glass Science and Technology*. Published by the Royal  
Society of Chemistry. Second Edition.

Smoke, E. J. (1951). Ceramic Compositions having Negative Linear Thermal Expansion. *Journal of the American Ceramic Society*. 34(3), 87-90.

Strnad, Z. (1986). *Glass-Ceramics Materials in Glass Science and Technology*. Elsevier, Amsterdam, The Netherlands.

Sunday, A. (2011). Effect of Varying Corn Cob and Rice Husk Ashes on Properties of Moulding Sand. *Journal of Minerals & Materials Characterization & Engineering*. 10 (15), 1449-1455.

Suzuki, S. and Tanaka, M. (1997). Glass-Ceramics from Sewage Sludge Ash. *Journal of Material Science*. 32, 1775-1779.

Tashiro, M. (1985). Crystallization of Glasses, Science and Technology. *Journal of Non-Crystalline Solids*. 73, 575-584.

Teixeira, S.R., Romero, M., Rinco Ma, J., Magalhaes, R.S., Souza, A.E., Santos, G.T.A and Silva, R. A. (2011). Glass-Ceramics Materials from the CaO-Al<sub>2</sub>O<sub>3</sub>-SiO<sub>2</sub> System using Sugarcane Bagasse Ash. *Journal of Material Science and Engineering*. 18 (2011) 112020.

Thiana, B., Vladimir, M. Fokin, Edgar, D. Zanotto (2008). New Large grain, highly crystalline, transparent glass-ceramics. *Journal of Non-crystalline Solids*. 354, 1721-1730.

- Tomohiro T., Yoshihiro T., Yoshikazu K. and Kiyoshi, O. (2004). Preparation and Properties of CaO-MgO-Al<sub>2</sub>O<sub>3</sub>- SiO<sub>2</sub> Glass ceramic from Kaolin Clay Refining Waste (Kera) and Dolomite. *Ceramics International*. 30, 983-989.
- Torres, F.J.and Alarcon, J. (2004). Mechanism of Crystallization of Pyroxene-based Glass-Ceramics Glazes. *Journal of Non Crystalline Solids*. 34, 45-51.
- Tulyaganov, D.U., Ribeiro, M.J. and Labrincha, J.A. (2002). Development of Glass-Ceramic by Sintering and Crystallization of Fine Powders of Calcium-Magnesium-Aluminosilicate Glasses. *Journal of Ceramics International*. 28, 515-520.
- Tulyaganov, D.U., Agathopoulos, J.M., Ventura, M.A. , Karakassides, Fabrichnaya, O. and Ferreira, J.M.F. (2006).Synthesis of Glass-Ceramics in the CaO-MgO-SiO<sub>2</sub> System with B<sub>2</sub>O<sub>3</sub>, P<sub>2</sub>O<sub>5</sub>,Na<sub>2</sub>O and CaF<sub>2</sub> Additives. *Journal of the European Ceramic Society*. 26, 1463-1471.
- Varshneya, A. K. (1994). Fundamentals of Inorganic Glasses. Academic Press, INC. Harcourt Brace & Company, Publishers.
- Wadsworth, I. and Stevens. R. (1992). The Influence of Whisker Dimension on the Mechanical Properties of Cordierite/ SiC Whisker Composites. *Journal of European Ceramic Society*. 9, 153-163.
- Wada, M. and Nimomiya, M.(1995).Glass Ceramic Architectural Cladding Materials. *Journal of Science Technology, Composition and Materials*. 30, 46-50.
- Wang, S.M., Kuang, F.H., Yan, Q.Z., Zhang, Q.C. and Ge, C.C. (2010). Crystallization Behaviour of a New Transparent Glass-creamics. *Advanced Material Research*.105(106), 597-599
- Wang,J., Chao, L., Gaoke, Z., Jun,X., Jianjun, H. and Xiujian,Z.(2015). Crystallization Properties of Magnesium Alumino silicate Glass-ceramics with and without rare-earth oxides.*Journal of Non-Crystalline Solids*. 19,1-5

Whitney, D.L. (2002). Coexisting Andalusite, Kyanite and Sillimanite: Sequential Formation

of Three  $Al_2SiO_5$  Polymorphs during Progressive Metamorphism near Triple Point, Sivrihisar, Turkey. *Journal of American Mineralogist*. 87(4), 405-416

Yehia, A. and Al-Wakeel, M. (2013). Role of Mineralogy in Selecting Beneficiation Route For Magnesite-dolomite Separation. *Journal of Physico-chemical Problems of Mineral Processing*. 49(2), 525-534.

Zanotto, E. D. (1981). The role of Amorphous Phase Separation in Crystal Nucleation in Splat Cooled  $Li_2O-SiO_2$  Glasses. *Journal of Materials Science*. 16, 973-982.

Appendix A: Effect of Heat Treatment Time and Titania ( $TiO_2$ ) Addition on Some Properties of Glass-Ceramics Samples.

Sample	HD HV	AD g/cm <sup>3</sup>	P (%)	WA (%)	1M HCl g/cm <sup>3</sup>	1M NaOH g/cm <sup>3</sup>
GLCS0PTHHT1H	192	2.1233	5.9886	4.9876	0.6831	0.8432
GLCS2PTHHT1H	389	2.3094	5.9185	2.7312	0.6558	0.83243
GLCS4PTHHT1H	554	2.3846	5.6223	2.5420	0.6352	0.8113
GLCS6PTHHT1H	720	2.4390	5.4236	2.5823	0.6045	0.7722
GLCS8PTHHT1H	750	2.7861	3.7619	1.7328	0.5842	0.72401
GLCS10PTHHT1H	912	2.8434	0.7912	0.3558	0.5836	0.68874
GLCS0PTHHT2H	221	2.1399	5.9068	4.9742	0.5825	0.6876
GLCS2PTHHT2H	398	2.3126	5.8741	2.7092	0.5653	0.6864
GLCS4PTHHT2H	582	2.4021	5.5027	2.4638	0.5548	0.67955
GLCS6PTHHT2H	746	2.4397	5.3623	2.5099	0.5440	0.67850
GLCS8PTHHT2H	772	2.8062	5.7101	1.6881	0.5339	0.6748
GLCS10PTHHT2H	919	2.8692	0.7387	0.3134	0.5263	0.6703
GLCS0PTHHT3H	288	2.1700	5.8641	4.9465	0.4653	0.6524

GLCS2PTHTT3H	502	2.3715	5.7506	2.6978	0.4582	0.6332
GLCS4PTHTT3H	635	2.4300	5.4450	2.4004	0.4548	0.6283
GLCS6PTHTT3H	762	2.5569	5.3059	2.4572	0.4431	0.6162
GLCS8PTHTT3H	792	2.8114	3.5104	1.6315	0.4355	0.5928
GLCS10PTHTT3H	966	2.8703	0.5194	0.2240	0.4374	0.5736
GLCS0PTHTT4H	418	2.1849	5.7541	4.2427	0.4253	0.5458
GLCS2PTHTT4H	505	2.3719	5.6895	2.3077	0.4002	0.4711
GLCS4PTHTT4H	657	2.4387	5.3604	2.3682	0.3765	0.4623
GLCS6PTHTT4H	835	2.6192	5.2365	2.4087	0.3434	0.4611
GLCS8PTHTT4H	876	2.8170	3.2867	1.5238	0.3032	0.4602
GLCS10PTHTT4H	988	2.8873	0.1422	0.0598	0.2443	0.3211

Appendix B: Summary of the Crystalline Phases Developed in the Glass-Ceramic Samples,

their Chemical Name and Chemical Formula after Heat Treatment.

Sample	Crystalline Phase	Chemical name	Chemical formula
GLCS2PTHTT2H	Hematite Quartz	Iron (III) Oxide Silicon dioxide	$Fe_2O_3$ $SiO_2$
GLSC2PTHTT4H	Hematite Andradite Cordierite	Iron (III) Oxide Calcium iron silicate Magnesium alumino silicate	$Fe_2O_3$ $3CaO.Fe_2O_3.3SiO_2$ $2MgO.2Al_2O_3.5SiO_2$
GLCS4PTHTT2H	Albite Monticellite Quartz	Sodium alumino silicate Calcium magnesium silicate Silicon dioxide	$Na_2O.Al_2O_3.3SiO_2$ $CaO.MgO.SiO_2$ $SiO_2$
GLCS4PTHTT4H	Albite	Sodium alumino silicate	$Na_2O.Al_2O_3.3SiO_2$

	Monticellite Witherite	Calcium magnesium silicate Barium carbonate	CaO.MgO.SiO <sub>2</sub> BaCO <sub>3</sub>
GLCS6PTHTT2H	Quartz Albite Dolomite	Silicon dioxide Sodium alumino silicate Calcium magnesium carbonate	SiO <sub>2</sub> Na <sub>2</sub> O.Al <sub>2</sub> O <sub>3</sub> .3SiO <sub>2</sub> CaMg(CO <sub>3</sub> ) <sub>2</sub>
GLCS6PTHTT4H	Albite Quartz Witherite Wollastonite	Sodium alumino silicate Silicon dioxide Barium carbonate Calcium silicate	Na <sub>2</sub> O.Al <sub>2</sub> O <sub>3</sub> .3SiO <sub>2</sub> SiO <sub>2</sub> BaCO <sub>3</sub> CaO.SiO <sub>2</sub>
GLSC8PTHTT2H	Albite Wollastonite Calcite	Sodium alumino silicate Calcium silicate Calcium carbonate	Na <sub>2</sub> O.Al <sub>2</sub> O <sub>3</sub> .3SiO <sub>2</sub> CaO.SiO <sub>2</sub> CaCO <sub>3</sub>
GLCS10PTHTT2H	Quartz Andradite Cordierite Monticellite Wollastonite	Silicon dioxide Calcium iron silicate Magnesium alumino silicate Calcium magnesium silicate Calcium silicate	SiO <sub>2</sub> 3CaO.Fe <sub>2</sub> O <sub>3</sub> .3SiO <sub>2</sub> 2MgO.2Al <sub>2</sub> O <sub>3</sub> .5SiO <sub>2</sub> CaO.MgO.SiO <sub>2</sub> CaO.SiO <sub>2</sub>
GLCS10PTHTT4H	Albite Quartz Titanate Hematite Calcite Wollastonite Microcline Andradite Cordierite Monticellite	Sodium alumino silicate Silicon dioxide Calcium titanium silicate Iron (III) Oxide Calcium carbonate Calcium silicate Potassium alumino silicate Calcium iron silicate Magnesium alumino silicate	Na <sub>2</sub> O.Al <sub>2</sub> O <sub>3</sub> .3SiO <sub>2</sub> SiO <sub>2</sub> CaO.TiO <sub>2</sub> SiO <sub>2</sub> Fe <sub>2</sub> O <sub>3</sub> CaCO <sub>3</sub> CaO.SiO <sub>2</sub> K <sub>2</sub> O.Al <sub>2</sub> O <sub>3</sub> .6SiO <sub>2</sub> 3CaO.Fe <sub>2</sub> O <sub>3</sub> .3SiO <sub>2</sub> 2MgO.2Al <sub>2</sub> O <sub>3</sub> .5SiO <sub>2</sub> CaO.MgO.SiO <sub>2</sub>

		Calcium magnesium silicate	
--	--	-------------------------------	--



